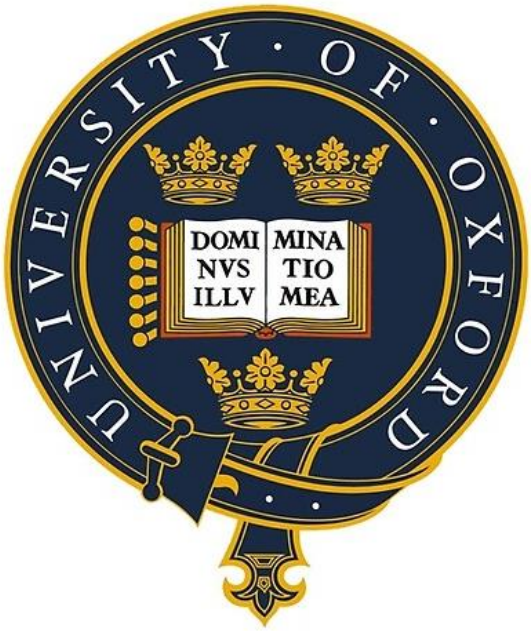
REPLICATION CATASTROPHE INDUCED BY CYCLIC HYPOXIA LEADS TO INCREASED APOBEC3B ACTIVITY



Samuel Bernard Bader

Wolfson College

Thesis submitted to the University of Oxford in accordance with the requirements for the degree of Doctor of Philosophy

Michaelmas Term, 2020
University of Oxford

Abstract

Regions of low oxygen (hypoxia) occur in most human solid tumours and correlate with a poor patient prognosis as hypoxic regions are resistant to most cancer therapies and have an increased metastatic potential. Hypoxia is a highly dynamic state, characterised by oxygen fluctuations on the order of minutes, hours, and days occurring simultaneously in regions throughout the tumour. Dynamic changes in tumour oxygenation are referred to as “cyclic hypoxia” that can span a wide range of oxygen tensions. Cells that experience severe levels of hypoxia (<0.1% O_2) are characterised by replication stress and the activation of the DNA damage response, in the absence of DNA damage. The apolipoprotein B mRNA editing enzyme, catalytic polypeptide-like (APOBEC) proteins are a family of eleven conserved cytidine deaminases that play a critical role in viral immunity through the deamination of viral transcripts. APOBECs have been shown to be responsible for the generation of mutational signatures in human cancers through their capability to deaminate cytosine bases to uracil in genomic DNA. How these mutational signatures arise in human cancer is currently unknown. Recently it was shown that hydroxyurea induced replication stress resulted in an up regulation of APOBEC3B and an increase in cellular deamination *in vitro*. This finding led us to ask if APOBEC activity would be increased in response to the physiologically relevant stress of hypoxia, which also induces replication stress. In contrast to our original hypothesis, we show that in response to chronic hypoxia (<0.1% O_2), the expression of APOBEC3B and APOBEC mediated deamination decreased. However, in response to cyclic hypoxia, APOBEC3B expression and activity increased. Most importantly, APOBEC3B induction in cyclic hypoxia was found to be dependent on replication catastrophe as opposed to replication stress. Furthermore, we provide evidence of hypoxia-dependent regulation of APOBEC-mediated activity in patient tumours. Specifically, a positive correlation can be seen between hypoxia and both the number of APOBEC mutations and the expression of A3B in human tumour samples. These data suggest that replication catastrophe induced by cyclic hypoxia is a plausible mechanism for the generation of the APOBEC mutation signatures in human cancer.

“You gotta break a few glass plates to make maracas”

-Nat

Acknowledgements

As I sit here at 12:18am on the night before submission day I can only imagine Ester's blood pressure rising in her dreams as I type these acknowledgements. Ester, I can't thank you enough for all that you've done for me. You were the one who believed in me and gave me a real shot to accomplish something that I was passionate about (even though I'm a pesky international student). I could always count on you to provide support when I needed it and to help me see a clear path when science seemed to be coming at me from 1000 directions at once. I have immensely enjoyed the time that I've spent in your lab. I'll never forget the feeling coming back from the bathroom at the Black Horse Pub and seeing 4 plates of half-finished sticky toffee puddings waiting for me. It was at that moment that I felt welcome in a totally new place and knew that the next 4 years would be some of the best of my life.

I would like to thank Adrian Harris and Peter McHugh for taking the time to sit with me and discuss my project as my thesis committee. I always appreciate an opportunity to receive constructive criticism.

I would also like to thank Andy Blackford and Tim Fenton for conducting a very thorough and challenging viva that I immensely enjoyed.

To my favourite teacher….who would have thought!! I can't believe that I can finally say these words to you. GG you are a massive reason why I have succeeded over the past 4 years. I couldn't imagine anyone taking more time or effort to teach an annoying Canadian student all that you did. You have no idea how much I appreciated all your help. I remember thinking soon after I got to know you that I hope I become even half the scientist that you are by the time I'm finished. I hope that I've lived up to this lofty expectation.

To Nat, I have absolutely no clue what I would have done without you these past 4 years. From Tindairy Fridays to that time we autocorrected your paper (cerevwowiae!!) I could always count on you to make everything bearable. I could fill this entire thesis with things we've laughed about over the years. You are a true friend and I'm honoured to (hopefullly) be graduating with you this year. See you at the LOTR marathon.

To all the present and past members of the Hammond lab who made a significant impact on my life and research: Tiffany, Hannah, Shaliny, Ania, Liz, Kasia, Hasan, Karin, Greg, Ishna, Anna, Ming, Eva, Ewen, Juan, Ryan, Joe, Sarah, I couldn't be more grateful to have been able to share such an experience with people like you….except for Ishna, I still don't like Ishna.

I also need to give a big shout out to the members of other labs who made life about a thousand times better with their "banter" as you Brits would say. Jen, Sovan, Eliot, Sam, thanks so much for everything.

Laia, you are really a part of this thesis! I'll never forget the time I spent in lockdown living with you. You are the most wonderful and supportive person and girlfriend that a guy could ask for. I hope you know how much I appreciate everything you've done for me.

Last but of course not least I want to thank my parents, Gayle and Marc. You were both the never-failing support behind all the hard work I put into this degree. It was difficult being so far away from you and from my true home for so long, but the times I got to come back to visit gave me the "reset" I needed to put in the work to achieve something that I can be proud of. I love you both so much, I owe so much of my success to you.

Thank you all!

Table of Contents

Abstract ***1***

Acknowledgements ***3***

List of Tables ***10***

List of Figures ***11***

List of Abbreviations ***14***

Chapter 1 ..... ***20***

Introduction **20**

Cancer 20

Hypoxia and cancer 24

Tumour hypoxia 24

The dynamic nature of hypoxia 26

Reactive oxygen species (ROS) 31

The transcriptional response to hypoxia, HIF1 35

Radiotherapy 39

Chemotherapy 43

Metastasis 44

Replication stress 46

DNA Replication 46

Origin licensing 48

An abundance of licensed origins 49

Replication stress 50

Responses to replication stress 53

RPA Exhaustion 56

Hypoxia-induced replication stress 60

The APOBEC family of proteins 63

Cytidine deaminases 63
Viral restriction 64
RNA editing 66
Retroelement restriction 68
Uracil in genomic DNA 71
The APOBEC mutation signature 74
Which APOBEC is the culprit? 76
Deamination of genomic DNA 79
Consequences of genomic DNA deamination (tumour) 82
Consequences of genomic DNA deamination (cell) 85
APOBEC3 regulation 87

AIMS 90

Chapter 2 91

Materials and Methods 91

Reagents 91
Hypoxia Treatments 97
Chronic Hypoxia (<0.1% O_2) 97
Cyclic and 2% O_2 97
Laboratory Techniques 98
Western Blot 98
Deamination assay 98
Small interfering RNA gene knockdown (siRNA) 99
RNA extraction and purification 100
cDNA library creation 100
Quantitative reverse transcriptase PCR (RT-qPCR) 101
Immunofluorescence (IF) microscopy 101
Flow cytometry (FACS) 102

Bioinformatics 103
Hypoxia expression signature (hypmet) 103
Group of hypoxia-inducible p53 target genes (p53genes) 103
APOBEC mutations 103
Statistical Analysis 104
Chapter 3 105
Expression and activity of APOBECs in chronic hypoxia 105
Introduction 105
Results 107
3.1 - Chronic hypoxia causes replication stress in an oxygen dependent manner 107
3.2 - HU induces the expression of multiple APOBECs 107
3.3 - Multiple APOBEC3s are induced at the mRNA level in chronic hypoxia (<0.1% O_2) in an oxygen dependent manner 108
3.4 – A3D and A3H are induced in chronic hypoxia in a HIF1 independent manner 110
3.5 - A3D and A3H are induced in chronic hypoxia in a p53 dependent manner 113
3.6 - A3B mRNA and protein expression decreases in chronic hypoxia in a p53 independent manner 114
3.7 - An in vitro deamination assay to determine the functional activity of APOBECs 116
3.8 - Deamination decreases in chronic hypoxia 118
Discussion 119
Chapter 4 122
Investigation of hypoxic conditions which lead to replication catastrophe 122
Introduction 122
Results 124
4.1 - DNA Replication is severely compromised in chronic hypoxia but continues with HU treatment 124
4.2 – Ongoing replication in HU treated cells includes origin firing 125

4.3 – Cells experience replication catastrophe with HU treatment but not chronic hypoxia .. 126
4.4 - A novel in vitro system for studying hypoxia..... 127
4.5 - Cyclic hypoxia causes prolonged replication stress..... 129
4.6 - DNA replication is maintained in cyclic hypoxia..... 130
4.7 - Cells arrest in the G2-phase of the cell cycle in cyclic hypoxia 132
4.8 – DNA replication is maintained through new origin firing in cyclic hypoxia..... 133
4.9 - Cyclic hypoxia causes replication catastrophe 134
Discussion 138
Chapter 5..... 140
A3B is upregulated by replication catastrophe 140
Introduction..... 140
Results 141
5.1 - A3B expression increases in cyclic hypoxia..... 141
5.2 - Deamination increases in cyclic hypoxia..... 141
5.3 - Increased deamination in cyclic hypoxia is dependent on A3B..... 142
5.4 - A3B induction in cyclic hypoxia does not alter the cell cycle..... 144
5.5 - A3B induction in cyclic hypoxia does not affect DDR signalling 146
5.6 – A3B induction in cyclic hypoxia is p53 independent..... 146
5.7 - Decreasing origin firing decreases replication catastrophe in cyclic hypoxia..... 147
5.8 - Decreasing origin firing in cyclic hypoxia abrogates A3B expression and activity..... 149
5.9 - Decreasing ROS in cyclic hypoxia abrogates A3B expression and activity 149
5.10 – A3B is upregulated in cyclic hypoxia in an NFκB dependent manner 151
5.11 - A3B is upregulated in cyclic hypoxia in an ATR dependent manner 151
5.12 - Loss of ATR in cyclic hypoxia leads to a G1 arrest..... 153
5.13 - A3C, A3D, A3F, A3G, and A3H expression positively correlates with a group of hypoxia-inducible p53 response genes 155
5.14 - The APOBEC mutation signature correlates with a validated hypoxia signature 156

5.15 - A3A and A3B expression correlates with a validated hypoxia signature 159

Discussion 161

Chapter 6..... 164

Discussion 164

APOBECs as a clinical target 166

APOBEC inhibition in combination with cancer therapy 169

Future directions 170

Appendices..... 171

Appendix I – Conferences and travel awards 171

Conferences attended 171

Travel awards 171

Appendix II – Published papers from this thesis 172

References..... 173

List of Tables

Table 1.1 – Summary of published studies describing cycling hypoxia. 31

Table 2.1 - General laboratory and cell culture reagents 91

Table 2.2 - Cell lines 92

Table 2.3 - Drug treatments 93

Table 2.4 – Primary antibodies 94

Table 2.5 – Secondary antibodies 95

Table 2.6 – RT-qPCR primers 96

Table 2.7 - siRNA 96

Table 2.8 - Oligonucleotides 97

Table 5.1 – Summary of bioinformatic analysis conducted 160

List of Figures

Figure 1.1 – The Edwin Smith papyrus 20

Figure 1.2 – The next generation hallmarks of cancer 23

Figure 1.3 – A hypoxic gradient in a solid tumour mass 25

..... 27

Figure 1.4 – An illustration of a vessel mismatch experiment 27

Figure 1.5 – Factors that influence ROS homeostasis and their consequences 33

Figure 1.6 – The impact of cyclic hypoxia on HIF signalling 37

Figure 1.7 – The effect of cyclic hypoxia on different stages in metastasis 45

Figure 1.8 – Licensing of DNA origins of replication in G1 47

Figure 1.9 – Sources of replication stress 51

..... 55

Figure 1.10 – The global role of ATR in replication stress response signalling 55

Figure 1.11 – Factors that influence RPA exhaustion and replication catastrophe 58

Figure 1.12 – Cytosine deamination reaction 63

Figure 1.13 – APOBEC viral restriction 65

Figure 1.14 – Proposed model of APOBEC3 mediated restriction of non-LTR retrotransposons

..... 69

Figure 1.15 – Consequences of genomic deamination 73

Figure 1.16 – Mutational signatures identified in human cancers 76

Figure 1.17 – Opportunities for APOBEC deamination of ssDNA 80

Figure 1.18 – Consequences of APOBEC-mediated deamination on the level of the tumour and the cell 83

Figure 3.1 – Replication stress signaling increases in chronic hypoxia (<0.1% O_2) 107

Figure 3.2 – mRNA expression of multiple APOBEC3s increases in response to HU..... 108

Figure 3.3 – mRNA expression of multiple APOBEC3s increases in response to chronic hypoxia (<0.1% O_2) 110

Figure 3.4 – mRNA induction of *A3D* and *A3H* in chronic hypoxia is HIF1 independent 112

Figure 3.5 - mRNA induction of *A3D* and *A3H* in chronic hypoxia is p53 dependent 114

Figure 3.6 – A3B expression decreases in chronic hypoxia in a p53 independent manner 116

Figure 3.7 – *In vitro* deamination assay schematic 117

Figure 3.8 – Deamination decreases in response to chronic hypoxia <0.1% O_2 118

Figure 4.1 – Chronic hypoxia and HU results in decreases in DNA replication to differing levels 125

Figure 4.2 – inhibiting new origins stops DNA replication with HU treatment but has no impact in chronic hypoxia 126

Figure 4.3 – Replication catastrophe in cells treated with HU but not chronic hypoxia..... 127

Figure 4.4 – Oxygen conditions used to model cyclic hypoxia *in vitro* 128

Figure 4.5 – Cyclic hypoxia causes replication stress that is maintained 130

Figure 4.6 – BrdU incorporation persists in cyclic hypoxia 132

Figure 4.7 – A G2 cell cycle arrest in cyclic hypoxia 133

Figure 4.8 – New origins fire in cyclic hypoxia 134

Figure 4.9 – Cyclic hypoxia causes replication catastrophe..... 137

Figure 5.1 – Cyclic hypoxia increases the expression of A3B protein 141

Figure 5.2 – Cyclic hypoxia increases APOBEC mediated deamination..... 142

Figure 5.3 – Deamination increase in cyclic hypoxia is A3B dependent 144

Figure 5.4 – No A3B dependent cell cycle effects in cyclic hypoxia..... 145

Figure 5.5 – A3B induction in cyclic hypoxia does not affect DDR signalling 146

Figure 5.6 – A3B induction in cyclic hypoxia is p53 independent..... 147

Figure 5.7 – Replication catastrophe caused by cyclic hypoxia depends on the firing of new origins 148

Figure 5.8 – A3B induction in cyclic hypoxia is dependent on new origin firing 149

Figure 5.9 – NAC abrogates replication catastrophe and A3B induction in cyclic hypoxia . 150

Figure 5.10 – A3B induction in cyclic hypoxia is NFκB dependent..... 151

Figure 5.11 – ATR treatment abrogates A3B induction and activity in cyclic hypoxia 153

Figure 5.12 – Cells treated with VX-970 in cyclic hypoxia arrest in G1 154

Figure 5.13 – Correlations between a group of hypoxia inducible p53 response genes and individual APOBEC3 genes..... 156

Figure 5.14 – Correlations between the hypoxia metagene and APOBEC mutations 157

Figure 5.15 – Correlations between the hypoxia metagene and APOBEC mutations 158

Figure 5.16 – Correlations between the hypoxia metagene and individual APOBEC3 genes 159

Figure 6.1 – Replication catastrophe induced by cyclic hypoxia leads to increased APOBEC3B activity..... 166

List of Abbreviations

A3A – APOBEC3A

A3B – APOBEC3B

A3C – APOBEC3C

A3D – APOBEC3D

A3F – APOBEC3F

A3G – APOBEC3G

A3H – APOBEC3H

ABCB1 – ATP binding cassette subfamily B member 1

AID – activation induced deaminase

APE1 – apurinic/apyrimidinic endonuclease-1

APH – aphidicolin

APOB – apolipoprotein B

APOBEC – apolipoprotein B mRNA editing enzyme, catalytic polypeptide-like

ATM – ataxia telangiectasia mutated

ATP – adenosine triphosphate

ATR – ataxia telangiectasia mutated and rad3-related protein

Bcl-xL – B-cell lymphoma extra-large

BCNU – carmustine

BER – base excision repair

BORF2 – ribonucleoside-diphosphate reductase large subunit

BrdU – bromo deoxyuridine

BSA – bovine serum albumin

CBS – clustered base substitutions

Cdc – cell division cycle

CDK – cyclin dependent kinase

CDT – chromatin licensing and DNA replication factor

CFS – common fragile site

ChIP – chromatin immunoprecipitation

Chk1 – checkpoint kinase 1

CMG – cdc45-MCM-GINS

$CoCl_2$ – cobalt chloride

CQ – chloroquine

DAPI – 4′,6-diamidino-2-phenylindole

DBS – doublet base substitutions

DDR – DNA damage response

DEPC – diethylpyrocarbonate

DFO – desferoxamine

DMEM – Dulbecco's modified Eagle's medium

DMSO – dimethylsulphoxide

DNA – deoxyribonucleic acid

DNase1 – deoxyribonuclease 1

dNDP – deoxyribonucleoside diphosphate

dNTP – deoxynucleotide

DOX – doxorubicin

DREAM – dimerization partner, RB-like, E2F and MuvB

DSB – double strand break

DSBs – double strand breaks

DTT – dithiothreitol

E2F1 – E2F transcription factor 1

EBV – Epstein-Barr virus

ECM – extracellular matrix

EDTA – ethylenediaminetetraacetic acid

eIF2α – eukaryotic translation initiation factor 2α

EMEM – Eagle's minimum essential media

EMT – epithelial to mesenchymal transfer

EPRI – electron paramagnetic resonance imaging

ETC – electron transport chain

ETP – etoposide

FBS – fetal bovine serum

GINS – Go, Ichi, Nii, and San

H2AX – H2A histone family member X

HCl – hydrochloric acid

HEPES – 4-(2-hydroxyethyl)-1-piperazineethanesulfonic acid

HIF1 – hypoxia-inducible factor

HIV – human immunodeficiency virus

HU – hydroxyurea

ID – insertion and deletion

IFN – interferon

LINE – long interspersed nuclear element

LTR – long terminal repeat

MCM – minichromosome maintenance

MEGM – mammary epithelial cell growth medium

MEPS – monocyte enriched PBMCs

MIBC – muscle invasive bladder cancer

MnTMPyP – manganese (III) tetrakis(1-methyl-4-pyridyl)porphyrin

MRI – magnetic resonance imaging

mRNA – messenger RNA

MYC – MYC proto-oncogene

NAC – N'acetylcysteine

NaCl – sodium chloride

NaOH – sodium hydroxide

NDP – ribonucleoside diphosphate

NFκB – nuclear factor kappa-light-chain-enhancer of activated B cells

NOS – nitric oxide synthase

NOX – NADPH oxidase

NRF2 – nuclear factor erythroid 2-related factor 2

NSCLC – non-small cell lung cancer

NTP – ribonucleotide

OER – oxygen enhancement ratio

ORC – origin recognition complex

PBMC – peripheral blood mononuclear cells

PBS – phosphate buffered saline

PCR – polymerase chain reaction

PET – positron electron tomography

PHD – prolyl hydroxylase domain

PI – propidium iodide

PIK3CA – phosphatidylinositol-4,5-Bisphosphate 3-Kinase Catalytic Subunit Alpha

PKA – protein kinase A

PMA – phorbol myristate acetate

Pol – polymerase

preRC – pre-replication complex

PTEN – phosphatase and tensin homolog

REV1 – REV1 DNA directed polymerase

RNA – ribonucleic acid

RNaseA – ribonuclease A

RNP – ribonucleoprotein

RNR – ribonucleotide reductase

ROS – reactive oxygen species

RPA – replication protein A

RRM2 – ribonucleotide reductase regulatory subunit M2

RT-PCR – reverse transcription polymerase chain reaction

RT-qPCR – quantitative reverse transcription polymerase chain reaction

SBS – single base substitutions

SDHB – succinate dehydrogenase B

SDS – sodium dodecyl sulphate

SINE – short interspersed nuclear element

siRNA – small interfering RNA

SLC25A1 – solute carrier family 25 member 1

SLC25A10 – solute carrier family 25 member 10

SMARCAL1 – SWI/SNF related, matrix associated, actin dependent regulator of chromatin, subfamily A-like 1

SOD – superoxide dismutase

ssDNA – single stranded DNA

T-ALL – T cell acute leukaemia

TCGA – the Cancer Genome Atlas

TLS – translesion synthesis polymerase

TMZ – temozolomide

TP – triapene

UGI – uracil glycosylase inhibitor

UNG – uracil DNA glycosylase

UPR – unfolded protein response

UV – ultraviolet

VHL – bon Hippel Lindau

VIF – virion infectivity factor

vMSOT – volumetric multispectral optoacoustic tomography

XO – xanthine oxidase

Chapter 1

Introduction

Cancer

The earliest recorded documentation of cancer dates back to almost 3000 BC, in the time of the ancient Egyptians. Unfortunately for humans at this time the prognosis for patients who developed cancer was a death sentence. The ancient Edwin Smith Papyrus soberly states that the "bulging tumour of the breast was a grave disease and there was no treatment for it" (Figure 1.1) (Feldman and Goodrich, 1999; Hajdu, 2011; Sudhakar, 2009). Cancer is very broadly defined as changes to cell physiology that lead to abnormal cell growth (neoplasia) (Seyfried and Shelton, 2010). Unfortunately, even today cancer is far from cured. Cancer is the second leading cause of death across the world with 18 million new diagnosis every year and 9.6 million deaths in 2018 (WHO, 2019).



Figure 1.1 – The Edwin Smith papyrus
This image is an excerpt from the Edwin Smith papyrus, a document written in approximately 3000 BC. The papyrus contains 48 separate medical case reports that are written on a 15-foot-long sheet of papyrus. The segment shown here details a case that scholars today believe refers to the first documented breast cancer patient. Reprinted from (Hajdu, 2011), with permission from John Wiley and Sons, License Number: 4935951436708.

Over the course of time the human race has sought to understand cancer on a higher level. A plethora of theories as to what cancer is and how it arises have been proposed over the years. The humoral theory in 1300 BC claimed that there were four bodily fluids: blood, phlegm, yellow bile, and black bile and that an imbalance between these fluids favouring black bile could cause cancer (Weinstein and Case, 2008). The trauma theory dating to the 1920s stated that cancer occurred as a result of physical tissue trauma (Ewing, 1935). More recently, the identification of oncogenes and tumour suppressors genes, genes that both promote and protect the body from cancer respectively, formed a basis for the underlying cause of cancer occurrence and progression that is still fundamental in research today (Bister, 2015; Classon and Harlow, 2002).

Today our knowledge of cancer has been advanced by the discovery of a defined set of cellular features and behaviours that are common to all cells as they transition from normal cells into cancerous tissue. These characteristics have been termed the “hallmarks of cancer” (Hanahan and Weinberg, 2000). The first 6 hallmarks of cancer were identified in the year 2000 and include sustained proliferative signalling, apoptotic resistance, replicative immortality, growth suppressor evasion, invasion and metastasis, and angiogenesis (Hanahan and Weinberg, 2000). Only 11 years later our understanding grew to include 4 new distinct hallmarks (Hanahan and Weinberg, 2011). A graphical illustration of the 10 known hallmarks of cancer highlighting the 4 new additions is shown in Figure 1.2. In addition to these hallmarks, it is becoming increasingly apparent from a therapeutic perspective that it is crucial to consider not only individual cellular behaviours, but the interplay between cells and their surrounding environment (Albini and Sporn, 2007; Hanahan and Weinberg, 2011; Petrova et al., 2018).

The environment that surrounds and influences cancer cells is referred to as the “tumour microenvironment”. The tumour microenvironment is a broad term that encompasses a variety of factors including immune cell infiltration, deregulated extracellular matrix (ECM) deposition, expanded tumour vasculature, and low oxygen regions (hypoxia) (Petrova et al.,

2018). Interplay between cells within a tumour and their surrounding environment can influence both the acquisition and impact of each of the 10 hallmarks (Hanahan and Weinberg, 2011). The tumour microenvironment is a crucial factor to consider as it can have stark implications concerning patient prognosis in a wide variety of cancer types (Albini and Sporn, 2007; Nijkamp et al., 2013; Scott and Gascoyne, 2014). Tumour hypoxia is a feature of the tumour microenvironment of particular interest due to its proven negative prognostic impact on multiple treatment modalities including radiotherapy, chemotherapy, small molecule inhibitor treatment, and immunotherapy (Bristow and Hill, 2008; Chouaib et al., 2017; Craig et al., 2020; Dewhirst et al., 2008; Ward et al., 2013). The definition and consequences associated with tumour hypoxia will be discussed in detail in the next section.

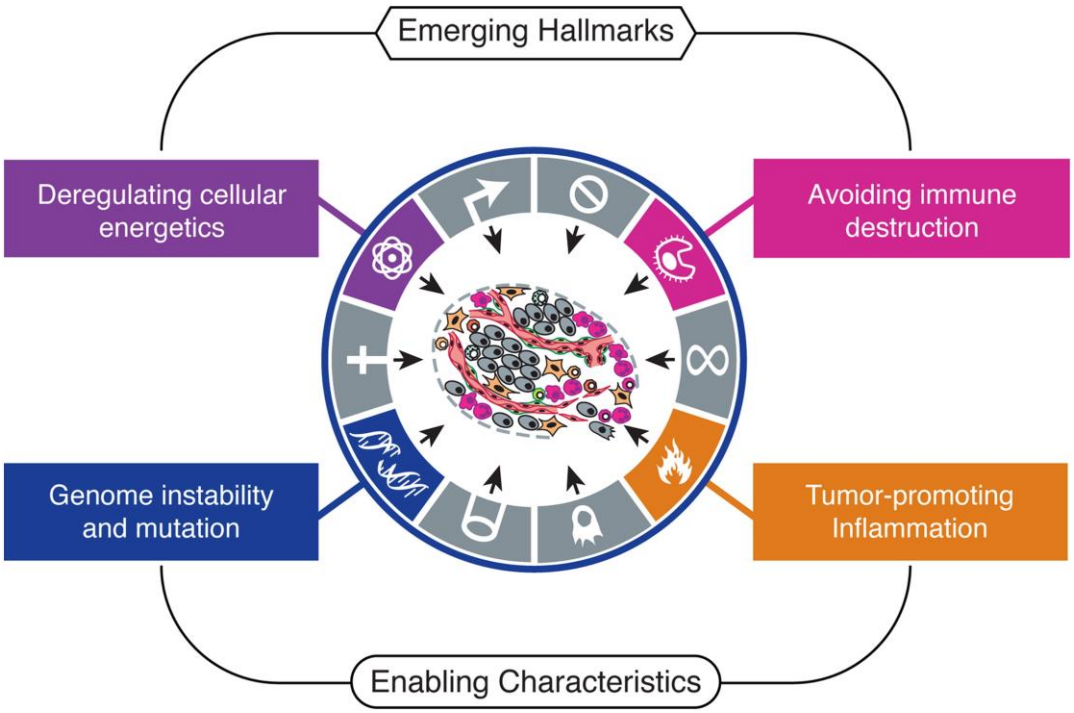


Figure 1.2 – The next generation hallmarks of cancer
The initial 6 hallmarks of cancer including proliferative signalling, apoptotic resistance, replicative immortality, growth suppressor evasion, invasion and metastasis, and angiogenesis are shown in grey. The updated hallmarks are divided into emerging hallmarks and enabling characteristics. Emerging hallmarks are newly discovered and distinct cellular behaviours that cells utilise as they transition into malignant cells. “Deregulated cellular energetics” refers to modifications to cellular metabolism that support abnormal cell growth. “Avoiding immune destruction” refers to mechanisms that protect the tumour from immune cell mediated destruction, typically by T and B lymphocytes, macrophages, or natural killer cells. Enabling characteristics primarily serve to increase the cellular adoption of the other 8 hallmarks. “Genome stability and mutation” refers to alternations to the genetic code that allow for the increased acquisition of oncogenic mutations or the increased inactivation of tumour suppressors. “Tumour-promoting inflammation” refers to the co-option of immune cell functions for the benefit of the growing tumour. Adapted and reprinted from (Alexandrov et al., 2013), with permission from Elsevier, License Number: 4935410536283.

Hypoxia and cancer

Tumour hypoxia

Oxygen has afforded humans and other complex multicellular organisms the ability to generate sufficient energy to maintain advanced biological systems (Brahimi-Horn and Pouyssegur, 2007). As such, the maintenance of sufficient tissue oxygenation is a key challenge that all aerobic organisms face. The availability of oxygen in human tissue is governed by the balance of supply and demand (Wigerup et al., 2016). For example, a mountaineer climbing Mount Everest is faced with two key challenges to maintain sufficient tissue oxygenation. Physical exertion increases tissue demand for oxygen, while the thinness of the air limits supply. In tumours, the demand for oxygen increases due to the increased metabolic demand of rapidly proliferating cancer cells, while the supply is limited by the malformed tumour vasculature (Chitneni et al., 2011; Hockel and Vaupel, 2001). Due to increased demand and decreased supply of oxygen, oxygen cannot access all tumour sections in sufficient quantities, resulting in a phenomenon known as tumour hypoxia.

The percentage of oxygen in the tumour microenvironment commonly associated with tumour hypoxia is between 0 and 6% O_2 (0-45.6 mmHg) (Vaupel et al., 2002; Vaupel et al., 1989). This range is highly contextual however as the physiological levels of oxygen in different tissues vary significantly. For example, normal arterial blood oxygenation is 13.2%, the liver is 4.1%, and the breast is 9% (Hammond et al., 2014; Koh and Powis, 2012; Vaupel et al., 2002). Importantly, hypoxia should be thought of as a gradient as opposed to a binary state. A gradient of oxygen tensions manifests as cells proliferate further and further away from the vasculature within a solid tumour. Mild (<2.0% O_2) and severe (<0.1% O_2) hypoxia have been suggested as terms to define the degree of hypoxia, as the oxygenation level can have profoundly different impacts on tumour cell biology (Bertout et al., 2008; Hammond et al., 2014). Importantly, the furthest distance where cells can access oxygen away from the blood supply is 200 μm. This distance represents the maximum measured diffusion distance of oxygen in tissue. The growth of tumour masses past 200 μm results in regions of necrosis

appearing in the core of the tumour (Figure 1.3) (Brahimi-Horn and Pouyssegur, 2007; Chitneni et al., 2011; Wilson and Hay, 2011).

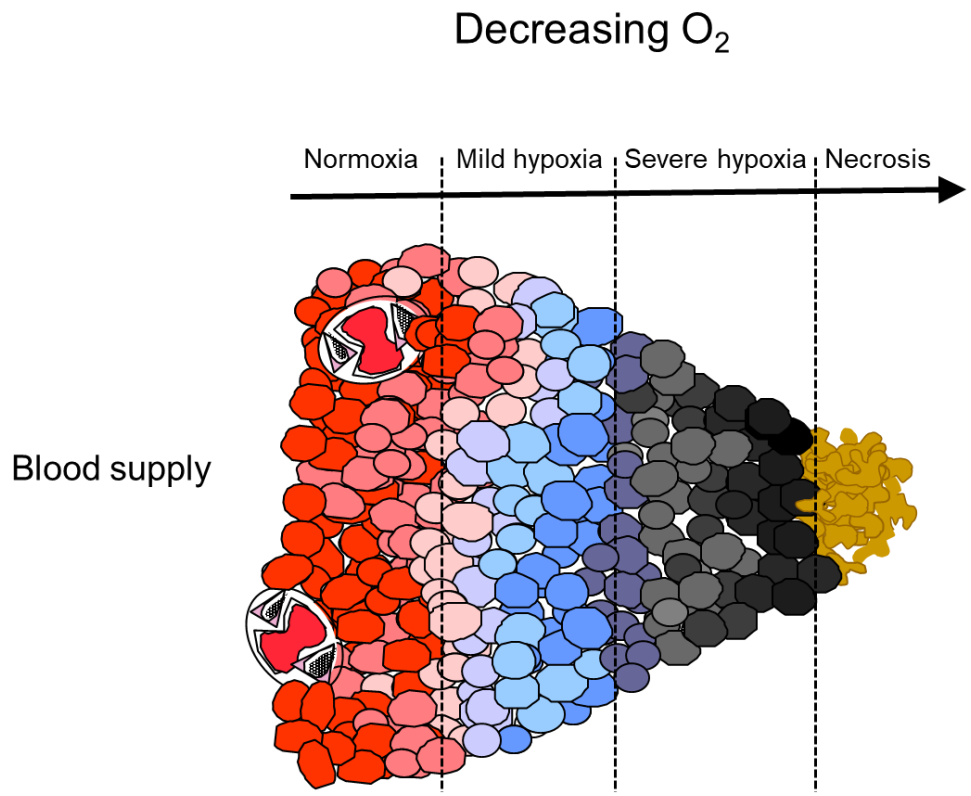


Figure 1.3 – A hypoxic gradient in a solid tumour mass
Tissue in close proximity to blood vessels is supplied with oxygen first and thus is adequately oxygenated. These regions are shown in red. Less oxygen reaches cells further away from blood vessels due to the high metabolic demand of tumour cells close to the vessels as well as the malformed vasculature providing inadequate supply. Cells further away from the blood supply can be labelled as mild or severe hypoxia and are shown in blue and black respectively. Cells furthest away from the vessels, where virtually no oxygen reaches due to the diffusion distance limit of oxygen in tissue (>200 μM), form a necrotic core shown in yellow.

Hypoxia is a relevant prognostic factor in cancer treatment as it is associated with highly aggressive tumours, poor patient prognosis, and a decrease in overall survival (Bertout et al., 2008). Unfortunately, hypoxic imaging in the clinic is seldom used in routine practice (Horsman et al., 2012; O'Connor et al., 2019). The Eppendorf needle electrode system was a promising technique that had the capability to directly measure tumour tissue oxygenation *in vivo*. Use of this technique was discontinued however due to its highly invasive nature limiting its usage to the most easily accessible tumours (O'Connor et al., 2019). Though mostly limited to occasions where it is necessary to remove the tissue of interest for other purposes, the

majority of hypoxic detection in patient tumours is currently through *ex vivo* immunohistochemical staining of biopsied tumour sections for markers associated with hypoxia (Bonnitcha et al., 2018; Chitneni et al., 2011). A key caveat of this technique is that it only provides a snapshot of tissue oxygenation. Snapshots fail to account for the highly dynamic nature of tumour hypoxia which will be discussed further in the following section.

The dynamic nature of hypoxia

The first indication of dynamic tumour oxygenation came from studies utilising animal-embedded window chambers. Window chambers are surgically implanted titanium frames that allow visualisation of the growth of xenograft tumours. Studies demonstrated that although blood flow to the growing tumour was compromised due to the malformed tumour vasculature as expected, it was also intermittent, suggesting that the amount of blood reaching the tumour and thus the amount of oxygen reaching the tumour may fluctuate (Eddy and Casarett, 1973; Goodall et al., 1965). Further work in this field utilised a vessel mismatch experiment to demonstrate that cells in close proximity to blood vessels that would normally be well oxygenated could become hypoxic (Figure 1.4). Researchers demonstrated this phenomenon utilising two different nuclear stains, Hoechst 33342 and DiOC7. Both compounds were injected into the same mouse with a 20-minute delay between one stain and the other. Each stain would stain any cells with sufficient blood perfusion to that area. Upon observation of the vasculature they noticed that the dye patterns did not overlap, suggesting that the oxygenation status of these regions had changed within the 20-minute delay in dye injection (Trotter et al., 1989). Studies suggest that the hypoxia status of approximately 20-60% of cells within solid tumour masses fluctuates (Bennewith et al., 2002; Chaplin et al., 1987; Ron et al., 2019; Yasui et al., 2010).

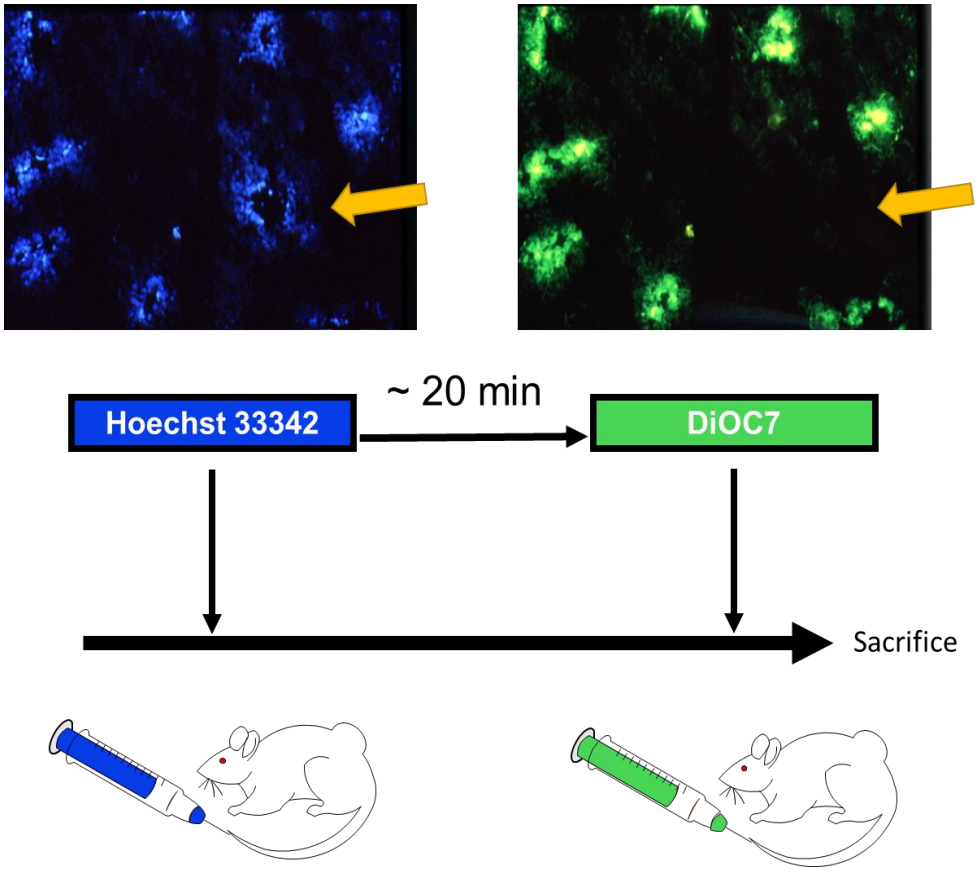


Figure 1.4 – An illustration of a vessel mismatch experiment
Two different nuclear stains, Hoechst 33342 and DiOC7, are injected into the same mouse with a 20-minute delay in between injections. The dye will stain any cells adjacent to functioning blood vessels. Importantly, the dyes will only stain these regions if the blood vessels are functional 2-3 minutes following injection. A region of interest is marked with a yellow arrow where the area was well perfused initially but became hypoxic after the 20-minute delay interval. Images of stained tumour sections were kindly provided by Professor Ester Hammond

Today the terms “cyclic hypoxia” or “intermittent hypoxia” are used to refer to dynamic changes in tumour oxygenation. Another commonly used term is “acute hypoxia” which refers to local and transient regions of hypoxia caused by perfusion issues within the tumour microenvironment. Conversely a state of hypoxia that remains static over time is referred to as “chronic hypoxia” (Bristow and Hill, 2008; Dewhirst et al., 2008; Dewhirst et al., 1996). A wide variety of imaging techniques have been utilised to measure cyclic, chronic, and acute hypoxia *in vivo* including: positron electron tomography (PET), magnetic resonance imaging (MRI), electron paramagnetic resonance imaging (EPRI), volumetric multispectral

optoacoustic tomography (vMSOT), and hyperspectral imaging (Hillestad et al., 2020; Matsumoto et al., 2010; O'Connor et al., 2019; Ron et al., 2019; Yasui et al., 2010). Studies utilising EPRI imaging in multiple xenograft tumour models have detected tumour regions with oxygen concentrations that fluctuate between 0-4.6% O_2 over the course of 30-minute intervals. Interestingly, these studies also show that in addition to areas of cyclic hypoxia, areas of chronic hypoxia can also be present in different regions of the same tumour. Regions of chronic hypoxia were found to remain under <0.5% O_2 for the duration of the 30-minute time period measured (Matsumoto et al., 2010; Yasui et al., 2010). Further studies utilising vMSOT and hyperspectral imaging support these data in terms of the magnitude and frequency of the oxygen fluctuations found in the xenograft tumour models (Palmer et al., 2010; Ron et al., 2019).

Imaging studies have also shown that the oxygen concentration in cells experiencing cyclic hypoxia fluctuates with two overlapping yet distinct periodicities. The first is a rapid cycle that has been attributed to changes in the flow rate of red blood cells in the tumour vasculature, termed red blood cell flux (Dewhirst et al., 2008). Studies concurrently measuring red blood cell flux and tumour oxygenation in xenograft models show a close association between the two. Oxygen levels were found to fluctuate with a periodicity of up to 60 minutes (Dewhirst et al., 1996; Kimura et al., 1996; Ron et al., 2019; Yasui et al., 2010). The longer frequency oxygen fluctuations occur on the order of hours to days. Studies monitoring tumour growth with window chamber xenograft models, as well as PET imaging in human patients showed stark changes in the tumour vasculature over the course of multiple days (Cao et al., 2005; Nehmeh et al., 2008). These longer cycles are hypothesised to occur due to vasculature remodelling resulting from angiogenic signalling (Dewhirst et al., 2008).

The largest challenge facing the research field of cyclic hypoxia today is the lack of applicability of the *in vitro* models used to the cyclic hypoxia conditions found in patients. Most *in vitro* models use hypoxia chambers to fluctuate oxygen concentrations in the cellular environment between two defined levels, termed here as the upper and lower bound

(Table 1.1). The use of ambient air oxygen concentrations of 21% O_2 to model the upper bound is particularly non-comparable to oxygen measurements taken from mouse and human tumours (Hillestad et al., 2020; Matsumoto et al., 2010; Ron et al., 2019; Yasui et al., 2010). A further limitation is the inability of most hypoxia chambers to cycle between oxygen tensions fast enough to mimic cycling hypoxia that occurs on the order of minutes (Dewhirst et al., 2008). Technology now exists however that is capable of rapidly cycling oxygen tensions, which can be utilised to create a more comprehensive picture of the biological responses to cyclic hypoxia (Minoves et al., 2017). In contrast, *in vivo* studies use incubation chambers for mice or rats with regulated gas supplies where the environmental oxygen tension can be fluctuated with a defined frequency (Table 1.1). These models more closely mimic clinically relevant tumour oxygenation levels as multiple studies have demonstrated physiologically relevant intratumoural oxygen tensions using intracellular oxygen probes (Cairns and Hill, 2004; Cairns et al., 2001; Hsieh et al., 2011; Kalliomaki et al., 2009; Rofstad et al., 2010).

Lack of *in vitro* clinical relevance brings up a pressing need for more physiologically relevant models of tumour hypoxia that fit within measured oxygen tensions and cycle frequencies. High variability between cyclic conditions used can also make comparison between studies difficult, however despite differing treatment conditions many common themes do seem to emerge. The remainder this section will discuss the biological consequences of hypoxia with a focus on the impact of cyclic hypoxia on tumour signalling and therapy resistance.

Cycling conditions (% O_2 and length of exposure)	**Number of Cycles**	**Ref**
1% O_2 (6.67 min) - 21% O_2 (6.67 min)	72	(Liu et al., 2016)
<0.02% O_2 (1 hr) - 21% O_2 (1 hr)	2-5	(Rouschop et al., 2013)
<0.02% O_2 (1 hr) - 21% O_2 (1 hr)	2-5	(Rouschop et al., 2009)
<0.02% O_2 (16 hr) - 21% O_2 (1 hr)	1	(Hammond et al., 2003a)
1% O_2 (1 hr) - 21% O_2 (30 min)	4	(Toffoli et al., 2009)

<1% O_2 (1 hr) - 21% O_2 (30 min)	3	(Martinive et al., 2009)
1% O_2 (2 hr) - 21% O_2 (2 hr)	1-3	(Malec et al., 2010)
0.5-1% O_2 (1 hr) - 21% O_2 (30 min)	3	(Martinive et al., 2006)
0.5-1% O_2 (1 hr) - 21% O_2 (30 min)	3	(Hsieh et al., 2010)
0.5-1% O_2 (10 min) - 21% O_2 (10 min)	12	(Hsieh et al., 2011)
0.5-1% O_2 (10 min) - 21% O_2 (10 min)	12	(Hsieh et al., 2012)
1.5% O_2 (30 s) - 21% O_2 (5 min)	60	(Yuan et al., 2008)
0.5-1% O_2 (1 hr) - 21% O_2 (30 min)	3	(Chen et al., 2015)
0.1% O_2 (24 hr) - 21% O_2 (72 hr)	20	(Liu et al., 2010b)
1% O_2 (48 hr) - 21% O_2 (24, 48, 72 hr)	1	(Schlaepfer et al., 2015)
1% O_2 (24 hr) - 21% O_2 (24 hr)	1, 5, 10	(Bhaskara et al., 2012)
1% O_2 (12 hr) - 21% O_2 (12 hr)	7	(Miao et al., 2014)
1% O_2 (12 hr) - 21% O_2 (12 hr)	5	(Zhu et al., 2014)
1% O_2 (12 hr) - 21% O_2 (12 hr)	5, 10, 15, 20	(Liu et al., 2017c)
0.5-1% O_2 (1 hr) - 21% O_2 (30 min)	3	(Chou et al., 2012)
<1% O_2 ('shots' for 8,72 hr) - 21% O_2 (n/a)	1,3/week	(Alhawarat et al., 2019)
1% O_2 (48 hr) - 21% O_2 (48 hr)	18-20	(Gupta et al., 2011)
0.1% O_2 (8 hr) - 21% O_2 (2, 4, 6, 8 hr)	1	(Liu et al., 2017b)
1% O_2 (24 hr) - 21% O_2 (24 hr)	5	(Chen et al., 2018)
<0.1% O_2 (5 min) - 7.76% O_2 (5 min)	36 or 108	(Martinez et al., 2019)
1% O_2 + nutrient deprivation (7 days) - 21% O_2 (1-3 weeks)	1-3	(Louie et al., 2010)
0.5% O_2 (1 hr) - 21% O_2 (30 min)	3	(Daneau et al., 2010)
1% O_2 (1 hr) - 21% O_2 (30 min)	4	(Delprat et al., 2020)
<1% O_2 (48 hr) - 21% O_2 (120 hr)	16 or 25	(Hlouschek et al., 2018a)
<1% O_2 (48 hr) - 21% O_2 (120 hr)	16 or 25	(Hlouschek et al., 2018b)
<0.1% O_2 (30 min or 3 hr) - 7% O_2 (30 min)	21 or 72	(Kumareswaran et al., 2015)
<0.1% O_2 (48 hr) - 21% O_2 (120 hr)	16 or 25	(Matschke et al., 2016)
1% O_2 (1 hr) - 21% O_2 (30 min)	4	(Tellier et al., 2015)
0.2 or 1% O_2 (8, 16, 24 hr) - 21% O_2 (8, 16, 24 hr)	3, 6, 50	(Verduzco et al., 2015)

7% O_2 (1 hr) - 21% O_2 (30 min)	3	(Hsieh et al., 2010)
5% O_2 (30 s) - 21% O_2 (1 min)	180/day (21 days)	(Li et al., 2018)
7% O_2 (10 min) - 21 % O_2 (10 min)	12	(Hsieh et al., 2011)
10% O_2 (~3 min) - 21% O_2 (~3 min)	80/day (7 days)	(Snyder et al., 2017)
7% O_2 (10 min) - 21% O_2 (10 min)	12/day (5/week for 6 weeks)	(Kalliomaki et al., 2008)
7% O_2 (10 min) - 21% O_2 (10 min)	6 or 12/day (5/week for 6 weeks)	(Kalliomaki et al., 2009)
7% O_2 (1 hr) - 21% O_2 (30 min)	3	(Martinive et al., 2006)
5-7% O_2 (10 min) - 21% O_2 (10 min)	12/day	(Cairns et al., 2001)
7% O_2 (10 min) – 21% O_2 (10 min)	12/day (21 days)	(Cairns and Hill, 2004)
7% O_2 (10 min) - 21% O_2 (10 min)	12	(Chen et al., 2015)
8% O_2 (10 min) - 21% O_2 (10 min)	12/day (35 days)	(Zhang et al., 2014b)
8% O_2 (10 min) - 21% O_2 (10 min)	12/day	(Rofstad et al., 2010)
7% O_2 (1 hr) - 21% O_2 (30 min)	3/day (1 day)	(Tellier et al., 2015)

Table 1.1 – Summary of published studies describing cycling hypoxia.
Studies highlighted in **grey** are *in vitro* studies which include reoxygenation to 21% O_2. Studies in **blue** are those which include reoxygenation to 21% O_2 but do not include multiple cycles i.e. a single reoxygenation event. Those in **green** are *in vitro* cyclic hypoxia studies which include cycling between two physiologically relevant oxygen concentrations. Finally, those in **orange** are *in vivo* studies and indicate the concentration of oxygen in the air the mice were given to breathe and for how long.

Reactive oxygen species (ROS)

A key biological consequence of both chronic and cyclic hypoxia that has profound influences on cell signalling as well as treatment resistance is the creation of reactive oxygen species (ROS). ROS is a broad term used to describe reactive chemical species that contain oxygen, typically generated during cellular metabolism. Two key mechanisms for ROS generation are enzymes that produce ROS as a by-product and electrons that “leak” from the electron transport chain (ETC) and subsequently interact with oxygen to form ROS (Galanis et al., 2008; Raedschelders et al., 2012). The reactive nature of ROS stems from an unpaired

electron contained in their outermost electron orbital. As reactive molecules can perturb normal cellular function, the cell tightly manages the amount of ROS produced. In addition, the cell is capable of detoxifying ROS to quench their reactivity through antioxidants such as glutathione and enzymes such as superoxide dismutase (SOD). When the amount of ROS created exceeds the amount detoxified, oxidative stress occurs. Oxidative stress results in damage to proteins, lipids, and DNA and can result in cell death (Finkel and Holbrook, 2000; Nathan and Cunningham-Bussel, 2013). Interestingly, ROS have also been implicated in signalling pathways within the cell that are critical for proliferation, host cell defence, autophagy, and stem cell differentiation (Figure 1.5) (Finkel and Holbrook, 2000; Martinez-Reyes et al., 2020; Reczek and Chandel, 2015; Sena and Chandel, 2012). A key mechanism by which ROS regulates these processes is through the modification of cysteine residues on redox sensitive proteins. For example, cysteine oxidation can negatively regulate many key regulatory phosphatases such as phosphatase and tensin homolog (PTEN), resulting in increased cellular proliferation (Koritzinsky and Wouters, 2013; Lee et al., 2002).

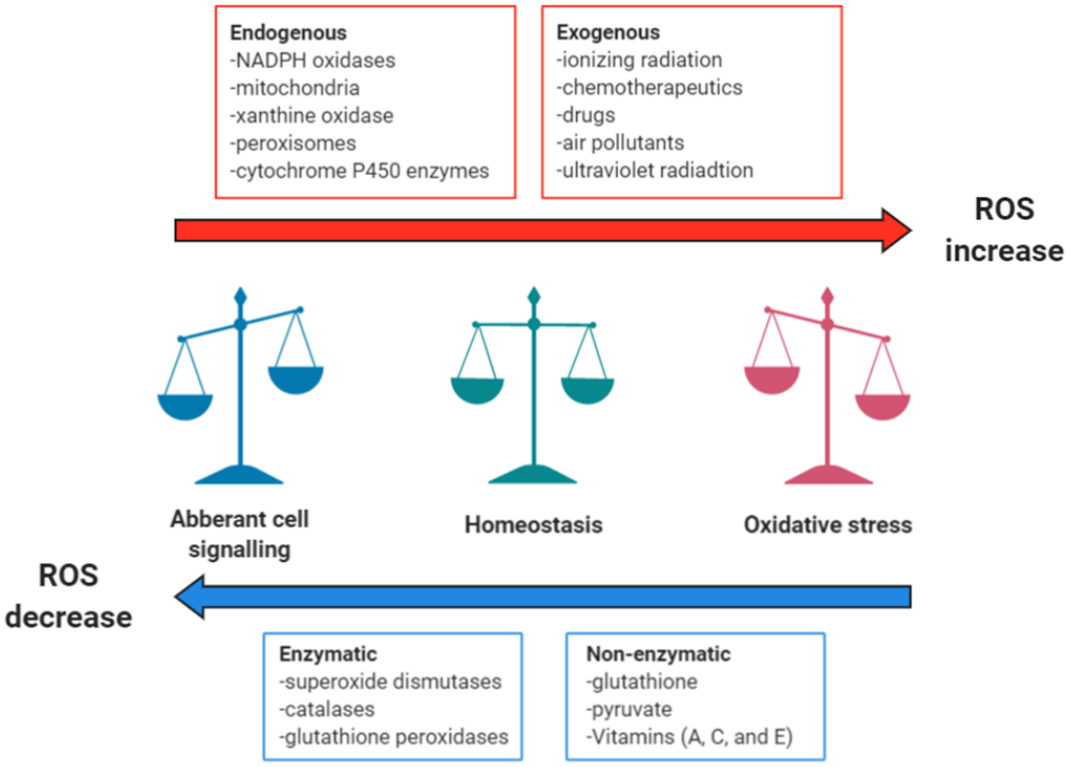


Figure 1.5 – Factors that influence ROS homeostasis and their consequences
The effects of different levels of ROS are illustrated with coloured scales. Aberrant cell signalling occurs if there is insufficient cellular ROS, while oxidative stress occurs if there is too much. A balance between ROS creation (red boxes) and ROS detoxification (blue boxes) results in homeostasis. Image created using Biorender.

Paradoxically, even with no oxygen present in the surrounding cellular environment, ROS have been shown to increase in chronic hypoxia primarily due to mitochondrial dysfunction, resulting in more electrons being released from the ETC (Bell et al., 2007; Chandel et al., 1998; Guzy et al., 2005). In addition, though not as well characterised, the expression of enzymes that produce ROS as a by-product such as NADPH oxidase 4 (NOX4) have also been shown to increase in hypoxic conditions (Li et al., 2008; Raedschelders et al., 2012). In response to reoxygenation the increase in ROS production has been extensively studied and attributed to a much wider array of phenomena including NADPH oxidase (NOX), nitric oxide synthase (NOS), and xanthine oxidase (XO) signalling, in addition to further damage to the ETC (Granger and Kvietys, 2015; Raedschelders et al., 2012). Cyclic hypoxia

has also been shown to increase levels of ROS in cancer both *in vitro* and *in vivo* (Li et al., 2018; Malec et al., 2010; Rouschop et al., 2013; Rouschop et al., 2009; Yuan et al., 2008). Correspondingly, in cyclic hypoxia an increase in the mRNA and protein expression of NOX and NOS have been shown (Hsieh et al., 2011; Hsieh et al., 2012; Malec et al., 2010; Martinive et al., 2009; Yuan et al., 2008). When compared directly, ROS have been shown to increase in cyclic hypoxia to a greater extent than in chronic hypoxia (Chen et al., 2015; Hsieh et al., 2010; Hsieh et al., 2011; Hsieh et al., 2012). To support this observation, levels of NOX4 and NOX1 mRNA and protein were measured in cyclic and chronic hypoxia *in vitro* and found to increase to a greater extent in cyclic hypoxia (Hsieh et al., 2011; Hsieh et al., 2012; Malec et al., 2010). Evidence demonstrating that the expression of NOX4 and NOX1 appreciably contributes to overall ROS levels can be seen by the fact that the increased ROS levels in cyclic hypoxia could be attenuated by the inducible knockdown of these NOX proteins both *in vitro* and *in vivo* (Hsieh et al., 2011; Hsieh et al., 2012; Malec et al., 2010).

As mentioned previously, if the amount of ROS generated exceeds the detoxification capability of the cell, then oxidative stress occurs. *In vivo* models of cyclic hypoxia have shown increases in a variety of oxidative stress markers, including increased expression of p22phox and NRF2 (Li et al., 2018; Snyder et al., 2017). As a key consequence of oxidative stress is DNA damage (Finkel and Holbrook, 2000; Nathan and Cunningham-Bussel, 2013), a variety of studies have quantified different forms of DNA damage in response to cyclic hypoxia *in vitro* and *in vivo*. Studies focusing on a single hypoxic and reoxygenation event demonstrate damage to genomic DNA in a ROS dependent manner (Hammond et al., 2003a). Other indications of DNA damage in cyclic hypoxic come from studies examining the creation of aberrant DNA bases. Guanine bases damaged by ROS are converted into 8-oxoguanine bases. An increase in 8-oxoguanine bases in cyclic hypoxia has been observed *in vivo,* although this appears to depend on the mouse model utilised (Kalliomaki et al., 2008; Kalliomaki et al., 2009; Snyder et al., 2017). Furthermore, an *in vitro* model of cyclic hypoxia utilising a comet assay to detect DNA damage, found a significant increase in cyclic hypoxia compared to normoxia (Liu et al., 2016).

In extreme cases, levels of oxidative stress can lead to intolerable levels of damage that result in cell death via apoptosis or necrosis (Finkel and Holbrook, 2000; Nathan and Cunningham-Bussel, 2013). Importantly, to facilitate cell survival in the face of oxidative stress, transcription factors such as NFκB, which stimulate pro-survival effects in oxidative stress conditions, are upregulated in cyclic hypoxia (Morgan and Liu, 2011). Multiple studies have observed increased activation of NFκB in cyclic hypoxia by measuring NFκB phosphorylation on serine 536 as well as downstream NFκB signalling targets (Delprat et al., 2020; Li et al., 2018; Tellier et al., 2015). Even with the protective effects of factors like NFκB, colony survival assays conducted in cyclic hypoxia show an overall decrease in cell viability. This decrease in cell viability is dependent on ROS as treatment with the ROS scavenging agent N'acetylcysteine (NAC) rescues cell viability (Rouschop et al., 2013; Rouschop et al., 2009).

The transcriptional response to hypoxia, HIF1

An important regulator of the hypoxic response is the HIF1 transcription factor. HIF1 is composed of two subunits, HIF1α and HIF1β. In normoxic conditions the HIF1α subunit is hydroxylated by members of the prolyl hydroxylase domain (PHD) protein family. Hydroxylation targets HIF1α for proteasomal degradation mediated by von Hippel Lindau (VHL). When stabilised in hypoxia, HIF1α binds to HIF1β which permits DNA binding to regulate the transcription of a wide variety of effector genes that manage cellular functions including metabolism, angiogenesis, growth, and apoptosis (Brahimi-Horn and Pouyssegur, 2009; Keith et al., 2011). Importantly, HIF1 is stabilised and able to activate transcription of these pathways in a wide variety of oxygen concentrations ranging from <0.1 to 3% O_2 (Dobrynin et al., 2017; Koumenis and Wouters, 2006; Schofield and Ratcliffe, 2004).

More recently, the alternate α subunits HIF2α and HIF3α have been identified as other key transcriptional regulators in hypoxia that can bind HIF1β and transactivate hypoxia response genes (Duan, 2016; Poon et al., 2009). Similar to HIF1α, HIF2α is also regulated through degradation mediated by VHL dependent hydroxylation and is rapidly stabilised in

response to hypoxia, though in a more tissue specific manner (Carroll and Ashcroft, 2006; Krieg et al., 2000). The expression of many HIF1α transcriptional targets are also transactivated by HIF2α, however HIF2α has also been shown to transactivate a distinct subset of genes (Hu et al., 2003; Raval et al., 2005; Wiesener et al., 1998). Less is known about HIF3α mainly due to the difficulties in separating the functions of the 8 different known variants that exist (Maynard et al., 2003). Interestingly, HIF3α has been shown to bind to HIF1β in a dominant negative fashion to form a non-functional transcription factor as a mechanism to negatively regulate HIF1/2α signalling (Makino et al., 2001; Makino et al., 2007).

A key regulatory component of HIF1 stability are ROS, which as previously discussed are increased in chronic hypoxia and to a greater degree in cyclic hypoxia. ROS mediate HIF1α stability by inhibiting the function of PHDs, allowing HIF1α to escape proteasomal degradation (Chandel et al., 1998; Mansfield et al., 2005; Niecknig et al., 2012) (Figure 1.6). Measurements of HIF1α protein levels consistently show that HIF1α is stabilised in cyclic hypoxia, and in all but one case is more highly expressed in cyclic compared to chronic hypoxia (Bhaskara et al., 2012; Chen et al., 2015; Daneau et al., 2010; Hsieh et al., 2010; Malec et al., 2010; Martinez et al., 2019; Martinive et al., 2009; Toffoli et al., 2009). HIF1 signalling measured through transcriptional reporter constructs also demonstrated an increase in HIF1 activity in cyclic compared to chronic hypoxia (Chen et al., 2015; Hsieh et al., 2010; Hsieh et al., 2011). Interestingly, while all of these studies used 21% O_2 as the upper oxygen bound, one study that rapidly cycled oxygen tensions every 5 minutes between <0.1-7.76% O_2 showed that while HIF expression increased in cyclic hypoxia, it accumulated to a lesser extent in cyclic than in chronic hypoxia (Martinez et al., 2019). As this study represents the sole *in vitro* study assaying for HIF stabilisation that is conducted with a physiologically relevant upper bound and rapid oxygen fluctuations, this observation requires further study. The increase in HIF1 stability and signalling in cyclic hypoxia is dependent on ROS as treatment with ROS scavenging agents such as tempol and manganese (III) tetrakis(1-methyl-4-pyridyl)porphyrin (MnTMPyP) in cyclic hypoxia abrogate the increase in HIF1 stability and

signalling (Hsieh et al., 2010; Hsieh et al., 2011; Li et al., 2018; Yuan et al., 2008). An additional mechanism by which HIF1 signalling increases in cyclic hypoxia occurs independently of HIF1 stabilisation in the nucleus. In chronic hypoxia, the cell packages a multitude of key mRNA transcripts generally associated with various stress responses, including HIF1, into cytoplasmic compartments termed stress granules (Buchan and Parker, 2009). Upon reoxygenation these stress granules disaggregate and their material is released which can amplify HIF1 downstream signalling (Moeller et al., 2004). The mechanisms by which cyclic hypoxia can influence HIF1 stabilisation and signalling are summarised in Figure 1.6.

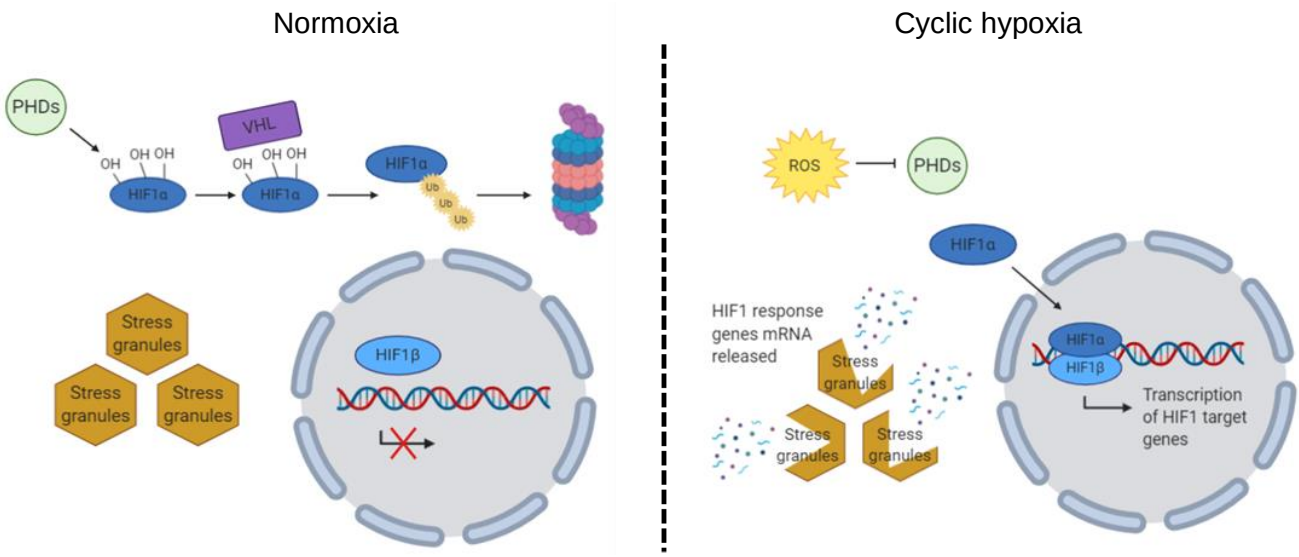


Figure 1.6 – The impact of cyclic hypoxia on HIF signalling
In normoxia HIF1α is hydroxylated by PHD enzymes, ubiquitinated by VHL, and degraded by the proteasome. Stress granules remain intact. In cyclic hypoxia ROS inhibits the function of PHDs so HIF1α can successfully enter the nucleus, bind to HIF1β, and drive the expression of HIF1 target genes. Additionally, in cyclic hypoxia stress granules disaggregate leading to the release of HIF1 response gene transcripts. Image created using Biorender.

Due to the biological complexity of HIF stabilisation and signalling, mathematical modelling has emerged as a useful way to increase our understanding of HIF biology. Though HIF dynamics in response to cyclic hypoxia have not been explicitly modelled, this strategy represents a promising way to decipher biological responses to complex variables such as oxygen concentration and cycling frequency without the need to test every condition

experimentally. By reducing the complex system that controls HIF-1 regulation to a simpler "core" system, existing biological knowledge of the interplay of the components within the core system can be used to inform the model to make predictions on situations that have not been experimentally tested (Cavadas et al., 2013). The first HIF1 modelling study utilised the HIF1 heterodimer, PHD, and VHL as its core system. This study identified switch-like responses in HIF1 signalling in response to both oxygen levels and the level of HIF1 synthesis (Kohn et al., 2004). Since then studies have modelled more complex systems such as HIF signalling within a 3D spheroid. In this study, oxygen tensions in different regions of a spheroid were measured with intracellular probes which were then used to inform the parameters of a mathematical model. A spheroid was then subjected to an *in silico* decrease in oxygen concentration from both 8 to 3% O_2 and from 21 to 1% O_2 and HIF1 activity was modelled over time. The model predicted that cells on the periphery of the spheroid would have the highest level of HIF1 signalling once exposed to hypoxia even though the core of the spheroid was initially the most hypoxic region. This somewhat counter intuitive finding was hypothesised to occur due to the relative speed of the change in oxygen concentration at the periphery of the spheroid relative to the hypoxic core, where the faster change results in a larger initial accumulation of HIF1 (Leedale et al., 2014).

Mathematical modelling has also been used to investigate the impact of a dynamic oxygen environment on different cellular characteristics. In one study, Cancer Genome Atlas (TCGA) datasets were deconvoluted based on the expression of genes known to be expressed in conditions of hypoxia or reoxygenation and divided into two distinct subpopulations. Though this study did not use any direct measures of tissue oxygenation they were able to infer how oxygenation status could influence cellular behaviours such as proliferation and angiogenesis based on the known function of genes specifically expressed in each subpopulation (Zhang et al., 2014a). Furthermore, another mathematical model created a population of cells with a continuous gradient of metabolic potentials ranging from fully oxidative to fully glycolytic to model the metabolic variation present in patient tumours. The values of these variables were then used to inform a mathematical model as to the

distribution of oxygen across the tumour and where regions of cyclic hypoxia would arise. Analysis was then carried out to determine how the subpopulations interacted with one another under the given oxygen conditions. A key finding was that in conditions where the oxygen level tended to fluctuate, a higher phenotypic variation became a competitive advantage in terms of managing oxygen consumption in a changing environment (Ardaseva et al., 2020). Finally, cross talk between HIF1 signalling and the expression of hypoxia inducible p53 apoptotic effector genes has been investigated and was found to vary according to the oxygen conditions input into the model (Bagnall et al., 2014). These studies all further the notion that distinct biological signalling occurs depending on the oxygen dynamics present in tumours and that mathematical modelling may be useful in dissecting the complex contribution of the dynamic oxygen environment to this signalling.

Radiotherapy

It has been well-established that hypoxic regions of tumours decrease the effectiveness of radiotherapy. The oxygen enhancement ratio (OER) has been described where tumours in hypoxic conditions are found to be 2.5-3 times more radioresistant than their oxygenated counterparts (Hammond et al., 2014; Horsman et al., 2012; Palcic et al., 1982). The presence of oxygen increases the effectiveness of radiotherapy as oxygen can react with DNA damage to form organic peroxides which are difficult for the cell to repair (Bertout et al., 2008). A biological component of the OER, distinct from the concentration of oxygen present during irradiation was first proposed by Shrieve and Harris. They found that cells irradiated in oxic conditions after prior treatment in longer periods of chronic hypoxic compared to shorter periods displayed increased radiosensitivity (Shrieve and Harris, 1985). Since then, multiple studies have utilised different chronic and cyclic hypoxia treatment schedules prior to irradiation under the same oxygen tension, to demonstrate a biologically relevant component of the OER that is dependent on hypoxic response signalling. Clonogenic assays demonstrate that cells pre-treated with cyclic hypoxia are radioresistant and are also more radioresistant

when compared to cells pre-treated with chronic hypoxic (Hlouschek et al., 2018a; Hlouschek et al., 2018b; Hsieh et al., 2010; Hsieh et al., 2012; Kumareswaran et al., 2015; Liu et al., 2010b; Martinive et al., 2006). This has also been confirmed *in vivo* where tumours irradiated in mice exposed to cyclic hypoxia were more radioresistant than their chronic hypoxia counterparts (Hsieh et al., 2010). As cells exposed to cyclic hypoxia have more ROS, oxidative stress, and DNA damage compared to cells exposed to chronic hypoxia, cyclic hypoxia promoting radioresistance is surprising. The elements of cell signalling in response to cyclic hypoxia that account for this surprising result will be discussed further in this section. These data demonstrate that the OER can also be affected by a biological component, distinct from the oxygen concentration at the time of irradiation and suggest that this biological component could be influenced by the hypoxic response.

HIF1 was the first identified hypoxic response factor thought to influence the OER. It was hypothesised that since a key determinant of the overall response to radiation was the sensitivity of the tumour vasculature to radiation, that the effectiveness of radiation could be improved by inhibiting a factor like HIF1 that controls downstream signalling of a variety of angiogenic factors (Garcia-Barros et al., 2003). Following from this logic, an experiment combining radiation with the HIF1 inhibitor YC-1 in a xenograft tumour model demonstrated increased radiosensitivity in the YC-1 inhibitor treated condition (Moeller et al., 2004). HIF1 has also been shown to promote radioresistance in chronic hypoxia *in vitro* through the induction of hypoxia response genes involved in cellular processes such as metabolism and cell cycle regulation (Barker et al., 2015; Harada, 2016; Hsieh et al., 2010; Liu et al., 2010a). Conversely, HIF1 targets that promote radiosensitivity have also been identified. It is not surprising however, given the diverse and numerous targets of HIF1, that a context dependent balance between HIF-mediated radiosensitivity and radioresistance is possible, although the net effect is likely radioresistance (Moeller and Dewhirst, 2006; Moeller et al., 2005). Following from the effects of HIF1 in chronic hypoxia, it was hypothesised that due to increased HIF1 stabilisation in cyclic relative to chronic hypoxia, that HIF1 could contribute to the increased

radioresistance observed in cyclic relative to chronic hypoxia (Bhaskara et al., 2012; Chen et al., 2015; Daneau et al., 2010; Hsieh et al., 2010; Malec et al., 2010; Martinez et al., 2019; Martinive et al., 2009; Toffoli et al., 2009).

In vitro and *in vivo* experiments demonstrated that the increased radioresistance in conditions of cyclic hypoxia was dependent on HIF1 signalling, as the ablation of HIF1 signalling radiosensitised cells (Hsieh et al., 2010; Liu et al., 2010b; Martinive et al., 2006). The radioprotective effect of HIF1 in cyclic hypoxia *in vivo* was thought to occur through HIF1-mediated protection of the tumour vasculature. A key observation that lead to this hypothesis was the fact that HIF1 signalling was found to increase following radiation *in vivo* but not *in vitro* (Lee et al., 2018; Moeller et al., 2004). Irradiation of cells *in vivo* has been shown to cause tumour reoxygenation resulting from decreased oxygen demand following the death of the metabolically demanding normoxic tissue (Crokart et al., 2005). In this way, radiation contributes to an increase in HIF1 signalling due to an increase in cellular ROS, akin to the mechanism of HIF1 induction in cyclic hypoxia (Dewhirst et al., 2008). Experiments testing the radioprotective capacity of HIF1 signalling demonstrated that the HIF1 signalling increase *in vivo* following irradiation protects the tumour vasculature from radiation induced damage. HIF1 mediated protection of endothelial cells could also be demonstrated *in vitro* (Martinive et al., 2006; Martinive et al., 2009; Moeller et al., 2004; Toffoli et al., 2009).

More recently, proteins associated with tolerance to oxidative stress have been implicated in the increased radioresistance of cells in cyclic hypoxia. Eukaryotic translation initiation factor 2α (eIF2α) has been identified as a factor that can influence the OER in hypoxic contexts (Rouschop et al., 2013). eIF2α is typically associated with the unfolded protein response (UPR), though it also plays a role in regulating the expression of enzymes involved in the synthesis of key antioxidants such as glutathione and cysteine. Inhibition of eIF2α, using a doxycycline inducible construct preventing eIF2α phosphorylation and downstream signalling, leads to increased radiosensitivity *in vivo* (Rouschop et al., 2013). Though cyclic hypoxia was neither directly measured with a probe, nor artificially created with regulated gas

supplies, the presence of cyclic hypoxia in xenograft tumours was inferred from analysis of pimonidazole positive and negative tumour regions. Interestingly, radiosensitisation only occurred if eIF2α was inhibited prior to irradiation, likely due to the role of eIF2α in mediating the cellular response to ROS. Inhibition of eIF2α prior to irradiation rendered cells incapable of managing the increased ROS generated by irradiation-induced reoxygenation. Supportive *in vitro* experiments showed that cell death caused by cyclic hypoxia increased further if eIF2α was inhibited, and that this depend on the presence of ROS. Furthermore, enzymes involved in the creation of the antioxidants glutathione and cysteine were shown to increase in cyclic hypoxia in an eIF2α dependent manner (Rouschop et al., 2013). Many other studies have also shown an upregulation of proteins that increase cellular antioxidant capabilities in response to cyclic hypoxia including solute carrier family 25 member 10 (SLC25A10) and solute carrier family 25 member 1 (SLC25A1) (Hlouschek et al., 2018a; Hlouschek et al., 2018b; Matschke et al., 2016). Supporting the notion that proteins contributing to the oxidative stress response in cyclic hypoxia contribute to radioresistance, SLC25A10 and SLC25A1, amongst others, have also been shown to directly contribute to the radioresistant nature of cyclic hypoxia (Hlouschek et al., 2018a; Hlouschek et al., 2018b; Hsieh et al., 2012; Matschke et al., 2016).

Autophagy is also likely a pathway that could impact the OER in hypoxic conditions though it has not yet been formally tested. Autophagy is a pathway involved in digestion of cellular components as a means for cell survival in adverse conditions (Koritzinsky and Wouters, 2013). It has been shown that the decrease in cell viability in cyclic hypoxia can be exacerbated through treatment with chloroquine (CQ), an inhibitor of autophagy. Autophagy is thought to protect cells in cycling hypoxia through the promotion of mitophagy which would lessen the amount of ROS produced through the ETC (Rouschop et al., 2009). Inhibiting autophagy in combination with irradiation in cyclic hypoxia would be an interesting direction of future study.

Chemotherapy

Hypoxic tumours demonstrate increased chemoresistance due to a variety of factors including: large diffusion distances from blood vessels, decreased cellular drug uptake, decreased apoptosis, altered pH, and decreased proliferation (Bristow and Hill, 2008; Cosse and Michiels, 2008). Many of these chemoresistant features are mediated by HIF-1 signalling (Cosse and Michiels, 2008; Monti and Gariboldi, 2011). Increased drug efflux and apoptotic resistance have been studied in the context of cyclic hypoxia and were demonstrated to contribute to a higher chemoresistance than cells treated in chronic hypoxia (Chen et al., 2015; Chou et al., 2012).

In cyclic hypoxia, a HIF1 dependent mechanism resulted in the upregulation of the cell membrane efflux pump, ATP Binding Cassette Subfamily B Member 1 (ABCB1). Cells in cyclic hypoxia demonstrated an increased capacity to efflux the chemotherapeutic drug Rh123 compared to cells in chronic hypoxia in an ABCB1-dependent manner. This ability to efflux chemotherapy drugs in cyclic hypoxia translated into increased resistance of glioblastoma cells to doxorubicin and carmustine (BCNU) *in vitro* (Chou et al., 2012). Cells in cyclic hypoxia also demonstrated an increased ability to resist apoptosis in response to chemotherapeutics. The anti-apoptotic gene, B-cell lymphoma extra-large (Bcl-xL), was shown to be upregulated to a greater extent in cyclic hypoxia compared to chronic hypoxia in a HIF-1 dependent manner (Chen et al., 2015; Gupta et al., 2011). Treating cells in cyclic hypoxia with temozolomide (TMZ) combined with Bcl-xL inhibition resulted in increased cell kill compared to TMZ alone. Interestingly, Bcl-xL upregulation was also found to occur in a ROS-dependent manner in cyclic hypoxia. Consequently, *in vivo* ROS scavenging with Tempol increased the effectiveness of TMZ treatment (Chen et al., 2015). Furthermore, exposure to a course of cyclic hypoxia spanning 50 days led to selection for loss of the p53 tumour suppressor gene. Loss of p53 translated into increased survival of sub clones from the cells treated in cyclic hypoxia compared to normoxia when treated with the chemotherapeutic etoposide (Verduzco et al., 2015).

Metastasis

Metastasis is the formation of secondary malignant growths in the body at distant sites from the primary tumour (Chambers et al., 2002). Understanding the processes that contribute to metastasis is essential as the vast majority of deaths from cancer result from metastatic growth (Steeg, 2016). To metastasise, cancer cells must undertake a variety of rate-limiting steps including: the epithelial to mesenchymal transfer (EMT), invasion and migration out of the basement layer, survival in blood circulation, and the ability to proliferate in the target location (Chambers et al., 2002; Lu and Kang, 2010; Rankin and Giaccia, 2016). The tumour microenvironment has been shown to contribute to multiple steps in the progression of metastasis (Joyce and Pollard, 2009). Hypoxia in particular aids cancer cells in completing these steps primarily through HIF1 signalling (Lu and Kang 2010) (Rankin and Giaccia 2016). Utilising regulated gas supplies to modulate the oxygen level in the environment of mice with xenograft tumours, it has been demonstrated that mice treated with cyclic hypoxia develop more metastasis than mice exposed to normal oxygen conditions. (Cairns and Hill, 2004; Li et al., 2018; Rofstad et al., 2010; Zhang et al., 2014b). Additionally, studies that have compared the ability of tumours to form metastasis in xenograft mice treated with cyclic and chronic hypoxia show that tumours from mice treated with cyclic hypoxia have more metastatic growths (Cairns et al., 2001; Chen et al., 2018; Daneau et al., 2010; Rofstad et al., 2007). The effect of cyclic hypoxia on the cellular abilities required to successfully metastasise are summarised in Figure 1.7.

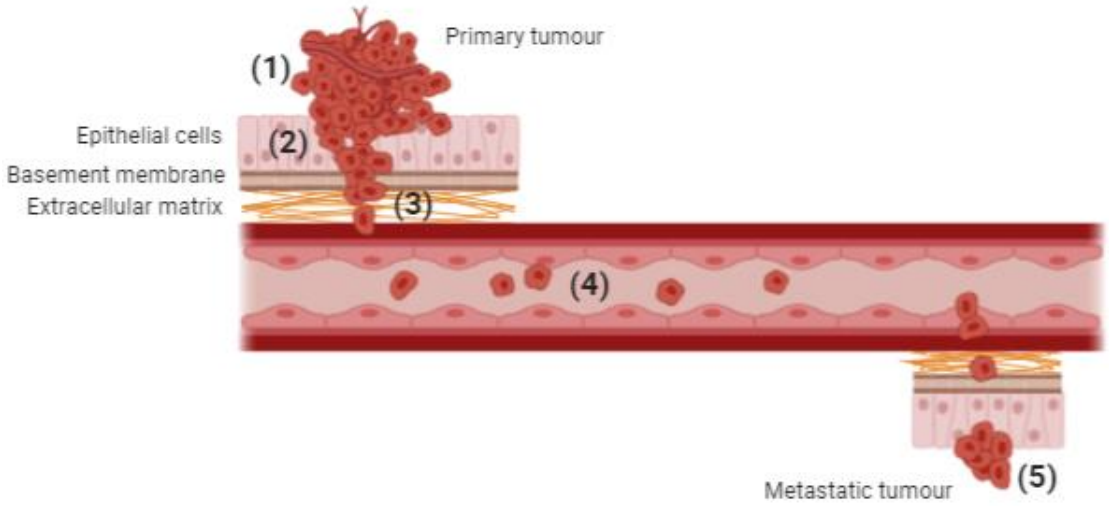


Figure 1.7 – The effect of cyclic hypoxia on different stages in metastasis
Cells treated in cyclic hypoxia in each of these studies demonstrated an increased capability for each of these processes crucial to metastasis.

(1) – EMT/stemness: (Bhaskara et al., 2012; Chen et al., 2018; Gupta et al., 2011; Louie et al., 2010; Miao et al., 2014; Zhu et al., 2014)

(2) – Invasion/migration: (Alhawarat et al., 2019; Liu et al., 2017c; Miao et al., 2014; Schlaepfer et al., 2015; Zhu et al., 2014)

(3) – ECM modulation: (Gutsche et al., 2016)

(4) – Survival in blood circulation: (Daneau et al., 2010)

(5) – Proliferation in target organ: (Cairns and Hill, 2004; Cairns et al., 2001; Chen et al., 2018; Daneau et al., 2010; Li et al., 2018; Rofstad et al., 2007; Rofstad et al., 2010; Zhang et al., 2014b). Image created using Biorender.

Replication stress

DNA Replication

DNA replication is a tightly regulated and highly conserved process in eukaryotes. Faithful replication is crucial to ensure that the important information contained within the genomic sequence of a cell is maintained upon cell division. Mis-regulation of DNA replication can lead to under or over replication of genetic material, mutation, or cell death in extreme cases (Gaillard et al., 2015; Mechali, 2010). Regulation of DNA replication occurs in two key phases: the licensing of origins of replication and the activation of a subset of those origins.

The licensing of origins accomplishes two main goals. The first is to select the locations in the genome where replication forks will originate. The second is to form a scaffold for the helicase complex that will be responsible for unwinding the DNA duplex ahead of the DNA polymerases. Origin licensing begins in the G1-phase of the cell cycle. It is crucial that the licensing of origins occurs before the DNA is replicated in S-phase so that no new origins can be licensed once DNA replication has begun. This ensures that no section of the DNA can be replicated more than once which could result in gene duplications or larger order chromosomal rearrangements (Blow et al., 2011; Gaillard et al., 2015).

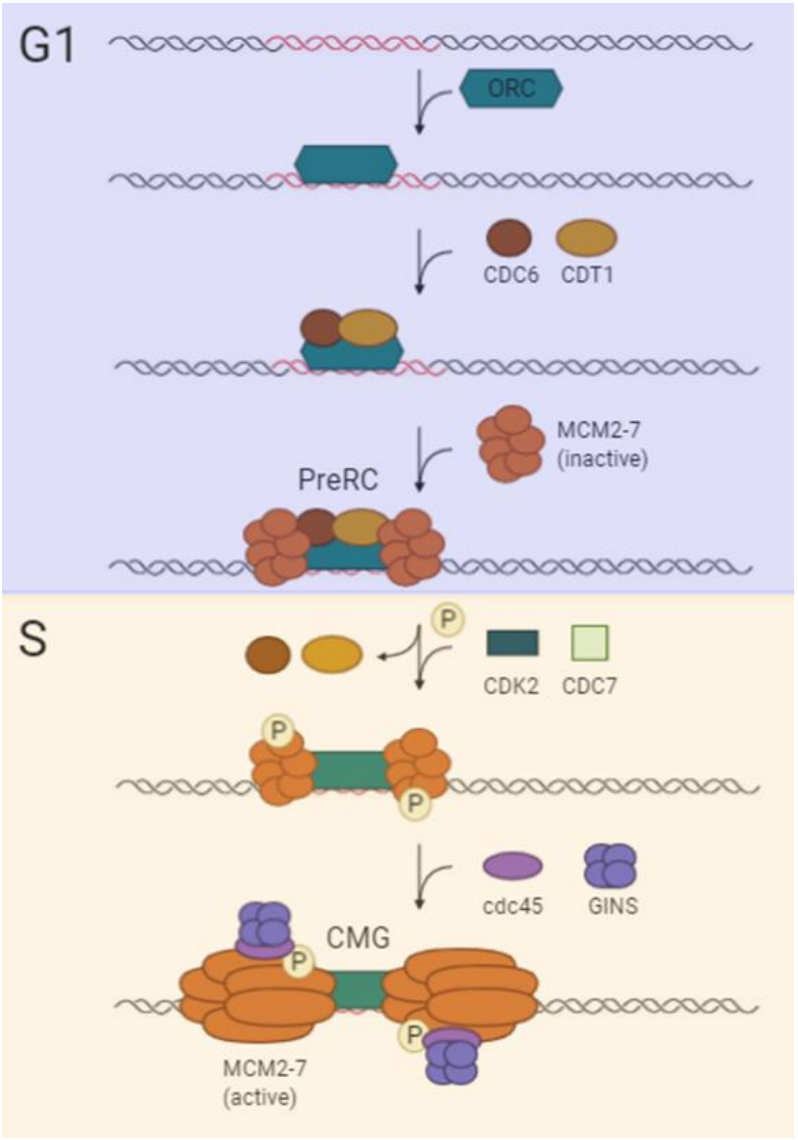


Figure 1.8 – Licensing of DNA origins of replication in G1
The red section of the DNA duplex represents the area designated to be licensed for replication. ORC initially binds to this area, however how this area is selected is largely unknown. Cdc6, CDT1, and the inactive MCM2-7 helicase bind to ORC and form the pre-replication complex (preRC). cdc6 and CDT1 dissociation from ORC, along with phosphorylations from CDK2 and Cdc7 allow cdc45 and GINS to bind ORC and form the cdc45-MCM-GINS (CMG) complex. The CMG complex features an activated MCM2-7 complex capable of unwinding DNA in S-phase. The blue box denotes events that occur in the G1-phase of the cell cycle while the orange box denotes events that occur in S-phase. Image created using Biorender.

Origin licensing

A graphical illustration of origin licensing is included in Figure 1.8. To begin licensing, the origin recognition complex (ORC) binds to specific locations in the genome. How ORC selects regions of the genome to become replication origins is still largely unknown, although AT rich regions of DNA seem to be preferred (Kong et al., 2003; Wang et al., 2006). Following ORC binding to the DNA, two proteins, cell division cycle 6-related protein kinase (cdc6) and chromatin licensing and DNA replication factor-1 (CDT1) are recruited, which load the minichromosome maintenance protein (MCM) 2-7 helicase complex onto the DNA (Evrin et al., 2009; Remus et al., 2009). The MCM2-7 complex is a hexameric complex consisting of 6 similar yet distinct subunits that can unwind the DNA duplex in an adenosine triphosphate (ATP) dependent manner when activated. Once the MCM2-7 complex is recruited, the complex is termed the pre-replication complex (preRC) (Gaillard et al., 2015; Mechali, 2010). A G1 licensing checkpoint exists where if insufficient origins are licensed then the cell arrests in G1 until it has licensed more. The G1 licensing checkpoint is a critical step in the regulation of DNA replication as cells that are terminally differentiated or moving into G0 lose the ability to license origins. Multiple cancers have been shown to have mutations that allow origins to be licensed without the proper regulatory signals (Blow et al., 2011).

Upon entry into S-phase, cdc6 and CDT1 dissociate, and preRCs are activated via phosphorylation by cyclin dependent kinase 2 (CDK2) and cdc7 (Zou and Stillman, 2000). These phosphorylations are key events to ensure the MCM2-7 complex is activated only once the cell moves into S-phase (Gaillard et al., 2015). Origin firing is a largely stochastic process as not much is known about how CDK2 and cdc7 select origins to fire. It has been observed however that groups of origins tend to fire in different periods in S-phase, classified as early, mid, and late firing origins (Aparicio et al., 1999; Zeman and Cimprich, 2014). CDK2 and cdc7 dependent phosphorylations allow the binding of Cdc45 and the Go, Ichi, Nii, and San complex (GINS) which modifies the conformation of MCM2-7 around the DNA strand and activates the helicase activity of the complex. The complex is now referred to as the cdc45-MCM-GINS (CMG) complex (Ilves et al., 2010). The CMG complex then proceeds to bi-directionally

unwind the DNA duplex. This allows the polymerases access to the DNA to begin replication. DNA polymerase (Pol) α primes the DNA and the polymerases Pol ε and Pol δ synthesise new DNA on the leading and lagging strand respectively (Gaillard et al., 2015; Mechali, 2010). Upon successful completion of replication, the cell will proceed into the G2-phase of the cell cycle and prepare for mitosis.

An abundance of licensed origins

During the process of DNA replication, mammalian cells license approximately 500,000 replication origins (Ge et al., 2007; Woodward et al., 2006). DNA replication originating from multiple origins is a strategy the cell utilises to replicate its genome more efficiently. If replication started from one origin, then S-phase alone would take upwards of 20 days to complete (Mechali, 2010). Interestingly, it has been shown that the cell only fires approximately 10-30% of the origins that it initially licenses in G1 (Moiseeva and Bakkenist, 2019). The cell manages the amount of origins that fire in S-phase through limiting the supply of factors required to fire licensed origins, such as CDK2 and cdc7, as these proteins are not abundant enough to fire all origins simultaneously (Mechali, 2010).

The strongest evidence demonstrating the need for an excess of licensed origins comes from experiments where levels of MCM proteins are experimentally modulated. Hypomorphic MCM protein mutations that decrease MCM protein expression without eliminating expression entirely can serve to limit the number of origins that are licensed without disrupting the process of DNA replication. This creates a scenario where origins are not licensed in excess and the effects can be studied. Two such models have been described, utilising MCM2 or MCM4 hypomorphic mutations in both mice and yeast (Pruitt et al., 2007; Shima et al., 2007). Yeast cells grown with a MCM4 hypomorphic mutation developed significantly more chromosome breaks than the wild type. Additionally, cells isolated from mice grown with MCM2 or MCM4 hypomorphic mutations show a significant increase in the formation of micronuclei and phosphorylation of H2A histone family member X (γH2AX) foci

compared to cells from a control mouse, indicating genome instability and DNA damage respectively. Finally, mice grown with hypomorphic MCM2 or MCM4 mutations exhibited the spontaneous occurrence of mammary adenocarcinomas and B/T cell lymphomas respectively (Pruitt et al., 2007; Shima et al., 2007).

It is important to consider that in both of these studies the mechanism of DNA replication itself was unperturbed by MCM2 and MCM4 knockdown, as origins were still successfully licensed (Pruitt et al., 2007; Shima et al., 2007). This begs the question of why decreasing the number of origins can lead to DNA damage and genome instability if DNA replication is still functioning normally? The accepted hypothesis is that decreasing the number of licensed origins renders the cell incapable of managing issues that arise during DNA replication (Kawabata et al., 2011; Klotz-Noack and Blow, 2011; Woodward et al., 2006). Normally facing a replication issue, the cell can re-start replication from a new origin to continue replicating DNA. In these two hypomorphic MCM models this is not possible due to the fact that there is no excess of origins (Pruitt et al., 2007; Shima et al., 2007). In support of this hypothesis, factors that directly interfere with DNA replication combined with a limited number of licensed origins result in more severe genomic instability and DNA damage phenotypes. For example, the number of micronuclei in cells with the MCM4 hypomorphic mutation significantly increased when cells were treated with hydroxyurea (HU), a compound that can interfere with DNA replication through the inhibition of nucleotide synthesis (Shima et al., 2007). Furthermore, treatment with non-toxic levels of HU results in cell death if MCM proteins are inhibited concurrently (Ge et al., 2007; Woodward et al., 2006). These data highlight the need for an excess of licensed origins to deal with perturbations to DNA replication and also introduce the concept of replication stress.

Replication stress

Replication stress is defined as conditions which stall or impede active DNA replication forks (Figure 1.9) (Puigvert et al., 2016; Zeman and Cimprich, 2014). The mechanism of ssDNA accumulation is typically ascribed to the CMG complex continuing to unwind DNA while

the polymerase is obstructed or stalled (Byun et al., 2005; Pacek and Walter, 2004). Replication stress is present to some degree in the majority of human cancers and has recently been classified as a hallmark of cancer (Macheret and Halazonetis, 2015). The causes of replication stress can be both endogenous and exogenous and have been grouped into 4 major categories, including aberrant origin firing, physical impediments to the replication fork, conflicts between replication and transcription machinery, and replication under inappropriate metabolic conditions (Magdalou et al., 2014). Many sources of replication stress could however fall into more than one of these 4 categories.

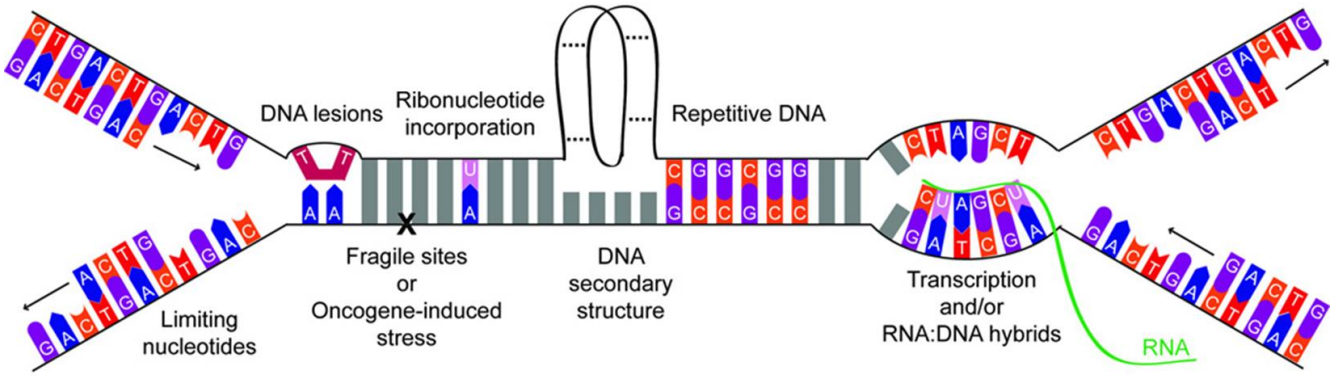


Figure 1.9 – Sources of replication stress
Many factors can interfere with the DNA replication machinery and cause replication stress, resulting in the accumulation of ssDNA. Sources of replication stress include DNA lesions, ribonucleotide incorporation, repetitive stretches of DNA, limited quantities of nucleotides, fragile sites, oncogene-induced stress, DNA secondary structures, and transcription/RNA:DNA hybrids. Adapted and reprinted from (Zeman and Cimprich, 2014), with permission from Nature Publishing Group, License Number: 4939430815514.

Aberrant origin firing causing an increased number of active forks can cause replication stress through the exhaustion of key resources required to complete DNA replication. For example, if too many origins fire simultaneously, then nucleotides quickly become the limiting factor and replication stalls (Beck et al., 2012; Bester et al., 2011; Poli et al., 2012). In addition, each replication fork requires the recruitment and coordination of over 50 factors. Too many active forks can quickly deplete cellular stocks of necessary replication factors, and impede

the faithful completion of replication (Mantiero et al., 2011). In contrast, a decrease in the number of active forks can also cause replication stress. This concept can be seen in areas of genome that naturally take much longer to replicate, termed common fragile sites (CFS) (Le Tallec et al., 2011; Letessier et al., 2011). CFSs take longer to replicate due to the demonstrated lack of replication origins that form in these regions (Zeman and Cimprich, 2014). Fewer origins render the cell unable to manage issues that arise during DNA replication, where normally replication could be restarted from a new origin. The hypomorphic MCM2 and MCM4 mutants discussed earlier are also an example where a lack of licensed replication origins leads to replication stress (Pruitt et al., 2007; Shima et al., 2007).

Physical impediments to the replication machinery are obstacles that stall or slow the DNA polymerase or CMG complex (Labib and Hodgson, 2007). These obstacles can be created by exogenous stresses, but interestingly can also arise due to normally occurring cellular events and structures (Mirkin and Mirkin, 2007). Examples of exogenous agents that result in replication stress include ultraviolet (UV) light, chemotherapeutics, irradiation, and cigarette smoke (Ciccia and Elledge, 2010). An example of a naturally occurring impediment to DNA replication can be a specific DNA sequence, such as a trinucleotide repeat, that can be predisposed to the formation of secondary structures (Lambert and Carr, 2013; Mirkin and Mirkin, 2007). Additionally, the misincorporation of ribonucleotides can also serve as a naturally occurring barrier to replication (Zeman and Cimprich, 2014).

The accumulation of ssDNA associated with replication stress has a variety of cellular consequences. Long stretches of ssDNA can be mutagenic as they can be cleaved by endonucleases causing chromosome breakages (Lopes et al., 2006). In addition, exposed ssDNA bases can be targeted by cellular deaminases resulting in point mutations or larger chromosomal arrangements depending on the distance between mutations (Alexandrov et al., 2013). To avoid more severe mutagenic outcomes the cell has specialised polymerases, termed translesion synthesis polymerases (TLS) that can replicate over a DNA lesion such as a long stretch of ssDNA. TLS polymerases are highly error prone however and induce significant numbers of point mutations (Mailand et al., 2013). In extreme cases replication

stress can lead to incomplete DNA synthesis which can yield negative outcomes upon entry into mitosis, including larger order chromosomal rearrangement and cell death (Magdalou et al., 2014).

Responses to replication stress

In the presence of replication stress, cells use a variety of signalling pathways to attempt to faithfully complete DNA replication and to avoid the negative consequences caused by sustained replication stress (Ciccia and Elledge, 2010; Gaillard et al., 2015). The most well characterised response to replication stress is the ataxia telangiectasia and Rad3 related (ATR) signalling pathway (Blackford and Jackson, 2017). When ssDNA is exposed in the nucleus it is rapidly bound by replication protein A (RPA) (Wold, 1997). RPA then serves as a template for the recruitment of ATR-interacting protein (ATRIP) which localises ATR to an ssDNA region where the ATR kinase can then initiate downstream signalling through the phosphorylation of target proteins (Zou and Elledge, 2003). The roles of ATR in mediating replication stress can be thought of as global effects that impact cell-wide processes, and local effects that stabilise individual replication forks (Blackford and Jackson, 2017; Magdalou et al., 2014; Zeman and Cimprich, 2014).

The global response to replication stress is primarily mediated through the Chk1 kinase. A graphical illustration of the roles of ATR/Chk1 in replication stress signalling is shown in Figure 1.10. The function of this signalling pathway is three-fold. Firstly, to inhibit the firing of new origins through the inhibition of CDK2 to provide the cell time to remedy the underlying issues causing replication stress (Buisson et al., 2015; Feijoo et al., 2001; Heffernan et al., 2002; Syljuasen et al., 2005). As discussed previously, CDK2 is one of two kinases that are required for the activation of licensed origins in S-phase, and thus inhibition of CDK2 delays the firing of late origins. The mechanism of Chk1 mediated inhibition of CDK enzymes is via the proteasomal degradation of cdc25A. cdc25A is a phosphatase that functions to remove inhibitory phosphorylations from CDK enzymes to promote their activity. Thus increasing

cdc25A degradation represses the enzymatic function of CDKs (Bartek et al., 2004). Secondly, Chk1 mediated CDK2 inhibition promotes the expression of the ribonucleotide reductase regulatory subunit M2 (RRM2) subunit of ribonucleotide reductase (RNR) to increase the production of deoxyribonucleotide triphosphates (dNTPs) needed for replication. Normally CDK2 restricts RRM2 expression through inactivating phosphorylations on the E2F transcription factor 1 (E2F1) transcription factor which promotes RRM2 expression (Buisson et al., 2015). Finally, the last major role of Chk1 in replication stress signalling is the imposition of a G2 cell cycle arrest via the inhibition of CDK1 (Jackson et al., 2000; Liu et al., 2000). CDK1 is also inhibited via Chk1 mediated cdc25A proteasomal degradation. A G2 cell cycle arrest ensures that the cell does not mitose before its genetic material has been faithfully duplicated.

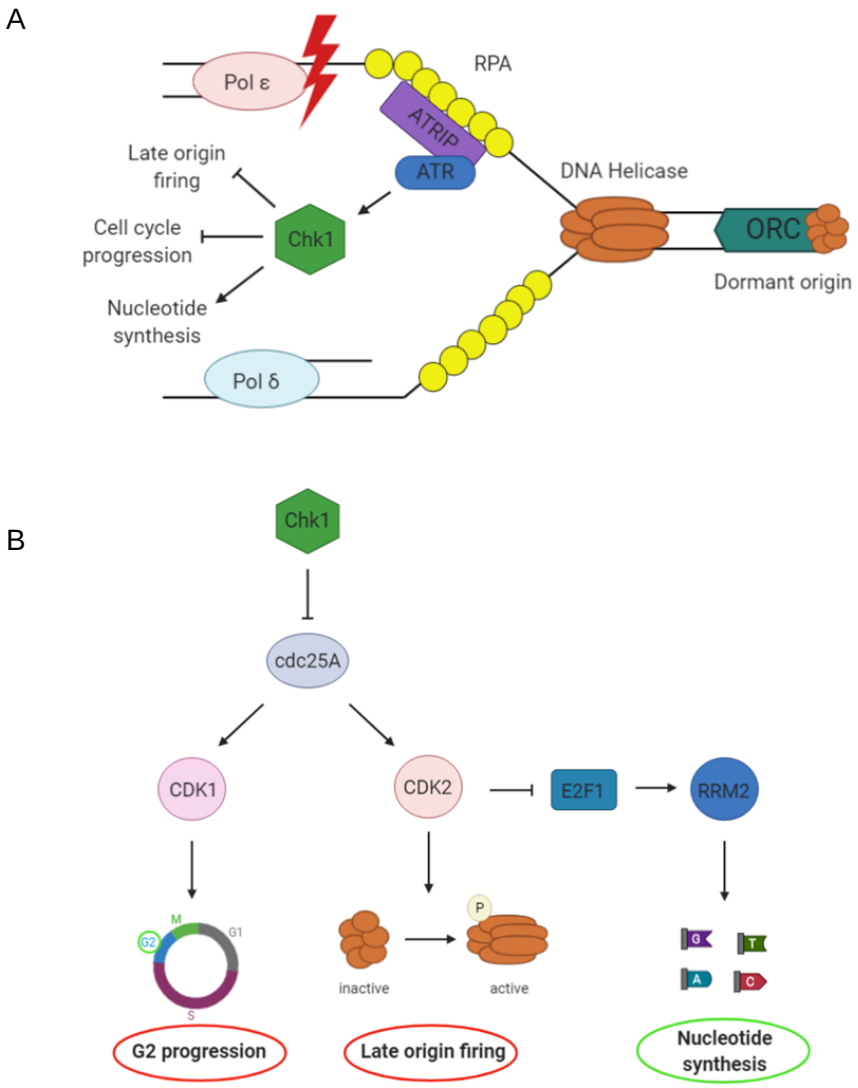


Figure 1.10 – The global role of ATR in replication stress response signalling

(A) A situation is depicted where the DNA polymerase has been stalled by a lesion on the DNA (red lightning) resulting in replication stress. While the polymerase stalls until the damage is fixed, the helicase proceeds to unwind the DNA, resulting in an accumulation of ssDNA. RPA then binds to the ssDNA, and ATRIP binds to the RPA recruiting the ATR kinase. ATR phosphorylates Chk1 which can then mediate the global functions of ATR replication response signalling including blocking late origin firing, blocking cell cycle progression, and promoting nucleotide synthesis. Image created using Biorender.

(B) An enhanced view of the roles of Chk1 in mediating the global response to replication stress. Chk1 phosphorylates cdc25A, targeting it for proteasomal degradation. In the absence of Chk1, cdc25A has a variety of functions associated with promoting DNA replication. Cdc25A removes inhibitory phosphorylations from CDK1 and CDK2 to maintain cell cycle progression and the firing of late origins of replication respectively. CDK2 additionally inhibits the E2F1 transcription factor, which normally promotes the expression of RRM2, a subunit of RNR required for nucleotide synthesis. Red and green circles denote cellular functions that Chk1 inhibits and promotes respectively when replication stress is present. Image created using Biorender.

The importance of Chk1 in the replication stress response has been demonstrated in experiments that ectopically increase or decrease the level of Chk1 (Lam et al., 2004; Lopez-Contreras et al., 2012). Mouse cells with an extra copy of Chk1 showed improved colony survival upon treatment with the replication stress inducing agents HU and aphidicolin (APH), demonstrating an improved capability of managing replication stress (Lopez-Contreras et al., 2012). Conversely, conditional Chk1 deletion in mouse mammary cells resulted in a slower completion of S-phase and increased DNA damage, even in the absence of an exogenous replication stress inducing agent, due to a decreased capacity to manage endogenous replication stress (Lam et al., 2004).

The local function of ATR at individual replication forks was first suggested stemming from experiments in yeast where ATR was shown to directly phosphorylate a variety of proteins present at stalled replication forks (Lopes et al., 2001; Tercero and Diffley, 2001). In mammalian cells, SWI/SNF related, matrix associated, actin dependent regulator of chromatin, subfamily A-like 1 (SMARCAL1) has been proposed to regulate the stability of individual replication forks in an ATR dependent manner (Couch et al., 2013). SMARCAL1 is a replication fork remodelling protein that stabilises and protects stalled replication forks (Betous et al., 2012). If left unregulated however, SMARCAL1 dependent remodelling can expose the replication fork to cleavage by the SLX4/MUS81 nuclease complex (Couch et al., 2013; Forment et al., 2011). ATR phosphorylates SMARCAL1 on serine 652 to limit its fork remodelling functions and thus protects the fork from nuclease mediated cleavage (Couch et al., 2013).

RPA Exhaustion

Recently, the concept of RPA exhaustion has been proposed as a link that unifies the global and local functions of ATR and other mediators of replication stress (Toledo et al., 2017; Toledo et al., 2013). RPA exhaustion occurs when the amount of ssDNA present in the cell exceeds the amount of free RPA that is capable of binding ssDNA. Naked ssDNA has been

demonstrated to be prone to massive fork breakage events in a phenomenon termed “replication catastrophe” (Brown and Baltimore, 2003; Nghiem et al., 2001; Toledo et al., 2013). Replication catastrophe is categorised by the presence of both replication stress and an accumulation of S-phase specific DNA damage in the same cell. Furthermore, an increase in the level of chromatin bound RPA can also be observed, indicating an exhaustion of the available pool of RPA (Toledo et al., 2017).

In the RPA exhaustion model, any factor that mediates replication stress, including ATR, serves to limit the amount of exposed ssDNA at replication forks such that the cellular supply of RPA remains abundant. In this way, any factor that influences levels of RPA through mediation of a global cellular process, such as inhibiting new origin firing, serves to locally stabilise replication forks by ensuring that there is sufficient RPA to bind any ssDNA that is exposed. There are a wide variety of factors that can increase or limit the generation of ssDNA in the nucleus. Examples of some of these methods along with their effect on replication fork dynamics and replication catastrophe are summarised in Figure 1.11.

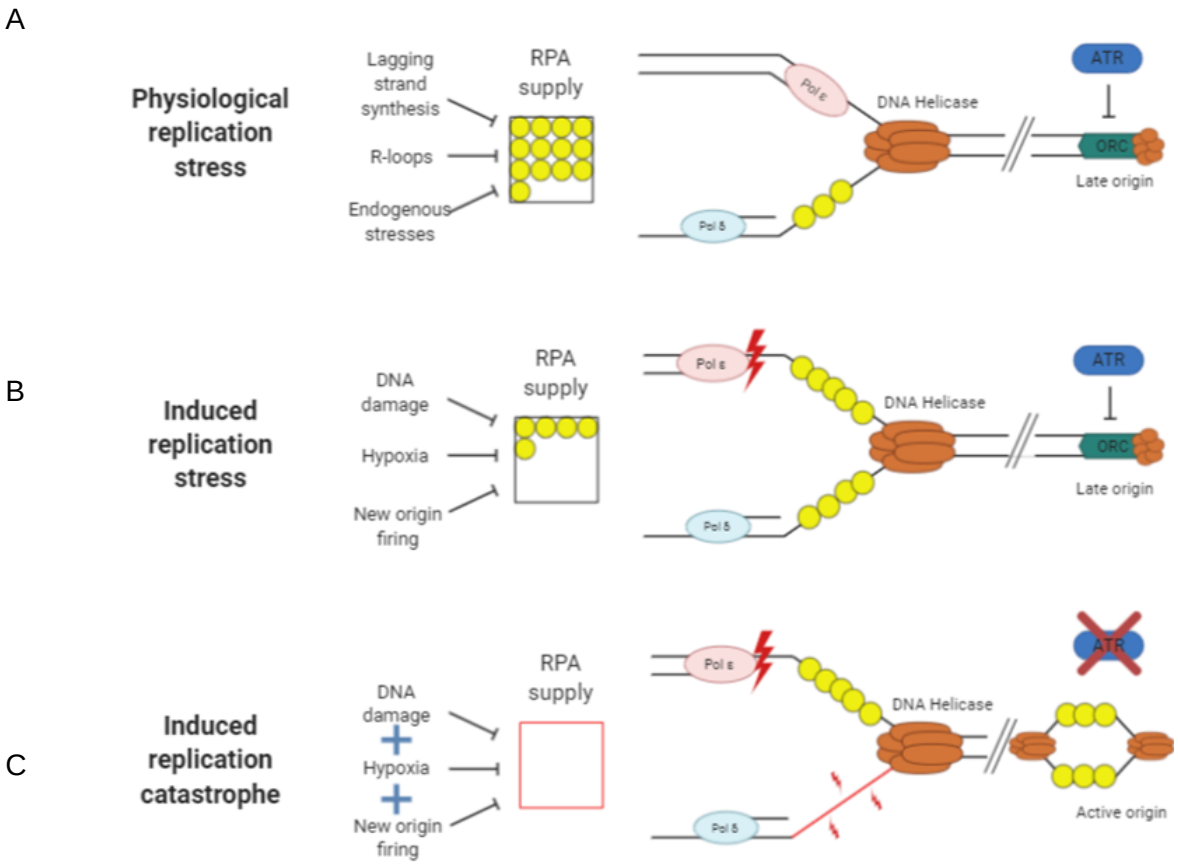


Figure 1.11 – Factors that influence RPA exhaustion and replication catastrophe
Different scenarios that could arise during DNA replication are depicted. On the left, boxes of RPA signify the amount of free RPA that the cell has in reserve to bind to ssDNA that accumulates during DNA replication. Factors that can contribute to RPA depletion are also shown. In the final scenario (C), these factors occur simultaneously. On the right are examples of replication fork dynamics detailing physiological replication stress, induced replication stress, and induced replication catastrophe. Image created using Biorender.
(A) Lagging strand synthesis causes an accumulation of RPA at the replication fork. Reserve RPA is still in abundance.
(B) Treatment with a DNA damaging agent causes a DNA lesion that has stalled the DNA polymerase. The continuation of the DNA helicase while the polymerase stalls creates longer stretches of ssDNA. More RPA is required to bind the accumulating ssDNA; however, all exposed ssDNA still gets bound by RPA.
(C) Treatment with a DNA damaging agent in combination with ATR inhibition leads to the same situation as in (B) but ATR cannot inhibit the firing of late origins of replication. This leads to RPA exhaustion as the amount of RPA remaining cannot cope with the amount of ssDNA present in the cell. ssDNA that is not coated with RPA is prone to breakage resulting in DNA damage. The uncoated segment of ssDNA prone to damage is shown in red.

ATR signalling protects the cell from RPA exhaustion. ATR mediated Chk1 signalling reduces the number of active replication forks via inhibition of late origin firing and thus reduces the amount of ssDNA present. This means that inhibition of ATR should increase the occurrence of RPA exhaustion and replication catastrophe (Toledo et al., 2013). Conversely, any attempt to inhibit the firing of new origins should delay the occurrence of RPA exhaustion, as less ssDNA accumulates. In these opposing methods, promoting and inhibiting the firing of new origins, one should be able to detect corresponding increases and decreases in S-phase specific DNA damage accompanying replication stress by treating with compounds or inhibitors that modulate the number of origins that fire in S-phase (Toledo et al., 2017).

The RPA exhaustion model also explains scenarios when checkpoint signalling is inhibited in otherwise normal replication conditions and replication stress still occurs. With checkpoint signalling inhibited, the cell is now less capable of managing replication stresses that arise during normal DNA replication (Figure 1.11 A). For this reason, the ATR signalling pathway is considered an essential pathway for normal cellular function, not just exclusively in response to stresses that cause replication stress (Blackford and Jackson, 2017; Buisson et al., 2015; Toledo et al., 2017). ssDNA occurs to varying degrees during normal replication mostly due to lagging strand synthesis (Zellweger et al., 2015). Normally the point in the cell cycle with the highest demand for RPA is in early S-phase (Buisson et al., 2015). Here the cell licenses new origins to fire to start DNA synthesis which comes with an increase in ssDNA. Additionally, the upregulation of RRM2 to generate nucleotides to be used for DNA synthesis is just beginning and it has not reached a high level at this point (Buisson et al., 2015; D'Angiolella et al., 2012). Even with these intrinsic increases in ssDNA the cell contains approximately 6-10 times the amount of RPA needed to coat any ssDNA generated during unperturbed DNA synthesis (Toledo et al., 2017).

Hypoxia-induced replication stress

There are a variety of methods employed to detect replication stress that depend on either the activation of replication stress response signalling or the global level of DNA replication. Firstly, RPA-S33 and Chk1-S345 are two phosphorylation marks that occur in an ATR dependent manner, that are commonly used as markers of replication stress (Olson et al., 2006; Zeman and Cimprich, 2014). Furthermore, bromo deoxyuridine (BrdU) or $^{[3H]}$thymidine incorporation assays utilise nucleotide analogues that can be directly incorporated into DNA during replication. The amount of the nucleotide analogue incorporated in each cell can then be quantified to determine the proportion of cells that are actively replicating (Hammond et al., 2003b; Pires et al., 2010). Finally, DNA fiber/combing methodology can also be used to study replication fork dynamics at the single molecule level (Bianco et al., 2012; Foskolou et al., 2016). Briefly, two different nucleotides are incorporated sequentially into the nascent DNA strand produced during DNA replication. Each nucleotide can then be individually stained and visualised by fluorescent microscopy. Both quantitative data on the rates of replication fork progression as well as qualitative data detailing the status of individual replication forks (stalled, ongoing, new origins) can be collected from this analysis.

Replication stress was first detected in hypoxic conditions when DNA synthesis using $^{[3H]}$thymidine incorporation was measured. It was found that in severe oxygen tensions (<0.1% O_2) DNA synthesis was almost completely abrogated (Hammond et al., 2002). When multiple oxygen concentrations were tested for active DNA replication via BrdU incorporation, active DNA replication was maintained in the range of 1-0.1% O_2. Only treatment at <0.1% O_2 could stop the incorporation of BrdU, indicating a lack of DNA replication (Pires et al., 2010). This has been further confirmed through use of the DNA fiber technique. Severe levels of hypoxia (<0.1% O_2) lead to a significant increase in stalled forks as well as a decrease in new origins that fire. At mild levels of hypoxia (2% O_2), replication dynamics are unchanged from those in normoxic conditions (21% O_2) (Foskolou et al., 2017; Olcina et al., 2013; Pires et al., 2010). Replication stress signalling including RPA-S33 phosphorylation and the accumulation

of RPA foci was also detected in an oxygen dependent manner (Olcina et al., 2013; Pires et al., 2010). The oxygen dependency of replication stress is proposed to occur at least in part due to decreased RRM2 efficiency in the absence of oxygen, which is an essential co-factor for RNR (Foskolou et al., 2017). RNR is the sole human enzyme responsible for the conversion of ribonucleoside diphosphates (NDP) to deoxyribonucleoside diphosphates (dNDP) which is the rate limiting step in the synthesis of dNTPs, the precursor to DNA (Mathews, 2015). A decrease in RNR efficiency leads to replication stress resulting from a lack of nucleotides required for DNA replication (Foskolou et al., 2017).

Hypoxia induced replication stress has been shown to occur in the absence of DNA damage (Bencokova et al., 2009; Hammond et al., 2002; Hammond et al., 2003b; Olcina et al., 2013). This was first demonstrated by comet assays, showing that while replication stress inducing agents such as HU and APH caused DNA damage, in response to chronic hypoxia (<0.1% O_2) no detectable DNA damage was observed (Hammond et al., 2002; Hammond et al., 2003b). Further experiments showed that even in the absence of DNA damage, ataxia telangiectasia mutated (ATM), the signalling pathway most well characterised for responding to DNA damage, is activated in chronic hypoxia (<0.1% O_2) (Bencokova et al., 2009). Both ATM and ATR have been identified as signalling pathways that protect hypoxic cells from DNA damage. Inhibiting either ATM or ATR results in a significant accumulation of DNA damage in hypoxic conditions and a decrease in colony survival (Olcina et al., 2013; Pires et al., 2012). This is hypothesised to occur because ATM and ATR contribute to the regulation of replication fork stability in hypoxic conditions through limiting the firing of new origins (Olcina et al., 2013; Pires et al., 2012). Contrasting the effects seen in chronic hypoxia, cells treated with hypoxia followed by reoxygenation (21% O_2) show a significant increase in DNA damage. Reoxygenation induced DNA damage likely occurs due to replication restart in conditions that lack the proper supplies for replication, such as nucleotides, or ROS induced damage (Hammond et al., 2003a; Hammond et al., 2004; Pires et al., 2012).

As previously discussed, hypoxia is negative prognostic factor in cancer treatment as it is associated with highly aggressive tumours, poor patient outcomes, and a decrease in overall survival (Bertout et al., 2008). Importantly, the levels of hypoxia that have been shown to cause replication stress (<0.1% O_2) represent the most treatment resistant fraction of the tumour (Brown and Wilson, 2004; Hammond et al., 2014; Horsman et al., 2012). As an example, hypoxia causes radioresistance in an oxygen dependent manner, where the oxygen enhancement ratio (OER) increases radioresistance by 2.5-3 times exclusively in near anoxic levels of hypoxia (Hall and Giaccia, 2006; Nordsmark et al., 2005).

The APOBEC family of proteins

Cytidine deaminases

The apolipoprotein B mRNA editing enzyme, catalytic polypeptide-like (APOBEC) proteins are a family of eleven cytidine deaminases. Their primary function is to bind to ssDNA or RNA transcripts and deaminate cytosine bases to uracil. While all APOBEC family members are capable of deaminating cytosines in ssDNA, only APOBEC1, APOBEC3A, and APOBEC3G have been proven to deaminate cytosines present in RNA, though all APOBECs are capable of RNA binding (Adolph et al., 2018; Henderson and Fenton, 2015; Prohaska et al., 2014). The deamination reaction is mediated by a conserved zinc coordination motif present within the catalytic domain of the APOBEC protein. A zinc molecule coordinates the reaction of a water molecule with an existing cytosine base to generate a uracil base as well as a molecule of ammonia as a by-product (Nabel et al., 2012; Olson et al., 2018) (Figure 1.12)

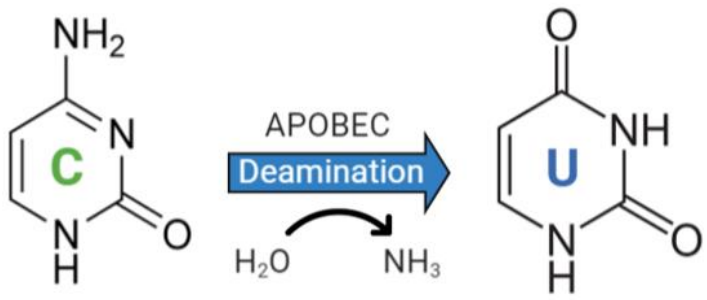


Figure 1.12 – Cytosine deamination reaction
Cytosine deamination catalysed by APOBEC proteins uses a water molecule to covert a cytosine base into a uracil base, yielding ammonia as an additional by-product. Image created using Biorender.

Though all APOBECs contain a similarly conserved zinc binding domain to deaminate cytosine, their functions within the cell have been found to be quite diverse. The first APOBEC discovered was APOBEC1 which was identified as a mechanism to edit the mRNA transcript of a gene called apolipoprotein B (APOB). The deamination of a cytosine base to uracil in the *APOB* transcript creates a stop codon that results in the translation of a different protein

isoform. This isoform is crucial for the proper uptake of lipids in the human small intestine (Smith et al., 2012). Another well studied APOBEC is activation induced deaminase (AID). AID functions primarily in immune cells and is involved in somatic hypermutation and class switch recombination (Muramatsu et al., 2000; Shinkura et al., 2004). APOBEC2 and 4 are catalytically inactive and their function unknown (Siriwardena et al., 2016). The remaining 7 APOBEC proteins, which comprise the APOBEC3 protein family, consist of APOBEC3A (A3A), APOBEC3B (A3B), APOBEC3C (A3C), APOBEC3D (A3D), APOBEC3F (A3F), APOBEC3G (A3G), and APOBEC3H (A3H). The regulation and function of the APOBEC3 protein family will be discussed in detail.

Viral restriction

The most well studied APOBEC protein to date is A3G. A3G was identified as a form of cellular innate immunity that could act as a viral restriction factor against the human immunodeficiency (HIV) virus. Since then A3D, A3F, and A3H have also been identified as HIV viral restriction factors (Harris and Liddament, 2004; Olson et al., 2018). To restrict the HIV virus, A3G deaminates cytosines present in the HIV viral genome to impair its normal function. Up to 10% of cytosines contained within the genome of an HIV virus can be deaminated by A3G in a single round of viral replication (Harris et al., 2003; Harris and Dudley, 2015). An excess of mutations proves lethal for the virus as it is unable to successfully carry out the functions required to infect other cells such as host genome integration and capsid formation. Mechanistically, it has been shown that A3G deaminates cytosines which are exposed when the virus is in its ssDNA intermediate phase (Yu et al., 2004). Upon reverse transcription of the viral RNA into a ssDNA intermediate form, A3G binds to the ssDNA transcript and deaminates cytosines to uracil. To have access to the virus in its ssDNA intermediate state, A3G must enter the viral capsid when the capsid forms in a cell that has already been infected. This is because once the capsid reaches a new cell and fuses with the cell membrane, a barrier remains around the virus preventing any restriction factors present

in the cytoplasm of the uninfected cell from accessing the virus (Figure 1.13) (Adolph et al., 2018; Harris and Liddament, 2004; Olson et al., 2018). In addition to deamination dependent viral restriction, it has also been shown that APOBEC proteins can bind to viral RNA. RNA binding serves to sterically hinder the progress of the viral reverse transcriptase enzyme, thus impairing the ability of the virus to transition through its ssDNA intermediate phase (Adolph et al., 2018; Narvaiza et al., 2012; Olson et al., 2018).

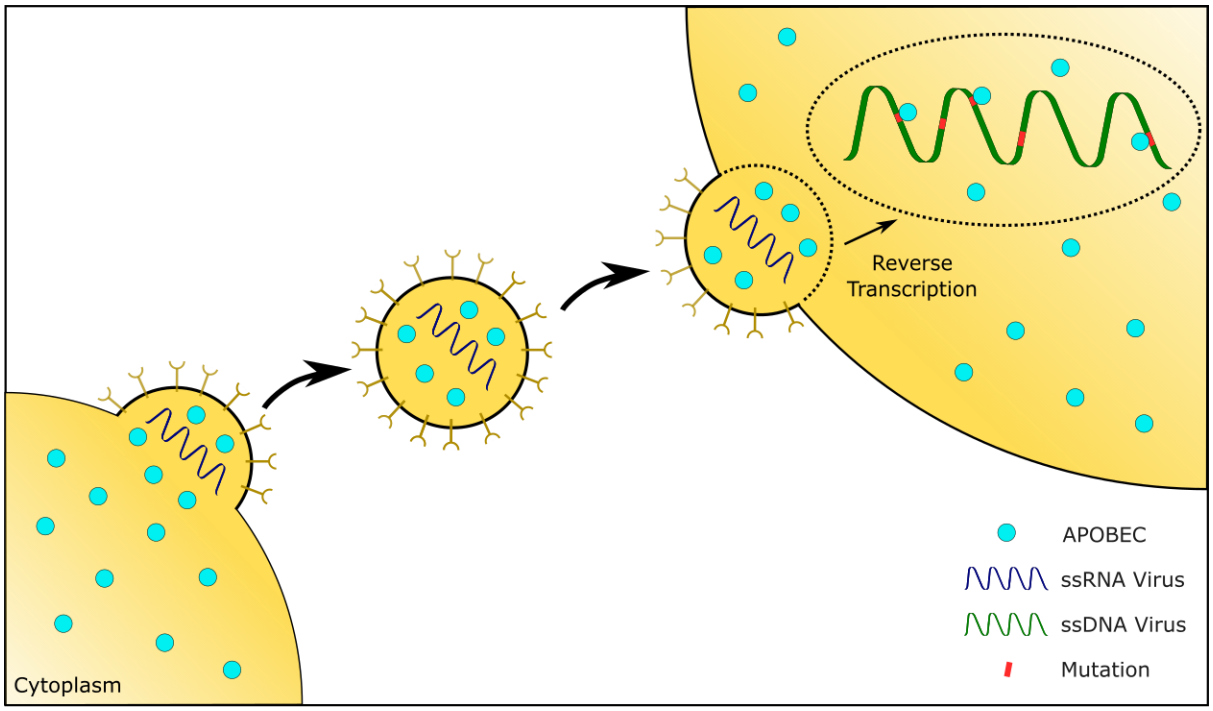


Figure 1.13 – APOBEC viral restriction
APOBEC proteins are included with the RNA virus within the viral capsid (solid black line) as it buds off an already infected cell. The viral capsid fuses with the membrane of an uninfected cell. A membrane is still present around the virus in the uninfected cell that prohibits proteins present in the host cell from interacting with the virus (dotted black line). The APOBEC proteins that travelled with the virus deaminate cytosine bases to uracil after the virus has undergone reverse transcription into its ssDNA intermediate phase.

This poses the question, if humans have such an effective defence against the HIV virus then why is it so prevalent in our population? The answer is that many viruses, including the HIV virus, have evolved a system to combat the deleterious effect of APOBEC deamination. HIV encodes a protein called virion infectivity factor (VIF) which is also included within the viral capsid. VIF recruits host proteins that ubiquitinate and target A3G for

proteasomal degradation (Schrofelbauer et al., 2004; von Schwedler et al., 1993). Interestingly, it has been demonstrated that even in the presence of VIF, a sub lethal level of mutation dependent on A3G induced deamination is still observed in the viral genome. It is hypothesised that this sub lethal level of mutation in the HIV genome serves as an important source of mutation that allows the virus to continue to adapt to its host's viral defence systems (Olson et al., 2018).

Another prominent example of viral adaptation to combat APOBEC deamination can be seen with the Epstein-Barr virus (EBV) and A3B. The EBV encodes a protein called ribonucleoside-diphosphate reductase large subunit (BORF2) which has been shown to bind directly to A3B. Instead of targeting the APOBEC for degradation as Vif does, BORF2 inhibits the deamination potential of A3B by localising it to the ER such that it does not have access to the replicating viral DNA in the nucleus (Cheng et al., 2019). All APOBEC3 proteins can restrict viruses with varying efficiencies. Viruses demonstrated to be APOBEC3 substrates include human t cell lymphotropic virus, hepatitis B virus, hepatitis c virus, human papillomavirus, and human herpesvirus (Harris, 2015; Rebhandl et al., 2015; Smith and Fenton, 2019).

RNA editing

As previously mentioned, a characterised function of APOBEC1 is to edit the mRNA transcript of the ApoB gene to ensure expression of the correct isoform in the small intestine. Since this discovery a limited number of studies have implicated A3A and A3G in mRNA editing (Sharma et al., 2016; Sharma et al., 2015). mRNA editing can be measured on the single gene or global level. For a single gene, an *in vitro* RNA editing assay is used. Briefly, a plasmid containing a gene of interest is transcribed and the resulting RNA product is mixed with cell lysate from different treatment conditions. RNA editing is then assessed by allele-specific RT-PCR which can detect single base differences between RNA products. Additionally, multiple candidate genes can be assayed for RNA editing by reverse transcribing

mRNA transcripts generated under different treatment conditions to cDNA followed by sanger sequencing. Global changes in mRNA editing can be demonstrated by sequencing the total RNA content (RNA-seq) of cell populations under different treatment conditions.

The *in vitro* mRNA editing assay has been used to demonstrate that A3A is capable of editing the mRNA of the succinate dehydrogenase B (SDHB) gene (Sharma et al., 2015). SDHB is a subunit of the succinate dehydrogenase complex which has been shown to be inactivated by a stop codon in normal peripheral blood mononuclear cells (PBMCs) and childhood T cell acute leukaemia (T-ALL) tumour samples. Interestingly, the stop codon was found to occur by means of a C>U mutation in the *SDHB* mRNA transcript, as opposed to a mutation in the DNA sequence of the SDHB gene (Baysal, 2007). The frequency of this editing event has been shown to increase when monocyte enriched PBMCs (MEPS) are exposed to mild levels of hypoxia (1% O_2) (Baysal et al., 2013). The A3A dependence of this upregulation was assessed in MEPS and M1 macrophages in response to interferon (IFN) and hypoxia (1% O_2) and both were shown to have increased levels of A3A-dependent *SDHB* mRNA editing (Sharma et al., 2015).

A global increase in RNA editing in hypoxia (1% O_2) was also seen, however the A3A dependence is unclear as *A3A* mRNA expression was shown to decrease. In support of A3A dependent global mRNA editing, when A3A was ectopically expressed in HEK-293T cells in normoxia, over 3000 mRNA editing events were observed that affected the translation of 1,110 proteins (Sharma et al., 2017). Similarly, when A3G was overexpressed in HEK-293T cells it was seen that the mRNA of over 600 genes was edited in an A3G dependent manner in normoxia. Interestingly, the groups of genes edited by A3A and A3G were distinct, suggesting that they have a mechanism for selectively editing specific subsets of mRNAs (Sharma et al., 2016).

Retroelement restriction

Another function of the APOBEC family is the restriction of retroelement mobility. Human cells contain a variety of retroelements that can copy their genomic material and reintegrate in a new location in the genome. The function of these elements is likely a means by which genetic diversity increases and new beneficial alleles arise. If left uncontrolled however, this system could overwhelm the cell with lethal levels of genomic rearrangements (Deininger and Batzer, 2002; Esnault et al., 2005). For this reason, the cell has various defence mechanisms against retroelements such that a correct balance is achieved.

The human genome contains two different types of retroelements: long terminal repeat (LTR) retrotransposons and non-LTR retrotransposons. Non-LTR retrotransposons represent the highest fraction of the genome in terms of bases and can be further subdivided into long interspersed nuclear elements (LINE) and short interspersed nuclear elements (SINE) elements. LTR retrotransposons are thought of an “endogenous retroviruses” as their replication cycle and reverse transcriptase steps function analogously to that of a retrovirus such as HIV. The key difference between LTR retrotransposons and retroviruses is the former lacks the ability to form a viral capsid, and thus lacks the ability to infect other cells aside from the host. Like HIV, LTR retrotransposons reverse transpose their genome to a ssDNA intermediate phase in the cytoplasm before moving back into the nucleus for integration into the host genome. Contrasting LTR retrotransposons, non-LTR retrotransposons are distinct in that their ssDNA intermediate phase occurs only in the nucleus (Deininger and Batzer, 2002; Kazazian, 2004).

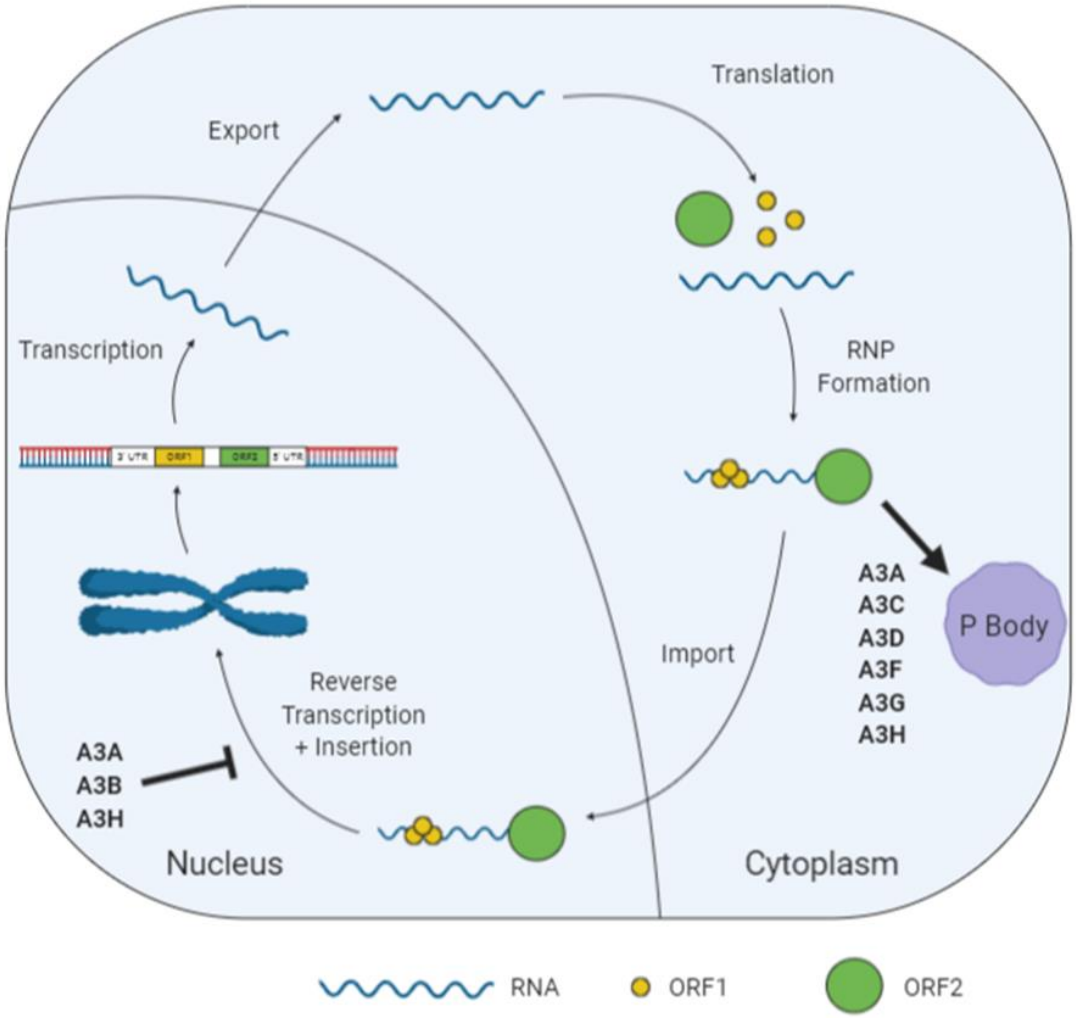


Figure 1.14 – Proposed model of APOBEC3 mediated restriction of non-LTR retrotransposons

The protein coding regions of non-LTR retrotransposons are transcribed in the nucleus. The mRNA transcript is then exported to the cytoplasm and translated. The translated proteins associate with the mRNA transcript to form a ribonucleoprotein (RNP) complex. Cytoplasmic APOBEC3s can sequester RNP complexes within cytoplasmic compartments termed P-bodies to limit their ability to access the nucleus and reinsertion. RNPs that are imported back into the nucleus can be deaminated by nuclear APOBEC3s to restrict functionality upon genome insertion. Image created using Biorender.

All APOBEC3 proteins have been shown to restrict at least one type of retroelement utilising either deamination dependent or independent mechanisms (Esnault et al., 2005; Feng et al., 2017; Henderson and Fenton, 2015; Kinomoto et al., 2007; Koito and Ikeda, 2013). The

mechanism and affinity each APOBEC3 possess against each retroelement largely depends the subcellular localisation of APOBEC3 proteins. A3C, A3D, A3F, and A3G are all constitutively localised to the cytoplasm and thus unable to access the nuclear compartment. A3B is constitutively localised to the nucleus while A3A and A3H have been detected in both compartments (Rebhandl et al., 2015; Starrett et al., 2016). Restriction of LTR retrotransposons is mechanistically analogous to the APOBEC3-mediated restriction of the HIV virus and will not be discussed further (Figure 1.13) (Koito and Ikeda, 2013). In regard to non-LTR retrotransposons, only A3A, A3B, and A3H are capable of restriction in a deamination dependent manner as they can access the non-LTR retrotransposon in its nuclear ssDNA intermediate phase (Figure 1.14) (Feng et al., 2017; Kinomoto et al., 2007; Koito and Ikeda, 2013). Interestingly, all APOBEC3 proteins have been shown to be able to restrict movement of non-LTR retrotransposons to some degree. Non-LTR retrotransposon restriction by cytoplasmic APOBEC3s is conducted by a deamination independent mechanism (Esnault et al., 2005; Kinomoto et al., 2007; Koito and Ikeda, 2013). Non-LTR retrotransposons have a brief cytoplasmic phase where their RNA enters the cytoplasm to facilitate translation of essential proteins. These proteins then associate with the non-LTR retroelement RNA to form a ribonucleoprotein (RNP) complex before shuttling back to the nucleus. While this has yet to be conclusively demonstrated, it is theorised that cytoplasmic localised APOBEC3s bind to the RNP and hinder its progression back into the nucleus. Sequestration of RNPs is possibly done through localisation to P-bodies, structures associated with the regulation of RNA species, found in the cytoplasm (Koito and Ikeda, 2013) (Figure 1.14). Though more research into the precise mechanism of retroelement restriction of each APOBEC3 is needed, it is clear that as a protein family the APOBEC3 proteins are capable of limiting the mobility of retroelements.

Uracil in genomic DNA

In addition to viruses, mRNA, and retroelements, it has been demonstrated that in certain circumstances APOBECs can deaminate genomic DNA (Adolph et al., 2018; Burns et al., 2013a). Deaminating a cytosine to uracil in genomic DNA can yield a wide variety of outcomes. Cells have many conserved mechanisms to deal with genomic uracil incorporation as the presence of uracil in genomic DNA does not always occur in an APOBEC dependent manner. For example, during DNA replication cells can incorporate uracil instead of cytosine into a newly synthesised DNA strand erroneously. Additionally, spontaneous deamination of methylated cytosine occurs throughout the genome, albeit with a relatively low frequency (Thompson and Cortez, 2020). The resulting uracil included in DNA from any of these scenarios is managed by the cell in a variety of possible ways.

The simplest outcome to resolve the incorporation of a genomic uracil is regular replication over the uracil base with a DNA polymerase. If a DNA polymerase reads an irregular DNA base, including uracil, it will preferentially insert an adenine across from it. This is referred to as the "A rule" (Strauss, 1991). Upon the next round of DNA replication, a thymine will be inserted across from the adenine where originally a cytosine was present. This ultimately results in a C>T mutation (Figure 1.15 A) (Adolph et al., 2018; Harris, 2015).

The enzyme responsible for locating and removing uracils present in genomic DNA is called uracil DNA glycosylase (UNG). UNG locates uracils and excises the uracil base resulting in an abasic site (Krokan et al., 2001). The UNG-mediated excision of uracil occurs very rapidly, so consequently a high proportion of uracils present in genomic DNA are converted to abasic sites (Harris, 2015). The question then becomes, what repair processes are implemented by the cell when an abasic site is detected? These outcomes are summarised in Figure 1.15 B. Apurinic/apyrimidinic endonuclease 1 (APE1) is an endonuclease that creates a nick in the DNA backbone such that DNA Pol β can insert the correct base into the abasic site. This is an error-free repair approach called base-excision repair (BER) that relies on utilising the guanine originally across from the cytosine as a

template (Sukhanova et al., 2005). If, however there are multiple deamination events in close proximity, then the nick caused by APE1 can result in double strand breaks and larger scale genomic rearrangements (Siriwardena et al., 2016). If APE1 does not create a nick in the DNA backbone, then translesion synthesis (TLS) can occur. The objective of TLS is to insert a base pair across from an abasic site even if it is incorrect, to avoid any larger scale chromosomal damages (Masutani et al., 2000). Pol η and REV1 DNA directed polymerase (REV1) are two such TLS polymerases (Thompson and Cortez, 2020). They both possess larger active sites than regular polymerases which allows them to read irregular DNA bases such as an abasic site. As with uracil, the A rule applies to this scenario where Pol η will preferentially read the abasic site as an adenine and insert a thymine upon replication resulting in the same C>T mutation. REV1 is unique in that it does not follow the A rule and will preferentially insert a cytosine across from an abasic site resulting in a C>G mutation upon replication (Chan et al., 2013). When considering these possible outcomes, it is notable that UNG is required for a C>G transition to occur, otherwise either a C>T transversion or no mutation will occur. Another factor that can affect the mutational outcome of genomic uracil incorporation is the availability of nucleotides. Any perturbations in the levels of specific nucleotides will affect their availability and therefore the chance they will be included by the acting DNA repair process (Helleday et al., 2014).

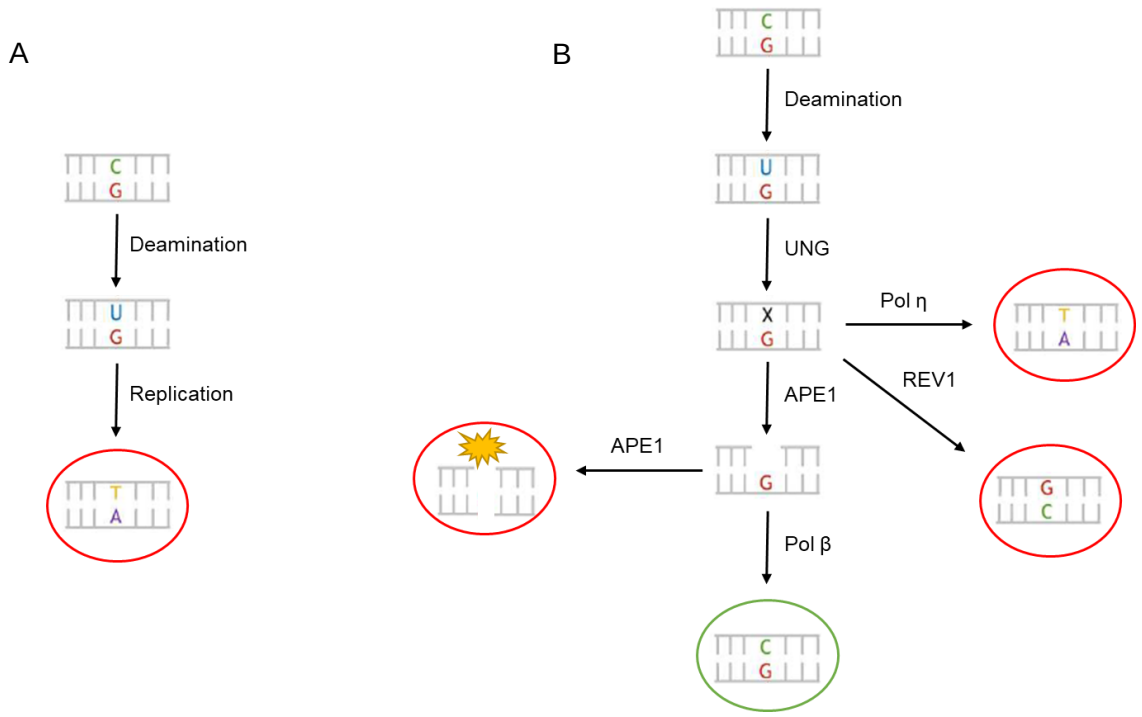


Figure 1.15 – Consequences of genomic deamination
Schematics indicating the multiple fates of a uracil inserted into genomic DNA. Red or green circles indicate a terminal mutagenic or error-free outcome. The fixation of each mutation is dependent upon the subsequent round of DNA replication after the initial deamination event occurs. Nucleotide bases are represented by their corresponding letters while an abasic site is represented by an X. (A) Consequences if the uracil base is replicated by a DNA polymerase and (B) consequences if the uracil base is converted into an abasic site by UNG are shown.

Though the outcomes are analogous, a key difference between the incorporation of a genomic uracil in an APOBEC dependent or independent manner is the sequence context that the uracil is contained in within the DNA. Through analysis of APOBEC mediated mutations on viral DNA and bacterial DNA with ectopically expressed APOBEC3s, it was observed that APOBEC3 proteins preferentially deaminate cytosines preceded by a thymine and followed by either a guanine or adenine base. The exception is A3G which prefers a cytosine preceded by another cytosine (Harris et al., 2002; Hultquist et al., 2011; Roberts et al., 2013b). This combined with the fact that genomic uracil insertion will preferentially lead to C>T or C>G mutations (Figure 1.15 A/B) led to the definition of APOBEC3 mutations as C>T or C>G mutations that occur within a TCW sequence context (W = adenine or thymine) (Alexandrov et al., 2013; Roberts et al., 2013b).

The APOBEC mutation signature

The concept of a mutational signature was first proposed when 21 breast cancer tumours were whole genome sequenced and single base substitution mutations were analysed (Nik-Zainal et al., 2012). For additional information on each individual mutation, the sequence data from one base directly proceeding and following each mutation was extracted. As there are 6 possible base substitutions (C>A, C>G, C>T, T>A, T>C, and T>G) and 16 possible combinations of flanking bases for each substitution, there are 96 possible single base mutations to analyse. From this wealth of mutational data, 5 mutational signatures were identified (Nik-Zainal et al., 2012). A mutational signature is a collection of mutations of the same type (out of the 96 possible single base substitutions) that occur at a high frequency relative to other mutations and that likely result from the same causative source. For example, many lung cancer samples were found to be dominated by G>C and C>A mutations. It was noticed that these mutations are consistent with those caused by tobacco exposure through smoking. For this reason, this mutational signature was attributed to smoking (Nik-Zainal et al., 2012). Since the initial 21 sequenced breast cancers, thousands more tumours have been sequenced across more than 30 cancer types and over 70 mutational signatures identified. Today, signatures exist for single base substitutions (SBS), doublet base substitutions (DBS), clustered base substitutions (CBS), and small insertion and deletion (ID) mutations. Additionally, the two bases preceding and following each somatic mutation are considered (Alexandrov et al., 2020; Alexandrov et al., 2013; Liu et al., 2017a).

Part of the power of classifying tumours by mutational signatures as opposed to looking for mutations in specific oncogenes or tumour suppressors is that mutational signatures allow for the inference of the relative contribution of different causative agents to the overall tumour mutational landscape (Helleday et al., 2014). For example, a tumour sample may have mutations that are characteristic of 3 different mutational signatures, although one may predominate, likely elucidating the most important driver of that cancer. Separating the relative contributions of different mutational signatures is crucial as almost every sequenced tumour

to date has contributing mutations from multiple signatures (Alexandrov et al., 2020; Alexandrov et al., 2013).

Similarly, to the mutational signature characterised by G>C and C>A mutations that was attributed to the use of tobacco smoke, two mutational signatures have been identified that contain a disproportionate amount of C>T and C>G mutations in the TCW sequence context, called single base substitution 2 (SBS2) and single base substitution 13 (SBS13). SBS2 and 13 are differentiated from each other solely on the basis of the relative amount of C>T versus C>G mutations present. These two mutational signatures have been identified in approximately 15% of all human cancers and 10% of cancer cell lines (Alexandrov et al., 2020; Alexandrov et al., 2013; Jarvis et al., 2018; Roberts et al., 2013b). Due to the sequence specificity of APOBEC deamination coupled with the fact that genomic uracil incorporation leads overwhelmingly to C>T and C>G mutations, these signatures were attributed to APOBEC activity. SBS2 and 13 are most prevalent in breast, head and neck, lung, bladder, cervical, and ovarian cancers although the signature has been detected in at least 16 different cancer types to some degree (Figure 1.16) (Alexandrov et al., 2020; Alexandrov et al., 2013). The relative contribution of the APOBEC mutational signature relative to other mutational signatures within a single cancer sample is highly variable. In some cases, up to 90% of all base substitution mutations in a tumour result from APOBEC activity (Olson et al., 2018). A key feature of the APOBEC mutational signatures is the occurrence of local regions of hypermutation (termed kataegis) where a large number of APOBEC mediated mutations occur within a relatively small stretch of DNA (Nik-Zainal et al., 2012; Petljak et al., 2019; Roberts et al., 2013b). These APOBEC mutational signatures give a powerful readout of APOBEC activity and have demonstrated widespread APOBEC signalling in human cancers.



Figure 1.16 – Mutational signatures identified in human cancers
Mutational signatures are listed on the left and the cancer types that were sequenced are listed at the top. Possible sources of each of the mutational signatures are also listed on the right along with the prevalence of each signature across all cancer types sequenced. Blue circles indicate the number of signatures contained within a given type of cancer, red circles indicate the number of cancer types that contain a given signature, and green circles show which signature is present in each cancer type. Red boxes indicate the APOBEC mutational signatures which are now referred to as SBS2 and 13. Adapted and reprinted from (Alexandrov et al., 2013), with permission from Springer Nature, License Number: 4840791156758

Which APOBEC is the culprit?

As there are 11 APOBECs and 7 members of the APOBEC3 family, it begs the question of which APOBEC is responsible for the generation of the APOBEC mutational signatures? or is it a combination of all of them? There is considerable debate on this topic. As previously mentioned, A3A, A3B, and A3H are the only APOBEC3 proteins that have been detected in the nuclear compartment and thus are the only APOBEC3 proteins with access to genomic DNA. A3H is distinct in that there are 7 different haplotypes with different affinities for nuclear vs. cytoplasmic localisation (Gu et al., 2016; Harari et al., 2009). Studies have shown that A3H haplotype 1 has a predominantly nuclear localisation and is enzymatically active though weaker than A3A and A3B (Li and Emerman, 2011; Starrett et al., 2016; Zhen et al.,

2012). It is widely agreed that A3B and A3A are primarily responsible for the signatures while A3H is suggested to contribute in situations where A3B and A3A are not present (Burns et al., 2013b; Chan et al., 2015; Starrett et al., 2016). The contrasting contributions of A3A, A3B, and A3H on the APOBEC mutational signatures will be discussed further in this section.

The evidence for A3B as the primary APOBEC responsible for the generation of the APOBEC mutational signatures is extensive. A3B is upregulated in tumour samples compared to matched normal samples in a wide variety of cancers and is also highly expressed in cancer cell lines (Ng et al., 2019). The largest differences in A3B expression in cancer relative to normal tissue can be seen in cancer types where the APOBEC mutational signature predominates. For example, in breast cancer, a cancer type where the APOBEC mutational signature occurs frequently, *A3B* mRNA is upregulated in 65% of patient-derived primary breast cancer specimens and 90% of breast cancer cell lines (Olson et al., 2018). Furthermore, out of all APOBECs the mRNA expression of *A3B* correlates most closely with the number of APOBEC mutations in tumours across a wide variety of tumour types. This relationship also holds true for kataegis, where a correlation between *A3B* mRNA expression and the number of kataegic foci exists in many cancers (Burns et al., 2013b; Roberts et al., 2013b). In addition to correlative evidence, it has also been shown that A3B ectopic overexpression in a cancer cell line with low endogenous A3B signalling results in the occurrence of the APOBEC mutational signature after 14 days of A3B expression (Akre et al., 2016; Nikkila et al., 2017). Evidence suggesting that A3B is not primarily responsible for the APOBEC mutational signature is mostly limited to tumours that display the APOBEC mutational signature yet are A3B null (Chan et al., 2015). Typically in this situation, it has been shown that these tumours have at least one copy of A3H haplotype 1 which is most likely to be able to deaminate genomic cytosines in the place of A3B due to its nuclear localisation (Starrett et al., 2016).

Utilising an antibiotic gene transfer assay, A3A has been shown to be the most potent deaminase enzyme of all APOBEC3 proteins. Briefly, different dishes of cells plated in media

containing antibiotics were transfected with each of the APOBEC3 proteins along with a gene transfer system. If the gene transfer system was not interrupted by APOBEC mediated deamination, then the cells would successfully acquire an antibiotic resistance gene and colonies would grow. The fewer colonies counted at the conclusion of the experiment, the more active the specific APOBEC3 deaminase was in disrupting the gene transfer system through deamination. The cells transfected with A3A resulted in 5 times less colonies than any other APOBEC3 and almost 10 times less than A3B (Stenglein et al., 2010). Even with the potent deamination ability of A3A, the largest hurdle to its widespread acceptance as the APOBEC responsible for the signature rests with its highly limited expression. In normal tissue A3A is only detected in specific immune cells including monocytes and macrophages (Burns et al., 2013b; Koning et al., 2009; Ng et al., 2019). A3A mRNA and protein expression has also shown to be sporadic in cancer cell lines and tumour samples (Ng et al., 2019). In addition, enzymatically A3A has been shown to rapidly cycle on and off substrates which makes it unlikely that it could cause the long stretches of strand coordinated mutations frequently seen in cancer (Adolph et al., 2017). Evidence in favour of A3A can be seen in a study that demonstrates that A3A and A3B possess different nucleotide preferences for deamination, where A3A prefers YTCA over RTCA (where Y is pyrimidine and R is a purine base) sequences for deamination (Chan et al., 2015). Further studies expanded on this and noticed that typically more mutations seen in tumour samples and cancer cell lines with the APOBEC signature tend to be YTCA, though this is dependent on the cancer type analysed (Alexandrov et al., 2020; Chan et al., 2015; Petljak et al., 2019). Though there is debate over the relative contributions of A3A, A3B and A3H to the APOBEC mutational signatures it is clear that either one of these or some combination of all of them accounts for the APOBEC mutational signatures in the vast majority of human cancers.

Deamination of genomic DNA

The high frequency of the APOBEC mutational signatures suggests that APOBECs are a major source of mutation in human cancers. For these mutations to occur however, APOBECs must deaminate cytosines present in genomic DNA and specifically ssDNA. There are a variety of opportunities that occur during both normal and aberrant cellular function in cancer cells where exposed ssDNA could be deaminated by an APOBEC enzyme. Importantly, it has been demonstrated that even though RPA rapidly coats any exposed genomic ssDNA, that APOBEC enzymes can actively compete with RPA for binding. Successful deamination of ssDNA oligonucleotides coated with RPA has been demonstrated in an *in vitro* system (Adolph et al., 2017). Clues as to the most likely opportunity where APOBEC enzymes can access ssDNA come from a wide variety of bioinformatic and enzymatic experiments. Whole genome sequencing data yields important information on the location of APOBEC mutations within the genome such as stand coordination, transcriptional strand bias, and mutational clustering. In addition, studies utilising purified APOBEC proteins and *in vitro* experimental set-ups meant to mimic endogenous cellular processes can inform our perception of how APOBECs work *in vivo*. DNA replication, DNA damage, transcription, and R-loops will be discussed further as opportunities for APOBECs to deaminate genomic DNA and are illustrated in Figure 1.17.

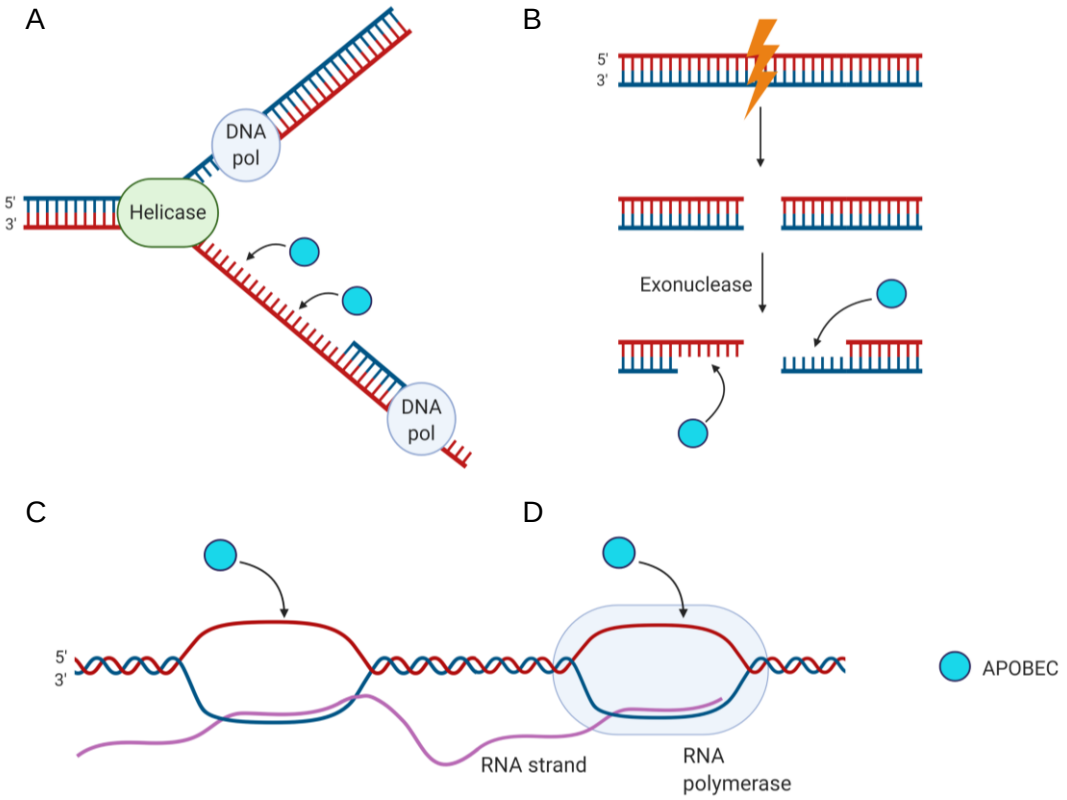


Figure 1.17 – Opportunities for APOBEC deamination of ssDNA
Graphical illustrations of (A) DNA replication (B) end resection following DNA damage, (C) R-loops, and (D) transcription outline the scenarios where APOBECs can access genomic ssDNA to deaminate cytosine bases. Image created using Biorender.

During normal DNA replication, the DNA polymerase is preceded by a helicase that unwinds the dsDNA duplex producing ssDNA. While DNA synthesis on the leading strand is rapid, on the lagging strand ssDNA persists for longer while the Okasaki fragments are filled (Okazaki et al., 1967). Difficulties experienced by cells attempting to replicate their genome such as replication fork stalling, incomplete lagging strand synthesis, and excessive origin firing can also serve to increase both the pool of ssDNA and the length of time the ssDNA is exposed such that cytosines are available for APOBEC mediated deamination (Adolph et al., 2017). The strongest evidence for APOBEC deamination during DNA replication comes from whole genome sequencing data showing that the majority of APOBEC mutations occur on the lagging DNA strand (Haradhvala et al., 2016; Hoopes et al., 2016; Seplyarskiy et al., 2016).

This suggests that the speed of replication is relevant to the number of APOBEC mutations observed. Additional studies utilised a minimal phage replication system that mimics the creation of Okasaki fragments on the lagging DNA strand. They found that the expression of A3A, A3B, and A3H were capable of successfully deaminating cytosines in this context while A3G was four times less efficient. This suggests that the deamination of cytosines present on the lagging DNA strand is at least possible *in vivo* (Figure 1.17 A) (Adolph et al., 2017).

One of the first steps in repairing a DNA double strand break (DSB) is for exonucleases to chew bases off the terminal ends of broken DNA fragments leaving ssDNA overhangs. As previously stated, whole genome sequencing data has shown that a disproportionate amount of APOBEC mutations occur within small stretches of DNA (kataegis) (Chan et al., 2015; Nik-Zainal et al., 2012; Swanton et al., 2015). These regions of kataegis were found to correspond with regions of chromosomal breakpoints (Petljak et al., 2019; Roberts et al., 2013b). The implication here is that APOBECs can deaminate cytosines present on the ssDNA overhangs after end resection has occurred and before the DNA is ligated back together (Figure 1.17 B).

Transcription is also a cellular process where ssDNA is exposed in the nucleus, however it has largely been ruled out as a major ssDNA substrate for APOBECs (Figure 1.17 C). This is primarily because the APOBEC mutational signature fails to demonstrate any transcriptional strand bias (Alexandrov et al., 2020; Alexandrov et al., 2013; Haradhvala et al., 2016). If ssDNA was deaminated during transcription, then a disproportionate amount of mutations would likely occur on the exposed non-coding DNA strand while transcription occurs on the coding strand. Furthermore, enzymatic data has shown that A3B requires oligomerisation before it is able to deaminate cytosines. Oligomerised A3B was found to be too large to efficiently deaminate cytosines within the transcription bubble (Adolph et al., 2017). Similarly, to transcription, *in vitro* enzymatic studies have shown that APOBECs are much less efficient at deaminating cytosines on the ssDNA strand of R-loops (Figure 1.17 D) (Adolph et al., 2017). These analyses of both the regions of DNA where APOBEC mutations are most likely to occur as well as the enzymatic properties

of APOBECs *in vitro* suggest that DNA replication and end-resection after DNA damage are the most likely events at which APOBECs access genomic ssDNA in human cancers.

Consequences of genomic DNA deamination (tumour)

Understanding the potential opportunities for APOBEC mediated deamination and recognising that the APOBEC mutational signature occurs in many human cancers, the next pertinent question becomes, what are the consequences associated with APOBEC mediated deamination in human cancer? The consequences are largely dependent on the quantity of deamination events that occur. The number of APOBEC mutations detected in different tumour samples can be highly variable even within the same type of cancer (Burns et al., 2013b; Roberts et al., 2013b). APOBEC mediated deamination will therefore occur in different magnitudes in different tumours and also in individual cells within a tumour. The consequences of such variable deamination can be thought of differently depending on whether you consider the effect on the level of the tumour, or the level of the cell (Figure 1.18).

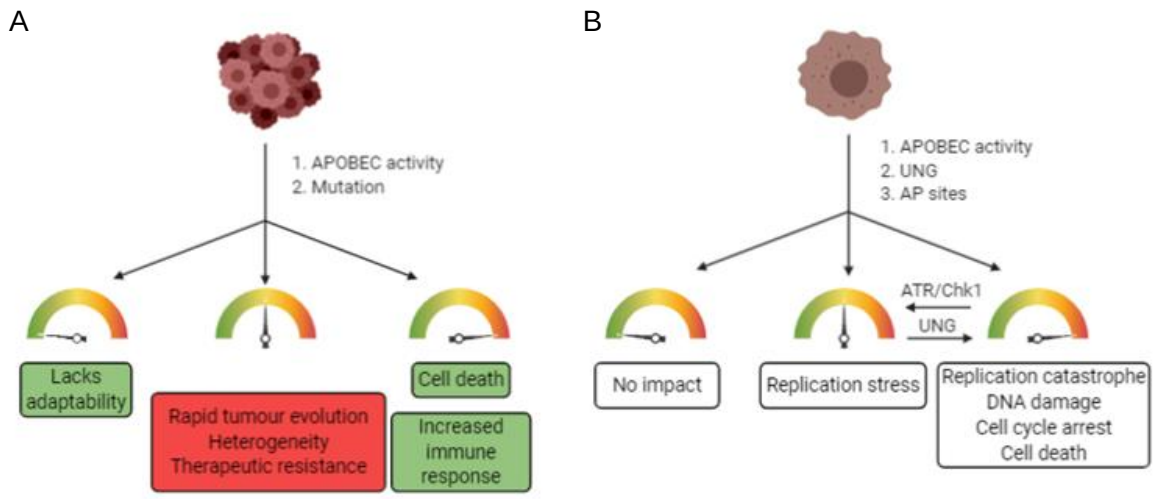


Figure 1.18 – Consequences of APOBEC-mediated deamination on the level of the tumour and the cell

(A) On the level of the tumour, APOBEC activity can be thought to increase the overall mutation rate within the tumour to varying degrees. Low, medium, and high levels of mutation are represented by dials. The consequences of each of these levels of APOBEC mediated deamination are displayed in boxes. Green colouring indicates a favourable outcome for the patient while red indicates an unfavourable outcome leading to a poor prognosis. Image created using Biorender.

(B) On the level of the cell, APOBEC activity can be thought to increase the number of abasic sites present in the genome of a cell to varying degrees. Low, medium, and high numbers of abasic sites are represented by dials. The consequences of each of these levels of APOBEC mediated abasic sites are displayed in boxes. ATR/Chk1 protects the cell from the consequences associated with the highest level of abasic sites. UNG creates more abasic sites and can push the cell into the consequences associated with the highest level. Image created using Biorender.

On the level of the tumour, many forms of chronic endogenous mutations have been shown to cause rapid tumour evolution, heterogeneity, and therapeutic resistance (Olson et al., 2018). This holds true for the deamination caused by APOBEC enzymes (Faltas et al., 2016; Law et al., 2016; Venkatesan et al., 2018). The prevailing hypothesis on how APOBEC mediated deamination can influence these negative prognostic traits, is that APOBEC activity is selected to provide tumours with a “just right” amount of mutation (Swanton et al., 2015). Too little mutation would render tumours unable to adapt to survive in the hostile tumour microenvironment. In contrast, too much mutation would result in the inability of a high proportion of cells within the tumour to perform their required functions. This “just right” level

of mutation can lead to a variety of undesirable outcomes for patients including treatment resistance and tumour heterogeneity (Figure 1.18 A). These negative effects can be seen when considering overall patient prognosis. For example, patients with ER+ breast tumours and non-small cell lung cancer (NSCLC) have decreased survival and response to treatment when their tumours are sorted by level of A3B expression (Kanu et al., 2016; Wang et al., 2018).

The most powerful experimental evidence of A3B expression actively promoting treatment resistance and accelerated tumourigenesis can be seen in an *in vivo* model where A3B overexpression and knockdown was combined with tamoxifen treatment in mice. The tumour volume of the mice treated with tamoxifen where A3B was overexpressed significantly increased compared to the vector control and did not increase when a catalytically dead version of A3B was overexpressed. The same paradigm also held true when A3B was inhibited alongside tamoxifen treatment where tumours significantly decreased in volume compared to the vector control (Law et al., 2016). Since A3B itself has no way to specifically target any of the genes required to respond to tamoxifen treatment, it stands to reason that the increased viability of the tumours was a product of the increased mutation rate afforded to the tumour by A3B mediated deamination, where mutations in various driver genes resulted in increased resistance to tamoxifen and accelerated tumourigenesis. To support this data other studies have directly shown that APOBEC activity can result in mutations in a wide variety of key cancer driver genes and tumour suppressors such as MYC proto-oncogene (MYC), p53, ATM, and Phosphatidylinositol-4,5-Bisphosphate 3-Kinase Catalytic Subunit Alpha (PIK3CA) (Henderson et al., 2014; Roberts et al., 2013b; Robertson et al., 2017).

In contrast, situations have also been observed where a stronger APOBEC mutational signature in a tumour cohort has correlated with an improved clinical outcome. A study that sequenced muscle invasive bladder cancer (MIBC) tumours showed that tumours with a high APOBEC burden of mutations have a significantly higher 5-year survival rate than those with a low number of APOBEC mutations (Robertson et al., 2017). They hypothesised that this

surprising result occurred due to the increased mutational burden, as these tumours expressed more neoantigens which could stimulate a stronger immune response. Another study utilising an *in vivo* mouse model showed that APOBEC expression in tumours resulted in increased expression of neoepitopes that could be detected by the immune system. Increased activation of the immune system coupled with A3B overexpression combined to increase the efficacy of immune checkpoint inhibitor treatment (Driscoll et al., 2020). These data suggest that the negative prognostic effects of APOBEC mutation on treatment resistance, tumourigenesis, and oncogene/tumour suppressor mutations could be counterbalanced by a positive prognostic effect of superior immune activation.

Consequences of genomic DNA deamination (cell)

APOBEC mediated deamination also results in a variety of consequences at the single cell level. As previously discussed, a possible outcome of APOBEC mediated deamination is the occurrence of an abasic site if the resulting uracil is excised by UNG (Figure 1.15 B). A large number of abasic sites contained within a relatively small genomic area can lead to a variety of cellular consequences such as replication stress, DNA damage and cell cycle arrest (Figure 1.18 B). Multiple studies using *in vitro* cell models have demonstrated that ectopic overexpression of A3A or A3B results in a significant increase in markers of replication stress such as phosphorylated Chk1 and RPA (Buisson et al., 2017; Green et al., 2017; Green et al., 2016; Landry et al., 2011; Nikkila et al., 2017; Serebrenik et al., 2019). Interestingly these effects have been shown to be dependent on the activity of UNG. A uracil incorporated into genomic DNA, while mutagenic, does not pose any immediate threat to the current replication cycle of the cell. The same cannot be said however for an abasic site created in an UNG dependent manner. When A3B is overexpressed and UNG is removed, replication stress signalling returns to the same levels as in cells where A3B is not expressed, as uracils are not converted into abasic sites that can stall DNA polymerases (Buisson et al., 2017; Serebrenik et al., 2019).

There are two main mechanisms by which APOBEC mediated deamination could lead to DNA damage. The first is UNG dependent persistent replication stress signalling leading to RPA exhaustion and replication catastrophe. The second is the fact that the DNA nicking action of APE1 on multiple abasic sites in a small genomic region could result in DSBs if too many nicks occur before they have a chance to be filled and repaired. There is currently debate in the literature as to the link between A3A/A3B expression and DNA damage. Some papers submit that ectopic A3A/A3B expression alone is sufficient to cause DNA damage as assayed by γH2AX expression, 53BP1 foci, and comet assay (Green et al., 2016; Landry et al., 2011; Nikkila et al., 2017; Serebrenik et al., 2019). As with replication stress induced by APOBEC mediated deamination, DNA damage was also found to be dependent on UNG (Serebrenik et al., 2019). A contrasting study posits that DNA damage and replication catastrophe will only occur in response to A3A/A3B overexpression if ATR/Chk1 is also inhibited, thus removing a key regulator protecting the cell from RPA exhaustion (Buisson et al., 2017). In this scenario ATR/Chk1 are protecting the cell against APOBEC mediated deamination leading to replication catastrophe. A supportive study finds that inhibiting ATR in combination with A3A overexpression results in massive cell death, supporting the notion that ATR protects cells against the consequences of APOBEC mediated deamination (Green et al., 2017). Finally, all studies that found DNA damage also found alterations in the cell cycle. BrdU and propidium iodide (PI) incorporation experiments showed that overexpressing A3A/A3B results in a G2/M or S-phase cell cycles arrest depending on the cell line tested (Green et al., 2017; Green et al., 2016; Nikkila et al., 2017).

Importantly, as the consequences of APOBEC mediated deamination are primarily determined by the quantity of deamination that occurs, it is important to consider the possible confounding factor of using ectopic overexpression systems to assay the consequences of APOBEC expression as opposed to the endogenous expression. One report tested the effects of both endogenously interferon-stimulated A3A and ectopically expressed A3A on cell viability and found that while ectopically expressed A3A significantly decreased cell viability, endogenously expressed A3A did not (Land et al., 2013). These data suggest that over-

expression studies should be carefully titrated to ensure the ectopically expressed APOBEC does not significantly differ in localisation or effect to the endogenous APOBEC. Additionally, the discrepancies between DNA damage observed in different studies could easily be accounted for by differences in the quantity of A3A/A3B ectopically overexpressed between the studies.

APOBEC3 regulation

Though it is clear that APOBEC mutations frequently occur in human cancers and are primarily caused by A3A or A3B, how these APOBECs become misregulated or upregulated such that they deaminate genomic ssDNA largely remains unclear. The few studies exploring APOBEC3 regulation have primarily focused on APOBEC3 responses to viruses or immune elements. This line of thinking is very intuitive as the primary function of APOBEC3 proteins is to restrict foreign viruses. *A3B* mRNA expression has been shown to increase in response to a variety of viruses including polyomavirus and human papilloma virus (Ohba et al., 2014; Smith and Fenton, 2019; Starrett et al., 2019; Verhalen et al., 2016; Vieira et al., 2014). Additionally, *A3A* mRNA expression was found to be induced by the immune signalling proteins IFN1 and IFNγ (Sharma et al., 2015; Thielen et al., 2010). A bioinformatic analysis also concluded that the expression of A3B in non-small cell lung cancer (NSCLC) correlates with the expression of an IFNγ expression signature (Wang et al., 2018). A contrasting bioinformatic analysis of groups of genes co-expressed with specific APOBEC3 genes, arrived at a very different conclusion. This study could not identify a correlation between the expression of either A3A or A3B and the expression of an immune related gene signature, though the expression of all the other APOBEC3 genes did correlate. Furthermore, A3A and A3B expression was found to most closely associate with genes involved in cellular proliferation and the cell cycle, specifically G2/M factors. A3B expression also specifically correlated with the expression a group of approximately 450 validated DNA damage response (DDR) effector genes (Ng et al., 2019; Pearl et al., 2015).

Experimentally it has been shown that A3B mRNA and protein expression is upregulated by agents that cause replication stress and DNA damage including HU, APH, and gemcitabine. In contrast, *A3G* mRNA expression was not increased in response to the same stimuli (Kanu et al., 2016). Treatment with exogenous nucleosides abrogated A3B expression in response to HU, suggesting a role for replication stress in A3B regulation. A3B induction in response to HU was also found to occur in an ATR dependent manner (Kanu et al., 2016). Furthermore, a wide variety of compounds which cause both DNA damage and replication stress as well as irradiation have been shown to increase the expression of the A3B protein (Shimizu et al., 2018; Yamazaki et al., 2020).

A small number of studies have sought to identify gene signalling pathways upstream of A3B in *in vitro* models. Studies have shown that all APOBEC3s are transcriptionally induced in response to p53. The exception is A3B which is repressed by the dimerisation partner, RB-like, E2F and MuvB (DREAM) complex binding to the A3B promoter. p53 response elements have been identified and confirmed in the promoters of all APOBEC3 proteins with the exception of A3D (Menendez et al., 2017). Supporting p53 dependent A3B repression, the expression of A3B in tumour samples was found to negatively correlate with the p53 status of the tumours (Periyasamy et al., 2017). Canonical and non-canonical nuclear factor kappa B (NFκB) signalling has also been found to play a role in the upregulation of A3B. An NFκB binding site has been identified in the A3B promoter and treatment with compounds that induce NFκB signalling such as phorbol myristate acetate (PMA) result in the increase in A3B mRNA and protein expression (Leonard et al., 2015; Maruyama et al., 2016). Another study has shown that protein kinase A (PKA) dependent phosphorylation of A3B on Thr214 leads to A3B inhibition, rendering A3B unable to deaminate ssDNA substrates *in vitro* (Matsumoto et al., 2019).

Events associated with retroelement mobility within the genome has also been suggested as a mechanism of APOBEC3 regulation. One study whole genome sequenced different generations of cell culture clones to be able to determine if and when APOBEC

signatures would arise in cancer cell lines. Many clones spontaneously developed APOBEC mutational signatures demonstrating characteristic clusters of APOBEC mutations (kataegis) without any stimulation or treatment (Petljak et al., 2019). The seemingly random nature of the advent of the APOBEC signature was hypothesised to occur due to an event associated with retroelement mobility within the cell. More research will be required to conclusively demonstrate this however as some cancers such as colorectal cancer have high rates of retro transposition while APOBEC mutagenesis is rare (Alexandrov et al., 2013). These studies represent a base for further research to conclusively determine how the APOBEC signature arises in human cancer.

AIMS

APOBEC proteins have been implicated in the generation of mutational signatures in a high percentage of human cancers (Alexandrov et al., 2020; Alexandrov et al., 2013). We sought to investigate a physiologically relevant mechanism by which the APOBEC mutational signatures could arise. Recently it was shown that hydroxyurea induced replication stress resulted in an up regulation of APOBEC3B and an increase in cellular deamination *in vitro* (Kanu et al., 2016). We tested the hypothesis that the physiologically relevant stress of hypoxia, which also causes replication stress, could lead to the upregulation of APOBEC expression and APOBEC mediated deamination. Further analysis of the cellular response to different types of hypoxia that induce replication stress was undertaken to test this hypothesis. Furthermore, we aimed to uncover evidence of hypoxia-mediated regulation of APOBEC activity in patient samples. Ultimately, we sought to further our understanding of the hypoxic stress response as well as the mechanism of APOBEC induction in human cancer.

Chapter 2

Materials and Methods

Reagents

Table 2.1 - General laboratory and cell culture reagents

Name	Producer/UK distributor
19 G syringe	Terumo
Acrylamide/Bis Solution 30%	BioRad
Agarose	Sigma-Aldrich
AllStars negative control siRNA	Qiagen
Anaerobic indicator strips	OXOID
Boric Acid	Sigma-Aldrich
Bromophenol blue	Sigma-Aldrich
BSA (bovine serum albumin)	Thermo Fisher Scientific
Calcium chloride	Thermo Fisher Scientific
Coverslips 20x20mm	VWR
Chloroform	Thermo Fisher Scientific
Deoxyribonuclease I (DNaseI)	New England Biolabs
DEPC (diethylpyrocarbonate) water	Thermo Fisher Scientific
DharmaFECT 1	Thermo Fisher Scientific
Dithiothreitol (DTT)	Sigma-Aldrich
DMEM (Dulbecco's modified Eagle's medium) media	Sigma-Aldrich
DMSO (dimethylsulphoxide)	Thermo Fisher Scientific
EDTA (ethylenediaminetetraacetic acid)	Sigma-Aldrich
EMEM (Eagle's minimum essential media)	Sigma-Aldrich
Ethanol	Thermo Fisher Scientific
FBS (foetal bovine serum)	Autogen Bioscience
Formaldehyde	Sigma-Aldrich
Gel loading buffer II	Thermo Fisher Scientific
Glycine	Sigma-Aldrich
Glycerol	Thermo Fisher Scientific
HCl (hydrochloric acid)	Sigma-Aldrich
HEK-Blue™ detection kit	Invivogen
HEPES (4-(2-hydroxyethyl)-1-piperazineethanesulfonic acid)	Sigma-Aldrich
Intercept blocking buffer LiCor	Li-Cor
Isopropanol	Thermo Fisher Scientific
Kaleidoscope protein ladder	BioRad
MEGM mammary epithelial cell growth medium bulletkit	Lonza

Methanol	Thermo Fisher Scientific
Mini-PROTEAN TGX pre-cast gels	BioRad
Nonidet P-40	Sigma-Aldrich
Paraformaldehyde	Thermo Fisher Scientific
PBS tablets (phosphate buffered saline)	Thermo Fisher Scientific
Ponceau solution	Sigma-Aldrich
Prolong gold antifade reagent with DAPI	Thermo Fisher Scientific
Propidium iodide (PI)	Sigma-Aldrich
Protease inhibitor cocktail tablets, EDTA-free	Roche
RNAse A (ribonuclease A)	Thermo Fisher Scientific
RMPI 1640 cell media	Sigma-Aldrich
Sodium chloride (NaCl)	Sigma-Aldrich
Sodium dodecyl sulphate (SDS)	Thermo Fisher Scientific
Sodium hydroxide (NaOH)	Sigma-Aldrich
Superfrost Plus microscope slides	Menzel Glaser
SYBR® Green	Thermo Fisher Scientific
TBE-Urea 15% gels	Novex
Trans-blot turbo midi 0.2 μL nitrocellulose transfer packs	BioRad
TRI reagent	Invitrogen
Tris-Glycine	Thermo Fisher Scientific
Triton-X-100	Thermo Fisher Scientific
Trizma Base	Sigma-Aldrich
Trypsin 0.05% EDTA	Sigma-Aldrich
Tween 20	Thermo Fisher Scientific
Ultra-low molecular weight ladder	Thermo Fisher Scientific
Uracil DNA glycosylase (UNG)	New England Biolabs
Uracil glycosylase inhibitor (UGI)	New England Biolabs
Urea	Thermo Fisher Scientific
Verso cDNA synthesis kit	Thermo Fisher Scientific
β-mercaptoethanol	Thermo Fisher Scientific

Table 2.2 - Cell lines

All cell media was supplemented with 10% FBS and cells were maintained in an incubator set to 37ºC and 5% CO_2. Cell lines were verified mycoplasma free using a HEK-Blue™ detection kit (Invivogen).

Cell line	Cell type	Media	Source	p53 status
RKO	colorectal carcinoma	DMEM	ATCC	wt[1]
HCT116	colorectal carcinoma	DMEM	CRUK	wt[2]
MCF7	breast adenocarcinoma	DMEM	Eric O'Neil (University of Oxford)	wt[3]
MCF10A	mammary epithelial	MEGM	Paul Span (Radboud University)	wt[4]
MDAMB231	breast adenocarcinoma	DMEM	Amanda Coutts (Nottingham Trent University)	missense[3]
MRC5	lung fibroblast	EMEM	ATCC	wt[5]
T24	bladder transitional cell carcinoma	DMEM	Anne Kiltie (University of Oxford)	nonsense[6]
VMCUB1	bladder transitional cell carcinoma	DMEM	Anne Kiltie (University of Oxford)	missense[6]
OE21	oesophageal squamous cell carcinoma	RPMI	Ricky Sharma (University College London)	deletion[6]

(Liu and Bodmer, 2006)[1]
(Abu El Maaty et al., 2017)[2]
(Leroy et al., 2014)[3]
(Lim et al., 2009)[4]
(Kollareddy et al., 2015)[5]
(Tym et al., 2016)[6]

Table 2.3 - Drug treatments

Name	Concentration used	Company
Cobalt chloride ($CoCl_2$)	150 μM	Sigma Aldrich
Hydroxyurea (HU)	2 mM	Sigma Aldrich
N'acetylcysteine (NAC)	5 mM	Sigma Aldrich
Bay 11-7085	10-20 μM	Tocris Biosciences
VX-970	1 μM	MedChem Express
AZD6738	5 μM	MedChem Express
BrdU	20 μM	Sigma Aldrich
Roscovitine	20 μM	Selleckchem
PHA-767491	20 μM	Selleckchem

Table 2.4 – Primary antibodies

Name	Species	Dilution	Company	Catalogue number	Application
p53	mouse	1:1000	Santa Cruz	sc-126	WB
p53 S15	rabbit	1:1000	Cell Signaling	9284	WB
RPA	rat	1:1000	Cell Signaling	2208	WB
KAP1	rabbit	1:1000	Bethyl	A300-274A	WB
KAP1 S824	rabbit	1:2000	Bethyl	A300-767A	WB
A3B	rabbit	1:1000	Abcam	ab184990	WB
HIF1α	mouse	1:500	BD biosciences	610958	WB
β-Actin	mouse	1:10000	Santa Cruz	sc-69879	WB
Chk1	mouse	1:1000	Santa Cruz	sc-8408	WB
Chk1 S345	rabbit	1:1000	Cell Signaling	2341	WB
Chk1 S296	rabbit	1:1000	Cell Signaling	D3O9F	WB
H3	mouse	1:1000	Cell Signaling	3638S	WB
H3 S10	rabbit	1:1000	Cell Signaling	9701	WB
ATR	mouse	1:1000	Santa Crus	sc-515173	WB
p65 S536	rabbit	1:1000	Cell Signaling	93H1	WB
Cyclin A	rabbit	1:1000	Abcam	ab181591	WB
53BP1	rabbit	1:500	Novus Biologicals	NB100-904	IF
RPA	rat	1:1000	Cell Signaling	2208	IF
BrdU	mouse	1:50	BD Biosciences	347580	FACS
H3 ser 10	rabbit	1:200	Cell Signaling	9701	FACS

Table 2.5 – Secondary antibodies

Name	Species	Dilution	Company	Catalogue number	Application
IRDye 800CW donkey anti-mouse IgG	mouse	1:10,000	LI-COR	926-32212	WB
IRDye 800CW donkey anti-rabbit IgG	rabbit	1:10,000	LI-COR	926-32213	WB
IRDye 800CW goat anti-rat IgG	rat	1:10,000	LI-COR	926-32219	WB
IRDye 680RD donkey anti-mouse IgG	mouse	1:10,000	LI-COR	926-68072	WB
IRDye 680RD donkey anti-rabbit IgG	rabbit	1:10,000	LI-COR	926-68073	WB
Alexa Fluor 488-conjugated goat anti-rabbit IgG	rabbit	1:200	Invitrogen	A-11008	IF
Alexa Fluor 488-conjugated goat anti-mouse IgG	mouse	1:200	Invitrogen	A-11001	IF/FACS
Alexa Fluor 594-conjugated goat anti-mouse IgG	mouse	1:200	Invitrogen	A11020	IF
Alexa Fluor 594-conjugated goat anti-rat IgG	rat	1:200	Invitrogen	A11007	IF

Table 2.6 – RT-qPCR primers

Gene	Oligonucleotide name	Sequence	Working concentration	Source
18S	18S F5 18S R5	TAGAGGGACAAGTGGCGTTC CGGACATCTAAGGGCATCAC	5 μM	Primer Blast
A3A	A3A_F1 A3A_R1	GGCCCAGACACTTGATGGAT TGTAGAAAGCCCCTGTGCTG	1 μM	Primer Blast
A3A	A3A_F2 A3A_R2	CAGCACAGGGGCTTTCTACA TTCTCCTGAAGGAACGCACG	1 μM	Primer Blast
A3A	A3A_F3 A3A_R3	GAAGGGACAAGCACATGGAAGC ATCTACTTGATCGGGAGCATAC	1 μM	Primer Blast
A3B	A3B_F2 A3B_R2	TCTATGGTCGGAGCTACACTTG GCACATTTCTGCGTGGTACTG	1 μM	Primer Blast
A3C	A3C_F1 A3C_R1	CAAGGACGCTGTAAGCAGGA TGCCTTCATCGGGTTTCTGA	2 μM	Primer Blast
A3D	A3D_F2 A3D_R1	GATAGAGATTGGCGGTGGGT CAGTATGCAAAGTCTTCATAGTCCA	2 μM	Primer Blast
A3F	A3F_F1 A3F_R1	CCGTTTGGACGCAAAGAT CCAGGTGATCTGGAAACACTT	2 μM	Primer Blast
A3G	A3G_F1 A3G_R1	CCGAGGACCCGAAGGTTAC TCCAACAGTGCTGAAATTCG	1 μM	Primer Blast
A3G	A3G_F2 A3G_R2	ACCCTGACCATCTTTGTTGC TCCAACAGTGCTGAAATTCG	1 μM	Primer Blast
A3G	A3G_F3 A3G_R3	GCATCGTGACCAGGAGTATG TCCAACAGTGCTGAAATTCG	1 μM	Primer Blast
A3H	A3H_F1 A3H_R1	GCCAGAAGCACAGATCAGAAAC GCGTCAGCTGGTAACACAAG	5 μM	Primer Blast
INPP5D	INPP5D_F1 INPP5D_R1	GAGAGGAGGGAGCAGAAGGT GCTTTCTGCTTGGTGTAGGC	1 μM	Primer Blast
GLUT1	GLUT1_F1 GLUT1_R1	ATACTCATGACCATCGCGCTAG AAAGAAGGCCACAAAGCCAAAG	4 μM	Primer Blast

Table 2.7 - siRNA

Name	Target	Sequence	Concentration	Company
siA3B_1	A3B	CCUGAUGGAUCCAGACACA[dt][dt]	50 nM	Sigma Aldrich
siA3B_2	A3B	GGUGUAUUUCAAGCCUCAGUU[dt][dt]	50 nM	Sigma Aldrich
siATR	ATR	CAGGCACTAATTGTTCTTCAAd[T]d[T]	50 nM	Invitrogen
sip53	p53	GUAAUCUACUGGGACGGAA[dT][dT]	50 nM	Ambion

Table 2.8 - Oligonucleotides

Name	Sequence	Application
Total probe 3	ATTATTATTANTCAAATGGATTTATTTATTTATTTATTTATTT'FAM (fluorescein)	Deamination Assay

Hypoxia Treatments

Chronic Hypoxia (<0.1% O_2)

A Bactron II anaerobic chamber (Shell Labs) was used for all chronic hypoxia treatments at <0.1% O_2. The oxygen concentration in the chamber was periodically tested with an Oxylite oxygen probe (Oxford Optronix) to ensure the oxygen level was below <0.1%. Additionally, anaerobic indicators (OXOID) were frequently used to detect any leaks. Cells were plated on glass dishes, as plastic dishes can retain oxygen, and grown at 37°C. Cells were lysed in the chamber to avoid reoxygenation.

Cyclic and 2% O_2

A Don Whitley M35 variable atmosphere workstation was used for all cyclic hypoxia and chronic hypoxia treatments at 2% O_2. Built-in oxygen, hydrogen, and CO_2 probes constantly measure the concentrations of these gasses in the chamber. The temperature of the whole chamber was set to 37°C. For cyclic treatments, the chamber was automatically set to cycle between the chosen oxygen concentrations for the chosen times. The oxygen probe was calibrated before every experiment and the hydrogen-activated palladium catalyst was changed every 3-6 months to ensure rapid elimination of oxygen. Cells were plated on glass dishes and harvested as in the Bactron II anaerobic chamber.

Laboratory Techniques

Western Blot

Cells were scraped into 1 mL PBS, pelleted, and lysed in 70-160 μL of HED lysis buffer (25 mM HEPES, 5 mM EDTA, 10% glycerol, 0.2% NP-40, 1 mM DTT (added fresh), 1X protease inhibitor (Roche) (added fresh)). Samples were sonicated for 20 s 2X with 5 s on ice in between before being pre-cleared by centrifugation at 16,200 g for 10 min at 4°C. Protein concentration was measured with a Nanodrop 1000 (Fisher Scientific) and 20-50 μg of protein was then mixed with sample buffer (3.3% SDS, 6 M urea, 17 mM Tris-HCl (pH 7.5), 0.07 M β-mercaptoethanol, 0.01% Bromophenol blue) and heated at 100°C for 10 min. 5 μL of kaleidoscope protein ladder (BioRad) was loaded into one of the lanes in order to allow analysis of the molecular weight of the bands. Samples were electrophoresed in Tris-glycine running buffer (25 mM Tris base, 192 mM glycine, 0.1% (w/v) SDS) on 4-20% Mini-PROTEAN TGX pre-cast gels (BioRad) at 120 V for 40-70 min. Gels were washed briefly in transfer buffer (25 mM Tris base, 150 mM glycine, 20% (v/v) methanol) and then electro-transferred onto 0.4 μm nitrocellulose membranes with a Transblot-Turbo machine (BioRad). The membranes were then blocked in Intercept blocking buffer (LI-COR) buffer diluted 1:1 in Tris-Buffered Saline (TBS) (50 mM Tris-HCl, pH 7.6, 150 mM NaCl) for 1 hr. Membranes were probed with primary antibody (diluted in 1:1 LI-COR buffer: TBS-Tween) overnight at 4°C while shaking. The antibodies used can be found in Table 2.4. Membranes were washed 3X in TBS-Tween for 5 min each time before being probed with IRDye 680 or 800 (LI-COR) secondary antibody (diluted to 1:10,000 in 1:1 LI-COR buffer: TBS-Tween) for 1-2 hr at room temperature (RT) with shaking. The membranes were then washed 3X in TBS-Tween. Membranes were developed using the Odyssey infrared imaging system.

Deamination assay

Cells were scraped into 1 mL PBS, pelleted, and lysed in 70-160 μL of HED lysis buffer (25 mM HEPES, 5 mM EDTA, 10% glycerol, 1X protease inhibitor, 1 mM DTT). Cells were then homogenised with a 19 G syringe (Terumo) before sonication with a bioruptor (Diagenode) on

the low intensity setting for 2 cycles of 10 s on, 20 s off. Samples were then pre-cleared by centrifugation at 16,200 g for 10 min at 4°C. Protein concentrations were equalised to 5 μg/mL using a Nanodrop 1000 (Fisher Scientific). A reaction mix to allow deamination was made containing 8.25 μL of each cleared lysate, 0.625 μL of RNase A (Fisher Scientific), 0.625 μL of 1X TE buffer and 0.5 μL of a 200 μM solution of a fluorescently tagged oligonucleotide containing an APOBEC deamination sequence (Table 2.8). After incubation at 37°C for 3 hr, 100 mM of NaOH was added and samples were heated to 95°C for 30 min. Samples were then mixed with Gel Loading Buffer II (Fisher Scientific) and heated at 70°C for 3 min before being run on a 15% TBE-urea gel for 70 min. Product and substrate bands denoting deamination were imaged with a Chemidoc touch imaging system (Biorad). Intensity of the product band denoting the amount of deamination that had occurred in that treatment condition was determined with Fiji image analysis software.

Small interfering RNA gene knockdown (siRNA)

Cells were seeded into 6-well plates such that they would be approximately 40% confluent the next day and left overnight to attach. Reaction mixtures A and B were made in cell media without FBS. Master mix A was made consisting of 5 μL of siRNA (20 μM stock), 20 μL of DEPC water (Thermo Fisher) and 25 μL of cell media without FBS per treatment condition well. As a negative control for each treatment condition an additional reaction mix A was made containing 5 μL of scrambled siRNA (Qiagen). Master mix B was made consisting of 5 μL of DharmaFECT (Dharmacon) and 345 μL cell media without FBS per treatment condition well. Reaction mixtures were incubated at RT for 5 min. The two mixtures were then gently mixed together and incubated for 20 min. Cell media was removed from the 6-well plates and 400 μL of the siRNA/Dharmafect reaction mixture was added to the cells. 1.6 mL of fresh media was then added such that the final concentration of siRNA in each well was 50 nM. Cells were incubated overnight and then then trypsinised and re-plated on glass dishes in preparation for

treatments. The cells were used 24-48 hr post-transfection. siRNA sequences used can be found in Table 2.7.

RNA extraction and purification

Cells were washed with 1 mL of PBS and then scraped into 1 mL of Trizol (Invitrogen). 200 μL of chloroform was added, samples were vortexed for 15 s and then centrifuged at 16,200 g for 15 min. The clear top layer on each sample which contains the RNA fraction was pipetted into a fresh Eppendorf and mixed with 500 μl of isopropanol. Samples were gently mixed and then centrifuged at 16,200 g for 10 min. The supernatant was pipetted off and the pellet mixed with 1 mL of 70% ethanol. Samples were vortexed briefly and then centrifuged at 7500 g for 5 min. As much supernatant as possible was pipetted off and the residual ethanol was left to evaporate off the pellet. After drying, the pellets were resuspended in 60 μL of DEPC water and the concentration of RNA was measured with a Nanodrop 1000 (Fisher Scientific). To degrade any residual DNA, 10 μg of RNA was mixed with DNaseI (NEB) and DNaseI reaction buffer (NEB) and incubated at 37°C for 30 min. 1 μL of EDTA (0.5 M) was then added to each sample to neutralise the DNaseI before a further incubation at 75°C for 10 min.

cDNA library creation

To reverse transcribe the RNA into cDNA the Verso enzyme kit (Thermo Scientific) was used. A reaction master mix was made containing 5X cDNA synthesis buffer, dNTP mix, random hexamers, RT enhancer, and verso enzyme added to the manufacturer's specifications. The master mix was combined with 1 μg of the RNA samples and spun down to ensure even mixing of reagents. Samples were then placed in a polymerase chain reaction (PCR) machine (Applied biosystems) and treated according to the following schedule to generate cDNA: 42°C for 60 min, 95°C for 2 min, and then 4°C. Samples were then placed in the freezer at -20°C until needed.

Quantitative reverse transcriptase PCR (RT-qPCR)

The SYBR Green PCR Master Mix kit (Applied Biosystems) was used for all RT-qPCR experiments. cDNA was first diluted 1/25 in DEPC water. Master mixes for the chosen primer sets were made combining 12.5 μL of SYBR green with 2.5 μL of the forward primer, 2.5 μL of the reverse primer, and 2.5 μL of DEPC water. 20 μL of the primer master mixes were mixed with 5 μL of the diluted cDNA samples in a 96 well plate and spun down. 3 technical replicates were run for each gene/primer set combination. Samples were run in a StepOne Real-Time PCR System (Thermo Scientific). Relative fold change values for tested genes relative to control were determined using the ΔΔct method using 18S as an endogenous control. Graphs were plotted using the mean of three biological replicates ± SEM. Primers sequences used are given in Table 2.6.

Immunofluorescence (IF) microscopy

Cells were seeded onto autoclaved cover slips (Menzel Glaser) before treatment. After treatment, cells were fixed with 4% fixation buffer (4% (w/v) paraformaldehyde in PBS) for 10 min at RT. Samples were permeabilised with 1% PBS-Triton X-100 (Thermo Fisher) for 10 min and blocked in 2% (w/v) bovine serum albumin (BSA) (Thermo Fisher) in 0.1% PBS-tween for 1 hr. Coverslips (VWR) were flipped cell side down onto 150 μL of primary antibody diluted with 2% BSA in 0.1% PBS-T on a parafilm covered surface for 90 min at 37°C. The primary antibodies used can be found in Table 2.4. Coverslips were then washed with chilled 0.25% PBS-T before incubation with secondary antibodies conducted in the same manner. After secondary antibody treatment, coverslips were again washed with 0.25% PBS-T and then mounted in Prolong gold antifade reagent with 4′,6-diamidino-2-phenylindole (DAPI) (Thermo Fisher) and left to set overnight. Nail polish was added to the corner of coverslips to bind them to the slide. Proteins were visualised with an LSM710 confocal microscope (Carl Zeiss Microscopy Ltd) and at least 150 cells were counted per condition. DNA damage and replication stress were quantified by counting cells with >5 53BP1 foci or >6 RPA foci

respectively. Foci were counted using a macro run on Fiji image analysis software. Briefly, cells are divided into individual entities based on the borders of their DAPI staining. An intensity threshold is then set that defines the minimum value for a foci to be counted. This threshold is then applied to each cell and any cells with >5 for 53BP1 or >6 for RPA are counted as having DNA damage or replication stress respectively present in that cell.

Flow cytometry (FACS)

BrdU (20 μM) was added to cells 1 hr before harvest and plates were placed in the dark. Cells were then washed in 1 mL PBS, trypsinised and transferred to 15 mL falcon tubes (BD Biosciences). Fresh media was added to the tubes to deactivate the trypsin and samples were centrifuged at 750 g for 5 min. The supernatant was removed, and cells were then fixed in ice-cold 70% ethanol added to the tube dropwise to avoid cell clumping. Cells were fixed for at least 30 min on ice before centrifuging at 750 g for 5 min and removing the supernatant. Samples were then treated with 2 M HCl (Sigma Aldrich) for 20 min after which 2 mL of PBS was added into the tubes to dilute the HCl and they were centrifuged at 1000 g for 5 min. The supernatant was removed, and samples were then blocked in 2% FBS in PBS solution, centrifuged at 1000 g and the supernatant removed. Samples were then treated with 100 μL of BrdU primary antibody (BD biosciences) diluted 1:50 in PBS overnight at 4°C while on a shaker. 1 mL of PBS was added, samples were centrifuged at 1000 g for 5 min and the supernatant removed. Samples were then incubated with 100 μL of Alexa Fluoro 488 (Invitrogen) diluted 1:200 in PBS. 1 mL of PBS was added to the samples before centrifugation at 1000 g for 5 min and after removal of the supernatant a mixture was added containing 1 mL PBS, 20 μL propidium Iodide (Sigma Aldrich), and 5 μL RNaseA (NEB) and samples were incubated at 37°C for 30 min. Samples were run on a BD FACSCaliber machine (BD biosciences) and BrdU/PI plots were analysed with FloJo software.

Bioinformatics

Hypoxia expression signature (hypmet)

RNA-seq expression data from TCGA firehose legacy datasets was accessed through http://www.cbioportal.org/. The raw expression of 51 genes within a validated hypoxia signature, termed the hypoxia metagene, (Buffa et al., 2010) in addition to the 7 APOBEC3 genes was downloaded from each dataset. First the median expression of each of the 51 genes was calculated across all samples in each dataset. The expression of each gene in a given sample was then normalised against the median expression of that gene in the whole dataset. Next the median of each of the 51 normalised gene values within a given sample was calculated and the log10 value of this was taken. This final value represents the "hypmet" for each given tumour in the dataset analysed. The hypmet for each tumour sample was then correlated with the expression of an individual APOBEC3 gene or the number of APOBEC mutations. A spearman coefficient was used to determine the strength of the correlation.

Group of hypoxia-inducible p53 target genes (p53genes)

Expression data for 6 hypoxia specific p53 target genes (BTG2, CYFIP2, INPP5D, KANK3, PHLDA3 and SULF2) (Leszczynska et al., 2015) was taken and analysed as with the hypmet. The final value represents the "p53genes" value for each given tumour in each dataset.

APOBEC mutations

Mutational data from different TCGA datasets was obtained from a previous study (Roberts et al., 2013a). 6 TCGA datasets were chosen where there were >100 samples with both available mutational and expression data (BRCA, KIRC, LUAD, STAD, LUSC, OV). APOBEC mutations were defined as the number of C to T or C to G mutations occurring in the TCW sequence context. 0.5 was added to the number of APOBEC mutations in each tumour so that tumours where no APOBEC mutations are present can still be graphically represented and the log10 of this value was calculated. The number of APOBEC mutations in each sample was then

correlated with the hypmet value of each sample in these 6 datasets. A spearman coefficient was used to determine the strength of the correlation.

Statistical Analysis

All experiments consist of three independent biological replicates unless otherwise indicated. Error bars represent standard error of the mean (SEM) of three independent biological repeats unless otherwise indicated. A two-tailed, unpaired t-test was used for the comparison of two means and a one-way analysis of variance (ANOVA) was used for the comparison of more than two means. Statistical significance was assumed if $p<0.05$ (* $p<0.05$, ** $p<0.01$, *** $p<0.001$).

Chapter 3

Expression and activity of APOBECs in chronic hypoxia

Introduction

Replication stress is defined as conditions which stall or impede active DNA replication forks, resulting in an accumulation of ssDNA (Puigvert et al., 2016). Many endogenous and exogenous agents can cause replication stress, such as a lack of materials required for DNA replication or DNA damage (Zeman and Cimprich, 2014). In hypoxic conditions, replication stress has been shown to occur through the depletion of nucleotides resulting from a decrease in the efficiency of the enzyme responsible for the rate limiting step in the production of dNTPs, ribonucleotide reductase (RNR) (Foskolou et al., 2017). Evaluation of DNA replication in hypoxia using the DNA fiber technique has shown a significant decrease in fork speeds as well as a significant increase in stalled replication forks that can be rescued by reoxygenation (Foskolou et al., 2017; Pires et al., 2010). Importantly only severe levels of hypoxia <0.1% O_2 have been shown to lead to nucleotide depletion and replication stress (Olcina et al., 2013).

As previously discussed, the APOBEC protein family was initially identified as a system of cellular viral immunity, however recently has been implicated as a source of genomic instability in cancer (Harris, 2015; Venkatesan et al., 2018). A3A and A3B have emerged as the APOBECs most likely to be responsible for the generation of the APOBEC mutational signature in human cancers (Alexandrov et al., 2013; Burns et al., 2013b; Roberts et al., 2013b). Though not much is known about the regulation of APOBECs in cancer, one study has demonstrated that treating cells with agents that cause replication stress induces the mRNA expression of *A3B* and *A3G* (Kanu et al., 2016). Additionally, p53 response elements have been identified in the promoters of all APOBEC3 genes and validated by chromatin immunoprecipitation (ChIP) with the exception of A3D (Menendez et al., 2017). Contrasting the rest of the family where p53 induces mRNA expression, p53 has been shown to repress *A3B* mRNA expression through DREAM complex (Periyasamy et al., 2017).

We hypothesised due to the fact that replication stress could regulate APOBECs, that hypoxia, through its effect on replication stress, could also be a mechanism of APOBEC regulation. Hypoxic APOBEC regulation could represent a possible explanation of how the APOBEC mutational signature arises in human cancers, as hypoxia is a physiologically relevant stress.

Results

3.1 - Chronic hypoxia causes replication stress in an oxygen dependent manner

To confirm the induction of replication stress, RKO cells were exposed to chronic hypoxia (<0.1% O_2) and phosphorylated RPA and Chk1 were measured by western blot. Both RPA and Chk1 are phosphorylated at specific residues by ATR in response to replication stress (Liu et al., 2012; Zhao and Piwnica-Worms, 2001). RPA32 phosphorylation increased in chronic hypoxia (<0.1% O_2) but then returned to near normoxic levels after longer exposure (20 hr). Phosphorylated Chk1 also followed the same pattern of expression. Importantly, the induction of replication stress in response to chronic hypoxia was confirmed to be oxygen dependent, with no replication stress observed at 2% O_2 (Figure 3.1). HIF1α was used as a positive control for hypoxic conditions as it is stabilised in <0.1 and 2 but not 21% O_2.

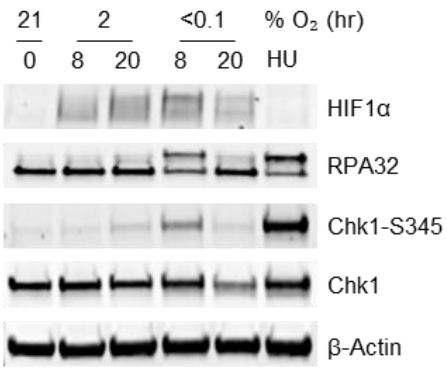


Figure 3.1 – Replication stress signaling increases in chronic hypoxia (<0.1% O_2)
RKO cells were exposed to the indicated oxygen concentrations or HU (2 mM, 20 hr) for the indicated times and western blotting was carried out; β-actin was used as a loading control.

3.2 - HU induces the expression of multiple APOBECs

It has been previously shown that replication stress can induce the expression of different members of the APOBEC3 family. A3B and A3G were both shown to increase in response to HU, an inhibitor of ribonucleotide reductase (RNR) that causes replication stress (Kanu et al., 2016). To determine if this held true in the RKO cell line, we treated cells with HU and assayed for the mRNA expression of all 7 APOBEC3 genes by RT-qPCR. Out of the 7 APOBEC3

genes, *A3A* and *A3G* could not be detected utilising three distinct primer sets for each gene. A significant increase in the mRNA expression of *A3B*, *A3C*, *A3D*, *A3F*, and *A3H* can be seen upon HU treatment (Figure 3.2 A-E).

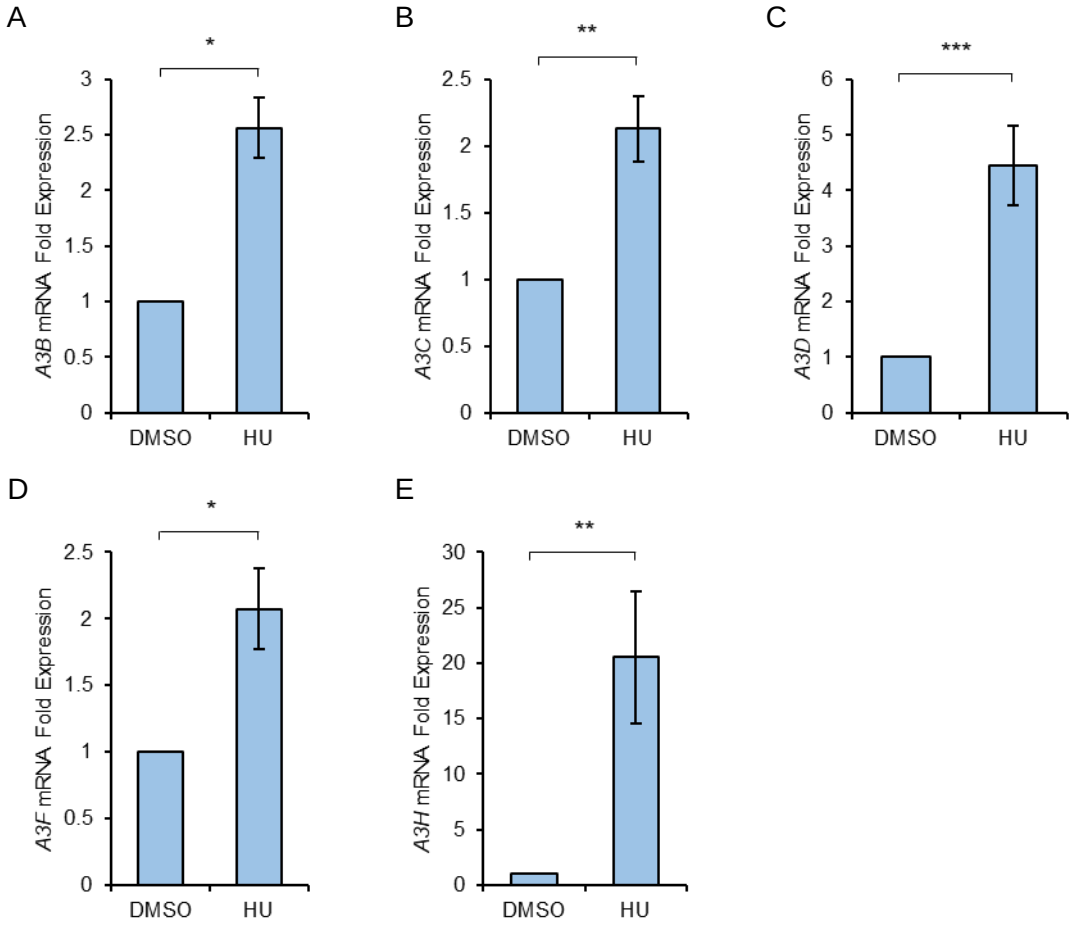


Figure 3.2 – mRNA expression of multiple APOBEC3s increases in response to HU
(A-E) RKO cells were treated with 2 mM HU or DMSO for 20 hr and RT-qPCR was carried out. The mRNA levels of (A) *A3B*, (B) *A3C*, (C) *A3D*, (D) *A3F*, and (E) *A3H* are shown as a relative fold change to the DMSO treated condition. Data show mean ± s.e.m. from n=3 biological experiments. A two-tailed unpaired t-test analysis was applied.

3.3 - Multiple APOBEC3s are induced at the mRNA level in chronic hypoxia (<0.1% O_2) in an oxygen dependent manner

We hypothesised that levels of chronic hypoxia low enough to cause replication stress (<0.1% O_2) should also lead to an increase in APOBEC3 expression. To determine the

expression of APOBEC3 family members in response to chronic hypoxia, RKO cells were exposed to <0.1 or 2% O_2 followed by RT-qPCR. 2% O_2 was included as a hypoxic treatment condition that does not cause replication stress (Figure 3.1) Of the 5 APOBEC3s detected, *A3D* and *A3H* were significantly induced in chronic hypoxia specifically in response to <0.1% O_2 (Figure 3.3 A, B). A similar pattern of expression was observed for *A3C* and *A3F* although this failed to reach statistical significance (Figure 3.3 C, D). To verify that APOBEC3 induction in response to <0.1% O_2 was not restricted to the RKO cell line, we determined the expression of *A3H* in the MCF-7 cell line and again observed a significant increase at multiple timepoints (Figure 3.3 E).

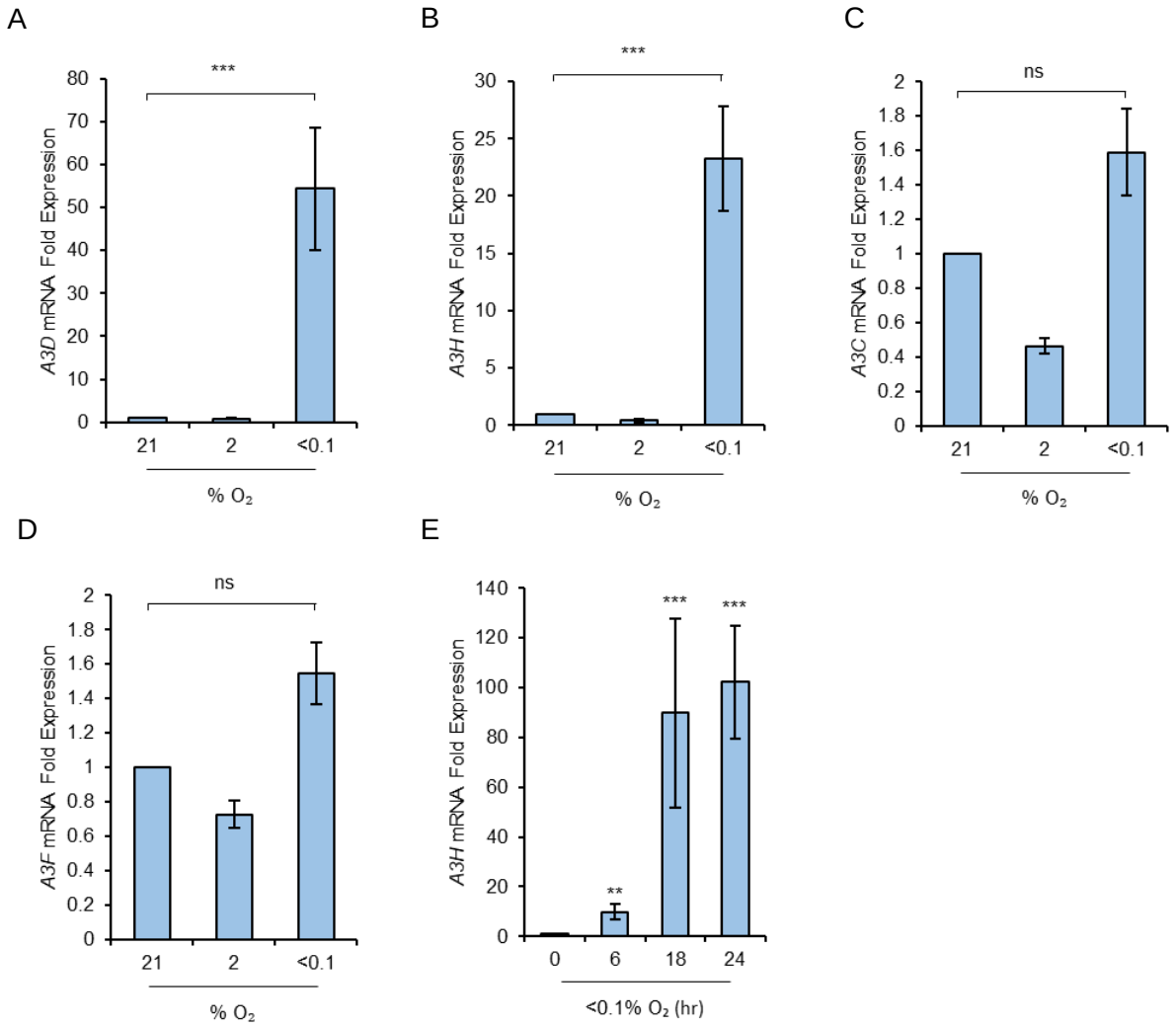


Figure 3.3 – mRNA expression of multiple APOBEC3s increases in response to chronic hypoxia (<0.1% O_2)

(A-D) RKO cells were treated with the indicated oxygen concentrations for 20 hr and RT-qPCR was carried out. The mRNA levels of (A) *A3D*, (B) *A3H*, (C) *A3F*, and (D) *A3C* are shown as a relative fold change to normoxic (21% O_2) levels. Data show mean ± s.e.m. from n=3 biological experiments. A one-way ANOVA analysis was applied.

(E) MCF7 cells were treated in <0.1% O_2 for the indicated times and RT-qPCR was carried out. Data show mean ± s.e.m. from n=3 biological experiments. A one-way ANOVA analysis was applied.

3.4 – A3D and A3H are induced in chronic hypoxia in a HIF1 independent manner

The induction of *A3D* and *A3H* at <0.1 but not at 2% O_2 suggests that HIF1 is not involved in APOBEC3 expression, as HIF1 is stabilised at both <0.1 and 2% O_2 (Figure 3.1). To

corroborate this, we utilised RKO cells with and without HIF1α (Dang et al., 2006). To confirm the loss of HIF1α in the RKO$^{HIF1α-/-}$ cells, we treated both RKO$^{HIF1α+/+}$ and RKO$^{HIF1α-/-}$ cells in chronic hypoxia (<0.1% O_2) and measured the mRNA levels of *GLUT1* by RT-qPCR. *GLUT1* mRNA expression is induced in response to HIF1 signalling in chronic hypoxia (Chen et al., 2001). As expected, we detected increased *GLUT1* mRNA expression at the 6 hr timepoint followed by a return to normoxic levels at later timepoints in the RKO$^{HIF1α+/+}$ cell line but not in the RKO$^{HIF1α-/-}$ cell line (Figure 3.4 A). Declining HIF1 target expression over time is also to be expected as HIF1 signalling upregulates negative feedback pathways to limit continuous HIF1 downstream signalling (Bardos and Ashcroft, 2005). To determine the HIF1 dependency of *A3D* and *A3H* induction in chronic hypoxia, RKO$^{HIF1α+/+}$ and RKO$^{HIF1α-/-}$ cells were treated with chronic hypoxia (<0.1% O_2) and the levels of *A3D* and *A3H* mRNA determined. Induction of *A3D* in response to chronic hypoxia was not changed by the lack of HIF1α while the induction of *A3H* in response to chronic hypoxia increased further in RKO$^{HIF1α-/-}$ cells, demonstrating the induction occurs in a HIF1 independent manner as well (Figure 3.4 B, C). To further test the HIF1 dependency of the *A3D* and *A3H* induction in chronic hypoxia, we utilised the iron chelator cobalt chloride ($CoCl_2$), which is capable of stabilising HIF1α in normoxic conditions (Figure 3.4 D). Neither *A3D* nor *A3H* was induced in response to $CoCl_2$, though robust HIF1α stabilisation was observed (Figure 3.4 D, E, F). These data demonstrate that neither *A3D* nor *A3H* were induced in a HIF1 dependent manner in chronic hypoxia.

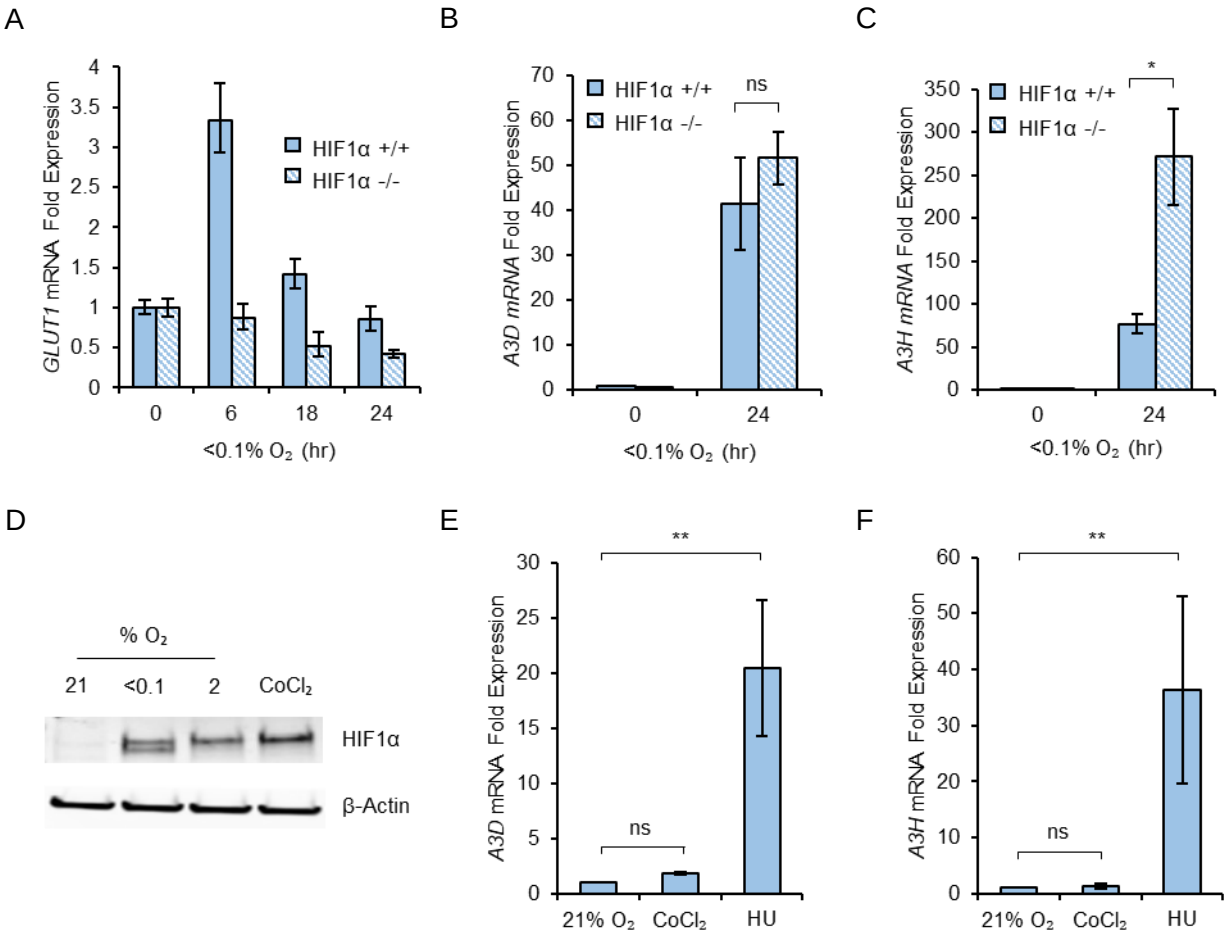


Figure 3.4 – mRNA induction of *A3D* and *A3H* in chronic hypoxia is HIF1 independent

(A) RKO$^{HIF1\alpha+/+}$ and RKO$^{HIF1\alpha-/-}$ cells were treated with <0.1% O_2 for the indicated times and RT-qPCR was carried out. Data show mean ± error bars calculated by StepOne software (Applied Biosystems) based on 3 technical replicates (n=1).

(B, C) RKO$^{HIF1\alpha+/+}$ and RKO$^{HIF1\alpha-/-}$ cells were treated with <0.1% O_2 for 24 hr and RT-qPCR was carried out. Data show mean ± s.e.m. from n=3 biological experiments. A two-tailed unpaired t-test analysis was applied.

(D) Western blot of RKO cells exposed to the indicated oxygen tensions or $CoCl_2$ (150 μM) for 20 hr.

(E, F) RKO cells were treated with $CoCl_2$ (150 μM) or HU (2 mM) for 20 hr and RT-qPCR was carried out. Data show mean ± s.e.m. from n=3 biological experiments. A one-way ANOVA analysis was applied.

3.5 - A3D and A3H are induced in chronic hypoxia in a p53 dependent manner

Both A3D and A3H have been described previously as targets of the p53 transcription factor, suggesting that chronic hypoxia-induced p53 could transactivate A3D/A3H (Menendez et al., 2017; Periyasamy et al., 2017). A p53 binding site has also been identified and experimentally confirmed in the A3H promoter (Menendez et al., 2017). In support of p53 dependent *A3D* and *A3H* induction, the stabilisation of activated p53 in chronic hypoxia shows the same oxygen dependency as observed for *A3D*/*A3H* induction (Figure 3.3 A, B, 3.5 A). Using siRNA specific for p53 (sip53) or a scrambled control (siSCR), expression of p53 was knocked down in normoxic (21% O_2) and chronic hypoxic (<0.1% O_2) conditions. Successful p53 knockdown was measured by a decrease in mRNA expression of a validated hypoxia inducible p53 target gene (Figure 3.5 B). As expected, in the absence of p53 the chronic hypoxia (<0.1% O_2) induced expression of both *A3D* and *A3H* was abrogated, demonstrating they are induced in a p53-dependent manner in chronic hypoxia (Figure 3.5 C, D).

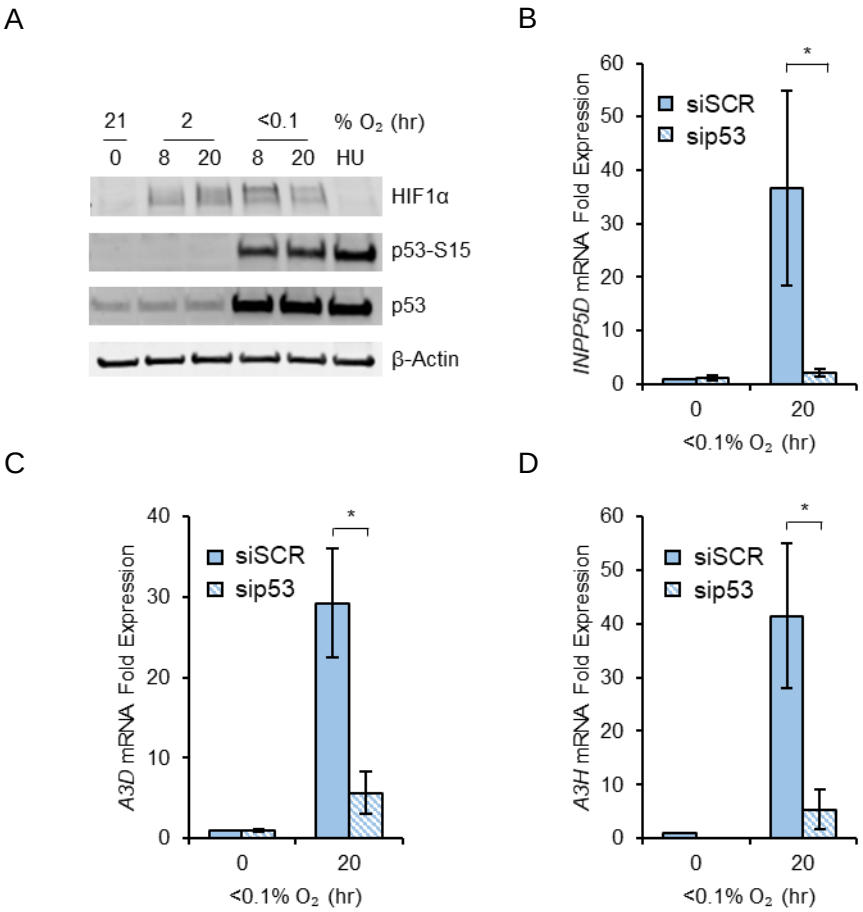


Figure 3.5 - mRNA induction of *A3D* and *A3H* in chronic hypoxia is p53 dependent
(A) RKO cells were exposed to the oxygen concentrations indicated for the times shown or HU (2 mM, 20 hr). Western blotting was carried out.
(B-D) RKO cells were treated with siRNA to p53 (sip53) or a scramble control (siSCR) followed by exposure to <0.1% O_2 for 20 hr. mRNA levels of *INPP5D* (B), *A3D* (C), and *A3H* (D) are shown relative to the normoxic control. Data show mean ± s.e.m. from n=3 biological experiments. A two-tailed unpaired t-test analysis was applied.

3.6 - A3B mRNA and protein expression decreases in chronic hypoxia in a p53 independent manner

In contrast to *A3D*, *A3H*, *A3C* and *A3F*, the expression of *A3B* mRNA decreased in response to chronic hypoxia (<0.1% O_2) (Figure 3.6 A). The level of A3B protein in response to chronic hypoxia also decreased while a clear induction was observed in HU treated cells (Figure 3.6 B). To confirm that the decreased A3B mRNA and protein expression in response

to chronic hypoxia was not restricted to RKO cells, we measured the levels of *A3B* mRNA in response to chronic hypoxia in 5 additional cancer and 2 non-cancerous cell lines, and saw a reduction in each (Figure 3.6 C). Previous reports have suggested that p53 can repress the expression of *A3B* mRNA via an indirect mechanism through the DREAM complex (Periyasamy et al., 2017). Additionally, a p53 binding site has been identified in the A3B promoter region (Menendez et al., 2017). Repression of A3B by p53 in chronic hypoxia seemed unlikely however, as decreased expression of *A3B* was observed in several p53 mutant cell lines (Figure 3.6 C, D). To formally verify this we depleted p53 by siRNA in chronic hypoxia. As previously shown a decrease in A3B protein expression in response to chronic hypoxia can be seen, however knocking down p53 had no impact (Figure 3.6 E).

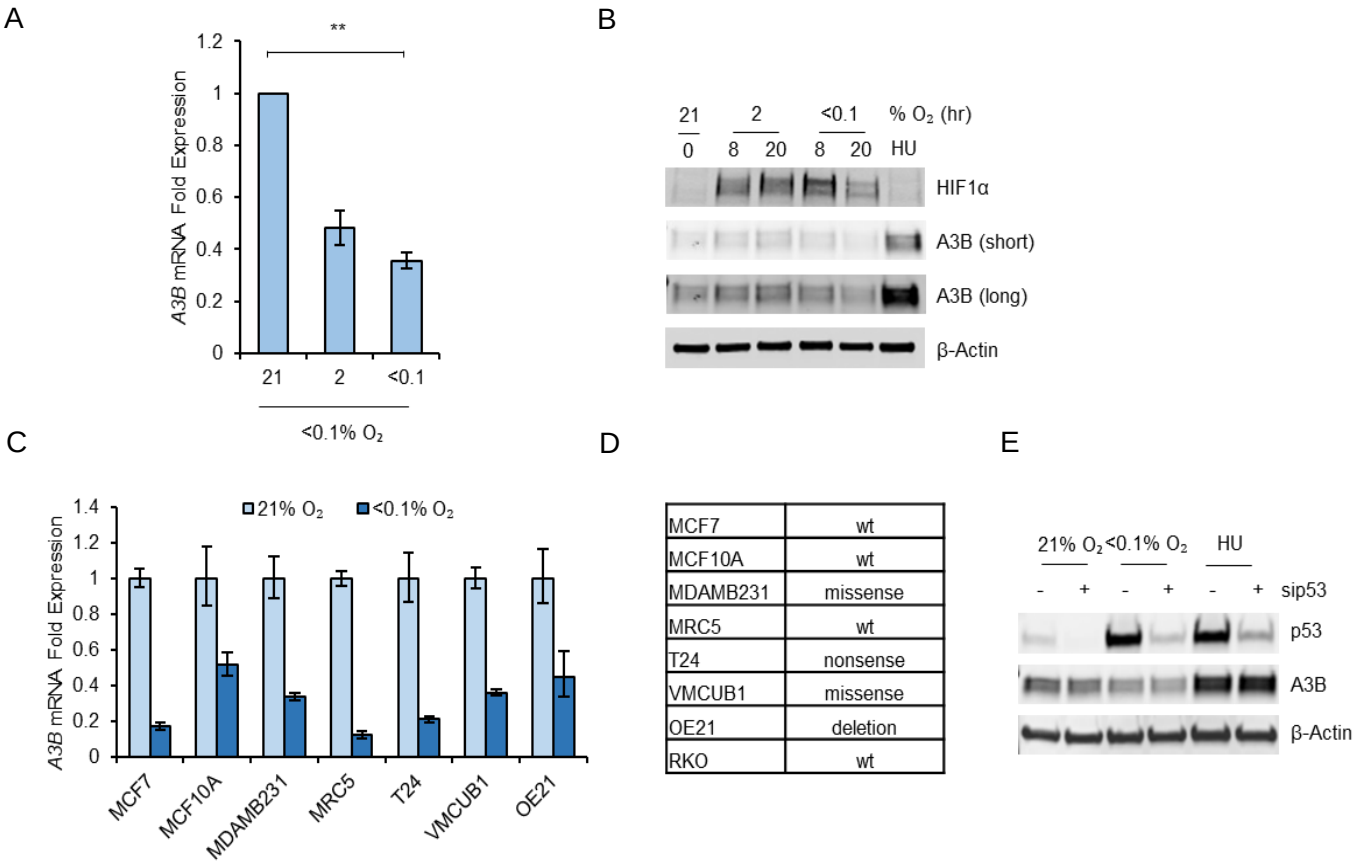


Figure 3.6 – A3B expression decreases in chronic hypoxia in a p53 independent manner
(A) RKO cells were exposed to the oxygen concentrations indicated for 20 hr and RT-qPCR was carried out. Data show mean ± s.e.m. from n=2 biological experiments. A one-way ANOVA analysis was applied.

(B) RKO cells were exposed to the oxygen concentrations indicated for the time shown or HU (2 mM, 20 hr) followed by western blotting. A3B long and short exposures are shown.

(C) Indicated cell lines were treated with <0.1% O_2 or normoxia for 20 hr before harvest. RT-qPCR was carried out for *A3B* mRNA expression. Data show mean ± error bars calculated by StepOne software (Applied Biosystems) based on 3 technical replicates (n=1).

(D) The p53 status of the cell lines in (C) are indicated.

(E) RKO cells were treated with siRNA to p53 (sip53) or a scramble control (siSCR) followed by exposure to the indicated oxygen concentration or HU (2 mM) for 20 hr. Western blotting was carried out (n=2).

3.7 - An in vitro deamination assay to determine the functional activity of APOBECs

To measure the output of APOBEC enzymatic activity, an *in vitro* deamination assay was used (Figure 3.7). This assay measures the ability of APOBEC proteins within in a sample lysate to

deaminate a ssDNA oligonucleotide containing the APOBEC consensus deamination sequence. The sequence of this probe can be found in Table 2.8. As there is very little difference between the deamination sequence preferences for each APOBEC3 protein, excluding A3G, this assay measures the amount of deamination resulting from the enzymatic activity of all APOBEC3 proteins except for A3G in a given treatment sample. To begin, the ssDNA oligonucleotide is mixed with the sample lysate and active APOBEC3 enzymes deaminate the cytosine present within the ssDNA oligonucleotide. If deamination has occurred, the endogenous UNG enzymes within the cells then excise the uracil base creating an abasic site. Upon treatment with NaOH and heat, any abasic sites are cleaved, breaking the oligonucleotide into smaller fragments. The intact and cleaved oligonucleotides can then be run on a gel and imaged. The intensity of the cleaved band can be used to assess how much deamination has occurred in that treatment sample (Kanu et al., 2016; Starrett et al., 2016).

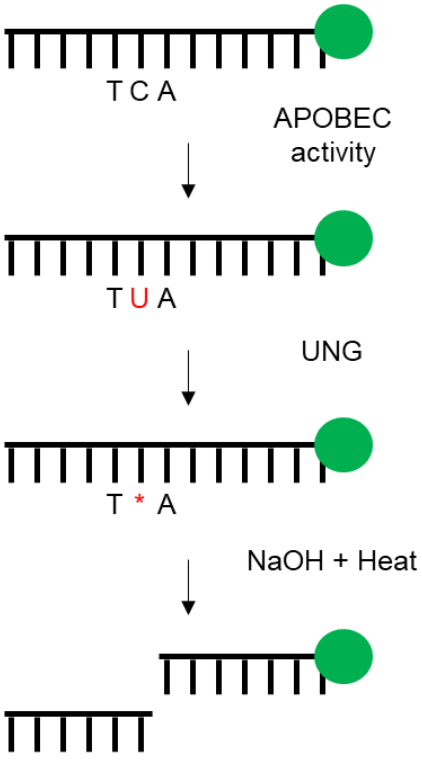


Figure 3.7 – *In vitro* deamination assay schematic
A schematic outlining the steps in the *in vitro* deamination assay. Individual black lines represent nucleotide bases and the green circle denotes the fluorescein tag. Treatments for the lysates at each step in the process are indicated.

3.8 - Deamination decreases in chronic hypoxia

As all members of the APOBEC3 family have deamination activity, we hypothesised that deamination would increase in response to chronic hypoxia (<0.1% O_2) as a result of increased expression of *A3D*, *A3H*, *A3C*, and *A3F*, despite the reduced expression of *A3B*. Using the *in vitro* deamination assay, we observed the expected increase in deamination in response to treatment with HU, however deamination significantly decreased in chronic hypoxia (<0.1% O_2) (Figure 3.8 A, B). These data suggested that the expression of A3B, which has been reported to be one of the two APOBECs primarily responsible for the generation of the APOBEC mutational signature, might also dictate the level of deamination in chronic hypoxia. Most interestingly, these data highlight a difference in the biological response to chronic hypoxia and HU induced replication stress, and suggest that APOBEC activity is not induced in response to all conditions which lead to replication stress.

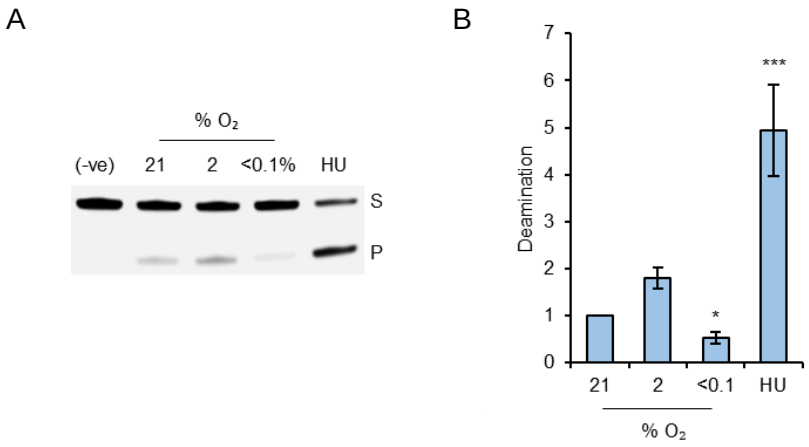


Figure 3.8 – Deamination decreases in response to chronic hypoxia <0.1% O_2
(A) An *in vitro* deamination assay was carried out on RKO cells exposed to the indicated oxygen concentrations or HU (2 mM) for 20 hr. The top band (S) is the substrate band and the bottom band (P) is the product band (n=2).
(B) Quantification of data in (A) where the average intensity of the product band (P) across 2 biological repeats is plotted relative to the intensity of the normoxic product band. Data show mean ± s.e.m. from n=2 biological experiments. A one-way ANOVA analysis was applied.

Discussion

Here we have shown that multiple APOBEC3 mRNA transcripts are induced in an oxygen dependent manner in response to chronic hypoxia (<0.1% O_2). The induction of *A3D* and *A3H* was found to be HIF1 independent and p53 dependent. Contrasting the other members of the APOBEC3 gene family, A3B mRNA and protein expression decreased in hypoxia in multiple cancerous and non-cancerous human cell lines. Using an *in vitro* deamination assay capable of detecting total APOBEC3 mediated deamination in different treatment conditions, we observed a decrease in deamination in chronic hypoxia. Though *A3D*, *A3H*, *A3C*, and *A3F* mRNA expression increased in chronic hypoxia (<0.1% O_2), the level of APOBEC mediated deamination mirrored that of *A3B* mRNA expression and decreased. This suggests that deamination in the RKO cell line depends primarily on the expression of A3B.

A limitation of our study was that A3A expression could not be detected in the RKO cell line. As previously discussed, in addition to A3B, A3A is thought to be the APOBEC3 gene primarily responsible for the generation of the APOBEC mutational signatures in human cancers. However, A3A expression is generally restricted to immune cells and is seldomly detected in cancer cell lines derived from other tissues (Burns et al., 2013b; Koning et al., 2009; Ng et al., 2019). Further study in alternative cell line models would be required to determine the effect of hypoxia on A3A expression and activity. A single study has shown that *A3A* mRNA expression decreases in response to mild chronic hypoxia (1% O_2) in MEPs and macrophages (Sharma et al., 2015).

An important area of further study concerns the functional purpose of *A3D*, *A3H*, *A3C*, and *A3F* induction in chronic hypoxia. As APOBEC3s can also bind RNA as a substrate, mRNA editing as an additional mechanism of gene regulation has been proposed as a possible function of the family. Recently, a limited number of studies have implicated both A3A and A3G in mRNA editing (Sharma et al., 2017; Sharma et al., 2016; Sharma et al., 2015). Interestingly, while there was overlap between the transcripts edited by A3A and A3G, many

were specifically edited by one or the other. These observations bring up two interesting questions. Firstly, whether the APOBECs upregulated in hypoxia can contribute to gene regulation through mRNA editing and secondly, if so, do they influence overlapping or distinct sets of genes? Furthermore, A3A was shown to edit the mRNA of a specific gene, SDHB, and this activity increased further in response to mild levels of chronic hypoxia (1% O_2) (Sharma et al., 2015). Further study would be required to determine whether hypoxic regulation of APOBEC mRNA editing by A3A is a global phenomenon or restricted to specific genes such as SDHB.

Contrasting data from other papers, where p53 dependent repression of A3B was demonstrated in response to compounds that stabilise p53 such as nutlin, the decrease in A3B expression in chronic hypoxia occurs in a p53 independent manner (Menendez et al., 2017; Periyasamy et al., 2017). Interestingly, it has been previously shown that hypoxia-induced p53 target genes differ significantly from classic p53 targets induced in response to DNA damage (Koumenis et al., 2001; Leszczynska et al., 2015). It is possible that A3B regulation is another example of a stress-specific p53-mediated response. We have yet to elucidate how A3B expression decreases in chronic hypoxia. One possibility is the fact that global gene transcription is repressed in hypoxic conditions (Johnson et al., 2008). Due to the hostile nature of hypoxia treatment, cells have been shown to halt the transcription of any genes that do not directly benefit their survival to conserve key cellular resources (Johnson et al., 2008). A3B may fall into this large group of genes.

A surprising result was seen in the fact that transcription of *A3H* mRNA in chronic hypoxia increased further in $RKO^{HIF1\alpha-/-}$ cells relative to $RKO^{HIF1\alpha+/+}$ cells. Though not experimentally determined, we theorise this could occur due to increased availability of a co-factor involved in the promotion of *A3H* transcription that is shared by HIF1 and p53. If availability of this co-factor is a limiting factor in p53 dependent *A3H* transcription, then lack of HIF1 could increase *A3H* transcription. A potential candidate is the transcriptional co-activator

p300, where p53 and HIF1 have been reported to compete for limited quantities to drive expression of their downstream targets (Schmid et al., 2004).

Our results suggest that not all agents that cause replication stress have the same impact on biological signalling. When considering the effects of replication stress inducing agents such as HU, it is important to consider the other effects that they may have on the cell such as DNA damage. Supporting this notion, DNA damage has been shown in response to HU treatment while no such damage is observed in response to chronic hypoxia (Bencokova et al., 2009; Petermann et al., 2010).

Chapter 4

Investigation of hypoxic conditions which lead to replication catastrophe

Introduction

An important distinction is whether a stress causes replication stress or replication catastrophe. The distinction is important as it can influence the biological response to the stress (Toledo et al., 2017). Replication catastrophe is a phenomenon where DNA damage occurs due to the exhaustion of the global pool of RPA. Cells experiencing replication catastrophe are characterised by the occurrence of replication stress and DNA damage markers in the same cell (King et al., 2015; Toledo et al., 2013; Warren and Eastman, 2019). Any cellular processes that result in RPA binding to ssDNA can potentially lead to RPA exhaustion and subsequent replication catastrophe (Toledo et al., 2017). An example is firing an excess of DNA replication origins, where more ssDNA is created than the cell has free RPA to coat.

It has been well established that treating cells in conditions of chronic hypoxia that cause replication stress (<0.1% O_2) does not lead to DNA damage/replication catastrophe (Bencokova et al., 2009; Foskolou et al., 2017; Olcina et al., 2013). The lack of DNA damage in chronic hypoxia (<0.1% O_2) has been attributed to the observed decrease in replication rates. In this situation, though exposed ssDNA is present, the lack of DNA replication likely serves to protect the cell from further ssDNA accumulation beyond the levels capable of being bound by free RPA, and thus the cells would not experience replication catastrophe. As previously discussed however, hypoxia *in vivo* is not a static state (Bristow and Hill, 2008; Dewhirst et al., 2008). Dynamic fluctuations in oxygen tensions within tumours span oxygen levels that can have markedly different effects on cells treated *in vitro*. For example, as previously shown, cells treated with <0.1% O_2 experience replication stress while cells treated with 2% O_2 do not (Figure 3.1) (Olcina et al., 2013). Contrasting our view on chronic hypoxia (<0.1% O_2), we hypothesised that *in vitro* oxygen fluctuations between levels of hypoxia that

cause replication stress (<0.1% O_2), and levels of oxygen that allow for normal DNA replication (2% O_2), could allow for the maintenance of DNA replication in hypoxic conditions through the firing of new DNA replication origins, and result in replication catastrophe. Here, we examine different hypoxic and drug (HU) induced stress conditions to determine the differences and similarities between key attributes such as the cell cycle and the propensity for replication catastrophe.

Results

4.1 - DNA Replication is severely compromised in chronic hypoxia but continues with HU treatment

To investigate the contrasting biological responses to chronic hypoxia (<0.1% O_2) and HU, we began by determining the impact of both stresses on DNA replication. RKO cells were exposed to HU or chronic hypoxia and both propidium iodide (PI) and bromodeoxyuridine (BrdU) incorporation was analysed. As expected, cells treated with chronic hypoxia arrested in G1 while cells treated with HU arrested in early S-phase (Figure 4.1 A, B) (Gardner et al., 2001; Kramer et al., 2008). Also, as expected, both chronic hypoxia (<0.1% O_2) and HU lead to a significant decrease in BrdU incorporation, indicating decreased DNA replication (Figure 4.1 C). Total levels of BrdU incorporation, and thus DNA replication, were measured by taking the mean value of the fluorescent intensity of the BrdU antibody signal in each cell, termed the mean fluorescence intensity (MFI). Surprisingly, the HU treated cells incorporated significantly more BrdU compared to the chronic hypoxic, cells suggesting ongoing DNA replication (Figure 4.1 C). The most noticeable difference between the two treatments was the presence of a sub-G1 population indicative of apoptosis in the chronic hypoxic cells but not the HU treated cells. This was surprising given that the induction of p53 is similar in both cases (Figure 3.5 A, 4.1 D).

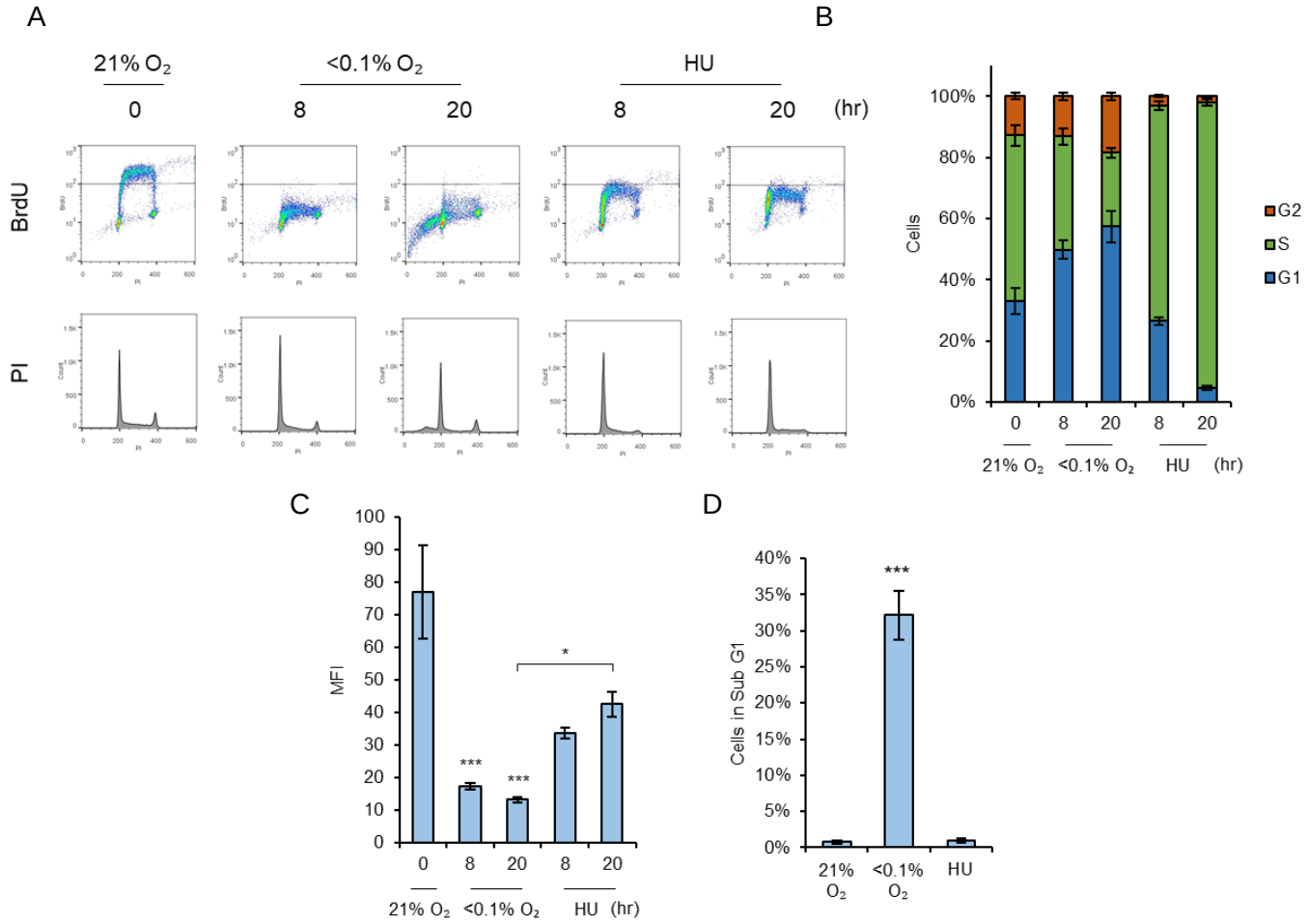


Figure 4.1 – Chronic hypoxia and HU results in decreases in DNA replication to differing levels

(A) RKO cells were exposed to <0.1% O_2 or HU (2 mM) for the indicated times. Cells were labeled with BrdU (20 μM) 1 hr prior to collection and analysed by FACS. A dotted line is provided as a reference for the comparison of BrdU intensity values between plots.

(B) The cell cycle phase of cells in each condition in (A) is shown

(C) The mean fluorescence intensity (MFI) of cells in each condition in (A) is shown. Data show mean ± s.e.m. from n=3 biological experiments. One-way ANOVA analysis was applied.

(D) The percentage of RKO cells treated with <0.1% O_2 or HU (2 mM) for 20 hr in the sub G1 cell cycle phase. Data show mean ± s.e.m. from n=3 biological experiments. One-way ANOVA analysis was applied.

4.2 – Ongoing replication in HU treated cells includes origin firing

Cells employ a variety of methods to attempt to continue DNA replication in conditions that cause replication stress (Mechali, 2010). To test if DNA replication in HU treated cells is

maintained by new origin firing, we used an inhibitor commonly used to restrict new origin firing via the inhibition of CDK1, 2, 5 and 7, roscovitine (Ros), and determined the impact on BrdU incorporation (Davies et al., 2007; Toledo et al., 2013). Inhibiting origin firing significantly decreased DNA replication in HU treated cells compared to control cells. No significant effect was seen upon addition of roscovitine to cells treated with chronic hypoxia (Figure 4.2 A, B).

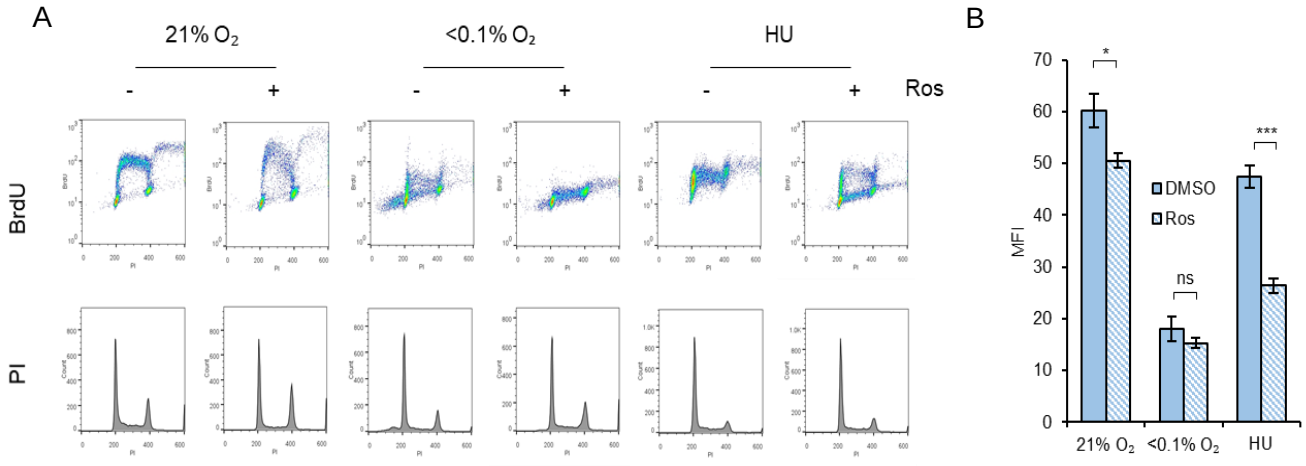


Figure 4.2 – inhibiting new origins stops DNA replication with HU treatment but has no impact in chronic hypoxia

(A) RKO cells were pre-treated with DMSO or roscovitine (20 μM) 30 min before exposure to the indicated oxygen tension or HU (2 mM) for 20 hr. Cells were pulsed with BrdU (20 μM) 1 hr prior to collection and analysed by FACS.

(B) Quantification of the data shown in (A) showing the mean fluorescence intensity in each condition. Data show mean ± s.e.m. from n=3 biological experiments. One-way ANOVA analysis was applied.

4.3 – Cells experience replication catastrophe with HU treatment but not chronic hypoxia

We hypothesised that ongoing DNA replication through new origin firing in HU treated cells would lead to RPA exhaustion and ultimately replication catastrophe (King et al., 2015; Toledo et al., 2017; Toledo et al., 2013). In contrast, cells in chronic hypoxia do not fire new origins, and thus should maintain a supply of available RPA and avoid replication catastrophe. To definitively confirm replication catastrophe in response to HU but not chronic hypoxia, we co-stained treated cells for a marker of DNA damage (53BP1) and replication stress (RPA) and

measured the proportion of cells that contained >5 53BP1 and >6 RPA foci. A significant increase in the number of cells with >5 53BP1 and >6 RPA foci was observed in the HU treated condition relative to normoxia, while there was no significant increase in chronic hypoxia (Figure 4.3 A, B). These data demonstrate that the conditions of HU induced replication stress, which lead to APOBEC activity, progress to replication catastrophe while replication catastrophe does not occur in response to chronic hypoxia. In addition to the large proportion of cells that experience replication catastrophe, approximately 80% of cells treated with HU experience replication stress (Figure 4.3 A, B). These data fit with our previous observations regarding the cell cycle in cells treated with HU, which show a large cell cycle arrest in early S-phase (Figure 4.1 A, B).

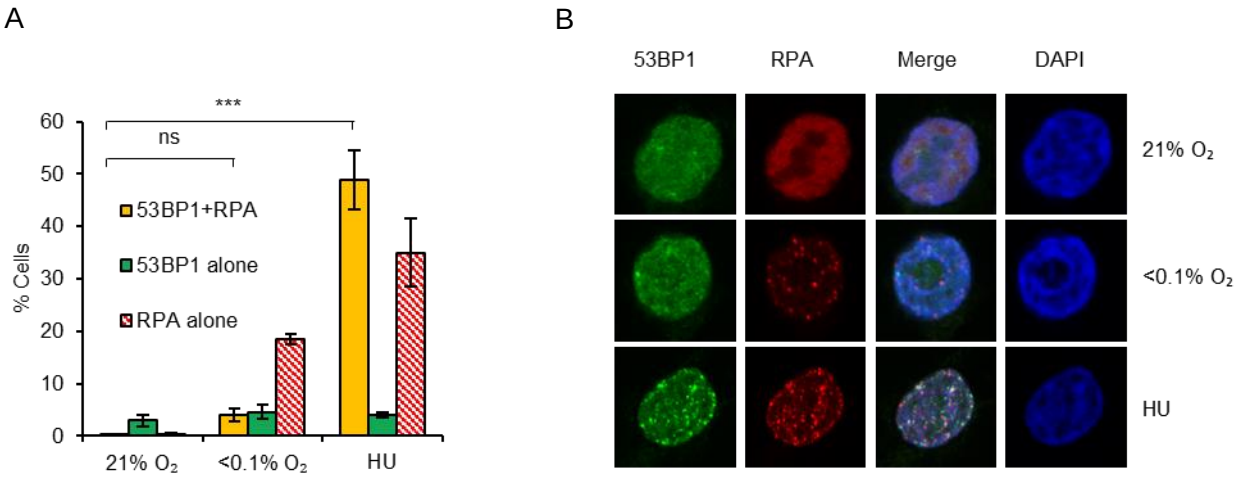


Figure 4.3 – Replication catastrophe in cells treated with HU but not chronic hypoxia
(A) RKO cells were exposed to <0.1% O_2 or HU (2 mM) for 20 hr. 53BP1 and RPA foci were visualised by immunofluorescence. The percentages of cells with >5 53BP1 and >6 RPA foci are shown. Data show mean ± s.e.m. from n=3 biological experiments. One-way ANOVA analysis was applied.
(B) Representative pictures of data shown in (A)

4.4 - A novel in vitro system for studying hypoxia

These data led us to refine our original hypothesis and consider that APOBEC activity is induced by replication catastrophe as opposed to replication stress. To test this hypothesis,

we considered hypoxic conditions which could include new origin firing, and thus could maintain active DNA replication, potentially leading to replication catastrophe. Specifically, we asked if including periods of milder hypoxia (2% O_2), which alone do not induce replication stress but stabilise HIF1, to cells treated in conditions of severe hypoxia that do cause replication stress (<0.1% O_2) might lead to the exhaustion of the available RPA pool and the DNA damage associated with replication catastrophe through ongoing replication. Using a hypoxia chamber capable of rapidly switching between multiple oxygen concentrations, we investigated conditions of cyclic hypoxia consisting of periods of <0.1% O_2 and 2% O_2 (Figure 4.4 A). Measurements of oxygen concentrations were taken using a built-in oxygen probe over the course of all cyclic experiments (Figure 4.4 B). Importantly, both levels of hypoxia used (<0.1 and 2% O_2) are physiologically relevant.

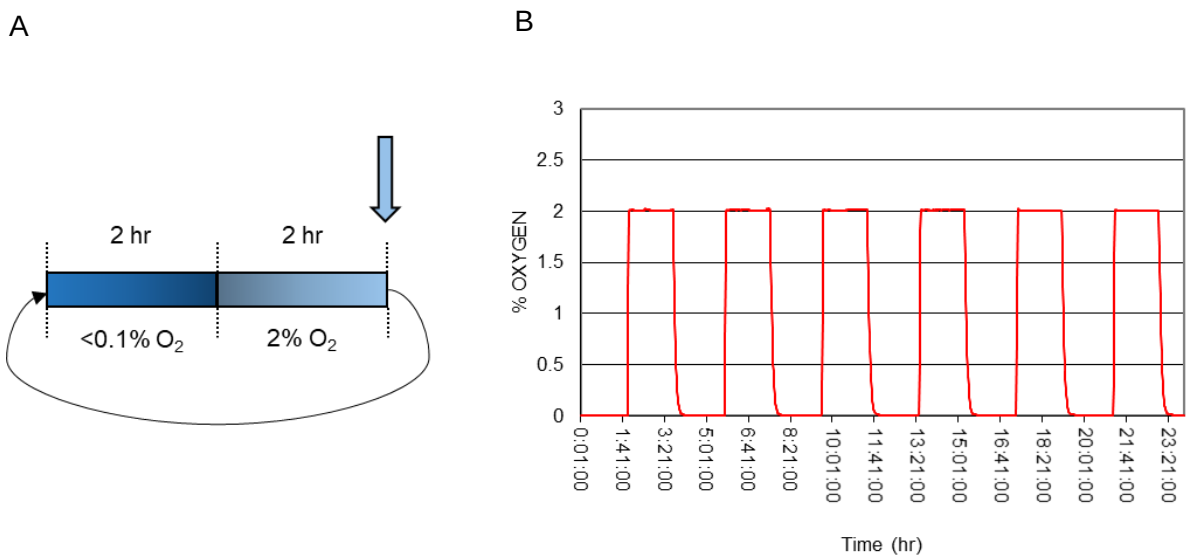


Figure 4.4 – Oxygen conditions used to model cyclic hypoxia *in vitro*
(A) A schematic outlining the cyclic hypoxia treatment schedule. Cells were treated with <0.1% O_2 for 2 hr followed by 2% O_2 for 2 hr. This cycle then repeats. The blue arrow indicates the point at which samples were harvested i.e. within the last 5 min of the 2% O_2 segment.
(B) A representative readout of the oxygen percentage over the course of an experiment from the built-in oxygen probe contained within the Don Whitley M35 variable atmosphere workstation.

4.5 - Cyclic hypoxia causes prolonged replication stress

Using our cyclic hypoxia time course, we confirmed that the addition of these periods of milder hypoxia (2% O_2) still led to replication stress by showing that both Chk1 and RPA were phosphorylated in cyclic hypoxia (Figure 4.5 A). As seen previously both RPA32 and Chk1 phosphorylation was reduced after 20 hr in chronic hypoxia (<0.1% O_2), however these phosphorylations appeared to be maintained in cyclic hypoxia. To investigate further, we determined the number of cells with >6 RPA foci in each condition and found that the percentage of cells with RPA foci increased over time in cyclic hypoxia, while in chronic hypoxia they formed and were then resolved (Figure 4.5 B, C). Interestingly, when we determined the number of RPA foci per cell, we saw that this number remained constant in cyclic conditions while it decreased over time in chronic (Figure 4.5 D). Together, these data suggest that replication stress persists in cyclic but not chronic hypoxia.

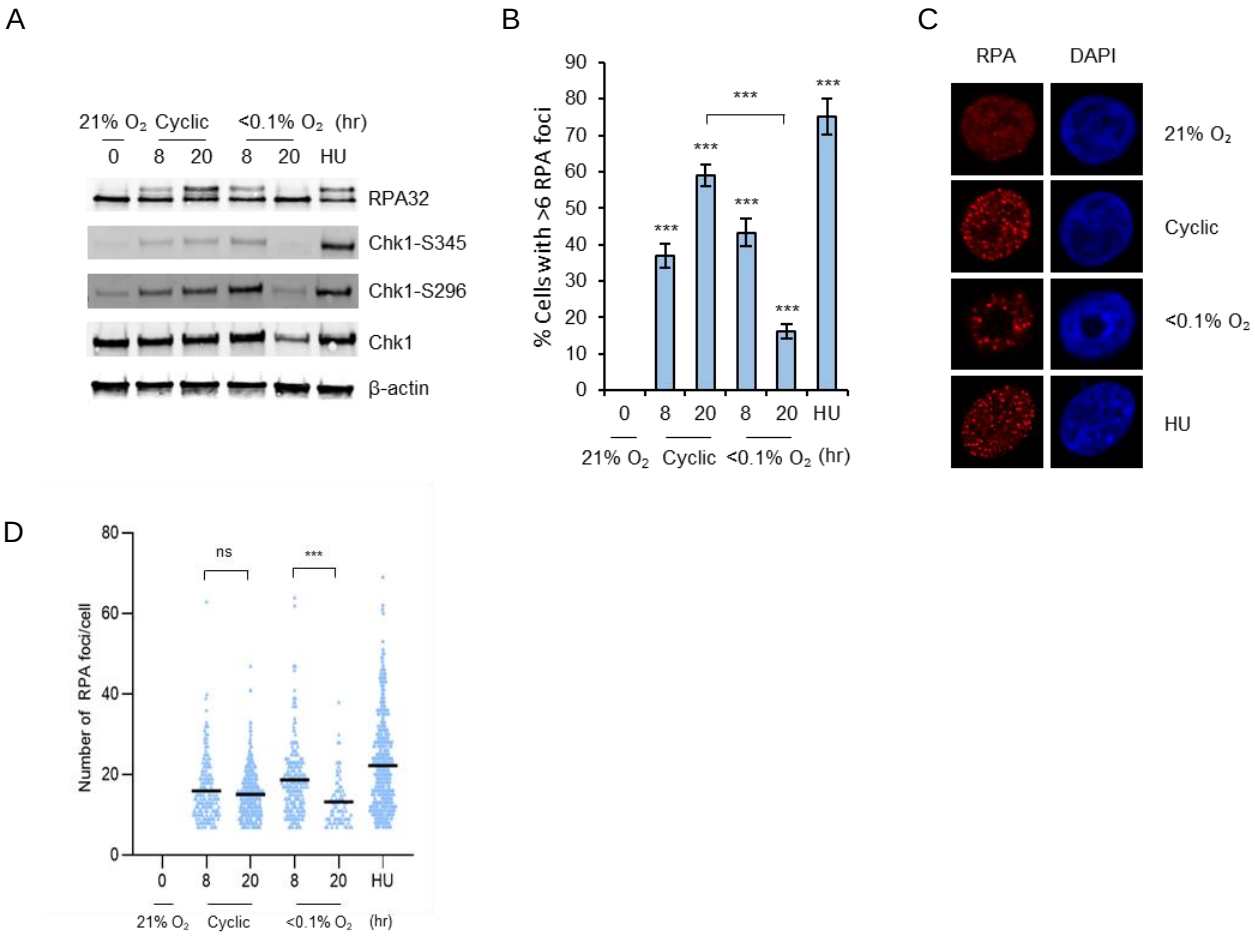


Figure 4.5 – Cyclic hypoxia causes replication stress that is maintained

(A) RKO cells were exposed to the oxygen concentrations indicated for the times shown or HU (2 mM, 20 hr). Western blotting was carried out.

(B) RPA foci were visualised by immunofluorescence in RKO cells treated with the indicated times of cyclic or chronic hypoxia (<0.1% O_2). The percentage of cells with >6 RPA foci is shown. Data show mean ± s.e.m. from n=3 biological experiments. One-way ANOVA analysis was applied.

(C) Representative images from data shown in (B).

(D) RKO cells were treated with the indicated oxygen concentrations or HU (2 mM) for the indicated times as in (B). The number of foci in every cell that had experienced replication stress (>6 RPA foci) under each treatment condition is shown. Black bars represent the mean number of RPA foci of all cells included in this analysis from n=3 biological experiments. One-way ANOVA analysis was applied.

4.6 - DNA replication is maintained in cyclic hypoxia

To assess both the nature of DNA replication and the cell cycle dynamics present in cyclic hypoxia, we carried out both BrdU incorporation and PI staining. In contrast to chronic hypoxia,

cells in cyclic hypoxia maintained incorporation of BrdU, demonstrating ongoing DNA replication. This can be seen by non-significant differences in the MFI when comparing different timepoints in cyclic hypoxia to normoxia (Figure 4.6 A, B). Quantification of the cell cycle phase showed that cells slowly moved through S-phase before eventually arresting in G2 (Figure 4.6 C). These data show that DNA replication is maintained in cyclic but not chronic hypoxia (<0.1% O_2).

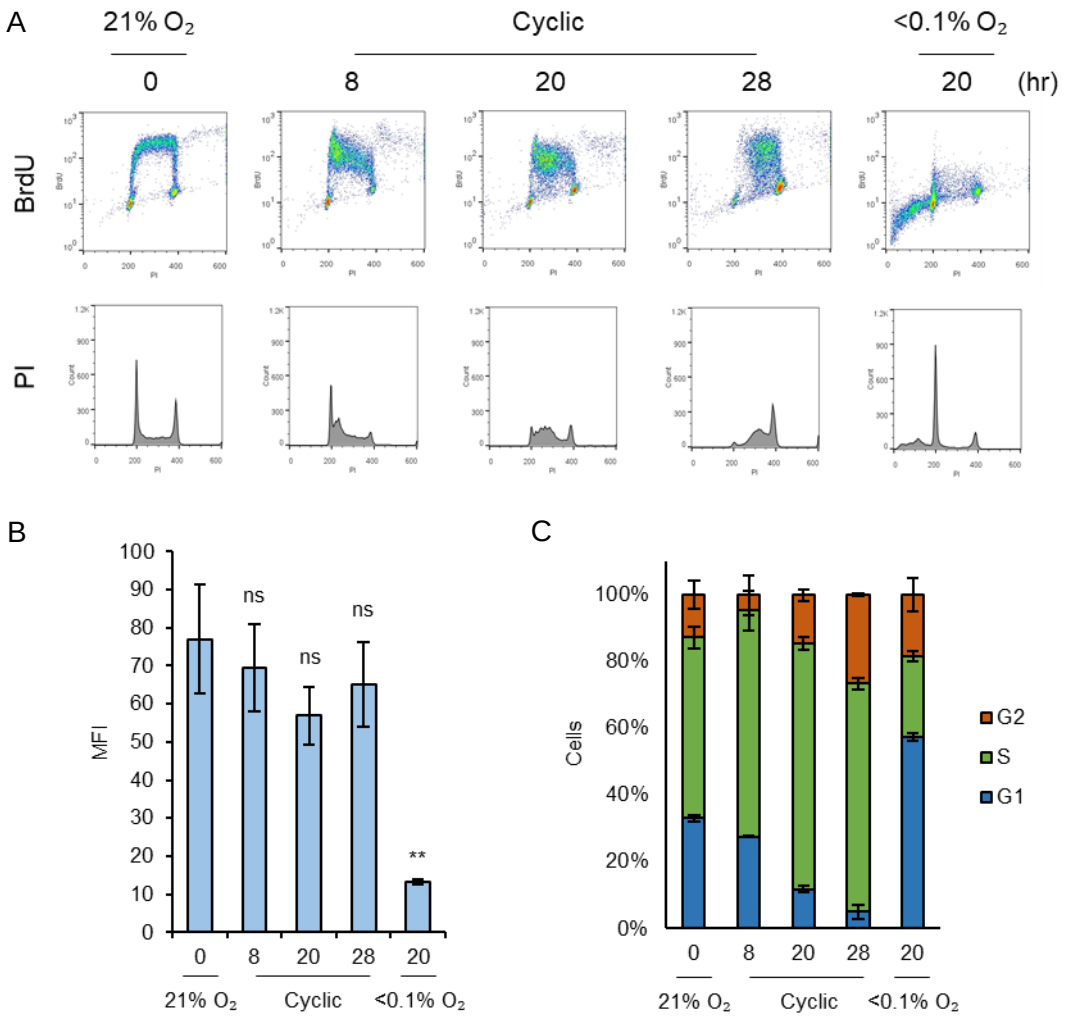


Figure 4.6 – BrdU incorporation persists in cyclic hypoxia

(A) RKO cells were exposed to cyclic or chronic hypoxia for the indicated times. Cells were labeled with BrdU (20 μM) 1 hr prior to collection and analysed by FACS. The chronic hypoxia data is taken from Figure 4.1 A for comparison

(B) Quantification of the data in (A) where the MFI is shown. The chronic hypoxia data is taken from Figure 4.1 C for comparison. Data show mean ± s.e.m. from n=3 biological experiments. One-way ANOVA analysis was applied.

(C) Quantification of the data in (A) where the percentage of cells in each phase of the cell cycle is shown. The chronic hypoxia data is taken from Figure 4.1 B for comparison

4.7 - Cells arrest in the G2-phase of the cell cycle in cyclic hypoxia

It has been previously shown that cells that experience replication catastrophe eventually arrest in the G2-phase of the cell cycle (Toledo et al., 2013). A G2 arrest in cyclic hypoxia was

confirmed by staining for histone 3 (H3) phosphorylation on serine 10, detected by both FACS and western blot. An H3 serine 10 phosphorylation is an indicator of mitosis, as it represents a crucial step in the mitotic pathway (Prigent and Dimitrov, 2003). The absence of this mark after 20 hours of cyclic hypoxia indicates a G2 arrest (Figure 4.7 A, B, C).

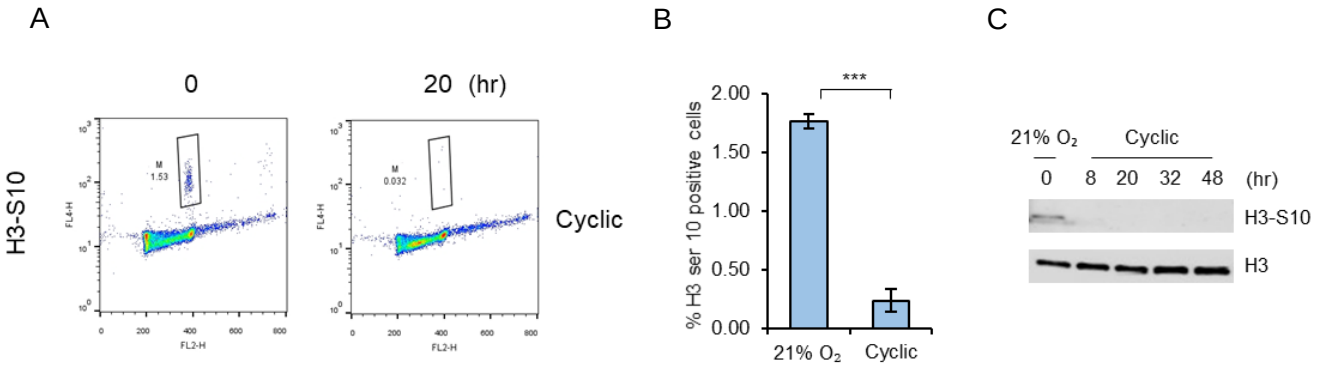


Figure 4.7 – A G2 cell cycle arrest in cyclic hypoxia
(A) RKO cells were exposed to cyclic hypoxia for 20 hr. FACS was carried out to assess the percentage of cells with H3 ser 10 positive staining. The x axis denotes the intensity of the PI staining.
(B) Quantification of data shown in (A). Data show mean ± s.e.m. from n=3 biological experiments. A two-tailed unpaired t-test was applied.
(C) RKO cells were exposed to cyclic hypoxia for the indicated timepoints. Western blotting was carried out (n=1).

4.8 – DNA replication is maintained through new origin firing in cyclic hypoxia

To determine whether the ongoing replication in cyclic hypoxia was also due to the firing of new origins, as it was with HU treatment, we again treated cells with roscovitine. A significant decrease in the MFI of Ros treated cells compared to the DMSO treated control cells was observed in cyclic hypoxia. This suggests that ongoing replication in cyclic hypoxia is due to the firing of new origins (Figure 4.8 A, B).

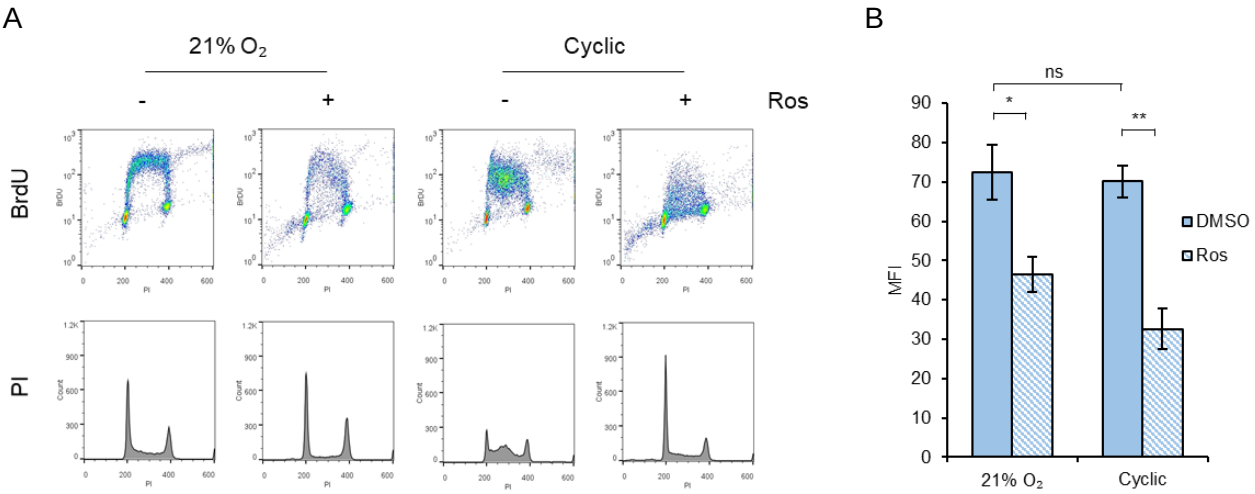


Figure 4.8 – New origins fire in cyclic hypoxia

(A) RKO cells were pretreated with DMSO or roscovitine (Ros) (20 μM) for 30 min and exposed to 21% O_2 or cyclic hypoxia for 20 hr. Cells were labeled with BrdU (20 μM) 1 hr prior to collection and analysed by FACS.

(B) Quantification of the data in (A) showing the mean fluorescence intensity in each condition. Data show mean ± s.e.m. from n=3 biological experiments. One-way ANOVA analysis was applied.

4.9 - Cyclic hypoxia causes replication catastrophe

Finally, we asked if continued DNA replication in cyclic hypoxia through the firing of new origins could lead to replication catastrophe. For this experiment we also used a hypoxic treatment schedule termed “reox”, in addition to our standard cyclic hypoxia model (Figure 4.9 A, B). We included the reox condition as cells that experience replication catastrophe demonstrate persistent replication stress and DNA damage signalling even after the stress is removed (Toledo et al., 2013). In our case we decided this could be modelled by keeping the oxygen concentration constant at 2% O_2 following the cyclic portion of the treatment. Co-staining for 53BP1 and RPA demonstrated that approximately 50% of cells in cyclic hypoxia were positive for both >5 53BP1 and >6 RPA foci (Figure 4.9 C, D). The fact that there was no significant increase in the number of cells with >5 53BP1 and <6 RPA foci, indicates that the DNA damage cause by cyclic hypoxia only arose in cells that experienced replication stress and

were thus in S-phase (Figure 4.9 C, D). Importantly, a similar number of cells were also positive for both >5 53BP1 and >6 RPA foci in the reox timecourse, indicating that the DNA damage and replication signalling persists after removal of the stress (Figure 4.9 C, D). Another key consequence of replication catastrophe is an increase in cell area over time, likely due to senescence resulting from persistent DDR signalling (Toledo et al., 2013). To assess if this held true in the cyclic and reox conditions, we divided treated cells into groups of cells that had experienced replication catastrophe (+RC) and those that had not (-RC). The mean nuclear area of each of these groups could then be determined. As predicted, the mean nuclear area of cells in cyclic hypoxia and reox that had experienced replication catastrophe was significantly bigger than those that did not. Cell area was also significantly increased in reox compared to cyclic, likely due to the increased amount of time associated with the reox treatment (Figure 4.9 E, F). Together, these data demonstrate that the *in vitro* cyclic hypoxia conditions used causes replication catastrophe.

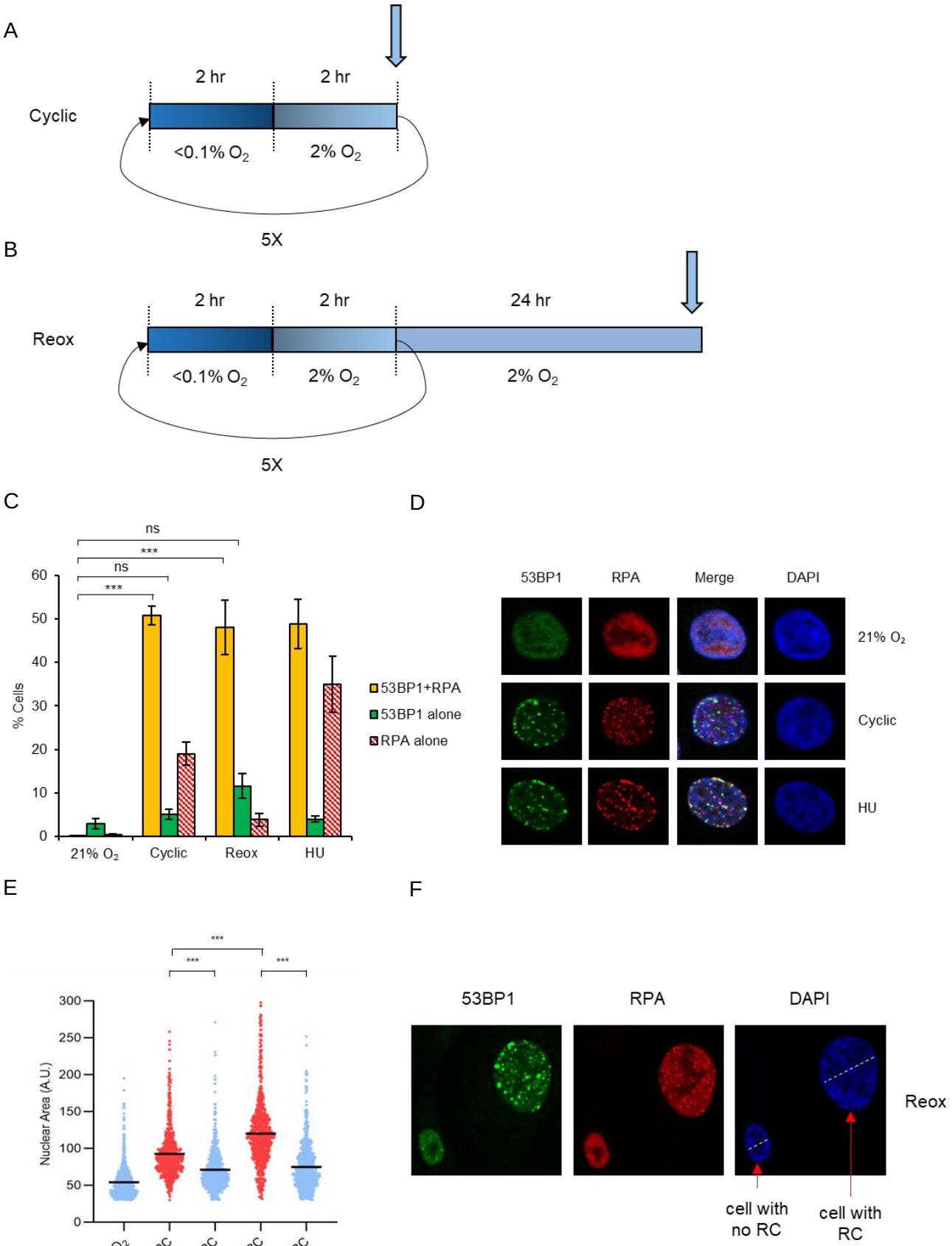

A
2 hr
2 hr
Cyclic
<0.1% O2
2% O2
5X
B
2 hr
2 hr
24 hr
Reox
<0.1% O2
2% O2
2% O2
5X
C
ns
***
ns
***
% Cells
60
50
40
30
20
10
0
21% O2
Cyclic
Reox
HU
53BP1+RPA
53BP1 alone
RPA alone
D
53BP1
RPA
Merge
DAPI
21% O2
Cyclic
HU
E
***
***
***
Nuclear Area (A.U.)
300
250
200
150
100
50
0
21% O2
Cyclic + RC
Cyclic -RC
Reox +RC
Reox -RC
F
53BP1
RPA
DAPI
Reox
cell with no RC
cell with RC

Figure 4.9 – Cyclic hypoxia causes replication catastrophe

(A) A schematic outlining the cyclic hypoxia treatment schedule as shown in (4.4 A), repeated 5 times

(B) A schematic outlining the reox treatment schedule. Cells were treated with <0.1% O_2 for 2 hr followed by 2% O_2 for 2 hr. This cycle was then repeated 5 times after which cells were left in 2% O_2 for 24 hr. The blue arrow indicates the point at which samples were harvested.

(C) RKO cells were treated with cyclic hypoxia or reox (see A, B) or HU (2 mM) for 20 hr and co-stained for 53BP1, RPA, and DAPI. Foci were visualised by immunofluorescence. Cells with >5 53BP1 and >6 RPA foci were counted and the percentage of cells with these foci was determined. Data show mean ± s.e.m. from n=3 biological experiments. One-way ANOVA analysis was applied.

(D) Representative images of data in (C).

(E) Cells treated in the conditions in (C) were grouped into cells that experienced replication catastrophe (+RC) and those that did not (-RC). The nuclear area of individual cells are plotted for each condition. Black bars represent the mean nuclear area of all cells from n=3 biological experiments. One-way ANOVA analysis was applied.

(F) Representative images of data in (C) where differences in the nuclear size of cells that experience replication catastrophe and those that do not can be seen.

Discussion

Here, we demonstrate that cells respond differently in terms of their cell cycle profile and propensity to experience replication catastrophe depending on whether they are treated with chronic hypoxia, cyclic hypoxia or HU. Cells treated with cyclic hypoxia were characterised by sustained DNA replication maintained through new origin firing, replication catastrophe, and a G2 cell cycle arrest. Though it has yet to be measured routinely in human tumours, a wealth of evidence from *in vivo* experiments suggests that cyclic hypoxia is commonplace in solid tumours (Cao et al., 2005; Hillestad et al., 2020; Nehmeh et al., 2008; O'Connor et al., 2019; Ron et al., 2019; Yasui et al., 2010). Though much study has been done to date on the effects of cyclic hypoxia on treatment modalities such as radiotherapy and chemotherapy *in vitro*, this has seldomly been conducted at oxygen concentrations that have been detected *in vivo.* The vast majority of studies utilise ambient air (21% O_2) for the reoxygenation portion of their cyclic schedule (Saxena and Jolly, 2019), while the maximum oxygen concentration predicted to occur in xenografts is closer to 5% O_2 (Yasui et al., 2010). Our cyclic hypoxia schedule therefore represents a physiologically relevant stress and the first description of an endogenous source of replication catastrophe that likely occurs in human tumours.

An important follow-up experiment to confirm the conclusions drawn from our data would be the use of DNA fibers to directly measure DNA replication at the single molecule level. DNA fibers could be used to assess both the speed of replication as well as to quantitatively measure the number of new origins that fire in response to different stresses (Foskolou et al., 2016). All of our experiments utilising BrdU incorporation to draw conclusions about DNA replication in response to different stresses could be solidified using the DNA fiber assay. Additionally, DNA fibers could be used to confirm that roscovitine has the desired effect of decreasing the number of new origins that fire in each treatment condition.

Another area of future work is the characterisation of cell fate in response to replication catastrophe. Determining the long term consequences of replication catastrophe is a

potentially important clinical question as a wide array of inhibitors used in the clinic have been shown to cause replication catastrophe *in vitro* (King et al., 2015; Toledo et al., 2013; Warren and Eastman, 2019). Thus far senescence has been proposed as a consequence of the sustained DDR signaling caused by replication catastrophe, though it has never been conclusively proven (Toledo et al., 2013). Senescence is a state of irreversible growth arrest that can have both oncogenic and tumour suppressive properties (Campisi, 2013). Our data supports a model suggesting that replication catastrophe causes senescence. All cells that experienced replication catastrophe in response to cyclic hypoxia demonstrated persistent DNA damage and replication stress signaling 24 hours after oxygen cycling was stopped as well as an increase in nuclear area, consistent with a senescent phenotype (Veitia, 2019). Senescence assays such as β-galactosidase and lamin B1 staining could be utlised to confirm that cyclic hypoxia pushes cells into senescence via replication catastrophe (Debacq-Chainiaux et al., 2009; Freund et al., 2012).

Chapter 5

A3B is upregulated by replication catastrophe

Introduction

Mutational signatures have been identified in human cancers and represent collections of similar mutations that likely originate from the same causative source (Nik-Zainal et al., 2012). Two mutational signatures, SBS2 and SBS13, have been attributed to the activity of APOBEC proteins, primarily A3A and A3B (Alexandrov et al., 2020; Alexandrov et al., 2013; Nik-Zainal et al., 2012; Roberts et al., 2013b). These signatures are defined by a high proportion of C>T and C>G mutations that occur within the APOBEC deamination motif, TCW (W = adenine or thymine). Currently the mechanisms by which the APOBEC mutational signatures arise in human cancer are unknown. Most studies studying APOBECs and cancer focus on either the consequences of ectopic APOBEC overexpression or the mechanism of APOBEC induction in response to stress inducing agents. Neither of these represents a plausible mechanism for the generation of the APOBEC mutational signature in human cancers. In contrast, cyclic hypoxia is a phenomenon that has been shown to occur in human tumours (Hillestad et al., 2020; Nehmeh et al., 2008; O'Connor et al., 2019). Cycles of tumour growth and angiogenesis result in corresponding cycles of hypoxia and reoxygenation that can fluctuate on the order of hours to days (Cao et al., 2005; Nehmeh et al., 2008). Here, we focus our analysis on A3B and test the hypothesis that replication catastrophe caused by cyclic hypoxia can lead to the upregulation of A3B expression and activity.

Results

5.1 - A3B expression increases in cyclic hypoxia

To determine if cyclic hypoxia causes increased A3B protein expression, RKO cells were exposed to either chronic (<0.1% O_2) or cyclic hypoxic conditions and western blotting was carried out (Figure 5.1 A). In the RKO cell line, an approximate 4-fold induction of A3B was seen in cycling but not chronic hypoxia (Figure 5.1 B). HCT116 cells were also treated in chronic (<0.1% O_2) or cyclic hypoxia to demonstrate that A3B protein induction in cyclic hypoxia is not cell line specific (Figure 5.1 C).

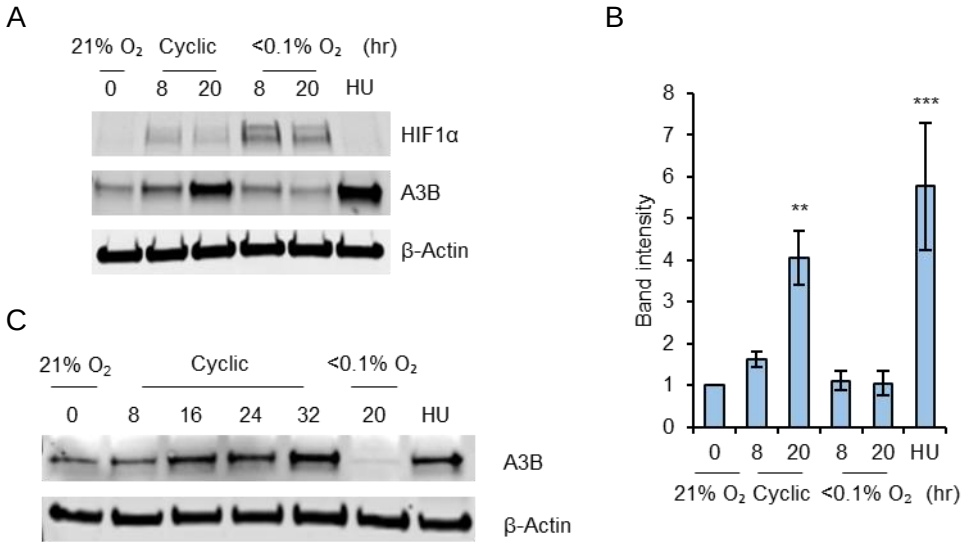


Figure 5.1 – Cyclic hypoxia increases the expression of A3B protein
(A) RKO cells were exposed to the oxygen concentrations indicated for the times shown or HU (2 mM, 20 hr). Western blotting was carried out.
(B) Quantification of the band intensities of the blots conducted in (A). Data show mean ± s.e.m. from n=3 biological experiments. One-way ANOVA analysis was applied.
(C) HCT116 cells were exposed to the oxygen concentrations indicated for the times shown or HU (2 mM, 20 hr). Western blotting was carried out (n=2).

5.2 - Deamination increases in cyclic hypoxia

Next, to determine if the A3B protein we saw induced in cyclic conditions was enzymatically active, we carried out deamination assays to measure APOBEC mediated deamination in

different hypoxic conditions. Deamination assays demonstrated that, as before, deamination decreased significantly in chronic hypoxia but was significantly increased in cyclic hypoxia (Figure 5.2 A, B). The pattern of APOBEC mediated deamination in response to cyclic and chronic hypoxia also mirrored that of the protein expression of A3B observed in RKO cells (Figure 5.1 A).

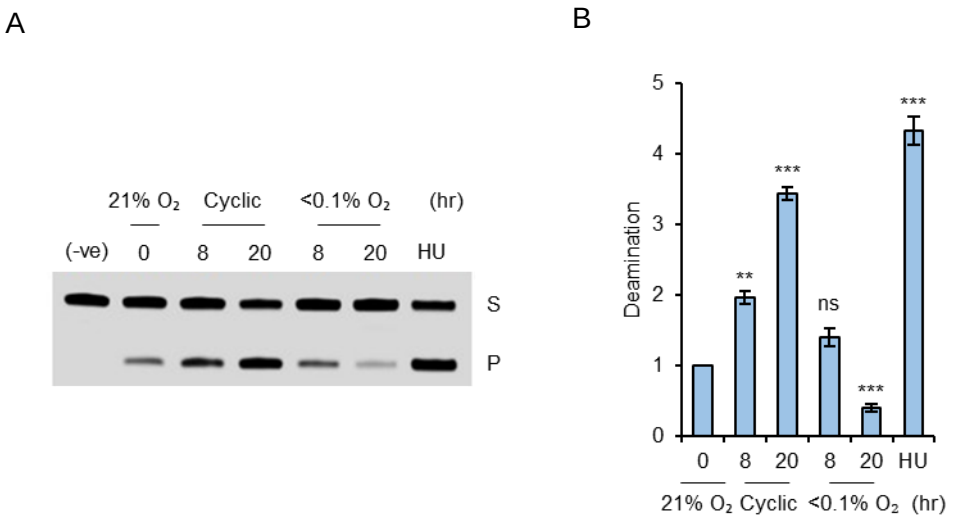


Figure 5.2 – Cyclic hypoxia increases APOBEC mediated deamination
(A) *In vitro* deamination assay measuring deamination activity in RKO cell line samples collected in the indicated hypoxic treatments for the indicated times or HU (2 mM, 20 hr). The top band is the substrate band (S) and the bottom band is the product band (P) (n=2).
(B) Quantification of deamination in (A), where the average intensity of the product band (P) (bottom) across 2 biological repeats is plotted relative to the intensity of the normoxic product band. Data show mean ± s.e.m. from n=2 biological experiments. One-way ANOVA analysis was applied.

5.3 - Increased deamination in cyclic hypoxia is dependent on A3B

We next considered if other APOBEC3 genes could also be induced in cyclic hypoxia and could potentially contribute to the increased APOBEC mediated deamination observed in cyclic hypoxia. The mRNA expression of both *A3C* and *A3H* was found to significantly increase in cyclic hypoxia (Figure 5.3 A, B). This raised the possibility that increased deamination in

cyclic hypoxia could be dependent on a number of APOBECs including A3B, A3C and A3H. However, based on our previous finding that the induction of *A3C* and *A3H* did not contribute to deamination levels in chronic hypoxia (Figure 3.3 B, C, Figure 3.8 A, B), we hypothesised that deamination in cyclic hypoxia might be A3B dependent. To test this hypothesis, we used siRNA to A3B to reduce A3B expression and determined the impact on deamination. Knocking down A3B abrogated both the increase in deamination in cyclic hypoxia as well as the baseline level of deamination seen in normoxic conditions in comparison to the scramble control (siSCR) (Figure 5.3 C). Successful A3B knockdown was confirmed with a western blot (Figure 5.3 D). These data show that the increase in deamination in cyclic hypoxia as well as the baseline level of deamination in normoxia is likely entirely dependent on A3B in the RKO cell line. Any residual deamination activity in cyclic hypoxia where A3B expression is knocked down with an siRNA is likely due to an A3B knockdown efficiency of less than 100% (Figure 5.3 C, D).

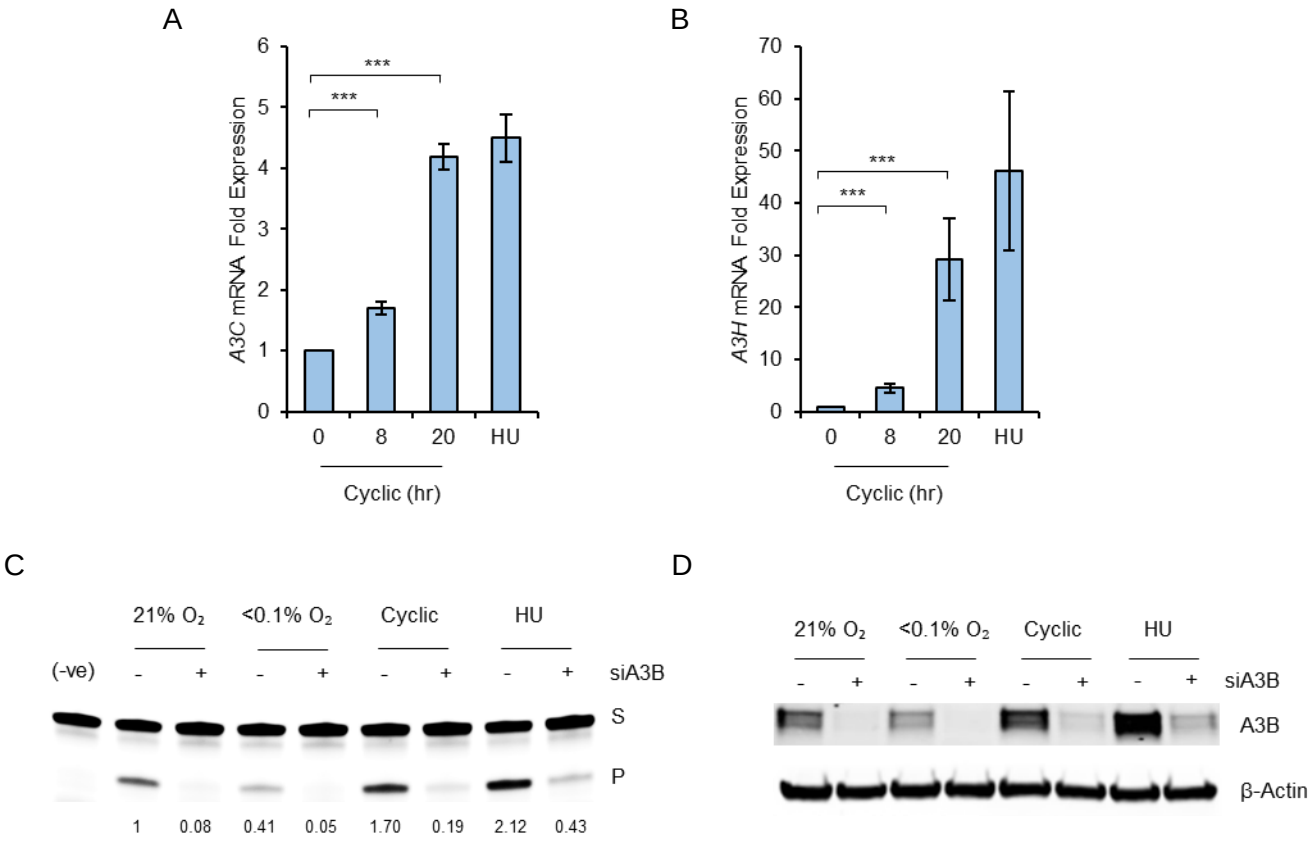


Figure 5.3 – Deamination increase in cyclic hypoxia is A3B dependent

(A, B) RKO cells were treated with cyclic hypoxia or HU (2 mM) for 20 hr and RT-qPCR was carried out. The mRNA levels of *A3C* (A) and *A3H* (B) as a relative fold change to normoxic (21% O_2) levels are shown. Data show mean ± s.e.m. from n=3 biological experiments. One-way ANOVA analysis was applied.

(C) RKO cells were treated with an siRNA to A3B (siA3B) or a scramble (siSCR) and then exposed to the hypoxic conditions indicated or HU (2 mM) for 20 hr, followed by a deamination assay. The intensity of the product band (P) for each condition relative to the normoxic siSCR condition is displayed below the blot (n=1).

(D) The samples from (C) were also analysed by western blot to confirm A3B knockdown (n=1).

5.4 - A3B induction in cyclic hypoxia does not alter the cell cycle

Previous reports have demonstrated that overexpression of A3B can impact cell cycle progression (Green et al., 2017; Green et al., 2016; Landry et al., 2011; Nikkila et al., 2017). Both G2/M-phase and S-phase arrests have both been demonstrated in a cell line-dependent

manner in response to ectopic overexpression of either A3B or A3A. We knocked down the expression of A3B with an siRNA and tested the impact on the cell cycle in cyclic hypoxia in comparison to a scramble control (siSCR). In contrast to previous studies, we found that A3B induction in cyclic hypoxia had no impact on the cell cycle, considering both the cell cycle phase as well as BrdU incorporation (Figure 5.4 A, B). Successful A3B knockdown was confirmed by western blot (Figure 5.4 C).

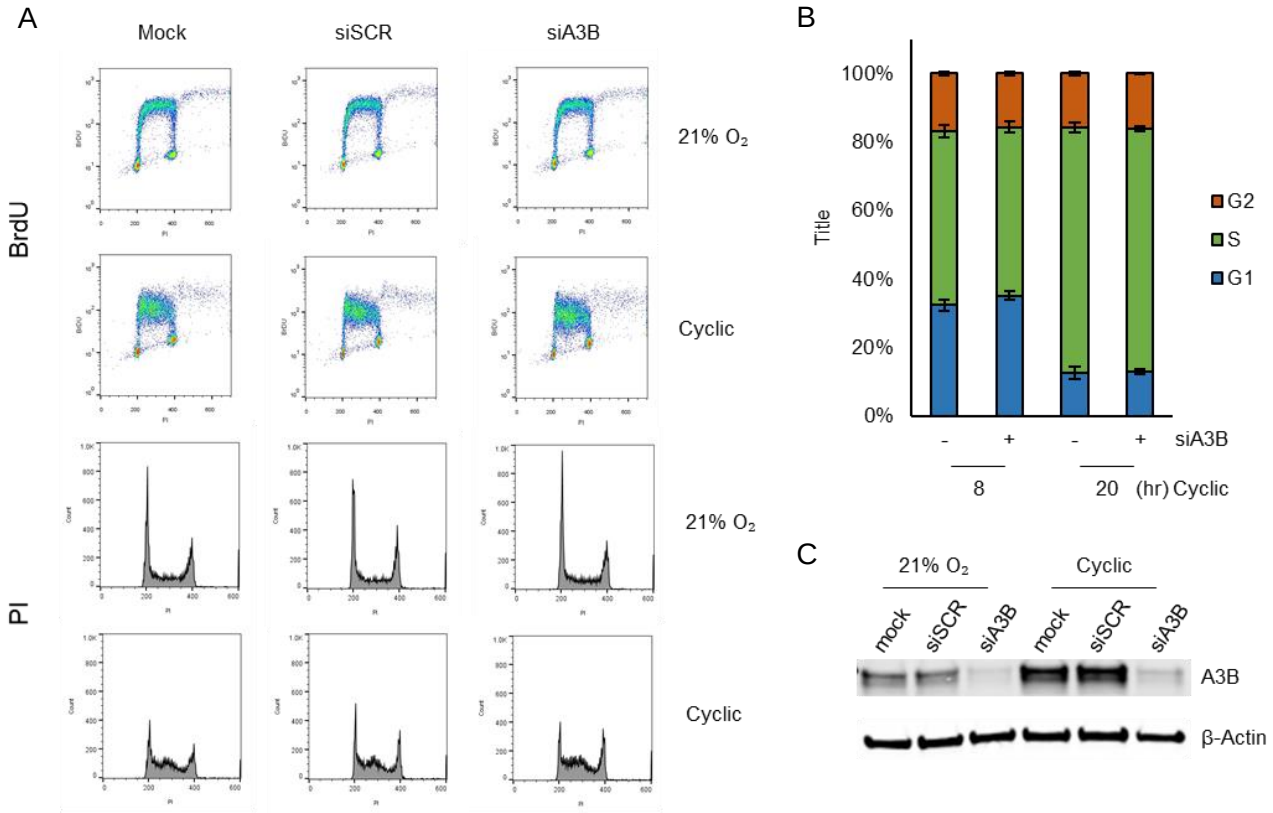


Figure 5.4 – No A3B dependent cell cycle effects in cyclic hypoxia
(A) RKO cells were treated with siRNA to A3B (siA3B), a scramble control (siSCR), or transfection agent alone (mock) followed by exposure to cyclic hypoxia for 20 hr. Cells were labeled with BrdU (20 μM) 1 hr prior to collection and analysed by FACS.
(B) Quantification of the data in (A) where the percentage of cells in each phase of the cell cycle is shown.
(C) Cells in (A) were assayed by western blot for successful A3B knockdown.

5.5 - A3B induction in cyclic hypoxia does not affect DDR signalling

In addition to the cell cycle, previous studies have also shown that A3B/A3A induction can result in an increase in DDR signalling (Buisson et al., 2017; Nikkila et al., 2017; Serebrenik et al., 2019). The activation of various DDR signalling proteins was assayed by western blot in cells treated with an siRNA to A3B (siA3B) or a scramble control (siSCR). Chk1 and RPA are phosphorylated in an ATR dependent manner in response to replication stress while KAP1 is phosphorylated in an ATM dependent manner in response to DNA damage (Bencokova et al., 2009; Olson et al., 2006; Ziv et al., 2006). No A3B dependent changes in the activation status of KAP1, Chk1, or RPA were observed in cyclic hypoxia. (Figure 5.5).

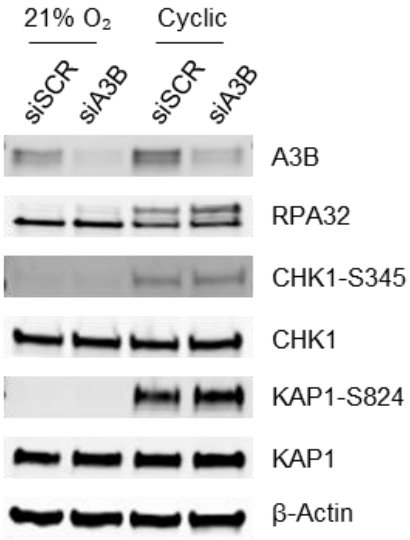


Figure 5.5 – A3B induction in cyclic hypoxia does not affect DDR signalling
RKO cells were treated with siA3B or siSCR and exposed to cyclic hypoxia for 20 hr. Western blotting was carried out.

5.6 – A3B induction in cyclic hypoxia is p53 independent

To determine the mechanism of A3B induction in cyclic hypoxia we first ruled out p53. p53 was an unlikely candidate as it had no impact on A3B protein expression in chronic hypoxia (Figure 3.6 E), and has been reported to repress A3B expression (Menendez et al., 2017;

Periyasamy et al., 2017). p53 had to be considered however as it can transactivate a different set of target genes in a stress specific manner (Leszczynska et al., 2015). We began by demonstrating that p53 is stabilised and activated in cyclic hypoxia through western blotting for serine 15 phosphorylation and total p53 protein levels (Figure 5.6 A) (Hammond et al., 2002). Once p53 activity in cyclic hypoxia was confirmed, we knocked down p53 expression in cyclic hypoxia using siRNA specific for p53 or a scramble control (siSCR). Successful p53 knockdown was confirmed by a decrease in total p53 protein level (Figure 5.6 B). As expected, in the absence of p53 the protein expression of A3B in cyclic hypoxia was unchanged (Figure 5.6 B).

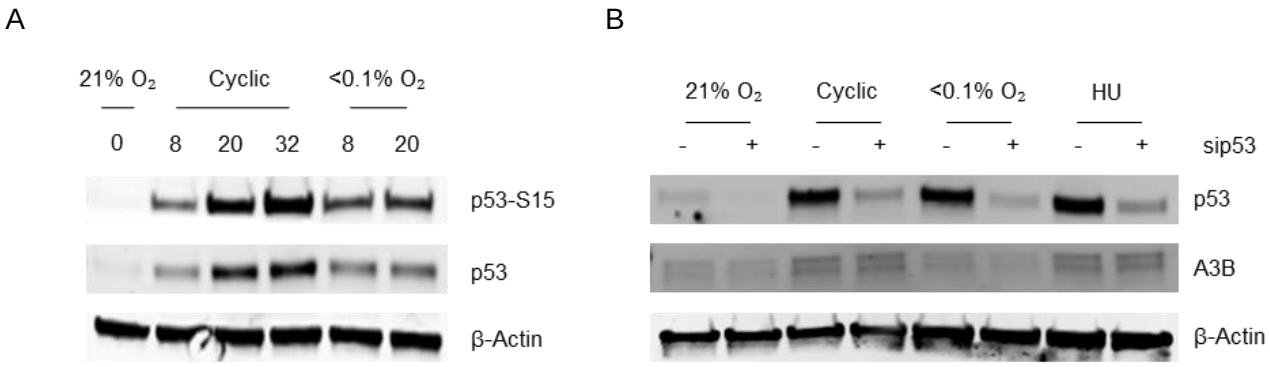


Figure 5.6 – A3B induction in cyclic hypoxia is p53 independent
(A) RKO cells were exposed to the oxygen concentrations indicated for the times shown. Western blotting was carried out.
(B) RKO cells were treated with siRNA to p53 (+) or a scramble control (-) followed by exposure to the oxygen concentration indicated or HU (2 mM) for 20 hr. Western blotting was carried out (n=2).

5.7 - Decreasing origin firing decreases replication catastrophe in cyclic hypoxia

To further inform our understanding of the mechanism of A3B induction in cyclic hypoxia, we tested our revised hypothesis that replication catastrophe is the signal that leads to A3B upregulation as opposed to replication stress. As discussed previously, replication catastrophe is characterised by the concurrent expression of DNA damage and replication stress markers

in the same cell. We previously showed that replication catastrophe as well as A3B expression increase in cyclic hypoxia (Figure 4.9 C, D, 5.1 A-C). To test our hypothesis, we used roscovitine (Ros) to inhibit new origin firing in cyclic hypoxia. We theorised that roscovitine should help protect cells against cyclic hypoxia induced replication catastrophe by decreasing the amount of exposed ssDNA present in the cell through inhibition of new origin firing. As predicted, the addition of roscovitine in cyclic hypoxia significantly decreased the number of cells experiencing replication catastrophe as determined by co-staining for 53BP1 and RPA foci (Figure 5.7 A, B). Additionally, an increase in cells with >5 53BP1 foci but <6 RPA foci was also observed in Ros treated conditions compared to DMSO. This is likely due to an off-target effect of roscovitine that induces DNA damage in the absence of replication stress, as a significant increase in cells with >5 53BP1 foci but <6 RPA foci is seen in normoxic cells treated with roscovitine compared to DMSO (Figure 5.7 A).

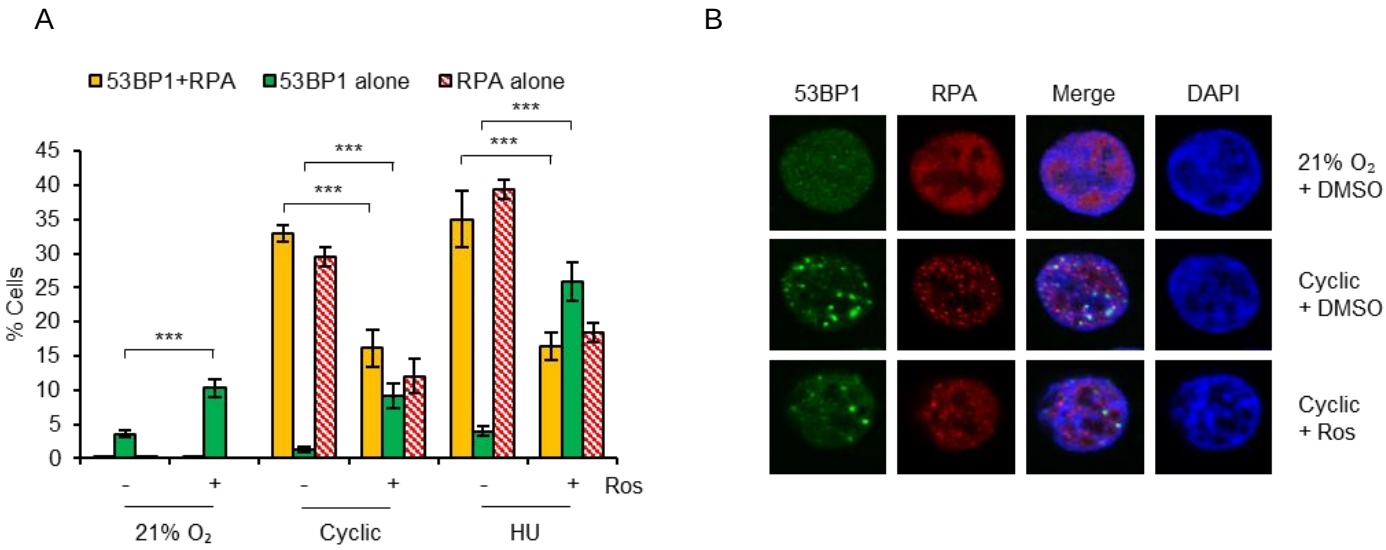


Figure 5.7 – Replication catastrophe caused by cyclic hypoxia depends on the firing of new origins

(A) RKO cells were pretreated with DMSO or roscovitine for 30 min (Ros) (20 μM) and exposed to 21% O_2, cyclic hypoxia, or HU (2 mM) for 20 hr. Cells were stained by immunofluorescence to detect cells with >5 53BP1 and >6 RPA foci and mounted in DAPI. Data show mean ± s.e.m. from n=3 biological experiments. One-way ANOVA analysis was applied.

(B) Representative images of data shown in (A)

5.8 - Decreasing origin firing in cyclic hypoxia abrogates A3B expression and activity

To directly link the decrease in replication stress observed in cyclic hypoxia upon treatment with roscovitine with A3B expression, we treated cells in cyclic hypoxia with roscovitine and assayed for A3B protein expression. In support of our hypothesis, cells in cyclic hypoxia treated with roscovitine accumulated less A3B protein than those treated with DMSO (Figure 5.8 A). The same effect could be seen utilising an alternative agent to inhibit new origin firing through the inhibition of cdc7 (PHA-767491) (Figure 5.8 B). These data demonstrate that the expression of A3B is increased in response to cyclic hypoxia due to replication catastrophe induced DNA damage.

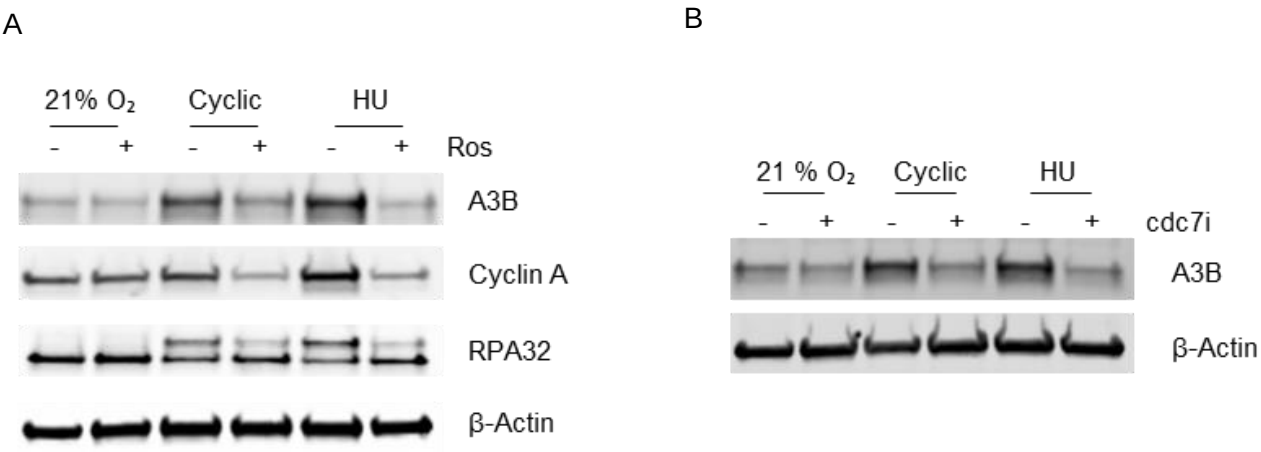


Figure 5.8 – A3B induction in cyclic hypoxia is dependent on new origin firing
(A) RKO cells were pretreated with DMSO or roscovitine (Ros) (20 μM) for 30 min and exposed to 21% O_2, cyclic hypoxia, or HU (2 mM) for 20 hr. Western blotting was carried out (n=2).
(B) RKO cells were pretreated with DMSO or cdc7i (20 μM) for 30 min and exposed to 21% O_2, cyclic hypoxia, or HU (2 mM) for 20 hr. Western blotting was carried out (n=1).

5.9 - Decreasing ROS in cyclic hypoxia abrogates A3B expression and activity

As discussed previously, many studies have shown that reactive oxygen species (ROS) accumulate in cyclic hypoxia (Li et al., 2018; Malec et al., 2010; Rouschop et al., 2013;

Rouschop et al., 2009; Yuan et al., 2008). We hypothesised that the activity of ROS would also likely contribute to replication catastrophe in cyclic hypoxia and the subsequent A3B induction through the creation of ROS-induced DNA damage (Finkel and Holbrook, 2000). Treatment with the ROS scavenger N' acetylcysteine (NAC) in cyclic hypoxia significantly decreased the proportion of cells experiencing replication catastrophe (Figure 5.9 A, B). In support of our hypothesis, cells treated with NAC and cyclic hypoxia showed a decrease in A3B protein expression compared to the DMSO control (Figure 5.9 C).

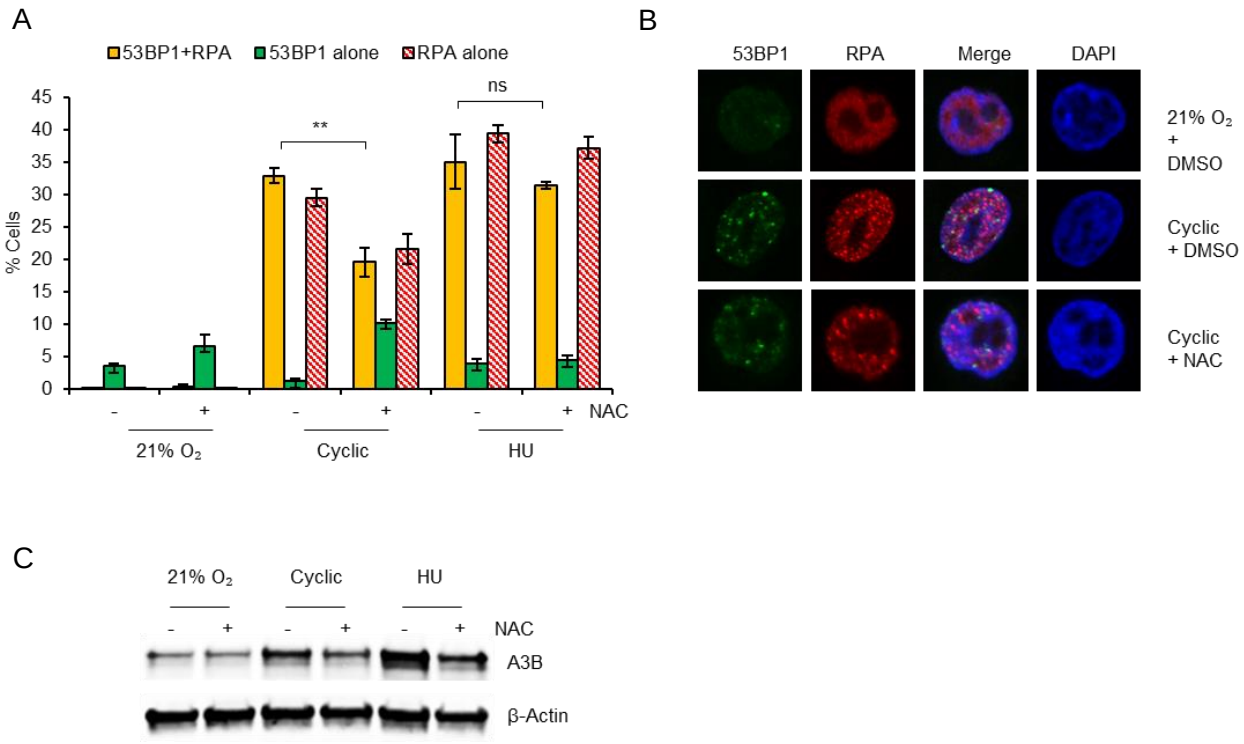


Figure 5.9 – NAC abrogates replication catastrophe and A3B induction in cyclic hypoxia
(A) RKO cells were pretreated with DMSO or NAC (5 mM) for 30 min and exposed to 21% O_2, cyclic hypoxia, or HU (2 mM) for 20 hr. Cells were stained by immunofluorescence to detect cells with >5 53BP1 and >6 RPA foci and mounted in DAPI. Data show mean ± s.e.m. from n=3 biological experiments. One-way ANOVA analysis was applied.
(B) Representative images of data shown in (A)
(C) RKO cells were pretreated with DMSO or NAC (5 mM) for 30 min and exposed to 21% O_2, cyclic hypoxia, or HU (2 mM) for 20 hr. Western blotting was carried out.

5.10 – A3B is upregulated in cyclic hypoxia in an NFκB dependent manner

Increased APOBEC expression, including A3B, has been linked to the NFκB transcription factor (Culver et al., 2010; Leonard et al., 2015). NFκB signalling has been shown to increase in response to both DNA damage and ROS, and therefore presented a potential mechanism for A3B induction in cyclic hypoxia. RKO cells in cyclic hypoxia were treated with an NFκB inhibitor (Bay11-7085) and partial reduction of A3B induction could be observed in a dose dependent manner (Figure 5.10). Successful inhibition of NFκB was determined by blotting for serine 536 phosphorylation on the p65 subunit of NFκB (Sakurai et al., 1999).

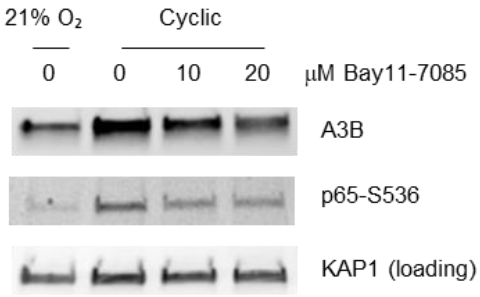


Figure 5.10 – A3B induction in cyclic hypoxia is NFκB dependent
RKO cells were pretreated with the indicated concentrations of Bay11-7085 for 30 min and exposed to cyclic hypoxia for 20 hr. Western blotting was carried out; KAP1 is used as a loading control.

5.11 - A3B is upregulated in cyclic hypoxia in an ATR dependent manner

Having implicated replication catastrophe as a key inducer of A3B expression, we hypothesised that further increasing replication catastrophe beyond the amount seen in cyclic hypoxia alone would result in higher A3B expression. To accomplish this, we inhibited ATR in combination with cyclic hypoxia. ATR inhibition combined with other agents that cause replication stress have previously been shown to increase the speed at which replication catastrophe occurs (Toledo et al., 2017; Toledo et al., 2013). This is because ATR protects cells against RPA exhaustion by limiting late origin firing through Chk1 signalling. Cells in

cyclic hypoxia were treated with inhibitors to ATR (VX-970, AZD6738) followed by western blotting for A3B. Surprisingly, inhibition of ATR abrogated the induction of A3B in cyclic hypoxia (Figure 5.11 A). This was further confirmed using siRNA to knock down ATR (Figure 5.11 B). Additionally, treatment with ATR inhibitors abrogated APOBEC activity in cyclic hypoxia as assayed by the *in vitro* deamination assay (Figure 5.11 C, D). These data were surprising as they suggest A3B is induced in cyclic hypoxia though an ATR-dependent mechanism.

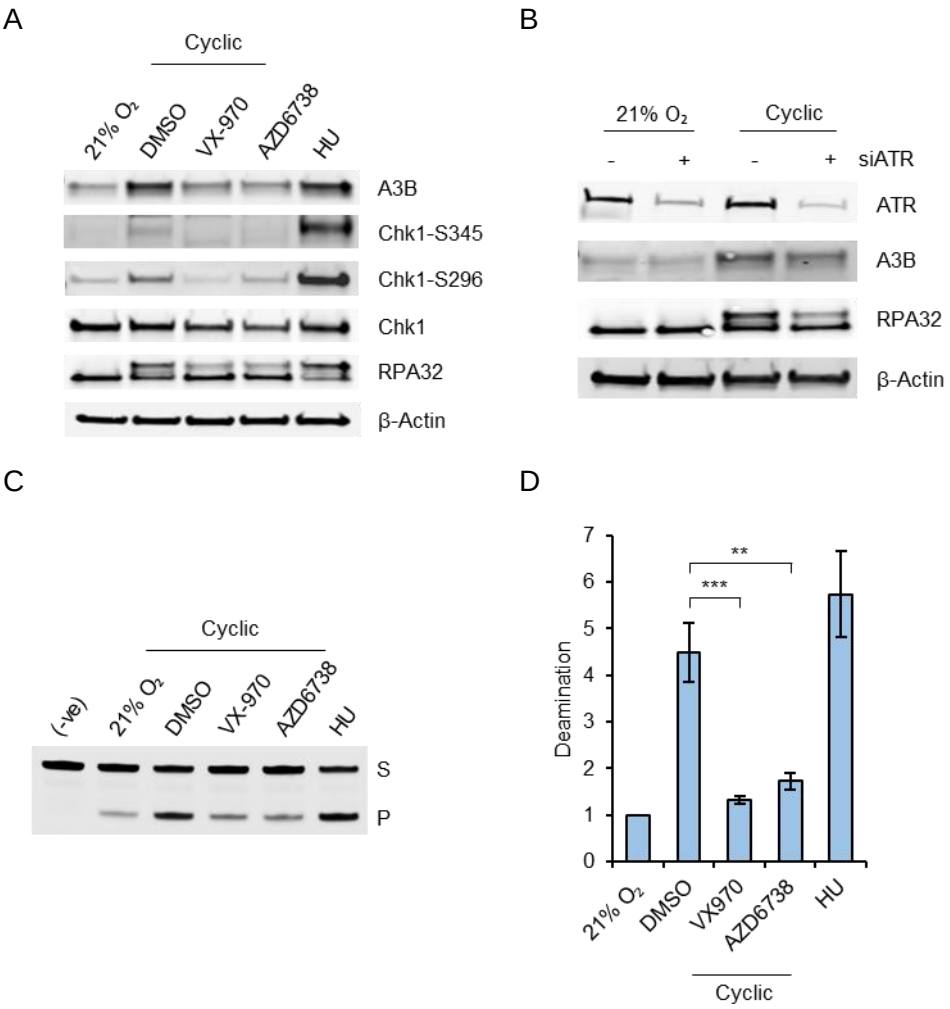


Figure 5.11 – ATR treatment abrogates A3B induction and activity in cyclic hypoxia

(A) RKO cells were exposed pre-treated with VX-970 (1 μM) or AZD6738 (5 μM) for 30 min and then exposed to 20 hr cyclic hypoxia or HU alone (2 mM, 20 hr). Western blotting was carried out.

(B) RKO cells were treated with siATR or siSCR and exposed to cyclic hypoxia for 20 hr. Western blotting was carried out (n=2).

(C) *In vitro* deamination assay on RKO cells pre-treated with VX-970 (1 μM) or AZD6738 (5 μM) for 30 min and exposed to 20 h cyclic hypoxia or HU alone (2 mM, 20 hr). Substrate (S) and product (P) bands are shown.

(D) Quantification of the bottom band intensity in samples from (C). Data show mean ± s.e.m. from n=3 biological experiments. One-way ANOVA analysis was applied.

5.12 - Loss of ATR in cyclic hypoxia leads to a G1 arrest

To further validate the conclusion that A3B induction in cyclic hypoxia is dependent on ATR, it was important to consider the impact of ATR inhibition on the cell cycle. Cells were exposed

to cycling hypoxia in the presence of an ATR inhibitor (VX-970) and the cell cycle analysed by BrdU/PI incorporation. Inhibition of ATR during cycling conditions prevented the accumulation of cells in S-phase, leading instead to a significant G1 accumulation (Figure 5.12 A, B). These data demonstrate that whilst A3B induction in cyclic hypoxia is ATR-dependent, this is due to a decreased S-phase population when ATR is inhibited. This further validates our conclusion that A3B is induced by replication catastrophe in cyclic hypoxia as replication catastrophe can only occur in S-phase.

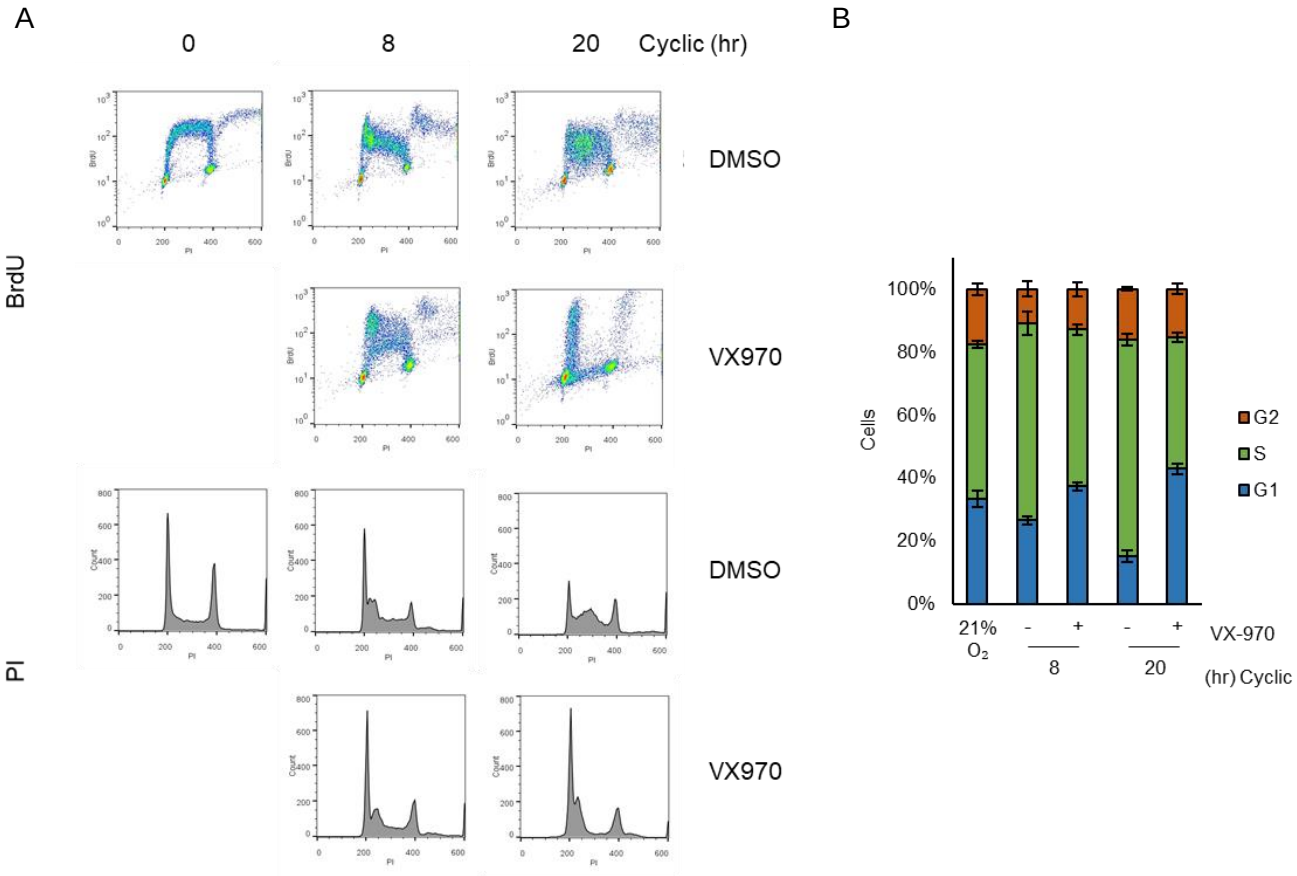


Figure 5.12 – Cells treated with VX-970 in cyclic hypoxia arrest in G1
(A) RKO cells were pre-treated with VX-970 for 30 min (1 μM) and then exposed to cyclic hypoxia (8 or 20 hr) followed by BrdU incorporation and FACS analysis.
(B) Quantification of the percentages of cells in each cycle phase of the data in (A).

5.13 - A3C, A3D, A3F, A3G, and A3H expression positively correlates with a group of hypoxia-inducible p53 response genes

Next, we sought to identify a link between tumour hypoxia and APOBEC expression/activity in patient samples. One of our original observations was that *A3D* and *A3H* were significantly induced in response to chronic hypoxia (<0.1% O_2) and that this occurred in a p53-dependent manner (Figure 3.3 A, B, 3.5 C, D). In a previous study we identified a set of 6 genes which are induced in hypoxia in a p53-dependent manner (Leszczynska et al., 2015). As A3D and A3H are also p53 target genes induced in hypoxia, we asked if the expression of these APOBECs would correlate with the 6 genes previously identified in patient samples. A significant positive correlation was found between A3C, A3D, A3F, A3G, and A3H and the 6 hypoxia-induced p53-dependent genes in the breast invasive carcinoma (BRCA) dataset, while in the colorectal adenocarcinoma dataset (COAD) all of these except for A3H were significantly correlated (Figure 5.13 A, B). These data demonstrate that our *in vitro* data showing APOBEC3 upregulation in an oxygen dependent manner in response to levels of hypoxia <0.1% O_2 likely holds true in patient tumours. Interestingly, expression of A3C and A3F also positively correlated with the 6 genes, suggesting that the non-significant increase in expression of A3C/A3F we observed in response to hypoxia *in vitro* (Figure 3.3 C, D) is likely significant in patient samples. Concerning A3B, a negative correlation was seen between A3B and the 6 genes in both BRCA and COAD (Figure 5.13 A, B). This suggests that A3B expression is repressed in areas of severe hypoxia in patient tumours which supports our *in vitro* data showing A3B repression in chronic hypoxia (<0.1% O_2) (Figure 3.6 A, B, C).

A

Breast invasive carcinoma TCGA (n=1100)		
Correlations	Spearman	*P*
p53genes vs APOBEC3A	-0.11	0.0003
p53genes vs APOBEC3B	-0.3	<0.0001
p53genes vs APOBEC3C	0.3	<0.0001
p53genes vs APOBEC3D	0.36	<0.0001
p53genes vs APOBEC3F	0.19	<0.0001
p53genes vs APOBEC3G	0.35	<0.0001
p53genes vs APOBEC3H	0.16	<0.0001

B

Colorectal adenocarcinoma TCGA (n=382)		
Correlations	Spearman	*P*
p53genes vs APOBEC3A	0.11	0.0376
p53genes vs APOBEC3B	-0.15	0.0041
p53genes vs APOBEC3C	0.31	<0.0001
p53genes vs APOBEC3D	0.21	<0.0001
p53genes vs APOBEC3F	0.2	<0.0001
p53genes vs APOBEC3G	0.27	<0.0001
p53genes vs APOBEC3H	0.1	0.0554

Figure 5.13 – Correlations between a group of hypoxia inducible p53 response genes and individual APOBEC3 genes

(A, B) Correlation between a group of hypoxia-induced p53 response genes (Leszczynska et al., 2015) and APOBEC3 mRNA expression in (A) BRCA or (B) COAD from the TCGA patient cohort. A spearman coefficient is used to assess the strength of the correlation and the significance of the correlation is displayed in column *P*

5.14 - The APOBEC mutation signature correlates with a validated hypoxia signature

We next sought to expand our analysis to patient tumours that likely experience cyclic hypoxia and determine whether a higher number of APOBEC mutations occur in these tumours. Cyclic hypoxia is a physiologically relevant condition although detailed study of this phenomenon has been hampered by difficulties in measuring the periodicity in patients. As of yet, there are no clinically useful markers of cyclic hypoxia. Therefore, we used a validated hypoxia signature, primarily made up of HIF target genes, to determine if a correlation between hypoxia and APOBEC mutations exists in patient tumours. Our rationale was that, even though we have concluded that A3B is not induced by chronic hypoxia alone, cells experiencing cyclic hypoxia still accumulate HIF and should therefore be positive for the hypoxia signature (Figure 5.1 A) (Buffa et al., 2010). To confirm the occurrence of the hypoxia signature in cyclic hypoxia *in vitro*, we measured the mRNA expression of 4 out of the 51 genes contained in the hypoxic signature in cyclic hypoxia and observed an increase in each (Figure 5.14 A-D).

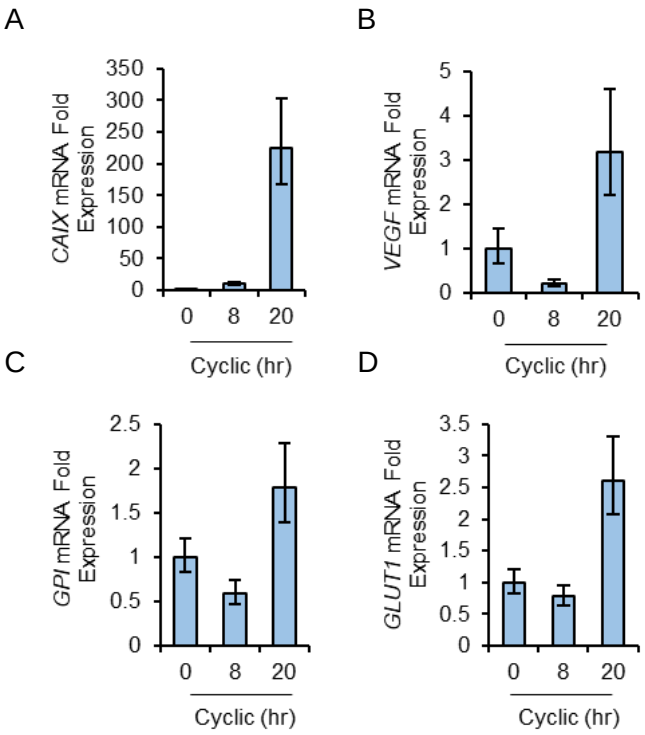


Figure 5.14 – Correlations between the hypoxia metagene and APOBEC mutations
(A-D) RKO cells were treated with cyclic hypoxia for the indicated times and RT-qPCR was carried out. The mRNA levels of (A) *CAIX*, (B) *VEGF*, (C) *GPI*, (D) *GLUT1* are shown as a relative fold change to the normoxic condition. Data show mean ± error bars calculated by StepOne software (Applied Biosystems) based on 3 technical replicates (n=1). This data was generated by Tiffany Ma.

To determine the number of APOBEC mutations in patient tumours we used a dataset curated by a previous study that sequenced patient tumours and quantified the number of APOBEC mutations present in each tumour (Roberts et al., 2013b). Using the TCGA patient cohort, we correlated the number of APOBEC mutations within individual tumours with the hypoxia signature and found a significant positive correlation between APOBEC signature mutations and the hypoxia signature. Specifically, a significant correlation could be seen between the number of APOBEC mutations present and the hypoxic signature in 4 out of the 6 datasets where there was sufficient APOBEC mutational data available (Figure 5.15 A-F). These data show that hypoxic patient tumours which likely experience cyclic hypoxia, have a higher number of APOBEC mutations than non-hypoxic tumours.

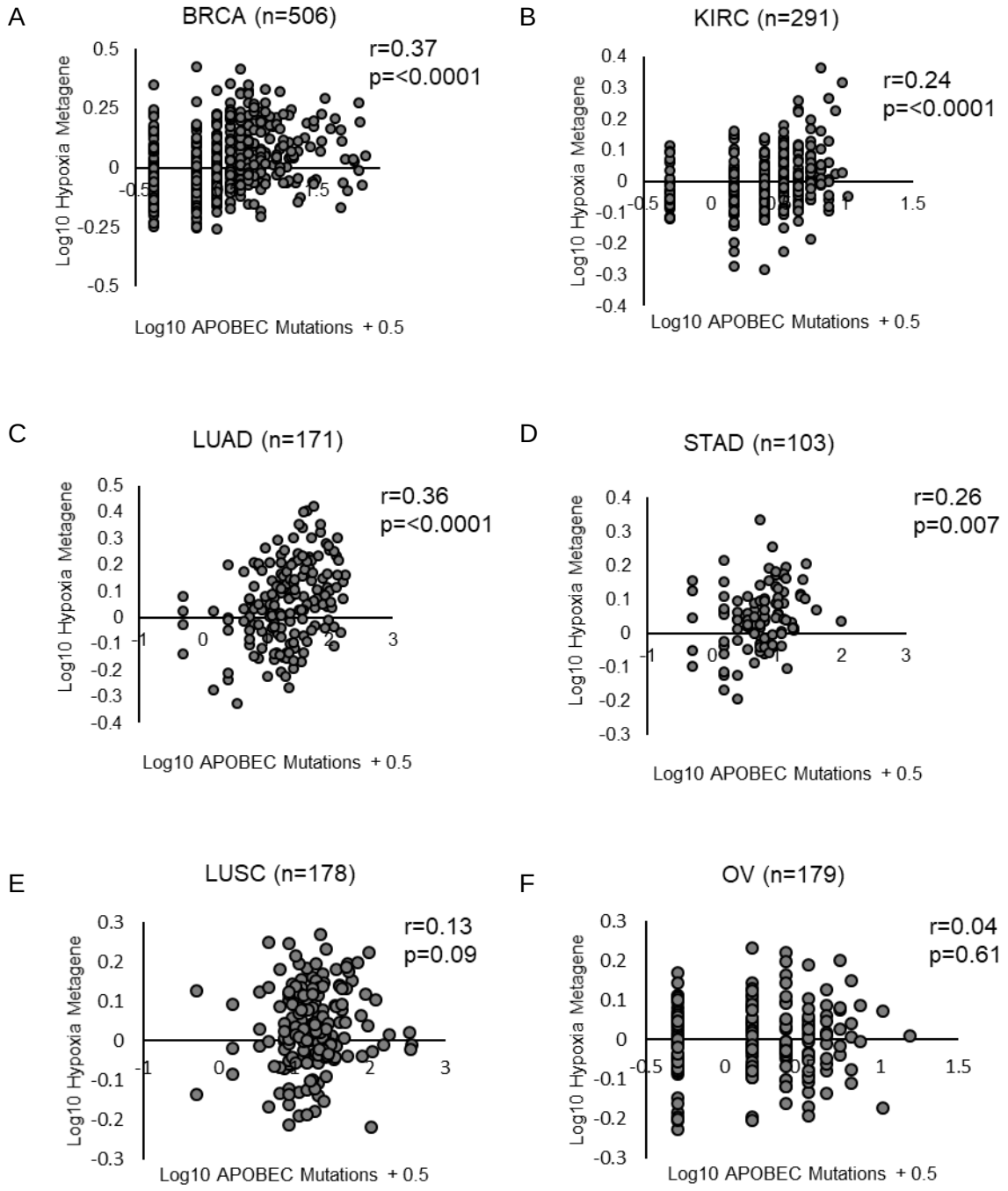


Figure 5.15 – Correlations between the hypoxia metagene and APOBEC mutations
(A-F) Correlation between the hypoxia metagene and the number of APOBEC mutations in a given tumour from the TCGA patient cohort. APOBEC mutations refers to the number of tCw to tTw and tCw to tGw changes. The log median expression of the hypoxia signature for each cancer dataset was compared to the log number of APOBEC mutations in each tumour sample. Mutation values are increased by 0.5 to display data from tumours with no observed APOBEC mutations. The spearman coefficient of the correlation and p value are displayed above. (A) BRCA (breast invasive carcinoma), (B) KIRC (kidney renal clear cell carcinoma), (C) LUAD (lung adenocarcinoma), (D) STAD (stomach adenocarcinoma), (E) LUSC (lung squamous cell carcinoma), (F) OV (ovarian cancer).

5.15 - A3A and A3B expression correlates with a validated hypoxia signature

To further support the conclusion that APOBEC mutations correlate with hypoxia we assessed whether a correlation existed between the expression of individual APOBEC3 genes and the hypoxia signature in patient samples. This analysis, while only correlative, should also give clues as to the APOBEC3 family member or members most responsible for the generation of APOBEC mutations in hypoxia. A significant positive correlation was found between the hypoxia signature and the expression of A3A and A3B in BRCA and COAD. None of the other APOBEC3 family members were significantly correlated with the hypoxia signature (Figure 5.16 A, B). These data show that expression of A3A and A3B correlates with hypoxia in patient tumours and also support previous studies showing that A3A and A3B are the APOBEC3 genes primarily responsible for the generation of the APOBEC mutational signatures (Burns et al., 2013b; Chan et al., 2015). A summary of all bioinformatic analysis conducted is displayed in Table 5.1.

A

Breast invasive carcinoma TCGA (n=1100)		
Correlations	**Spearman**	***P***
Hypmet vs APOBEC3A	0.35	<0.0001
Hypmet vs APOBEC3B	0.48	<0.0001
Hypmet vs APOBEC3C	-0.06	0.0517
Hypmet vs APOBEC3D	-0.11	0.0002
Hypmet vs APOBEC3F	0.01	0.65
Hypmet vs APOBEC3G	0.01	0.81
Hypmet vs APOBEC3H	0.1	0.014

B

Colorectal adenocarcinoma TCGA (n=382)		
Correlations	**Spearman**	***P***
Hypmet vs APOBEC3A	0.11	0.039
Hypmet vs APOBEC3B	0.16	0.0014
Hypmet vs APOBEC3C	-0.06	0.2149
Hypmet vs APOBEC3D	-0.11	0.0378
Hypmet vs APOBEC3F	-0.05	0.3365
Hypmet vs APOBEC3G	-0.08	0.1381
Hypmet vs APOBEC3H	-0.03	0.5016

Figure 5.16 – Correlations between the hypoxia metagene and individual APOBEC3 genes

(A, B) Correlation between the hypoxia metagene and APOBEC mRNA expression in (A) BRCA or (B) COAD from the TCGA patient cohort. A spearman coefficient is used to assess the strength of the correlation and the significance of the correlation is displayed in column *P*

	Significant correlation with		
	Hypoxia induced p53-dependent targets	Hypoxia signature	APOBEC-mediated mutations
Hypoxia signature	n/a	n/a	BRCA, KIRC, LUAD, STAD
A3A expression	BRCA, COAD	BRCA, COAD	BRCA[1]
A3B expression	BRCA, COAD	BRCA, COAD	BRCA, LUAD[1]
A3C expression	BRCA, COAD	(-)	(-)[1]
A3D expression	BRCA, COAD	BRCA, COAD	(-)[1]
A3F expression	BRCA, COAD	(-)	(-)[1]
A3G expression	BRCA, COAD	(-)	(-)[1]
A3H expression	BRCA	BRCA	(-)[1]

Table 5.1 – Summary of bioinformatic analysis conducted

The bioinformatic analysis contained in Figure 5.13, 5.14, and 5.16 are summarised here. Boxes are filled with TCGA datasets where a significant correlation was found between the listed categories in that dataset. Red and blue lettering denote a significant positive or negative correlation respectively. A (-) represents a non-significant correlation while (n/a) represents data that has not been collected.

[1](Roberts et al., 2013b)

Discussion

Here we have shown that replication catastrophe caused by cyclic hypoxia leads to an upregulation of A3B expression and APOBEC mediated deamination. The increase in APOBEC mediated deamination in cyclic hypoxia was dependent on A3B, and likely not impacted by an increase in *A3C* and *A3H* mRNA expression. Increased A3B expression in cyclic hypoxia did not impact the cell cycle or DDR signalling. New origin firing and ROS were identified as two factors that contributed to the replication catastrophe induced DNA damage and A3B induction in cyclic hypoxia. NFκB was also identified as a transcription factor induced in cyclic hypoxia that is required for A3B induction. Finally, we found that ATR inhibition protected cells from experiencing replication catastrophe due to a G1 cell cycle arrest.

The link between cyclic hypoxia and A3B expression represents a plausible explanation of how the APOBEC mutational signatures are generated in human cancers. Our hypothesis is that cycles of hypoxia which occur during tumour growth, progression, and treatment lead to an increase in A3B expression that results in APOBEC mediated mutations. To support this, we demonstrated that APOBEC mutations correlate with a hypoxia gene signature in patient tumours, suggesting that hypoxic tumours accumulate a greater number of APOBEC mutations than non-hypoxic tumours. Furthermore, a significant positive correlation was also seen between the expression of the two APOBEC genes most likely to cause the APOBEC mutational signatures, A3A and A3B, and the hypoxia signature. It is important to compare our *in vitro* data versus that from examining patient datasets. In chapter 3 we found no evidence of A3B induction in response to chronic hypoxia (at either 2 or <0.1% O_2), however in chapter 5 we saw a correlation between A3B and the hypoxia signature. Our conclusion is that the hypoxia signature can be used to inform on more than just chronic hypoxia and in this instance, it reflects cycling conditions. Our data also further suggests a currently unknown role for the other APOBEC3 genes (A3D, A3H, A3C, and A3F) in hypoxic regions of tumours.

Further experiments will be necessary to prove that NFκB transcriptionally upregulates A3B in cyclic hypoxia. Firstly, and most importantly, RT-qPCR to measure *A3B* mRNA expression in cyclic hypoxia to demonstrate that the induction occurs at the mRNA level. Secondly, chromatin immunoprecipitation (ChIP) experiments to confirm whether NFκB directly binds to the A3B promoter in cyclic hypoxia, or if it promotes expression through another NFκB target gene. Additional experiments will also be necessary to study the impact of ROS in cyclic hypoxia. The accumulation of ROS in cyclic hypoxia has only been demonstrated upon reoxygenation to 21% O_2 (Table 1.1), an oxygen concentration that is not relevant to human tumours. Both the amount of ROS as well as the type of ROS that predominate will have to be directly measured in the physiologically relevant oxygen tensions used to model cyclic hypoxia in our study. However, the fact that NAC decreased replication catastrophe in cyclic hypoxia makes it highly likely that ROS is present to some degree as NAC directly acts to quench intracellular ROS. An interesting question concerning ROS in cyclic hypoxia is whether it causes damage specifically in S-phase or throughout the cell cycle, and what the impact of damaged cells outside of S-phase would be on A3B? Immunofluorescence staining would suggest that the damage predominates in S-phase, as no significant increase in cells with DNA damage but no replication stress can be seen in cyclic hypoxia.

A surprising result was the fact that inhibition of ATR in cyclic hypoxia led to a G1 cell cycle arrest. We hypothesise that this occurs due to an accumulation of DNA damage prior to S-phase entry. While chronic hypoxia alone does not cause DNA damage, combining chronic hypoxia (<0.1% O_2) with ATR inhibition has been shown to lead to a significant increase in 53BP1 foci, indicating DNA damage (Pires et al., 2012). As ATR is inhibited 30 minutes prior to the start of treatment in cyclic hypoxia and the first stage in the cyclic treatment is <0.1% O_2 hypoxia (Figure 4.4 A), DNA damage could arise before the cells enter S-phase. DNA damage can trigger a G1 cell cycle arrest until the damage is resolved (Agarwal et al., 1995). A DNA damage dependent G1 cell cycle arrest in cyclic hypoxia could be further investigated

by determining the p53 dependence of the observed G1 arrest, as p53 is a key mediator of the G1 checkpoint through p21 signalling (Agami and Bernards, 2000). Additionally, testing to see if ATM inhibition would have the same impact on the cell cycle in cyclic hypoxia as ATR inhibition would further suggest DNA damage as the cause of the G1 cell cycle arrest.

Chapter 6

Discussion

Here, we have demonstrated that the biological response to replication stress is determined by the level of accompanying DNA damage (replication catastrophe) (Figure 6.1). Exposure to chronic hypoxia (<0.1% O_2) alone induces replication stress but this occurs in the absence of DNA damage (Bencokova et al., 2009; Hammond et al., 2002; Hammond et al., 2003b; Olcina et al., 2013). Expression of *A3D*, *A3H*, *A3C*, and *A3F* increased in chronic hypoxia while expression of A3B decreased. Mirroring the expression of A3B, a decrease in APOBEC mediated deamination was also observed in chronic hypoxia (<0.1% O_2). In contrast, replication stress induced by either HU or cyclic hypoxia lead to replication catastrophe due to ongoing DNA replication. Both new origin firing and ROS were implicated as two factors that contributed to cyclic hypoxia induced replication catastrophe. Both stresses also caused an increase in A3B expression and deamination. Most importantly, this induction was found to be dependent on replication catastrophe, as treatment with inhibitors of new origins and ROS abrogated A3B induction in cyclic hypoxia. NFκB was identified as a transcription factor expressed in cyclic hypoxia that drives expression of A3B. Surprisingly, ATR inhibition in cyclic hypoxia also abrogated the induction of A3B in cyclic hypoxia though likely through a G1 cell cycle arrest that prevented the accumulation of replication stress and DNA damage in S-phase. The importance of our finding was highlighted by evidence suggesting that cycling hypoxia leads to increased expression of A3B and increased APOBEC activity in patient samples. Overall, our study provides mechanistic insights into APOBEC induction and links this mechanism to the presence of APOBEC-mediated mutations in human cancers.

Numerous previous reports have described increased replication stress signaling and a G2/M phase cell cycle arrest following A3B overexpression (Buisson et al., 2017; Green et al., 2017; Green et al., 2016; Landry et al., 2011; Nikkila et al., 2017; Serebrenik et al., 2019). In contrast, we did not find an A3B-dependent effect on either replication stress or cell cycle profile in cyclic hypoxia. A notable difference between the previous studies and ours is the

method of A3B induction. Cyclic hypoxia induces the endogenous expression of A3B whereas previous reports rely on non-physiological levels of A3B resulting from exogenous overexpression. Differences in the overall quantity and localisation of A3B in the cell could potentially explain the discrepancy. Interestingly, one report tested the effects of both endogenously interferon-stimulated A3A and ectopically expressed A3A on cell viability and found that while ectopically expressed A3A significantly decreased cell viability, endogenously expressed A3A did not (Land et al., 2013).

Interestingly, a recent report investigating genes that are co-expressed with A3B/A3A demonstrated a correlation with a validated group of DDR effector genes. This contrasts with the rest of the APOBEC3 family that correlates with validated immune signatures (Ng et al., 2019). These data led to the conclusion that the increased expression of DDR factors was the result of APOBEC mediated deamination i.e. a form of DNA damage (Figure 1.18 B). Our data however would suggest otherwise, in our model angiogenesis and red blood cell flux leads to cyclic hypoxia and replication catastrophe/DNA damage which in turn results in the upregulation of A3B and APOBEC mediated deamination.

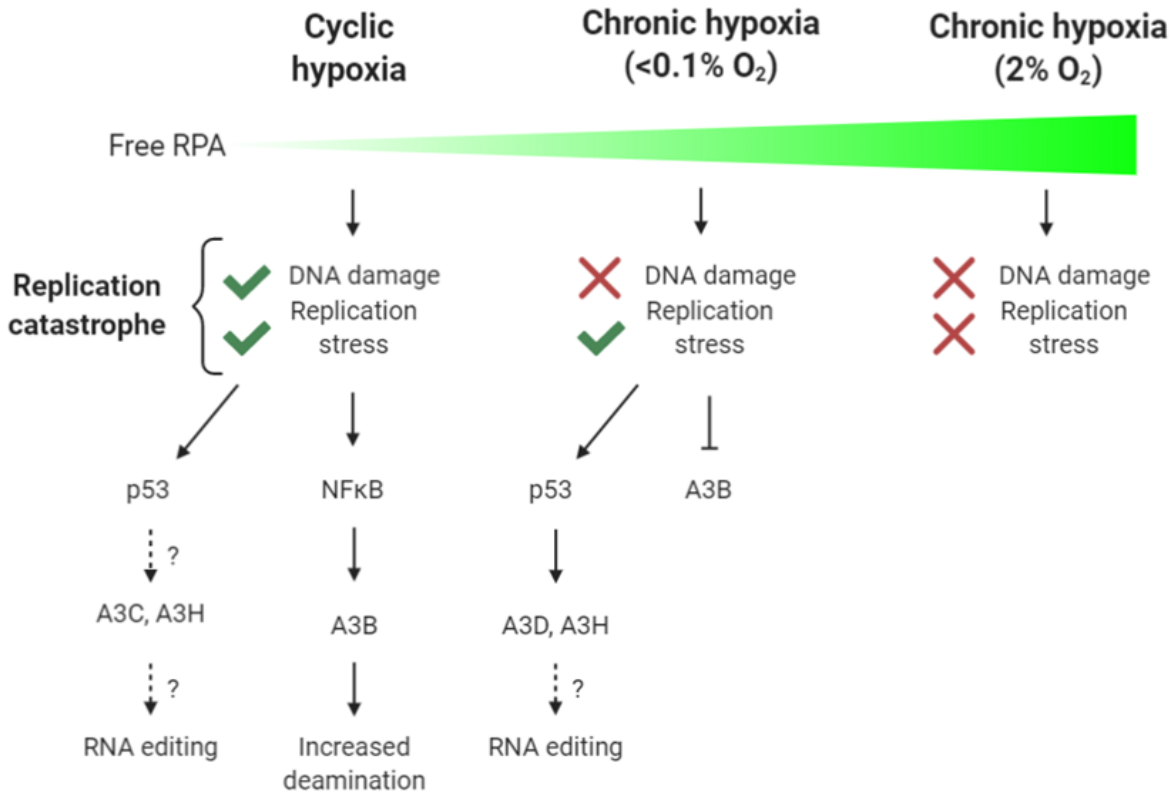


Figure 6.1 – Replication catastrophe induced by cyclic hypoxia leads to increased APOBEC3B activity
Different hypoxic treatments result in different quantities of exposed ssDNA. The amount of free RPA that is capable of binding ssDNA in each hypoxic condition is indicated by the green gradient. A lack of free RPA in cyclic hypoxia leads to replication catastrophe, which is characterised by the simultaneous occurrence of DNA damage and replication stress. Chronic hypoxia (<0.1% O_2) leads to replication stress in the absence of DNA damage while chronic hypoxia (2% O_2) leads to normal replication fork dynamics and no DNA damage. The consequences of each of these hypoxic treatments are detailed below. Dotted arrows are used to indicate hypothesised connections that our studies have not yet shown. Image created using Biorender.

APOBECs as a clinical target

Targeting APOBECs is an emerging clinical strategy. There are currently two main schools of thought of how modulation of APOBEC expressions in cancer could yield therapeutic benefits. The first strategy suggests decreasing APOBEC expression to limit tumourigenesis and the development of treatment resistance through a decreased mutation

rate. In this context, APOBEC inhibition can be thought of as a form of “sunscreen” (Harris, 2015). Sunscreen is applied to protect your skin from harmful UV rays from the sun which can increase the risk of developing harmful or tumourigenic mutations through the generation of thymidine dimers (Hart and Setlow, 1975). In the same way, APOBEC inhibition would shield the genome from the occurrence of APOBEC mutations that could generate mutagenic outcomes and contribute to tumourigenesis and treatment resistance (Harris, 2015; Olson et al., 2018). Supporting APOBEC inhibition as a clinical strategy, a study investigating the development of tamoxifen resistance *in vivo* showed a significant A3B dependent effect on the speed at which tumours developed treatment resistance to the chemotherapeutic tamoxifen (Law et al., 2016).

A key question concerning the inhibition of APOBECs is whether an inhibitor targeting a specific APOBEC or a pan-APOBEC inhibitor is preferred. A pan-APOBEC inhibitor would ensure that any mutagenic contributions from other APOBECs are also managed, as it has been shown that in the absence of A3B, A3H can compensate in function (Starrett et al., 2016). Another issue with a pan-inhibitor is it could also inhibit beneficial functions of other APOBECs, such as the roles of AID in class-switch recombination and somatic hypermutation (Longerich et al., 2006).

If a specific APOBEC was chosen for inhibition, A3B would be the most suitable candidate. A3B is a non-essential gene so inhibition could be included with a wide variety of other standard cancer therapies (Burns et al., 2013a). Additionally, due to the widespread expression of A3B resulting in the APOBEC mutation signatures in a wide variety of different cancer types, an A3B inhibitor could likely have an impact on the most patients (Burns et al., 2013b; Ng et al., 2019). Our data, through demonstrating that APOBEC mediated deamination is dependent on A3B in the RKO cell line, would suggest A3B as the primary candidate to have the largest impact on reducing APOBEC mediated deamination. Progress in developing an A3B inhibitor to be used in the clinic is still currently in preliminary stages. Proof of concept inhibitors demonstrating successful inhibition of a specific APOBEC3 family member targeting

A3G have been developed for the purpose of improving HIV treatment (Li et al., 2012; Olson et al., 2013). In this scenario A3G inhibitors were developed as a means to “hypomutate” the HIV genome so that it loses its ability to adapt (Olson et al., 2018).

Currently strategies to inhibit APOBEC activity include the development of a modified oligonucleotide that can be used to selectively inhibit A3B *in vitro* (Barzak et al., 2019; Kvach et al., 2019). Development of small molecule inhibitors to target A3B is currently hampered by the lack of data on the structure of A3B with a small molecule bound in its active site. Progress is however being made in a recent study that identified potential mechanisms for successful A3B inhibition with small molecules through the zinc binding domain (Shi et al., 2020). The development of more inhibitory compounds and preclinical testing will be required to determine if these strategies will prove efficacious in a clinical setting.

Somewhat controversially, it is worth considering that increasing APOBEC activity in cancers could be beneficial. There are two proposed mechanisms for how increasing APOBEC activity could yield therapeutic benefits. Firstly, in muscle invasive bladder cancer (MIBC), high APOBEC expression was shown correlate with a better patient prognosis as increased neoantigen presentation increased the immune response (Robertson et al., 2017). Regions of hypoxia have been demonstrated to be immune cold, meaning they have a lack of infiltrating T-cells (Schito, 2018; Terry et al., 2020). Further upregulating APOBEC activity could potentially increase efficacy of immune therapies in hypoxic regions of tumours. In support of this treatment strategy, increasing APOBEC expression has been shown to increase the efficacy of immune checkpoint blockade therapy due to increased neoepitope presentation (Driscoll et al., 2020). Secondly, further increasing APOBEC activity could potentially drive cells to cell death due to an accumulation of a deleterious quantity of mutations resulting from APOBEC activity (Olson et al., 2018). This strategy can be thought of as analogous to the mechanism by which APOBECs restrict viruses, by mutating their genome enough such that it becomes non-functional. Though there are many exciting theories

concerning the use of APOBEC inhibitors or agonists in clinical practice, much more needs to be uncovered before this becomes a reality.

APOBEC inhibition in combination with cancer therapy

Once inhibition of APOBEC is a reality, it will be important to consider in which clinical scenarios it will be effective. Considering APOBEC signalling alongside oxygen metabolism regulators and DDR inhibitors will be discussed further in this section. Though cyclic hypoxia is a naturally occurring phenomenon in cancer, oxygen conditions that resemble cyclic hypoxia are likely created through other cancer treatment modalities. Our data showing that cyclic hypoxia leads to replication catastrophe and APOBEC upregulation could suggest that this should be a relevant clinical consideration due to the negative impacts of A3B on treatment resistance. For example, it is well characterised that radiation leads to an increase in tumour oxygenation due to the decreased demand for oxygen from the normoxic cells killed by radiation therapy (Crokart et al., 2005). Another potential example is more recent therapeutics that act to decrease oxygen metabolism. The rationale behind these therapeutics is to decrease the demand for oxygen of cells in the periphery of tumours so that oxygen can penetrate to deeper areas that would have been hypoxic and thus radioresistant (Dewhirst, 2018). These therapeutics including metformin, papavarine, and atovaquone have been combined with radiotherapy and have demonstrated improved the efficacy of radiotherapy in xenograft tumour models (Ashton et al., 2016; Benej et al., 2018; Zannella et al., 2013). A pertinent question regarding these therapeutics is if they create a synthetic scenario of cyclic hypoxia? Atovaquone for example was administered for 7 days prior to tumour irradiation as that is the amount of time required for it to accumulate to clinically useful levels (Ashton et al., 2016; Dixon et al., 1996; Falloon et al., 1999). We would hypothesise that over this treatment period, the tumour would experience fluctuations in oxygen and APOBEC upregulation could occur.

Another clinical consideration suggested by our data is the effect of other DDR inhibitors on APOBEC expression. We showed that ATR inhibition with two inhibitors currently undergoing clinical trials for application in cancer therapy resulted in significant decreases in A3B expression and APOBEC mediated deamination. Though this was likely not due to a direct interaction it could still speak to an added benefit of these inhibitor treatments that was not previously known. If ATR inhibitor treatment can arrest cells experiencing cyclic hypoxia in G1 then replication catastrophe and APOBEC upregulation will not occur. In general, though the clinical implications of APOBEC have yet to be fully elucidated, they are likely to become a relevant consideration as a part of existing cancer therapies.

Future directions

To test if an increased APOBEC-mediated mutation rate is a consequence in cyclic hypoxia *in vitro*, experiments over a much longer time period would need to take place to see if cells treated in cyclic hypoxia would acquire mutations. One study has demonstrated that cells treated with 50 cycles of hypoxia and reoxygenation and then cultured over a period of months acquired mutations in genes including p53 and HIF1α (Verduzco et al., 2015). An interesting experiment would be to sequence cells treated in cyclic hypoxia over a long period of time to see if the APOBEC mutation signature would arise. These experiments could also be conducted in non-cancerous cell lines to show that cyclic hypoxia was a means by which cells could acquire activating tumour mutations.

Appendices

Appendix I – Conferences and travel awards

Conferences attended

1) The Association for Radiation Research Conference (Oxford) 2017 - poster presentation "**Severe Hypoxia Regulates Expression of Members of the APOBEC Family"**
2) 6th International Conference on Tumor Microenvironment and Cellular Stress: Signaling, Metabolism, Imaging and Therapeutic Targets (Crete) 2018 - poster presentation "**Hypoxia regulates expression and activity of the APOBEC family"**

Travel awards

Don Whitley Workstation Travel Grant (23/09/2019) – £250

Oxford Optronix Travel Grant (23/09/2019) - £200

Wolfson College Travel Grant (23/09/2019) - £300

Appendix II – Published papers from this thesis

1) **Bader, S.B.**; Ma, T.; Liang, J.; Maezono, S.E.B.; Buffa, F.M.; Hammond, E.M. Replication Catastrophe Induced by Cyclic Hypoxia Leads to Increased APOBEC3B Activity. (*Nucleic Acids Research, in review*)
2) **Bader, S.B.**; Dewhirst, M.W.; Hammond, E.M. Cyclic Hypoxia: An Update on Its Characteristics, Methods to Measure It and Biological Implications in Cancer. *Cancers* **2021**, *13*, 23.
3) Niemira, M.; Borowa-Mazgaj, B.; **Bader, S.B.**; Moszyńska, A.; Ratajewski, M.; Karaś, K.; Kwaśniewski, M.; Krętowski, A.; Mazerska, Z.; Hammond, E.M.; Skwarska, A. Anticancer Imidazoacridinone C-1311 is Effective in Androgen-Dependent and Androgen-Independent Prostate Cancer Cells. *Biomedicines* **2020**, *8*, 292.

References

Abu El Maaty, M.A., W. Strassburger, T. Qaiser, Y. Dabiri, and S. Wolfl. 2017. Differences in p53 status significantly influence the cellular response and cell survival to 1,25-dihydroxyvitamin D3-metformin cotreatment in colorectal cancer cells. *Mol Carcinog*. 56:2486-2498.

Adolph, M.B., R.P. Love, and L. Chelico. 2018. Biochemical Basis of APOBEC3 Deoxycytidine Deaminase Activity on Diverse DNA Substrates. *ACS Infect Dis*. 4:224-238.

Adolph, M.B., R.P. Love, Y. Feng, and L. Chelico. 2017. Enzyme cycling contributes to efficient induction of genome mutagenesis by the cytidine deaminase APOBEC3B. *Nucleic Acids Res*. 45:11925-11940.

Agami, R., and R. Bernards. 2000. Distinct initiation and maintenance mechanisms cooperate to induce G1 cell cycle arrest in response to DNA damage. *Cell*. 102:55-66.

Agarwal, M.L., A. Agarwal, W.R. Taylor, and G.R. Stark. 1995. p53 controls both the G2/M and the G1 cell cycle checkpoints and mediates reversible growth arrest in human fibroblasts. *Proc Natl Acad Sci U S A*. 92:8493-8497.

Akre, M.K., G.J. Starrett, J.S. Quist, N.A. Temiz, M.A. Carpenter, A.N. Tutt, A. Grigoriadis, and R.S. Harris. 2016. Mutation Processes in 293-Based Clones Overexpressing the DNA Cytosine Deaminase APOBEC3B. *PLoS One*. 11:e0155391.

Albini, A., and M.B. Sporn. 2007. The tumour microenvironment as a target for chemoprevention. *Nat Rev Cancer*. 7:139-147.

Alexandrov, L.B., J. Kim, N.J. Haradhvala, M.N. Huang, A.W. Tian Ng, Y. Wu, A. Boot, K.R. Covington, D.A. Gordenin, E.N. Bergstrom, S.M.A. Islam, N. Lopez-Bigas, L.J. Klimczak, J.R. McPherson, S. Morganella, R. Sabarinathan, D.A. Wheeler, V. Mustonen, P.M.S.W. Group, G. Getz, S.G. Rozen, M.R. Stratton, and P. Consortium. 2020. The repertoire of mutational signatures in human cancer. *Nature*. 578:94-101.

Alexandrov, L.B., S. Nik-Zainal, D.C. Wedge, S.A. Aparicio, S. Behjati, A.V. Biankin, G.R. Bignell, N. Bolli, A. Borg, A.L. Borresen-Dale, S. Boyault, B. Burkhardt, A.P. Butler, C. Caldas, H.R. Davies, C. Desmedt, R. Eils, J.E. Eyfjord, J.A. Foekens, M. Greaves, F. Hosoda, B. Hutter, T. Ilicic, S. Imbeaud, M. Imielinski, N. Jager, D.T. Jones, D. Jones, S. Knappskog, M. Kool, S.R. Lakhani, C. Lopez-Otin, S. Martin, N.C. Munshi, H. Nakamura, P.A. Northcott, M. Pajic, E. Papaemmanuil, A. Paradiso, J.V. Pearson, X.S. Puente, K. Raine, M. Ramakrishna, A.L. Richardson, J. Richter, P. Rosenstiel, M. Schlesner, T.N. Schumacher, P.N. Span, J.W. Teague, Y. Totoki, A.N. Tutt, R. Valdes-Mas, M.M. van Buuren, L. van 't Veer, A. Vincent-Salomon, N. Waddell, L.R. Yates, I. Australian Pancreatic Cancer Genome, I.B.C. Consortium, I.M.-S. Consortium, I. PedBrain, J. Zucman-Rossi, P.A. Futreal, U. McDermott, P. Lichter, M. Meyerson, S.M. Grimmond, R. Siebert, E. Campo, T. Shibata, S.M. Pfister, P.J. Campbell, and M.R. Stratton. 2013. Signatures of mutational processes in human cancer. *Nature*. 500:415-421.

Alhawarat, F.M., H.M. Hammad, M.S. Hijjawi, A.S. Sharab, D.A. Abuarqoub, M.A. Al Shhab, and M.A. Zihlif. 2019. The effect of cycling hypoxia on MCF-7 cancer stem cells and the impact of their microenvironment on angiogenesis using human umbilical vein endothelial cells (HUVECs) as a model. *PeerJ*. 7:e5990.

Aparicio, O.M., A.M. Stout, and S.P. Bell. 1999. Differential assembly of Cdc45p and DNA polymerases at early and late origins of DNA replication. *Proc Natl Acad Sci U S A*. 96:9130-9135.

Ardaseva, A., R.A. Gatenby, A.R.A. Anderson, H.M. Byrne, P.K. Maini, and T. Lorenzi. 2020. A Mathematical Dissection of the Adaptation of Cell Populations to Fluctuating Oxygen Levels. *Bull Math Biol*. 82:81.

Ashton, T.M., E. Fokas, L.A. Kunz-Schughart, L.K. Folkes, S. Anbalagan, M. Huether, C.J. Kelly, G. Pirovano, F.M. Buffa, E.M. Hammond, M. Stratford, R.J. Muschel, G.S.

Higgins, and W.G. McKenna. 2016. The anti-malarial atovaquone increases radiosensitivity by alleviating tumour hypoxia. *Nat Commun*. 7:12308.

Bagnall, J., J. Leedale, S.E. Taylor, D.G. Spiller, M.R. White, K.J. Sharkey, R.N. Bearon, and V. See. 2014. Tight control of hypoxia-inducible factor-alpha transient dynamics is essential for cell survival in hypoxia. *J Biol Chem*. 289:5549-5564.

Bardos, J.I., and M. Ashcroft. 2005. Negative and positive regulation of HIF-1: a complex network. *Biochim Biophys Acta*. 1755:107-120.

Barker, H.E., J.T. Paget, A.A. Khan, and K.J. Harrington. 2015. The tumour microenvironment after radiotherapy: mechanisms of resistance and recurrence. *Nat Rev Cancer*. 15:409-425.

Bartek, J., C. Lukas, and J. Lukas. 2004. Checking on DNA damage in S phase. *Nat Rev Mol Cell Biol*. 5:792-804.

Barzak, F.M., S. Harjes, M.V. Kvach, H.M. Kurup, G.B. Jameson, V.V. Filichev, and E. Harjes. 2019. Selective inhibition of APOBEC3 enzymes by single-stranded DNAs containing 2'-deoxyzebularine. *Org Biomol Chem*. 17:9435-9441.

Baysal, B.E. 2007. A recurrent stop-codon mutation in succinate dehydrogenase subunit B gene in normal peripheral blood and childhood T-cell acute leukemia. *PLoS One*. 2:e436.

Baysal, B.E., K. De Jong, B. Liu, J. Wang, S.K. Patnaik, P.K. Wallace, and R.T. Taggart. 2013. Hypoxia-inducible C-to-U coding RNA editing downregulates SDHB in monocytes. *PeerJ*. 1:e152.

Beck, H., V. Nahse-Kumpf, M.S. Larsen, K.A. O'Hanlon, S. Patzke, C. Holmberg, J. Mejlvang, A. Groth, O. Nielsen, R.G. Syljuasen, and C.S. Sorensen. 2012. Cyclin-dependent kinase suppression by WEE1 kinase protects the genome through control of replication initiation and nucleotide consumption. *Mol Cell Biol*. 32:4226-4236.

Bell, E.L., T.A. Klimova, J. Eisenbart, C.T. Moraes, M.P. Murphy, G.R. Budinger, and N.S. Chandel. 2007. The Qo site of the mitochondrial complex III is required for the transduction of hypoxic signaling via reactive oxygen species production. *J Cell Biol*. 177:1029-1036.

Bencokova, Z., M.R. Kaufmann, I.M. Pires, P.S. Lecane, A.J. Giaccia, and E.M. Hammond. 2009. ATM activation and signaling under hypoxic conditions. *Mol Cell Biol*. 29:526-537.

Benej, M., X. Hong, S. Vibhute, S. Scott, J. Wu, E. Graves, Q.T. Le, A.C. Koong, A.J. Giaccia, B. Yu, C.S. Chen, I. Papandreou, and N.C. Denko. 2018. Papaverine and its derivatives radiosensitize solid tumors by inhibiting mitochondrial metabolism. *Proc Natl Acad Sci U S A*. 115:10756-10761.

Bennewith, K.L., J.A. Raleigh, and R.E. Durand. 2002. Orally administered pimonidazole to label hypoxic tumor cells. *Cancer Res*. 62:6827-6830.

Bertout, J.A., S.A. Patel, and M.C. Simon. 2008. The impact of O2 availability on human cancer. *Nat Rev Cancer*. 8:967-975.

Bester, A.C., M. Roniger, Y.S. Oren, M.M. Im, D. Sarni, M. Chaoat, A. Bensimon, G. Zamir, D.S. Shewach, and B. Kerem. 2011. Nucleotide deficiency promotes genomic instability in early stages of cancer development. *Cell*. 145:435-446.

Betous, R., A.C. Mason, R.P. Rambo, C.E. Bansbach, A. Badu-Nkansah, B.M. Sirbu, B.F. Eichman, and D. Cortez. 2012. SMARCAL1 catalyzes fork regression and Holliday junction migration to maintain genome stability during DNA replication. *Genes Dev*. 26:151-162.

Bhaskara, V.K., I. Mohanam, J.S. Rao, and S. Mohanam. 2012. Intermittent hypoxia regulates stem-like characteristics and differentiation of neuroblastoma cells. *PLoS One*. 7:e30905.

Bianco, J.N., J. Poli, J. Saksouk, J. Bacal, M.J. Silva, K. Yoshida, Y.L. Lin, H. Tourriere, A. Lengronne, and P. Pasero. 2012. Analysis of DNA replication profiles in budding yeast and mammalian cells using DNA combing. *Methods*. 57:149-157.

Bister, K. 2015. Discovery of oncogenes: The advent of molecular cancer research. *Proc Natl Acad Sci U S A*. 112:15259-15260.

Blackford, A.N., and S.P. Jackson. 2017. ATM, ATR, and DNA-PK: The Trinity at the Heart of the DNA Damage Response. *Mol Cell*. 66:801-817.

Blow, J.J., X.Q. Ge, and D.A. Jackson. 2011. How dormant origins promote complete genome replication. *Trends Biochem Sci*. 36:405-414.

Bonnitcha, P., S. Grieve, and G. Figtree. 2018. Clinical imaging of hypoxia: Current status and future directions. *Free Radic Biol Med*. 126:296-312.

Brahimi-Horn, M.C., and J. Pouyssegur. 2007. Oxygen, a source of life and stress. *FEBS Lett*. 581:3582-3591.

Brahimi-Horn, M.C., and J. Pouyssegur. 2009. HIF at a glance. *J Cell Sci*. 122:1055-1057.

Bristow, R.G., and R.P. Hill. 2008. Hypoxia and metabolism. Hypoxia, DNA repair and genetic instability. *Nat Rev Cancer*. 8:180-192.

Brown, E.J., and D. Baltimore. 2003. Essential and dispensable roles of ATR in cell cycle arrest and genome maintenance. *Genes Dev*. 17:615-628.

Brown, J.M., and W.R. Wilson. 2004. Exploiting tumour hypoxia in cancer treatment. *Nat Rev Cancer*. 4:437-447.

Buchan, J.R., and R. Parker. 2009. Eukaryotic stress granules: the ins and outs of translation. *Mol Cell*. 36:932-941.

Buffa, F.M., A.L. Harris, C.M. West, and C.J. Miller. 2010. Large meta-analysis of multiple cancers reveals a common, compact and highly prognostic hypoxia metagene. *Br J Cancer*. 102:428-435.

Buisson, R., J.L. Boisvert, C.H. Benes, and L. Zou. 2015. Distinct but Concerted Roles of ATR, DNA-PK, and Chk1 in Countering Replication Stress during S Phase. *Mol Cell*. 59:1011-1024.

Buisson, R., M.S. Lawrence, C.H. Benes, and L. Zou. 2017. APOBEC3A and APOBEC3B Activities Render Cancer Cells Susceptible to ATR Inhibition. *Cancer Res*. 77:4567-4578.

Burns, M.B., L. Lackey, M.A. Carpenter, A. Rathore, A.M. Land, B. Leonard, E.W. Refsland, D. Kotandeniya, N. Tretyakova, J.B. Nikas, D. Yee, N.A. Temiz, D.E. Donohue, R.M. McDougle, W.L. Brown, E.K. Law, and R.S. Harris. 2013a. APOBEC3B is an enzymatic source of mutation in breast cancer. *Nature*. 494:366-370.

Burns, M.B., N.A. Temiz, and R.S. Harris. 2013b. Evidence for APOBEC3B mutagenesis in multiple human cancers. *Nat Genet*. 45:977-983.

Byun, T.S., M. Pacek, M.C. Yee, J.C. Walter, and K.A. Cimprich. 2005. Functional uncoupling of MCM helicase and DNA polymerase activities activates the ATR-dependent checkpoint. *Genes Dev*. 19:1040-1052.

Cairns, R.A., and R.P. Hill. 2004. Acute hypoxia enhances spontaneous lymph node metastasis in an orthotopic murine model of human cervical carcinoma. *Cancer Res*. 64:2054-2061.

Cairns, R.A., T. Kalliomaki, and R.P. Hill. 2001. Acute (cyclic) hypoxia enhances spontaneous metastasis of KHT murine tumors. *Cancer Res*. 61:8903-8908.

Campisi, J. 2013. Aging, cellular senescence, and cancer. *Annu Rev Physiol*. 75:685-705.

Cao, Y., C.Y. Li, B.J. Moeller, D. Yu, Y. Zhao, M.R. Dreher, S. Shan, and M.W. Dewhirst. 2005. Observation of incipient tumor angiogenesis that is independent of hypoxia and hypoxia inducible factor-1 activation. *Cancer Res*. 65:5498-5505.

Carroll, V.A., and M. Ashcroft. 2006. Role of hypoxia-inducible factor (HIF)-1alpha versus HIF-2alpha in the regulation of HIF target genes in response to hypoxia, insulin-like growth

factor-I, or loss of von Hippel-Lindau function: implications for targeting the HIF pathway. *Cancer Res*. 66:6264-6270.

Cavadas, M.A., L.K. Nguyen, and A. Cheong. 2013. Hypoxia-inducible factor (HIF) network: insights from mathematical models. *Cell Commun Signal*. 11:42.

Chambers, A.F., A.C. Groom, and I.C. MacDonald. 2002. Dissemination and growth of cancer cells in metastatic sites. *Nat Rev Cancer*. 2:563-572.

Chan, K., M.A. Resnick, and D.A. Gordenin. 2013. The choice of nucleotide inserted opposite abasic sites formed within chromosomal DNA reveals the polymerase activities participating in translesion DNA synthesis. *DNA Repair (Amst)*. 12:878-889.

Chan, K., S.A. Roberts, L.J. Klimczak, J.F. Sterling, N. Saini, E.P. Malc, J. Kim, D.J. Kwiatkowski, D.C. Fargo, P.A. Mieczkowski, G. Getz, and D.A. Gordenin. 2015. An APOBEC3A hypermutation signature is distinguishable from the signature of background mutagenesis by APOBEC3B in human cancers. *Nat Genet*. 47:1067-1072.

Chandel, N.S., E. Maltepe, E. Goldwasser, C.E. Mathieu, M.C. Simon, and P.T. Schumacker. 1998. Mitochondrial reactive oxygen species trigger hypoxia-induced transcription. *Proc Natl Acad Sci U S A*. 95:11715-11720.

Chaplin, D.J., P.L. Olive, and R.E. Durand. 1987. Intermittent blood flow in a murine tumor: radiobiological effects. *Cancer Res*. 47:597-601.

Chen, A., J. Sceneay, N. Godde, T. Kinwel, S. Ham, E.W. Thompson, P.O. Humbert, and A. Moller. 2018. Intermittent hypoxia induces a metastatic phenotype in breast cancer. *Oncogene*. 37:4214-4225.

Chen, C., N. Pore, A. Behrooz, F. Ismail-Beigi, and A. Maity. 2001. Regulation of glut1 mRNA by hypoxia-inducible factor-1. Interaction between H-ras and hypoxia. *J Biol Chem*. 276:9519-9525.

Chen, W.L., C.C. Wang, Y.J. Lin, C.P. Wu, and C.H. Hsieh. 2015. Cycling hypoxia induces chemoresistance through the activation of reactive oxygen species-mediated B-cell lymphoma extra-long pathway in glioblastoma multiforme. *J Transl Med*. 13:389.

Cheng, A.Z., J. Yockteng-Melgar, M.C. Jarvis, N. Malik-Soni, I. Borozan, M.A. Carpenter, J.L. McCann, D. Ebrahimi, N.M. Shaban, E. Marcon, J. Greenblatt, W.L. Brown, L. Frappier, and R.S. Harris. 2019. Epstein-Barr virus BORF2 inhibits cellular APOBEC3B to preserve viral genome integrity. *Nat Microbiol*. 4:78-88.

Chitneni, S.K., G.M. Palmer, M.R. Zalutsky, and M.W. Dewhirst. 2011. Molecular imaging of hypoxia. *J Nucl Med*. 52:165-168.

Chou, C.W., C.C. Wang, C.P. Wu, Y.J. Lin, Y.C. Lee, Y.W. Cheng, and C.H. Hsieh. 2012. Tumor cycling hypoxia induces chemoresistance in glioblastoma multiforme by upregulating the expression and function of ABCB1. *Neuro Oncol*. 14:1227-1238.

Chouaib, S., M.Z. Noman, K. Kosmatopoulos, and M.A. Curran. 2017. Hypoxic stress: obstacles and opportunities for innovative immunotherapy of cancer. *Oncogene*. 36:439-445.

Ciccia, A., and S.J. Elledge. 2010. The DNA damage response: making it safe to play with knives. *Mol Cell*. 40:179-204.

Classon, M., and E. Harlow. 2002. The retinoblastoma tumour suppressor in development and cancer. *Nat Rev Cancer*. 2:910-917.

Cosse, J.P., and C. Michiels. 2008. Tumour hypoxia affects the responsiveness of cancer cells to chemotherapy and promotes cancer progression. *Anticancer Agents Med Chem*. 8:790-797.

Couch, F.B., C.E. Bansbach, R. Driscoll, J.W. Luzwick, G.G. Glick, R. Betous, C.M. Carroll, S.Y. Jung, J. Qin, K.A. Cimprich, and D. Cortez. 2013. ATR phosphorylates SMARCAL1 to prevent replication fork collapse. *Genes Dev*. 27:1610-1623.

Craig, S.G., M.P. Humphries, M. Alderdice, V. Bingham, S.D. Richman, M.B. Loughrey, H.G. Coleman, A. Viratham-Pulsawatdi, K. McCombe, G.I. Murray, A. Blake, E. Domingo,

J. Robineau, L. Brown, D. Fisher, M.T. Seymour, P. Quirke, P. Bankhead, S. McQuaid, M. Lawler, D.G. McArt, T.S. Maughan, J.A. James, and M. Salto-Tellez. 2020. Immune status is prognostic for poor survival in colorectal cancer patients and is associated with tumour hypoxia. *Br J Cancer*. 123:1280-1288.

Crokart, N., B.F. Jordan, C. Baudelet, R. Ansiaux, P. Sonveaux, V. Gregoire, N. Beghein, J. DeWever, C. Bouzin, O. Feron, and B. Gallez. 2005. Early reoxygenation in tumors after irradiation: determining factors and consequences for radiotherapy regimens using daily multiple fractions. *Int J Radiat Oncol Biol Phys*. 63:901-910.

Culver, C., A. Sundqvist, S. Mudie, A. Melvin, D. Xirodimas, and S. Rocha. 2010. Mechanism of hypoxia-induced NF-kappaB. *Mol Cell Biol*. 30:4901-4921.

D'Angiolella, V., V. Donato, F.M. Forrester, Y.T. Jeong, C. Pellacani, Y. Kudo, A. Saraf, L. Florens, M.P. Washburn, and M. Pagano. 2012. Cyclin F-mediated degradation of ribonucleotide reductase M2 controls genome integrity and DNA repair. *Cell*. 149:1023-1034.

Daneau, G., R. Boidot, P. Martinive, and O. Feron. 2010. Identification of cyclooxygenase-2 as a major actor of the transcriptomic adaptation of endothelial and tumor cells to cyclic hypoxia: effect on angiogenesis and metastases. *Clin Cancer Res*. 16:410-419.

Dang, D.T., F. Chen, L.B. Gardner, J.M. Cummins, C. Rago, F. Bunz, S.V. Kantsevoy, and L.H. Dang. 2006. Hypoxia-inducible factor-1alpha promotes nonhypoxia-mediated proliferation in colon cancer cells and xenografts. *Cancer Res*. 66:1684-1936.

Davies, S.L., P.S. North, and I.D. Hickson. 2007. Role for BLM in replication-fork restart and suppression of origin firing after replicative stress. *Nat Struct Mol Biol*. 14:677-679.

Debacq-Chainiaux, F., J.D. Erusalimsky, J. Campisi, and O. Toussaint. 2009. Protocols to detect senescence-associated beta-galactosidase (SA-betagal) activity, a biomarker of senescent cells in culture and in vivo. *Nat Protoc*. 4:1798-1806.

Deininger, P.L., and M.A. Batzer. 2002. Mammalian retroelements. *Genome Res*. 12:1455-1465.

Delprat, V., C. Tellier, C. Demazy, M. Raes, O. Feron, and C. Michiels. 2020. Cycling hypoxia promotes a pro-inflammatory phenotype in macrophages via JNK/p65 signaling pathway. *Sci Rep*. 10:882.

Dewhirst, M.W. 2018. A potential solution for eliminating hypoxia as a cause for radioresistance. *Proc Natl Acad Sci U S A*. 115:10548-10550.

Dewhirst, M.W., Y. Cao, and B. Moeller. 2008. Cycling hypoxia and free radicals regulate angiogenesis and radiotherapy response. *Nat Rev Cancer*. 8:425-437.

Dewhirst, M.W., H. Kimura, S.W. Rehmus, R.D. Braun, D. Papahadjopoulos, K. Hong, and T.W. Secomb. 1996. Microvascular studies on the origins of perfusion-limited hypoxia. *Br J Cancer Suppl*. 27:S247-251.

Dixon, R., A.L. Pozniak, H.M. Watt, P. Rolan, and J. Posner. 1996. Single-dose and steady-state pharmacokinetics of a novel microfluidized suspension of atovaquone in human immunodeficiency virus-seropositive patients. *Antimicrob Agents Chemother*. 40:556-560.

Dobrynin, G., T.E. McAllister, K.B. Leszczynska, S. Ramachandran, A.J. Krieg, A. Kawamura, and E.M. Hammond. 2017. KDM4A regulates HIF-1 levels through H3K9me3. *Sci Rep*. 7:11094.

Driscoll, C.B., M.R. Schuelke, T. Kottke, J.M. Thompson, P. Wongthida, J.M. Tonne, A.L. Huff, A. Miller, K.G. Shim, A. Molan, C. Wetmore, P. Selby, A. Samson, K. Harrington, H. Pandha, A. Melcher, J.S. Pulido, R. Harris, L. Evgin, and R.G. Vile. 2020. APOBEC3B-mediated corruption of the tumor cell immunopeptidome induces heteroclitic neoepitopes for cancer immunotherapy. *Nat Commun*. 11:790.

Duan, C. 2016. Hypoxia-inducible factor 3 biology: complexities and emerging themes. *Am J Physiol Cell Physiol*. 310:C260-269.

Eddy, H.A., and G.W. Casarett. 1973. Development of the vascular system in the hamster malignant neurilemmoma. *Microvasc Res*. 6:63-82.

Esnault, C., O. Heidmann, F. Delebecque, M. Dewannieux, D. Ribet, A.J. Hance, T. Heidmann, and O. Schwartz. 2005. APOBEC3G cytidine deaminase inhibits retrotransposition of endogenous retroviruses. *Nature*. 433:430-433.

Evrin, C., P. Clarke, J. Zech, R. Lurz, J. Sun, S. Uhle, H. Li, B. Stillman, and C. Speck. 2009. A double-hexameric MCM2-7 complex is loaded onto origin DNA during licensing of eukaryotic DNA replication. *Proc Natl Acad Sci U S A*. 106:20240-20245.

Ewing, J. 1935. The Modern Attitude Toward Traumatic Cancer. *Bull N Y Acad Med*. 11:281-333.

Falloon, J., S. Sargent, S.C. Piscitelli, C. Bechtel, S.W. LaFon, B. Sadler, R.E. Walker, J.A. Kovacs, M.A. Polis, R.T. Davey, Jr., H.C. Lane, and H. Masur. 1999. Atovaquone suspension in HIV-infected volunteers: pharmacokinetics, pharmacodynamics, and TMP-SMX interaction study. *Pharmacotherapy*. 19:1050-1056.

Faltas, B.M., D. Prandi, S.T. Tagawa, A.M. Molina, D.M. Nanus, C. Sternberg, J. Rosenberg, J.M. Mosquera, B. Robinson, O. Elemento, A. Sboner, H. Beltran, F. Demichelis, and M.A. Rubin. 2016. Clonal evolution of chemotherapy-resistant urothelial carcinoma. *Nat Genet*. 48:1490-1499.

Feijoo, C., C. Hall-Jackson, R. Wu, D. Jenkins, J. Leitch, D.M. Gilbert, and C. Smythe. 2001. Activation of mammalian Chk1 during DNA replication arrest: a role for Chk1 in the intra-S phase checkpoint monitoring replication origin firing. *J Cell Biol*. 154:913-923.

Feldman, R.P., and J.T. Goodrich. 1999. The Edwin Smith Surgical Papyrus. *Childs Nerv Syst*. 15:281-284.

Feng, Y., M.H. Goubran, T.B. Follack, and L. Chelico. 2017. Deamination-independent restriction of LINE-1 retrotransposition by APOBEC3H. *Sci Rep*. 7:10881.

Finkel, T., and N.J. Holbrook. 2000. Oxidants, oxidative stress and the biology of ageing. *Nature*. 408:239-247.

Forment, J.V., M. Blasius, I. Guerini, and S.P. Jackson. 2011. Structure-specific DNA endonuclease Mus81/Eme1 generates DNA damage caused by Chk1 inactivation. *PLoS One*. 6:e23517.

Foskolou, I.P., D. Biasoli, M.M. Olcina, and E.M. Hammond. 2016. Measuring DNA Replication in Hypoxic Conditions. *Adv Exp Med Biol*. 899:11-25.

Foskolou, I.P., C. Jorgensen, K.B. Leszczynska, M.M. Olcina, H. Tarhonskaya, B. Haisma, V. D'Angiolella, W.K. Myers, C. Domene, E. Flashman, and E.M. Hammond. 2017. Ribonucleotide Reductase Requires Subunit Switching in Hypoxia to Maintain DNA Replication. *Mol Cell*. 66:206-220 e209.

Freund, A., R.M. Laberge, M. Demaria, and J. Campisi. 2012. Lamin B1 loss is a senescence-associated biomarker. *Mol Biol Cell*. 23:2066-2075.

Gaillard, H., T. Garcia-Muse, and A. Aguilera. 2015. Replication stress and cancer. *Nat Rev Cancer*. 15:276-289.

Galanis, A., A. Pappa, A. Giannakakis, E. Lanitis, D. Dangaj, and R. Sandaltzopoulos. 2008. Reactive oxygen species and HIF-1 signalling in cancer. *Cancer Lett*. 266:12-20.

Garcia-Barros, M., F. Paris, C. Cordon-Cardo, D. Lyden, S. Rafii, A. Haimovitz-Friedman, Z. Fuks, and R. Kolesnick. 2003. Tumor response to radiotherapy regulated by endothelial cell apoptosis. *Science*. 300:1155-1159.

Gardner, L.B., Q. Li, M.S. Park, W.M. Flanagan, G.L. Semenza, and C.V. Dang. 2001. Hypoxia inhibits G1/S transition through regulation of p27 expression. *J Biol Chem*. 276:7919-7926.

Ge, X.Q., D.A. Jackson, and J.J. Blow. 2007. Dormant origins licensed by excess Mcm2-7 are required for human cells to survive replicative stress. *Genes Dev*. 21:3331-3341.

Goodall, C.M., A.G. Sanders, and P. Shubik. 1965. Studies of vascular patterns in living tumors with a transparent chamber inserted in hamster cheek pouch. *J Natl Cancer Inst*. 35:497-521.

Granger, D.N., and P.R. Kvietys. 2015. Reperfusion injury and reactive oxygen species: The evolution of a concept. *Redox Biol*. 6:524-551.

Green, A.M., K. Budagyan, K.E. Hayer, M.A. Reed, M.R. Savani, G.B. Wertheim, and M.D. Weitzman. 2017. Cytosine Deaminase APOBEC3A Sensitizes Leukemia Cells to Inhibition of the DNA Replication Checkpoint. *Cancer Res*. 77:4579-4588.

Green, A.M., S. Landry, K. Budagyan, D.C. Avgousti, S. Shalhout, A.S. Bhagwat, and M.D. Weitzman. 2016. APOBEC3A damages the cellular genome during DNA replication. *Cell Cycle*. 15:998-1008.

Gu, J., Q. Chen, X. Xiao, F. Ito, A. Wolfe, and X.S. Chen. 2016. Biochemical Characterization of APOBEC3H Variants: Implications for Their HIV-1 Restriction Activity and mC Modification. *J Mol Biol*. 428:4626-4638.

Gupta, R., C. Chetty, P. Bhoopathi, S. Lakka, S. Mohanam, J.S. Rao, and D.E. Dinh. 2011. Downregulation of uPA/uPAR inhibits intermittent hypoxia-induced epithelial-mesenchymal transition (EMT) in DAOY and D283 medulloblastoma cells. *Int J Oncol*. 38:733-744.

Gutsche, K., E.B. Randi, V. Blank, D. Fink, R.H. Wenger, C. Leo, and C.C. Scholz. 2016. Intermittent hypoxia confers pro-metastatic gene expression selectively through NF-kappaB in inflammatory breast cancer cells. *Free Radic Biol Med*. 101:129-142.

Guzy, R.D., B. Hoyos, E. Robin, H. Chen, L. Liu, K.D. Mansfield, M.C. Simon, U. Hammerling, and P.T. Schumacker. 2005. Mitochondrial complex III is required for hypoxia-induced ROS production and cellular oxygen sensing. *Cell Metab*. 1:401-408.

Hajdu, S.I. 2011. A note from history: landmarks in history of cancer, part 1. *Cancer*. 117:1097-1102.

Hall, E.J., and A.J. Giaccia. 2006. Radiobiology for the Radiologist. Lippincott Williams & Wilkins.

Hammond, E.M., M.C. Asselin, D. Forster, J.P. O'Connor, J.M. Senra, and K.J. Williams. 2014. The meaning, measurement and modification of hypoxia in the laboratory and the clinic. *Clin Oncol (R Coll Radiol)*. 26:277-288.

Hammond, E.M., N.C. Denko, M.J. Dorie, R.T. Abraham, and A.J. Giaccia. 2002. Hypoxia links ATR and p53 through replication arrest. *Mol Cell Biol*. 22:1834-1843.

Hammond, E.M., M.J. Dorie, and A.J. Giaccia. 2003a. ATR/ATM targets are phosphorylated by ATR in response to hypoxia and ATM in response to reoxygenation. *J Biol Chem*. 278:12207-12213.

Hammond, E.M., M.J. Dorie, and A.J. Giaccia. 2004. Inhibition of ATR leads to increased sensitivity to hypoxia/reoxygenation. *Cancer Res*. 64:6556-6562.

Hammond, E.M., S.L. Green, and A.J. Giaccia. 2003b. Comparison of hypoxia-induced replication arrest with hydroxyurea and aphidicolin-induced arrest. *Mutat Res*. 532:205-213.

Hanahan, D., and R.A. Weinberg. 2000. The hallmarks of cancer. *Cell*. 100:57-70.

Hanahan, D., and R.A. Weinberg. 2011. Hallmarks of cancer: the next generation. *Cell*. 144:646-674.

Harada, H. 2016. Hypoxia-inducible factor 1-mediated characteristic features of cancer cells for tumor radioresistance. *J Radiat Res*. 57 Suppl 1:i99-i105.

Haradhvala, N.J., P. Polak, P. Stojanov, K.R. Covington, E. Shinbrot, J.M. Hess, E. Rheinbay, J. Kim, Y.E. Maruvka, L.Z. Braunstein, A. Kamburov, P.C. Hanawalt, D.A. Wheeler, A. Koren, M.S. Lawrence, and G. Getz. 2016. Mutational Strand Asymmetries in Cancer Genomes Reveal Mechanisms of DNA Damage and Repair. *Cell*. 164:538-549.

Harari, A., M. Ooms, L.C. Mulder, and V. Simon. 2009. Polymorphisms and splice variants influence the antiretroviral activity of human APOBEC3H. *J Virol*. 83:295-303.

Harris, R.S. 2015. Molecular mechanism and clinical impact of APOBEC3B-catalyzed mutagenesis in breast cancer. *Breast Cancer Res*. 17:8.

Harris, R.S., K.N. Bishop, A.M. Sheehy, H.M. Craig, S.K. Petersen-Mahrt, I.N. Watt, M.S. Neuberger, and M.H. Malim. 2003. DNA deamination mediates innate immunity to retroviral infection. *Cell*. 113:803-809.

Harris, R.S., and J.P. Dudley. 2015. APOBECs and virus restriction. *Virology*. 479-480:131-145.

Harris, R.S., and M.T. Liddament. 2004. Retroviral restriction by APOBEC proteins. *Nat Rev Immunol*. 4:868-877.

Harris, R.S., S.K. Petersen-Mahrt, and M.S. Neuberger. 2002. RNA editing enzyme APOBEC1 and some of its homologs can act as DNA mutators. *Mol Cell*. 10:1247-1253.

Hart, R.W., and R.B. Setlow. 1975. Direct evidence that pyrimidine dimers in DNA result in neoplastic transformation. *Basic Life Sci*. 5B:719-724.

Heffernan, T.P., D.A. Simpson, A.R. Frank, A.N. Heinloth, R.S. Paules, M. Cordeiro-Stone, and W.K. Kaufmann. 2002. An ATR- and Chk1-dependent S checkpoint inhibits replicon initiation following UVC-induced DNA damage. *Mol Cell Biol*. 22:8552-8561.

Helleday, T., S. Eshtad, and S. Nik-Zainal. 2014. Mechanisms underlying mutational signatures in human cancers. *Nat Rev Genet*. 15:585-598.

Henderson, S., A. Chakravarthy, X. Su, C. Boshoff, and T.R. Fenton. 2014. APOBEC-mediated cytosine deamination links PIK3CA helical domain mutations to human papillomavirus-driven tumor development. *Cell Rep*. 7:1833-1841.

Henderson, S., and T. Fenton. 2015. APOBEC3 genes: retroviral restriction factors to cancer drivers. *Trends Mol Med*. 21:274-284.

Hillestad, T., T. Hompland, C.S. Fjeldbo, V.E. Skingen, U.B. Salberg, E.K. Aarnes, A. Nilsen, K.V. Lund, T.S. Evensen, G.B. Kristensen, T. Stokke, and H. Lyng. 2020. MR Imaging Distinguishes Tumor Hypoxia Levels of Different Prognostic and Biological Significance in Cervical Cancer. *Cancer Res*.

Hlouschek, J., C. Hansel, V. Jendrossek, and J. Matschke. 2018a. The Mitochondrial Citrate Carrier (SLC25A1) Sustains Redox Homeostasis and Mitochondrial Metabolism Supporting Radioresistance of Cancer Cells With Tolerance to Cycling Severe Hypoxia. *Front Oncol*. 8:170.

Hlouschek, J., V. Ritter, F. Wirsdorfer, D. Klein, V. Jendrossek, and J. Matschke. 2018b. Targeting SLC25A10 alleviates improved antioxidant capacity and associated radioresistance of cancer cells induced by chronic-cycling hypoxia. *Cancer Lett*. 439:24-38.

Hockel, M., and P. Vaupel. 2001. Tumor hypoxia: definitions and current clinical, biologic, and molecular aspects. *J Natl Cancer Inst*. 93:266-276.

Hoopes, J.I., L.M. Cortez, T.M. Mertz, E.P. Malc, P.A. Mieczkowski, and S.A. Roberts. 2016. APOBEC3A and APOBEC3B Preferentially Deaminate the Lagging Strand Template during DNA Replication. *Cell Rep*. 14:1273-1282.

Horsman, M.R., L.S. Mortensen, J.B. Petersen, M. Busk, and J. Overgaard. 2012. Imaging hypoxia to improve radiotherapy outcome. *Nat Rev Clin Oncol*. 9:674-687.

Hsieh, C.H., C.H. Lee, J.A. Liang, C.Y. Yu, and W.C. Shyu. 2010. Cycling hypoxia increases U87 glioma cell radioresistance via ROS induced higher and long-term HIF-1 signal transduction activity. *Oncol Rep*. 24:1629-1636.

Hsieh, C.H., W.C. Shyu, C.Y. Chiang, J.W. Kuo, W.C. Shen, and R.S. Liu. 2011. NADPH oxidase subunit 4-mediated reactive oxygen species contribute to cycling hypoxia-promoted tumor progression in glioblastoma multiforme. *PLoS One*. 6:e23945.

Hsieh, C.H., C.P. Wu, H.T. Lee, J.A. Liang, C.Y. Yu, and Y.J. Lin. 2012. NADPH oxidase subunit 4 mediates cycling hypoxia-promoted radiation resistance in glioblastoma multiforme. *Free Radic Biol Med*. 53:649-658.

Hu, C.J., L.Y. Wang, L.A. Chodosh, B. Keith, and M.C. Simon. 2003. Differential roles of hypoxia-inducible factor 1alpha (HIF-1alpha) and HIF-2alpha in hypoxic gene regulation. *Mol Cell Biol*. 23:9361-9374.

Hultquist, J.F., J.A. Lengyel, E.W. Refsland, R.S. LaRue, L. Lackey, W.L. Brown, and R.S. Harris. 2011. Human and rhesus APOBEC3D, APOBEC3F, APOBEC3G, and APOBEC3H demonstrate a conserved capacity to restrict Vif-deficient HIV-1. *J Virol*. 85:11220-11234.

Ilves, I., T. Petojevic, J.J. Pesavento, and M.R. Botchan. 2010. Activation of the MCM2-7 helicase by association with Cdc45 and GINS proteins. *Mol Cell*. 37:247-258.

Jackson, J.R., A. Gilmartin, C. Imburgia, J.D. Winkler, L.A. Marshall, and A. Roshak. 2000. An indolocarbazole inhibitor of human checkpoint kinase (Chk1) abrogates cell cycle arrest caused by DNA damage. *Cancer Res*. 60:566-572.

Jarvis, M.C., D. Ebrahimi, N.A. Temiz, and R.S. Harris. 2018. Mutation Signatures Including APOBEC in Cancer Cell Lines. *JNCI Cancer Spectr*. 2.

Johnson, A.B., N. Denko, and M.C. Barton. 2008. Hypoxia induces a novel signature of chromatin modifications and global repression of transcription. *Mutat Res*. 640:174-179.

Joyce, J.A., and J.W. Pollard. 2009. Microenvironmental regulation of metastasis. *Nat Rev Cancer*. 9:239-252.

Kalliomaki, T.M., G. McCallum, S.J. Lunt, P.G. Wells, and R.P. Hill. 2008. Analysis of the effects of exposure to acute hypoxia on oxidative lesions and tumour progression in a transgenic mouse breast cancer model. *BMC Cancer*. 8:151.

Kalliomaki, T.M., G. McCallum, P.G. Wells, and R.P. Hill. 2009. Progression and metastasis in a transgenic mouse breast cancer model: effects of exposure to in vivo hypoxia. *Cancer Lett*. 282:98-108.

Kanu, N., M.A. Cerone, G. Goh, L.P. Zalmas, J. Bartkova, M. Dietzen, N. McGranahan, R. Rogers, E.K. Law, I. Gromova, M. Kschischo, M.I. Walton, O.W. Rossanese, J. Bartek, R.S. Harris, S. Venkatesan, and C. Swanton. 2016. DNA replication stress mediates APOBEC3 family mutagenesis in breast cancer. *Genome biology*. 17:185.

Kawabata, T., S.W. Luebben, S. Yamaguchi, I. Ilves, I. Matise, T. Buske, M.R. Botchan, and N. Shima. 2011. Stalled fork rescue via dormant replication origins in unchallenged S phase promotes proper chromosome segregation and tumor suppression. *Mol Cell*. 41:543-553.

Kazazian, H.H., Jr. 2004. Mobile elements: drivers of genome evolution. *Science*. 303:1626-1632.

Keith, B., R.S. Johnson, and M.C. Simon. 2011. HIF1alpha and HIF2alpha: sibling rivalry in hypoxic tumour growth and progression. *Nat Rev Cancer*. 12:9-22.

Kimura, H., R.D. Braun, E.T. Ong, R. Hsu, T.W. Secomb, D. Papahadjopoulos, K. Hong, and M.W. Dewhirst. 1996. Fluctuations in red cell flux in tumor microvessels can lead to transient hypoxia and reoxygenation in tumor parenchyma. *Cancer Res*. 56:5522-5528.

King, C., H.B. Diaz, S. McNeely, D. Barnard, J. Dempsey, W. Blosser, R. Beckmann, D. Barda, and M.S. Marshall. 2015. LY2606368 Causes Replication Catastrophe and Antitumor Effects through CHK1-Dependent Mechanisms. *Mol Cancer Ther*. 14:2004-2013.

Kinomoto, M., T. Kanno, M. Shimura, Y. Ishizaka, A. Kojima, T. Kurata, T. Sata, and K. Tokunaga. 2007. All APOBEC3 family proteins differentially inhibit LINE-1 retrotransposition. *Nucleic Acids Res*. 35:2955-2964.

Klotz-Noack, K., and J.J. Blow. 2011. A role for dormant origins in tumor suppression. *Mol Cell*. 41:495-496.

Koh, M.Y., and G. Powis. 2012. Passing the baton: the HIF switch. *Trends Biochem Sci*. 37:364-372.

Kohn, K.W., J. Riss, O. Aprelikova, J.N. Weinstein, Y. Pommier, and J.C. Barrett. 2004. Properties of switch-like bioregulatory networks studied by simulation of the hypoxia response control system. *Mol Biol Cell*. 15:3042-3052.

Koito, A., and T. Ikeda. 2013. Intrinsic immunity against retrotransposons by APOBEC cytidine deaminases. *Front Microbiol*. 4:28.

Kollareddy, M., E. Dimitrova, K.C. Vallabhaneni, A. Chan, T. Le, K.M. Chauhan, Z.I. Carrero, G. Ramakrishnan, K. Watabe, Y. Haupt, S. Haupt, R. Pochampally, G.R. Boss, D.G. Romero, C.G. Radu, and L.A. Martinez. 2015. Regulation of nucleotide metabolism by mutant p53 contributes to its gain-of-function activities. *Nat Commun*. 6:7389.

Kong, D., T.R. Coleman, and M.L. DePamphilis. 2003. Xenopus origin recognition complex (ORC) initiates DNA replication preferentially at sequences targeted by Schizosaccharomyces pombe ORC. *EMBO J*. 22:3441-3450.

Koning, F.A., E.N. Newman, E.Y. Kim, K.J. Kunstman, S.M. Wolinsky, and M.H. Malim. 2009. Defining APOBEC3 expression patterns in human tissues and hematopoietic cell subsets. *J Virol*. 83:9474-9485.

Koritzinsky, M., and B.G. Wouters. 2013. The roles of reactive oxygen species and autophagy in mediating the tolerance of tumor cells to cycling hypoxia. *Semin Radiat Oncol*. 23:252-261.

Koumenis, C., R. Alarcon, E. Hammond, P. Sutphin, W. Hoffman, M. Murphy, J. Derr, Y. Taya, S.W. Lowe, M. Kastan, and A. Giaccia. 2001. Regulation of p53 by hypoxia: dissociation of transcriptional repression and apoptosis from p53-dependent transactivation. *Mol Cell Biol*. 21:1297-1310.

Koumenis, C., and B.G. Wouters. 2006. "Translating" tumor hypoxia: unfolded protein response (UPR)-dependent and UPR-independent pathways. *Mol Cancer Res*. 4:423-436.

Kramer, O.H., S.K. Knauer, D. Zimmermann, R.H. Stauber, and T. Heinzel. 2008. Histone deacetylase inhibitors and hydroxyurea modulate the cell cycle and cooperatively induce apoptosis. *Oncogene*. 27:732-740.

Krieg, M., R. Haas, H. Brauch, T. Acker, I. Flamme, and K.H. Plate. 2000. Up-regulation of hypoxia-inducible factors HIF-1alpha and HIF-2alpha under normoxic conditions in renal carcinoma cells by von Hippel-Lindau tumor suppressor gene loss of function. *Oncogene*. 19:5435-5443.

Krokan, H.E., M. Otterlei, H. Nilsen, B. Kavli, F. Skorpen, S. Andersen, C. Skjelbred, M. Akbari, P.A. Aas, and G. Slupphaug. 2001. Properties and functions of human uracil-DNA glycosylase from the UNG gene. *Prog Nucleic Acid Res Mol Biol*. 68:365-386.

Kumareswaran, R., N. Chaudary, K. Jaluba, A. Meng, J. Sykes, A. Borhan, R.P. Hill, and R.G. Bristow. 2015. Cyclic hypoxia does not alter RAD51 expression or PARP inhibitor cell kill in tumor cells. *Radiother Oncol*. 116:388-391.

Kvach, M.V., F.M. Barzak, S. Harjes, H.A.M. Schares, G.B. Jameson, A.M. Ayoub, R. Moorthy, H. Aihara, R.S. Harris, V.V. Filichev, D.A. Harki, and E. Harjes. 2019. Inhibiting APOBEC3 Activity with Single-Stranded DNA Containing 2'-Deoxyzebularine Analogues. *Biochemistry*. 58:391-400.

Labib, K., and B. Hodgson. 2007. Replication fork barriers: pausing for a break or stalling for time? *EMBO Rep*. 8:346-353.

Lam, M.H., Q. Liu, S.J. Elledge, and J.M. Rosen. 2004. Chk1 is haploinsufficient for multiple functions critical to tumor suppression. *Cancer Cell*. 6:45-59.

Lambert, S., and A.M. Carr. 2013. Impediments to replication fork movement: stabilisation, reactivation and genome instability. *Chromosoma*. 122:33-45.

Land, A.M., E.K. Law, M.A. Carpenter, L. Lackey, W.L. Brown, and R.S. Harris. 2013. Endogenous APOBEC3A DNA cytosine deaminase is cytoplasmic and nongenotoxic. *J Biol Chem*. 288:17253-17260.

Landry, S., I. Narvaiza, D.C. Linfesty, and M.D. Weitzman. 2011. APOBEC3A can activate the DNA damage response and cause cell-cycle arrest. *EMBO Rep*. 12:444-450.

Law, E.K., A.M. Sieuwerts, K. LaPara, B. Leonard, G.J. Starrett, A.M. Molan, N.A. Temiz, R.I. Vogel, M.E. Meijer-van Gelder, F.C. Sweep, P.N. Span, J.A. Foekens, J.W. Martens, D. Yee, and R.S. Harris. 2016. The DNA cytosine deaminase APOBEC3B promotes tamoxifen resistance in ER-positive breast cancer. *Sci Adv*. 2:e1601737.

Le Tallec, B., B. Dutrillaux, A.M. Lachages, G.A. Millot, O. Brison, and M. Debatisse. 2011. Molecular profiling of common fragile sites in human fibroblasts. *Nat Struct Mol Biol*. 18:1421-1423.

Lee, D.E., K. Alhallak, S.V. Jenkins, I. Vargas, N.P. Greene, K.P. Quinn, R.J. Griffin, R.P.M. Dings, and N. Rajaram. 2018. A Radiosensitizing Inhibitor of HIF-1 alters the Optical Redox State of Human Lung Cancer Cells In Vitro. *Sci Rep*. 8:8815.

Lee, S.R., K.S. Yang, J. Kwon, C. Lee, W. Jeong, and S.G. Rhee. 2002. Reversible inactivation of the tumor suppressor PTEN by H2O2. *J Biol Chem*. 277:20336-20342.

Leedale, J., A. Herrmann, J. Bagnall, A. Fercher, D. Papkovsky, V. See, and R.N. Bearon. 2014. Modeling the dynamics of hypoxia inducible factor-1alpha (HIF-1alpha) within single cells and 3D cell culture systems. *Math Biosci*. 258:33-43.

Leonard, B., J.L. McCann, G.J. Starrett, L. Kosyakovsky, E.M. Luengas, A.M. Molan, M.B. Burns, R.M. McDougle, P.J. Parker, W.L. Brown, and R.S. Harris. 2015. The PKC/NF-kappaB signaling pathway induces APOBEC3B expression in multiple human cancers. *Cancer Res*. 75:4538-4547.

Leroy, B., L. Girard, A. Hollestelle, J.D. Minna, A.F. Gazdar, and T. Soussi. 2014. Analysis of TP53 mutation status in human cancer cell lines: a reassessment. *Hum Mutat*. 35:756-765.

Leszczynska, K.B., I.P. Foskolou, A.G. Abraham, S. Anbalagan, C. Tellier, S. Haider, P.N. Span, E.E. O'Neill, F.M. Buffa, and E.M. Hammond. 2015. Hypoxia-induced p53 modulates both apoptosis and radiosensitivity via AKT. *J Clin Invest*. 125:2385-2398.

Letessier, A., G.A. Millot, S. Koundrioukoff, A.M. Lachages, N. Vogt, R.S. Hansen, B. Malfoy, O. Brison, and M. Debatisse. 2011. Cell-type-specific replication initiation programs set fragility of the FRA3B fragile site. *Nature*. 470:120-123.

Li, L., F. Ren, C. Qi, L. Xu, Y. Fang, M. Liang, J. Feng, B. Chen, W. Ning, and J. Cao. 2018. Intermittent hypoxia promotes melanoma lung metastasis via oxidative stress and inflammation responses in a mouse model of obstructive sleep apnea. *Respir Res*. 19:28.

Li, M., S.M. Shandilya, M.A. Carpenter, A. Rathore, W.L. Brown, A.L. Perkins, D.A. Harki, J. Solberg, D.J. Hook, K.K. Pandey, M.A. Parniak, J.R. Johnson, N.J. Krogan, M. Somasundaran, A. Ali, C.A. Schiffer, and R.S. Harris. 2012. First-in-class small molecule inhibitors of the single-strand DNA cytosine deaminase APOBEC3G. *ACS Chem Biol*. 7:506-517.

Li, M.M., and M. Emerman. 2011. Polymorphism in human APOBEC3H affects a phenotype dominant for subcellular localization and antiviral activity. *J Virol*. 85:8197-8207.

Li, S., S.S. Tabar, V. Malec, B.G. Eul, W. Klepetko, N. Weissmann, F. Grimminger, W. Seeger, F. Rose, and J. Hanze. 2008. NOX4 regulates ROS levels under normoxic and hypoxic conditions, triggers proliferation, and inhibits apoptosis in pulmonary artery adventitial fibroblasts. *Antioxid Redox Signal*. 10:1687-1698.

Lim, L.Y., N. Vidnovic, L.W. Ellisen, and C.O. Leong. 2009. Mutant p53 mediates survival of breast cancer cells. *Br J Cancer*. 101:1606-1612.

Liu, D., P. Abbosh, D. Keliher, B. Reardon, D. Miao, K. Mouw, A. Weiner-Taylor, S. Wankowicz, G. Han, M.Y. Teo, C. Cipolla, J. Kim, G. Iyer, H. Al-Ahmadie, E. Dulaimi, D.Y.T. Chen, R.K. Alpaugh, J. Hoffman-Censits, L.A. Garraway, G. Getz, S.L. Carter, J. Bellmunt, E.R. Plimack, J.E. Rosenberg, and E.M. Van Allen. 2017a. Mutational

patterns in chemotherapy resistant muscle-invasive bladder cancer. *Nat Commun*. 8:2193.

Liu, H., F. Jiang, X. Jia, J. Lan, H. Guo, E. Li, A. Yan, and Y. Wang. 2017b. Cycling hypoxia affects cell invasion and proliferation through direct regulation of claudin1 / claudin7 expression, and indirect regulation of P18 through claudin7. *Oncotarget*. 8:10298-10311.

Liu, J., J. Zhang, X. Wang, Y. Li, Y. Chen, K. Li, J. Zhang, L. Yao, and G. Guo. 2010a. HIF-1 and NDRG2 contribute to hypoxia-induced radioresistance of cervical cancer Hela cells. *Exp Cell Res*. 316:1985-1993.

Liu, L., W. Liu, L. Wang, T. Zhu, J. Zhong, and N. Xie. 2017c. Hypoxia-inducible factor 1 mediates intermittent hypoxia-induced migration of human breast cancer MDA-MB-231 cells. *Oncol Lett*. 14:7715-7722.

Liu, Q., S. Guntuku, X.S. Cui, S. Matsuoka, D. Cortez, K. Tamai, G. Luo, S. Carattini-Rivera, F. DeMayo, A. Bradley, L.A. Donehower, and S.J. Elledge. 2000. Chk1 is an essential kinase that is regulated by Atr and required for the G(2)/M DNA damage checkpoint. *Genes Dev*. 14:1448-1459.

Liu, S., S.O. Opiyo, K. Manthey, J.G. Glanzer, A.K. Ashley, C. Amerin, K. Troksa, M. Shrivastav, J.A. Nickoloff, and G.G. Oakley. 2012. Distinct roles for DNA-PK, ATM and ATR in RPA phosphorylation and checkpoint activation in response to replication stress. *Nucleic Acids Res*. 40:10780-10794.

Liu, S., Z. Wang, B. Xu, K. Chen, J. Sun, and L. Ren. 2016. Intermittent hypoxia reduces microglia proliferation and induces DNA damage in vitro. *Iran J Basic Med Sci*. 19:497-502.

Liu, Y., and W.F. Bodmer. 2006. Analysis of P53 mutations and their expression in 56 colorectal cancer cell lines. *Proc Natl Acad Sci U S A*. 103:976-981.

Liu, Y., X. Song, X. Wang, L. Wei, X. Liu, S. Yuan, and L. Lv. 2010b. Effect of chronic intermittent hypoxia on biological behavior and hypoxia-associated gene expression in lung cancer cells. *J Cell Biochem*. 111:554-563.

Longerich, S., U. Basu, F. Alt, and U. Storb. 2006. AID in somatic hypermutation and class switch recombination. *Curr Opin Immunol*. 18:164-174.

Lopes, M., C. Cotta-Ramusino, A. Pellicioli, G. Liberi, P. Plevani, M. Muzi-Falconi, C.S. Newlon, and M. Foiani. 2001. The DNA replication checkpoint response stabilizes stalled replication forks. *Nature*. 412:557-561.

Lopes, M., M. Foiani, and J.M. Sogo. 2006. Multiple mechanisms control chromosome integrity after replication fork uncoupling and restart at irreparable UV lesions. *Mol Cell*. 21:15-27.

Lopez-Contreras, A.J., P. Gutierrez-Martinez, J. Specks, S. Rodrigo-Perez, and O. Fernandez-Capetillo. 2012. An extra allele of Chk1 limits oncogene-induced replicative stress and promotes transformation. *J Exp Med*. 209:455-461.

Louie, E., S. Nik, J.S. Chen, M. Schmidt, B. Song, C. Pacson, X.F. Chen, S. Park, J. Ju, and E.I. Chen. 2010. Identification of a stem-like cell population by exposing metastatic breast cancer cell lines to repetitive cycles of hypoxia and reoxygenation. *Breast Cancer Res*. 12:R94.

Lu, X., and Y. Kang. 2010. Hypoxia and hypoxia-inducible factors: master regulators of metastasis. *Clin Cancer Res*. 16:5928-5935.

Macheret, M., and T.D. Halazonetis. 2015. DNA replication stress as a hallmark of cancer. *Annu Rev Pathol*. 10:425-448.

Magdalou, I., B.S. Lopez, P. Pasero, and S.A. Lambert. 2014. The causes of replication stress and their consequences on genome stability and cell fate. *Semin Cell Dev Biol*. 30:154-164.

Mailand, N., I. Gibbs-Seymour, and S. Bekker-Jensen. 2013. Regulation of PCNA-protein interactions for genome stability. *Nat Rev Mol Cell Biol*. 14:269-282.

Makino, Y., R. Cao, K. Svensson, G. Bertilsson, M. Asman, H. Tanaka, Y. Cao, A. Berkenstam, and L. Poellinger. 2001. Inhibitory PAS domain protein is a negative regulator of hypoxia-inducible gene expression. *Nature*. 414:550-554.

Makino, Y., R. Uenishi, K. Okamoto, T. Isoe, O. Hosono, H. Tanaka, A. Kanopka, L. Poellinger, M. Haneda, and C. Morimoto. 2007. Transcriptional up-regulation of inhibitory PAS domain protein gene expression by hypoxia-inducible factor 1 (HIF-1): a negative feedback regulatory circuit in HIF-1-mediated signaling in hypoxic cells. *J Biol Chem*. 282:14073-14082.

Malec, V., O.R. Gottschald, S. Li, F. Rose, W. Seeger, and J. Hanze. 2010. HIF-1 alpha signaling is augmented during intermittent hypoxia by induction of the Nrf2 pathway in NOX1-expressing adenocarcinoma A549 cells. *Free Radic Biol Med*. 48:1626-1635.

Mansfield, K.D., R.D. Guzy, Y. Pan, R.M. Young, T.P. Cash, P.T. Schumacker, and M.C. Simon. 2005. Mitochondrial dysfunction resulting from loss of cytochrome c impairs cellular oxygen sensing and hypoxic HIF-alpha activation. *Cell Metab*. 1:393-399.

Mantiero, D., A. Mackenzie, A. Donaldson, and P. Zegerman. 2011. Limiting replication initiation factors execute the temporal programme of origin firing in budding yeast. *EMBO J*. 30:4805-4814.

Martinez-Reyes, I., L.R. Cardona, H. Kong, K. Vasan, G.S. McElroy, M. Werner, H. Kihshen, C.R. Reczek, S.E. Weinberg, P. Gao, E.M. Steinert, R. Piseaux, G.R.S. Budinger, and N.S. Chandel. 2020. Mitochondrial ubiquinol oxidation is necessary for tumour growth. *Nature*.

Martinez, C.A., B. Kerr, C. Jin, P.A. Cistulli, and K.M. Cook. 2019. Obstructive Sleep Apnea Activates HIF-1 in a Hypoxia Dose-Dependent Manner in HCT116 Colorectal Carcinoma Cells. *Int J Mol Sci*. 20.

Martinive, P., F. Defresne, C. Bouzin, J. Saliez, F. Lair, V. Gregoire, C. Michiels, C. Dessy, and O. Feron. 2006. Preconditioning of the tumor vasculature and tumor cells by intermittent hypoxia: implications for anticancer therapies. *Cancer Res*. 66:11736-11744.

Martinive, P., F. Defresne, E. Quaghebeur, G. Daneau, N. Crokart, V. Gregoire, B. Gallez, C. Dessy, and O. Feron. 2009. Impact of cyclic hypoxia on HIF-1alpha regulation in endothelial cells--new insights for anti-tumor treatments. *FEBS J*. 276:509-518.

Maruyama, W., K. Shirakawa, H. Matsui, T. Matsumoto, H. Yamazaki, A.D. Sarca, Y. Kazuma, M. Kobayashi, K. Shindo, and A. Takaori-Kondo. 2016. Classical NF-kappaB pathway is responsible for APOBEC3B expression in cancer cells. *Biochem Biophys Res Commun*. 478:1466-1471.

Masutani, C., R. Kusumoto, S. Iwai, and F. Hanaoka. 2000. Mechanisms of accurate translesion synthesis by human DNA polymerase eta. *EMBO J*. 19:3100-3109.

Mathews, C.K. 2015. Deoxyribonucleotide metabolism, mutagenesis and cancer. *Nat Rev Cancer*. 15:528-539.

Matschke, J., H. Riffkin, D. Klein, R. Handrick, L. Ludemann, E. Metzen, T. Shlomi, M. Stuschke, and V. Jendrossek. 2016. Targeted Inhibition of Glutamine-Dependent Glutathione Metabolism Overcomes Death Resistance Induced by Chronic Cycling Hypoxia. *Antioxid Redox Signal*. 25:89-107.

Matsumoto, S., H. Yasui, J.B. Mitchell, and M.C. Krishna. 2010. Imaging cycling tumor hypoxia. *Cancer Res*. 70:10019-10023.

Matsumoto, T., K. Shirakawa, M. Yokoyama, H. Fukuda, A.D. Sarca, S. Koyabu, H. Yamazaki, Y. Kazuma, H. Matsui, W. Maruyama, K. Nagata, F. Tanabe, M. Kobayashi, K. Shindo, R. Morishita, H. Sato, and A. Takaori-Kondo. 2019. Protein kinase A inhibits tumor mutator APOBEC3B through phosphorylation. *Sci Rep*. 9:8307.

Maynard, M.A., H. Qi, J. Chung, E.H. Lee, Y. Kondo, S. Hara, R.C. Conaway, J.W. Conaway, and M. Ohh. 2003. Multiple splice variants of the human HIF-3 alpha locus are targets of the von Hippel-Lindau E3 ubiquitin ligase complex. *J Biol Chem*. 278:11032-11040.

Mechali, M. 2010. Eukaryotic DNA replication origins: many choices for appropriate answers. *Nat Rev Mol Cell Biol*. 11:728-738.

Menendez, D., T.A. Nguyen, J. Snipe, and M.A. Resnick. 2017. The Cytidine Deaminase APOBEC3 Family Is Subject to Transcriptional Regulation by p53. *Mol Cancer Res*. 15:735-743.

Miao, Z.F., T.T. Zhao, Z.N. Wang, Y.Y. Xu, X.Y. Mao, J.H. Wu, X.Y. Liu, H. Xu, Y. You, and H.M. Xu. 2014. Influence of different hypoxia models on metastatic potential of SGC-7901 gastric cancer cells. *Tumour Biol*. 35:6801-6808.

Minoves, M., J. Morand, F. Perriot, M. Chatard, B. Gonthier, E. Lemarie, J.B. Menut, J. Polak, J.L. Pepin, D. Godin-Ribuot, and A. Briancon-Marjollet. 2017. An innovative intermittent hypoxia model for cell cultures allowing fast Po2 oscillations with minimal gas consumption. *Am J Physiol Cell Physiol*. 313:C460-C468.

Mirkin, E.V., and S.M. Mirkin. 2007. Replication fork stalling at natural impediments. *Microbiol Mol Biol Rev*. 71:13-35.

Moeller, B.J., Y. Cao, C.Y. Li, and M.W. Dewhirst. 2004. Radiation activates HIF-1 to regulate vascular radiosensitivity in tumors: role of reoxygenation, free radicals, and stress granules. *Cancer Cell*. 5:429-441.

Moeller, B.J., and M.W. Dewhirst. 2006. HIF-1 and tumour radiosensitivity. *Br J Cancer*. 95:1-5.

Moeller, B.J., M.R. Dreher, Z.N. Rabbani, T. Schroeder, Y. Cao, C.Y. Li, and M.W. Dewhirst. 2005. Pleiotropic effects of HIF-1 blockade on tumor radiosensitivity. *Cancer Cell*. 8:99-110.

Moiseeva, T.N., and C.J. Bakkenist. 2019. Dormant origin signaling during unperturbed replication. *DNA Repair (Amst)*. 81:102655.

Monti, E., and M.B. Gariboldi. 2011. HIF-1 as a target for cancer chemotherapy, chemosensitization and chemoprevention. *Curr Mol Pharmacol*. 4:62-77.

Morgan, M.J., and Z.G. Liu. 2011. Crosstalk of reactive oxygen species and NF-kappaB signaling. *Cell Res*. 21:103-115.

Muramatsu, M., K. Kinoshita, S. Fagarasan, S. Yamada, Y. Shinkai, and T. Honjo. 2000. Class switch recombination and hypermutation require activation-induced cytidine deaminase (AID), a potential RNA editing enzyme. *Cell*. 102:553-563.

Nabel, C.S., S.A. Manning, and R.M. Kohli. 2012. The curious chemical biology of cytosine: deamination, methylation, and oxidation as modulators of genomic potential. *ACS Chem Biol*. 7:20-30.

Narvaiza, I., S. Landry, and M.D. Weitzman. 2012. APOBEC3 proteins and genomic stability: the high cost of a good defense. *Cell Cycle*. 11:33-38.

Nathan, C., and A. Cunningham-Bussel. 2013. Beyond oxidative stress: an immunologist's guide to reactive oxygen species. *Nat Rev Immunol*. 13:349-361.

Nehmeh, S.A., N.Y. Lee, H. Schroder, O. Squire, P.B. Zanzonico, Y.E. Erdi, C. Greco, G. Mageras, H.S. Pham, S.M. Larson, C.C. Ling, and J.L. Humm. 2008. Reproducibility of intratumor distribution of (18)F-fluoromisonidazole in head and neck cancer. *Int J Radiat Oncol Biol Phys*. 70:235-242.

Ng, J.C.F., J. Quist, A. Grigoriadis, M.H. Malim, and F. Fraternali. 2019. Pan-cancer transcriptomic analysis dissects immune and proliferative functions of APOBEC3 cytidine deaminases. *Nucleic Acids Res*. 47:1178-1194.

Nghiem, P., P.K. Park, Y. Kim, C. Vaziri, and S.L. Schreiber. 2001. ATR inhibition selectively sensitizes G1 checkpoint-deficient cells to lethal premature chromatin condensation. *Proc Natl Acad Sci U S A*. 98:9092-9097.

Niecknig, H., S. Tug, B.D. Reyes, M. Kirsch, J. Fandrey, and U. Berchner-Pfannschmidt. 2012. Role of reactive oxygen species in the regulation of HIF-1 by prolyl hydroxylase 2 under mild hypoxia. *Free Radic Res*. 46:705-717.

Nijkamp, M.M., P.N. Span, J. Bussink, and J.H. Kaanders. 2013. Interaction of EGFR with the tumour microenvironment: implications for radiation treatment. *Radiother Oncol*. 108:17-23.

Nik-Zainal, S., L.B. Alexandrov, D.C. Wedge, P. Van Loo, C.D. Greenman, K. Raine, D. Jones, J. Hinton, J. Marshall, L.A. Stebbings, A. Menzies, S. Martin, K. Leung, L. Chen, C. Leroy, M. Ramakrishna, R. Rance, K.W. Lau, L.J. Mudie, I. Varela, D.J. McBride, G.R. Bignell, S.L. Cooke, A. Shlien, J. Gamble, I. Whitmore, M. Maddison, P.S. Tarpey, H.R. Davies, E. Papaemmanuil, P.J. Stephens, S. McLaren, A.P. Butler, J.W. Teague, G. Jonsson, J.E. Garber, D. Silver, P. Miron, A. Fatima, S. Boyault, A. Langerod, A. Tutt, J.W. Martens, S.A. Aparicio, A. Borg, A.V. Salomon, G. Thomas, A.L. Borresen-Dale, A.L. Richardson, M.S. Neuberger, P.A. Futreal, P.J. Campbell, M.R. Stratton, and C. Breast Cancer Working Group of the International Cancer Genome. 2012. Mutational processes molding the genomes of 21 breast cancers. *Cell*. 149:979-993.

Nikkila, J., R. Kumar, J. Campbell, I. Brandsma, H.N. Pemberton, F. Wallberg, K. Nagy, I. Scheer, B.G. Vertessy, A.A. Serebrenik, V. Monni, R.S. Harris, S.J. Pettitt, A. Ashworth, and C.J. Lord. 2017. Elevated APOBEC3B expression drives a kataegic-like mutation signature and replication stress-related therapeutic vulnerabilities in p53-defective cells. *Br J Cancer*. 117:113-123.

Nordsmark, M., S.M. Bentzen, V. Rudat, D. Brizel, E. Lartigau, P. Stadler, A. Becker, M. Adam, M. Molls, J. Dunst, D.J. Terris, and J. Overgaard. 2005. Prognostic value of tumor oxygenation in 397 head and neck tumors after primary radiation therapy. An international multi-center study. *Radiother Oncol*. 77:18-24.

O'Connor, J.P.B., S.P. Robinson, and J.C. Waterton. 2019. Imaging tumour hypoxia with oxygen-enhanced MRI and BOLD MRI. *Br J Radiol*. 92:20180642.

Ohba, K., K. Ichiyama, M. Yajima, N. Gemma, M. Nikaido, Q. Wu, P. Chong, S. Mori, R. Yamamoto, J.E. Wong, and N. Yamamoto. 2014. In vivo and in vitro studies suggest a possible involvement of HPV infection in the early stage of breast carcinogenesis via APOBEC3B induction. *PLoS One*. 9:e97787.

Okazaki, R., T. Okazaki, K. Sakabe, and K. Sugimoto. 1967. Mechanism of DNA replication possible discontinuity of DNA chain growth. *Jpn J Med Sci Biol*. 20:255-260.

Olcina, M.M., I.P. Foskolou, S. Anbalagan, J.M. Senra, I.M. Pires, Y. Jiang, A.J. Ryan, and E.M. Hammond. 2013. Replication stress and chromatin context link ATM activation to a role in DNA replication. *Mol Cell*. 52:758-766.

Olson, E., C.J. Nievera, V. Klimovich, E. Fanning, and X. Wu. 2006. RPA2 is a direct downstream target for ATR to regulate the S-phase checkpoint. *J Biol Chem*. 281:39517-39533.

Olson, M.E., R.S. Harris, and D.A. Harki. 2018. APOBEC Enzymes as Targets for Virus and Cancer Therapy. *Cell Chem Biol*. 25:36-49.

Olson, M.E., M. Li, R.S. Harris, and D.A. Harki. 2013. Small-molecule APOBEC3G DNA cytosine deaminase inhibitors based on a 4-amino-1,2,4-triazole-3-thiol scaffold. *ChemMedChem*. 8:112-117.

Pacek, M., and J.C. Walter. 2004. A requirement for MCM7 and Cdc45 in chromosome unwinding during eukaryotic DNA replication. *EMBO J*. 23:3667-3676.

Palcic, B., J.W. Brosing, and L.D. Skarsgard. 1982. Survival measurements at low doses: oxygen enhancement ratio. *Br J Cancer*. 46:980-984.

Palmer, G.M., A.N. Fontanella, G. Zhang, G. Hanna, C.L. Fraser, and M.W. Dewhirst. 2010. Optical imaging of tumor hypoxia dynamics. *J Biomed Opt*. 15:066021.

Pearl, L.H., A.C. Schierz, S.E. Ward, B. Al-Lazikani, and F.M. Pearl. 2015. Therapeutic opportunities within the DNA damage response. *Nat Rev Cancer*. 15:166-180.

Periyasamy, M., A.K. Singh, C. Gemma, C. Kranjec, R. Farzan, D.A. Leach, N. Navaratnam, H.L. Palinkas, B.G. Vertessy, T.R. Fenton, J. Doorbar, F. Fuller-Pace, D.W. Meek, R.C. Coombes, L. Buluwela, and S. Ali. 2017. p53 controls expression of the DNA

deaminase APOBEC3B to limit its potential mutagenic activity in cancer cells. *Nucleic Acids Res*. 45:11056-11069.

Petermann, E., M.L. Orta, N. Issaeva, N. Schultz, and T. Helleday. 2010. Hydroxyurea-stalled replication forks become progressively inactivated and require two different RAD51-mediated pathways for restart and repair. *Mol Cell*. 37:492-502.

Petljak, M., L.B. Alexandrov, J.S. Brammeld, S. Price, D.C. Wedge, S. Grossmann, K.J. Dawson, Y.S. Ju, F. Iorio, J.M.C. Tubio, C.C. Koh, I. Georgakopoulos-Soares, B. Rodriguez-Martin, B. Otlu, S. O'Meara, A.P. Butler, A. Menzies, S.G. Bhosle, K. Raine, D.R. Jones, J.W. Teague, K. Beal, C. Latimer, L. O'Neill, J. Zamora, E. Anderson, N. Patel, M. Maddison, B.L. Ng, J. Graham, M.J. Garnett, U. McDermott, S. Nik-Zainal, P.J. Campbell, and M.R. Stratton. 2019. Characterizing Mutational Signatures in Human Cancer Cell Lines Reveals Episodic APOBEC Mutagenesis. *Cell*. 176:1282-1294 e1220.

Petrova, V., M. Annicchiarico-Petruzzelli, G. Melino, and I. Amelio. 2018. The hypoxic tumour microenvironment. *Oncogenesis*. 7:10.

Pires, I.M., Z. Bencokova, M. Milani, L.K. Folkes, J.L. Li, M.R. Stratford, A.L. Harris, and E.M. Hammond. 2010. Effects of acute versus chronic hypoxia on DNA damage responses and genomic instability. *Cancer Res*. 70:925-935.

Pires, I.M., M.M. Olcina, S. Anbalagan, J.R. Pollard, P.M. Reaper, P.A. Charlton, W.G. McKenna, and E.M. Hammond. 2012. Targeting radiation-resistant hypoxic tumour cells through ATR inhibition. *Br J Cancer*. 107:291-299.

Poli, J., O. Tsaponina, L. Crabbe, A. Keszthelyi, V. Pantesco, A. Chabes, A. Lengronne, and P. Pasero. 2012. dNTP pools determine fork progression and origin usage under replication stress. *EMBO J*. 31:883-894.

Poon, E., A.L. Harris, and M. Ashcroft. 2009. Targeting the hypoxia-inducible factor (HIF) pathway in cancer. *Expert Rev Mol Med*. 11:e26.

Prigent, C., and S. Dimitrov. 2003. Phosphorylation of serine 10 in histone H3, what for? *J Cell Sci*. 116:3677-3685.

Prohaska, K.M., R.P. Bennett, J.D. Salter, and H.C. Smith. 2014. The multifaceted roles of RNA binding in APOBEC cytidine deaminase functions. *Wiley Interdiscip Rev RNA*. 5:493-508.

Pruitt, S.C., K.J. Bailey, and A. Freeland. 2007. Reduced Mcm2 expression results in severe stem/progenitor cell deficiency and cancer. *Stem Cells*. 25:3121-3132.

Puigvert, J.C., K. Sanjiv, and T. Helleday. 2016. Targeting DNA repair, DNA metabolism and replication stress as anti-cancer strategies. *FEBS J*. 283:232-245.

Raedschelders, K., D.M. Ansley, and D.D. Chen. 2012. The cellular and molecular origin of reactive oxygen species generation during myocardial ischemia and reperfusion. *Pharmacol Ther*. 133:230-255.

Rankin, E.B., and A.J. Giaccia. 2016. Hypoxic control of metastasis. *Science*. 352:175-180.

Raval, R.R., K.W. Lau, M.G. Tran, H.M. Sowter, S.J. Mandriota, J.L. Li, C.W. Pugh, P.H. Maxwell, A.L. Harris, and P.J. Ratcliffe. 2005. Contrasting properties of hypoxia-inducible factor 1 (HIF-1) and HIF-2 in von Hippel-Lindau-associated renal cell carcinoma. *Mol Cell Biol*. 25:5675-5686.

Rebhandl, S., M. Huemer, R. Greil, and R. Geisberger. 2015. AID/APOBEC deaminases and cancer. *Oncoscience*. 2:320-333.

Reczek, C.R., and N.S. Chandel. 2015. ROS-dependent signal transduction. *Curr Opin Cell Biol*. 33:8-13.

Remus, D., F. Beuron, G. Tolun, J.D. Griffith, E.P. Morris, and J.F. Diffley. 2009. Concerted loading of Mcm2-7 double hexamers around DNA during DNA replication origin licensing. *Cell*. 139:719-730.

Roberts, S.A., M.S. Lawrence, L.J. Klimczak, S.A. Grimm, D. Fargo, P. Stojanov, A. Kiezun, G.V. Kryukov, S.L. Carter, G. Saksena, S. Harris, R.R. Shah, M.A. Resnick, G. Getz,

and D.A. Gordenin. 2013a. An APOBEC cytidine deaminase mutagenesis pattern is widespread in human cancers. *Nature Genetics*. 45:970-+.

Roberts, S.A., M.S. Lawrence, L.J. Klimczak, S.A. Grimm, D. Fargo, P. Stojanov, A. Kiezun, G.V. Kryukov, S.L. Carter, G. Saksena, S. Harris, R.R. Shah, M.A. Resnick, G. Getz, and D.A. Gordenin. 2013b. An APOBEC cytidine deaminase mutagenesis pattern is widespread in human cancers. *Nat Genet*. 45:970-976.

Robertson, A.G., J. Kim, H. Al-Ahmadie, J. Bellmunt, G. Guo, A.D. Cherniack, T. Hinoue, P.W. Laird, K.A. Hoadley, R. Akbani, M.A.A. Castro, E.A. Gibb, R.S. Kanchi, D.A. Gordenin, S.A. Shukla, F. Sanchez-Vega, D.E. Hansel, B.A. Czerniak, V.E. Reuter, X. Su, B. de Sa Carvalho, V.S. Chagas, K.L. Mungall, S. Sadeghi, C.S. Pedamallu, Y. Lu, L.J. Klimczak, J. Zhang, C. Choo, A.I. Ojesina, S. Bullman, K.M. Leraas, T.M. Lichtenberg, C.J. Wu, N. Schultz, G. Getz, M. Meyerson, G.B. Mills, D.J. McConkey, T.R. Network, J.N. Weinstein, D.J. Kwiatkowski, and S.P. Lerner. 2017. Comprehensive Molecular Characterization of Muscle-Invasive Bladder Cancer. *Cell*. 171:540-556 e525.

Rofstad, E.K., K. Galappathi, B. Mathiesen, and E.B. Ruud. 2007. Fluctuating and diffusion-limited hypoxia in hypoxia-induced metastasis. *Clin Cancer Res*. 13:1971-1978.

Rofstad, E.K., J.V. Gaustad, T.A. Egeland, B. Mathiesen, and K. Galappathi. 2010. Tumors exposed to acute cyclic hypoxic stress show enhanced angiogenesis, perfusion and metastatic dissemination. *Int J Cancer*. 127:1535-1546.

Ron, A., X.L. Dean-Ben, S. Gottschalk, and D. Razansky. 2019. Volumetric Optoacoustic Imaging Unveils High-Resolution Patterns of Acute and Cyclic Hypoxia in a Murine Model of Breast Cancer. *Cancer Res*. 79:4767-4775.

Rouschop, K.M., L.J. Dubois, T.G. Keulers, T. van den Beucken, P. Lambin, J. Bussink, A.J. van der Kogel, M. Koritzinsky, and B.G. Wouters. 2013. PERK/eIF2alpha signaling protects therapy resistant hypoxic cells through induction of glutathione synthesis and protection against ROS. *Proc Natl Acad Sci U S A*. 110:4622-4627.

Rouschop, K.M., C.H. Ramaekers, M.B. Schaaf, T.G. Keulers, K.G. Savelkouls, P. Lambin, M. Koritzinsky, and B.G. Wouters. 2009. Autophagy is required during cycling hypoxia to lower production of reactive oxygen species. *Radiother Oncol*. 92:411-416.

Sakurai, H., H. Chiba, H. Miyoshi, T. Sugita, and W. Toriumi. 1999. IkappaB kinases phosphorylate NF-kappaB p65 subunit on serine 536 in the transactivation domain. *J Biol Chem*. 274:30353-30356.

Saxena, K., and M.K. Jolly. 2019. Acute vs. Chronic vs. Cyclic Hypoxia: Their Differential Dynamics, Molecular Mechanisms, and Effects on Tumor Progression. *Biomolecules*. 9.

Schito, L. 2018. Bridging angiogenesis and immune evasion in the hypoxic tumor microenvironment. *Am J Physiol Regul Integr Comp Physiol*. 315:R1072-R1084.

Schlaepfer, I.R., D.K. Nambiar, A. Ramteke, R. Kumar, D. Dhar, C. Agarwal, B. Bergman, M. Graner, P. Maroni, R.P. Singh, R. Agarwal, and G. Deep. 2015. Hypoxia induces triglycerides accumulation in prostate cancer cells and extracellular vesicles supporting growth and invasiveness following reoxygenation. *Oncotarget*. 6:22836-22856.

Schmid, T., J. Zhou, R. Kohl, and B. Brune. 2004. p300 relieves p53-evoked transcriptional repression of hypoxia-inducible factor-1 (HIF-1). *Biochem J*. 380:289-295.

Schofield, C.J., and P.J. Ratcliffe. 2004. Oxygen sensing by HIF hydroxylases. *Nat Rev Mol Cell Biol*. 5:343-354.

Schrofelbauer, B., Q. Yu, and N.R. Landau. 2004. New insights into the role of Vif in HIV-1 replication. *AIDS Rev*. 6:34-39.

Scott, D.W., and R.D. Gascoyne. 2014. The tumour microenvironment in B cell lymphomas. *Nat Rev Cancer*. 14:517-534.

Sena, L.A., and N.S. Chandel. 2012. Physiological roles of mitochondrial reactive oxygen species. *Mol Cell*. 48:158-167.

Seplyarskiy, V.B., R.A. Soldatov, K.Y. Popadin, S.E. Antonarakis, G.A. Bazykin, and S.I. Nikolaev. 2016. APOBEC-induced mutations in human cancers are strongly enriched on the lagging DNA strand during replication. *Genome Res*. 26:174-182.

Serebrenik, A.A., G.J. Starrett, S. Leenen, M.C. Jarvis, N.M. Shaban, D.J. Salamango, H. Nilsen, W.L. Brown, and R.S. Harris. 2019. The deaminase APOBEC3B triggers the death of cells lacking uracil DNA glycosylase. *Proc Natl Acad Sci U S A*. 116:22158-22163.

Seyfried, T.N., and L.M. Shelton. 2010. Cancer as a metabolic disease. *Nutr Metab (Lond)*. 7:7.

Sharma, S., S.K. Patnaik, Z. Kemer, and B.E. Baysal. 2017. Transient overexpression of exogenous APOBEC3A causes C-to-U RNA editing of thousands of genes. *RNA Biol*. 14:603-610.

Sharma, S., S.K. Patnaik, R.T. Taggart, and B.E. Baysal. 2016. The double-domain cytidine deaminase APOBEC3G is a cellular site-specific RNA editing enzyme. *Sci Rep*. 6:39100.

Sharma, S., S.K. Patnaik, R.T. Taggart, E.D. Kannisto, S.M. Enriquez, P. Gollnick, and B.E. Baysal. 2015. APOBEC3A cytidine deaminase induces RNA editing in monocytes and macrophages. *Nat Commun*. 6:6881.

Shi, K., O. Demir, M.A. Carpenter, S. Banerjee, D.A. Harki, R.E. Amaro, R.S. Harris, and H. Aihara. 2020. Active site plasticity and possible modes of chemical inhibition of the human DNA deaminase APOBEC3B. *FASEB Bioadv*. 2:49-58.

Shima, N., A. Alcaraz, I. Liachko, T.R. Buske, C.A. Andrews, R.J. Munroe, S.A. Hartford, B.K. Tye, and J.C. Schimenti. 2007. A viable allele of Mcm4 causes chromosome instability and mammary adenocarcinomas in mice. *Nat Genet*. 39:93-98.

Shimizu, A., H. Fujimori, Y. Minakawa, Y. Matsuno, M. Hyodo, Y. Murakami, and K.I. Yoshioka. 2018. Onset of deaminase APOBEC3B induction in response to DNA double-strand breaks. *Biochem Biophys Rep*. 16:115-121.

Shinkura, R., S. Ito, N.A. Begum, H. Nagaoka, M. Muramatsu, K. Kinoshita, Y. Sakakibara, H. Hijikata, and T. Honjo. 2004. Separate domains of AID are required for somatic hypermutation and class-switch recombination. *Nat Immunol*. 5:707-712.

Shrieve, D.C., and J.W. Harris. 1985. The in vitro sensitivity of chronically hypoxic EMT6/SF cells to X-radiation and hypoxic cell radiosensitizers. *Int J Radiat Biol Relat Stud Phys Chem Med*. 48:127-138.

Siriwardena, S.U., K. Chen, and A.S. Bhagwat. 2016. Functions and Malfunctions of Mammalian DNA-Cytosine Deaminases. *Chem Rev*. 116:12688-12710.

Smith, H.C., R.P. Bennett, A. Kizilyer, W.M. McDougall, and K.M. Prohaska. 2012. Functions and regulation of the APOBEC family of proteins. *Semin Cell Dev Biol*. 23:258-268.

Smith, N.J., and T.R. Fenton. 2019. The APOBEC3 genes and their role in cancer: insights from human papillomavirus. *J Mol Endocrinol*. 62:R269-R287.

Snyder, B., B. Shell, J.T. Cunningham, and R.L. Cunningham. 2017. Chronic intermittent hypoxia induces oxidative stress and inflammation in brain regions associated with early-stage neurodegeneration. *Physiol Rep*. 5.

Starrett, G.J., E.M. Luengas, J.L. McCann, D. Ebrahimi, N.A. Temiz, R.P. Love, Y. Feng, M.B. Adolph, L. Chelico, E.K. Law, M.A. Carpenter, and R.S. Harris. 2016. The DNA cytosine deaminase APOBEC3H haplotype I likely contributes to breast and lung cancer mutagenesis. *Nat Commun*. 7:12918.

Starrett, G.J., A.A. Serebrenik, P.A. Roelofs, J.L. McCann, B. Verhalen, M.C. Jarvis, T.A. Stewart, E.K. Law, A. Krupp, M. Jiang, J.W.M. Martens, E. Cahir-McFarland, P.N. Span, and R.S. Harris. 2019. Polyomavirus T Antigen Induces APOBEC3B Expression Using an LXCXE-Dependent and TP53-Independent Mechanism. *mBio*. 10.

Steeg, P.S. 2016. Targeting metastasis. *Nat Rev Cancer*. 16:201-218.

Stenglein, M.D., M.B. Burns, M. Li, J. Lengyel, and R.S. Harris. 2010. APOBEC3 proteins mediate the clearance of foreign DNA from human cells. *Nat Struct Mol Biol*. 17:222-229.

Strauss, B.S. 1991. The 'A rule' of mutagen specificity: a consequence of DNA polymerase bypass of non-instructional lesions? *Bioessays*. 13:79-84.

Sudhakar, A. 2009. History of Cancer, Ancient and Modern Treatment Methods. *J Cancer Sci Ther*. 1:1-4.

Sukhanova, M.V., S.N. Khodyreva, N.A. Lebedeva, R. Prasad, S.H. Wilson, and O.I. Lavrik. 2005. Human base excision repair enzymes apurinic/apyrimidinic endonuclease1 (APE1), DNA polymerase beta and poly(ADP-ribose) polymerase 1: interplay between strand-displacement DNA synthesis and proofreading exonuclease activity. *Nucleic Acids Res*. 33:1222-1229.

Swanton, C., N. McGranahan, G.J. Starrett, and R.S. Harris. 2015. APOBEC Enzymes: Mutagenic Fuel for Cancer Evolution and Heterogeneity. *Cancer Discov*. 5:704-712.

Syljuasen, R.G., C.S. Sorensen, L.T. Hansen, K. Fugger, C. Lundin, F. Johansson, T. Helleday, M. Sehested, J. Lukas, and J. Bartek. 2005. Inhibition of human Chk1 causes increased initiation of DNA replication, phosphorylation of ATR targets, and DNA breakage. *Mol Cell Biol*. 25:3553-3562.

Tellier, C., D. Desmet, L. Petit, L. Finet, C. Graux, M. Raes, O. Feron, and C. Michiels. 2015. Cycling hypoxia induces a specific amplified inflammatory phenotype in endothelial cells and enhances tumor-promoting inflammation in vivo. *Neoplasia*. 17:66-78.

Tercero, J.A., and J.F. Diffley. 2001. Regulation of DNA replication fork progression through damaged DNA by the Mec1/Rad53 checkpoint. *Nature*. 412:553-557.

Terry, S., A.S.T. Engelsen, S. Buart, W.S. Elsayed, G.H. Venkatesh, and S. Chouaib. 2020. Hypoxia-driven intratumor heterogeneity and immune evasion. *Cancer Lett*. 492:1-10.

Thielen, B.K., J.P. McNevin, M.J. McElrath, B.V. Hunt, K.C. Klein, and J.R. Lingappa. 2010. Innate immune signaling induces high levels of TC-specific deaminase activity in primary monocyte-derived cells through expression of APOBEC3A isoforms. *J Biol Chem*. 285:27753-27766.

Thompson, P.S., and D. Cortez. 2020. New insights into abasic site repair and tolerance. *DNA Repair (Amst)*. 90:102866.

Toffoli, S., A. Roegiers, O. Feron, M. Van Steenbrugge, N. Ninane, M. Raes, and C. Michiels. 2009. Intermittent hypoxia is an angiogenic inducer for endothelial cells: role of HIF-1. *Angiogenesis*. 12:47-67.

Toledo, L., K.J. Neelsen, and J. Lukas. 2017. Replication Catastrophe: When a Checkpoint Fails because of Exhaustion. *Mol Cell*. 66:735-749.

Toledo, L.I., M. Altmeyer, M.B. Rask, C. Lukas, D.H. Larsen, L.K. Povlsen, S. Bekker-Jensen, N. Mailand, J. Bartek, and J. Lukas. 2013. ATR prohibits replication catastrophe by preventing global exhaustion of RPA. *Cell*. 155:1088-1103.

Trotter, M.J., D.J. Chaplin, R.E. Durand, and P.L. Olive. 1989. The use of fluorescent probes to identify regions of transient perfusion in murine tumors. *Int J Radiat Oncol Biol Phys*. 16:931-934.

Tym, J.E., C. Mitsopoulos, E.A. Coker, P. Razaz, A.C. Schierz, A.A. Antolin, and B. Al-Lazikani. 2016. canSAR: an updated cancer research and drug discovery knowledgebase. *Nucleic Acids Res*. 44:D938-943.

Vaupel, P., S. Briest, and M. Hockel. 2002. Hypoxia in breast cancer: pathogenesis, characterization and biological/therapeutic implications. *Wien Med Wochenschr*. 152:334-342.

Vaupel, P., F. Kallinowski, and P. Okunieff. 1989. Blood flow, oxygen and nutrient supply, and metabolic microenvironment of human tumors: a review. *Cancer Res*. 49:6449-6465.

Veitia, R.A. 2019. DNA Content, Cell Size, and Cell Senescence. *Trends Biochem Sci*. 44:645-647.

Venkatesan, S., R. Rosenthal, N. Kanu, N. McGranahan, J. Bartek, S.A. Quezada, J. Hare, R.S. Harris, and C. Swanton. 2018. Perspective: APOBEC mutagenesis in drug resistance and immune escape in HIV and cancer evolution. *Ann Oncol*. 29:563-572.

Verduzco, D., M. Lloyd, L. Xu, A. Ibrahim-Hashim, Y. Balagurunathan, R.A. Gatenby, and R.J. Gillies. 2015. Intermittent hypoxia selects for genotypes and phenotypes that increase survival, invasion, and therapy resistance. *PLoS One*. 10:e0120958.

Verhalen, B., G.J. Starrett, R.S. Harris, and M. Jiang. 2016. Functional Upregulation of the DNA Cytosine Deaminase APOBEC3B by Polyomaviruses. *J Virol*. 90:6379-6386.

Vieira, V.C., B. Leonard, E.A. White, G.J. Starrett, N.A. Temiz, L.D. Lorenz, D. Lee, M.A. Soares, P.F. Lambert, P.M. Howley, and R.S. Harris. 2014. Human papillomavirus E6 triggers upregulation of the antiviral and cancer genomic DNA deaminase APOBEC3B. *mBio*. 5.

von Schwedler, U., J. Song, C. Aiken, and D. Trono. 1993. Vif is crucial for human immunodeficiency virus type 1 proviral DNA synthesis in infected cells. *J Virol*. 67:4945-4955.

Wang, L., C.M. Lin, J.O. Lopreiato, and M.I. Aladjem. 2006. Cooperative sequence modules determine replication initiation sites at the human beta-globin locus. *Hum Mol Genet*. 15:2613-2622.

Wang, S., M. Jia, Z. He, and X.S. Liu. 2018. APOBEC3B and APOBEC mutational signature as potential predictive markers for immunotherapy response in non-small cell lung cancer. *Oncogene*. 37:3924-3936.

Ward, C., S.P. Langdon, P. Mullen, A.L. Harris, D.J. Harrison, C.T. Supuran, and I.H. Kunkler. 2013. New strategies for targeting the hypoxic tumour microenvironment in breast cancer. *Cancer Treat Rev*. 39:171-179.

Warren, N.J.H., and A. Eastman. 2019. Inhibition of checkpoint kinase 1 following gemcitabine-mediated S phase arrest results in CDC7- and CDK2-dependent replication catastrophe. *J Biol Chem*. 294:1763-1778.

Weinstein, I.B., and K. Case. 2008. The history of Cancer Research: introducing an AACR Centennial series. *Cancer Res*. 68:6861-6862.

WHO. 2019. All cancers factsheet. World Health Organisation - International Agency for Reserach on Cancer, https://gco.iarc.fr/today/data/factsheets/cancers/39-All-cancers-fact-sheet.pdf.

Wiesener, M.S., H. Turley, W.E. Allen, C. Willam, K.U. Eckardt, K.L. Talks, S.M. Wood, K.C. Gatter, A.L. Harris, C.W. Pugh, P.J. Ratcliffe, and P.H. Maxwell. 1998. Induction of endothelial PAS domain protein-1 by hypoxia: characterization and comparison with hypoxia-inducible factor-1alpha. *Blood*. 92:2260-2268.

Wigerup, C., S. Pahlman, and D. Bexell. 2016. Therapeutic targeting of hypoxia and hypoxia-inducible factors in cancer. *Pharmacol Ther*. 164:152-169.

Wilson, W.R., and M.P. Hay. 2011. Targeting hypoxia in cancer therapy. *Nat Rev Cancer*. 11:393-410.

Wold, M.S. 1997. Replication protein A: a heterotrimeric, single-stranded DNA-binding protein required for eukaryotic DNA metabolism. *Annu Rev Biochem*. 66:61-92.

Woodward, A.M., T. Gohler, M.G. Luciani, M. Oehlmann, X. Ge, A. Gartner, D.A. Jackson, and J.J. Blow. 2006. Excess Mcm2-7 license dormant origins of replication that can be used under conditions of replicative stress. *J Cell Biol*. 173:673-683.

Yamazaki, H., K. Shirakawa, T. Matsumoto, Y. Kazuma, H. Matsui, Y. Horisawa, E. Stanford, A.D. Sarca, R. Shirakawa, K. Shindo, and A. Takaori-Kondo. 2020. APOBEC3B reporter myeloma cell lines identify DNA damage response pathways leading to APOBEC3B expression. *PLoS One*. 15:e0223463.

Yasui, H., S. Matsumoto, N. Devasahayam, J.P. Munasinghe, R. Choudhuri, K. Saito, S. Subramanian, J.B. Mitchell, and M.C. Krishna. 2010. Low-field magnetic resonance

imaging to visualize chronic and cycling hypoxia in tumor-bearing mice. *Cancer Res*. 70:6427-6436.

Yu, Q., R. Konig, S. Pillai, K. Chiles, M. Kearney, S. Palmer, D. Richman, J.M. Coffin, and N.R. Landau. 2004. Single-strand specificity of APOBEC3G accounts for minus-strand deamination of the HIV genome. *Nat Struct Mol Biol*. 11:435-442.

Yuan, G., J. Nanduri, S. Khan, G.L. Semenza, and N.R. Prabhakar. 2008. Induction of HIF-1alpha expression by intermittent hypoxia: involvement of NADPH oxidase, Ca2+ signaling, prolyl hydroxylases, and mTOR. *J Cell Physiol*. 217:674-685.

Zannella, V.E., A. Dal Pra, H. Muaddi, T.D. McKee, S. Stapleton, J. Sykes, R. Glicksman, S. Chaib, P. Zamiara, M. Milosevic, B.G. Wouters, R.G. Bristow, and M. Koritzinsky. 2013. Reprogramming metabolism with metformin improves tumor oxygenation and radiotherapy response. *Clin Cancer Res*. 19:6741-6750.

Zellweger, R., D. Dalcher, K. Mutreja, M. Berti, J.A. Schmid, R. Herrador, A. Vindigni, and M. Lopes. 2015. Rad51-mediated replication fork reversal is a global response to genotoxic treatments in human cells. *J Cell Biol*. 208:563-579.

Zeman, M.K., and K.A. Cimprich. 2014. Causes and consequences of replication stress. *Nat Cell Biol*. 16:2-9.

Zhang, C., S. Cao, and Y. Xu. 2014a. Population dynamics inside cancer biomass driven by repeated hypoxia-reoxygenation cycles. *Quantitative Biology*. 2:85-99.

Zhang, J., J. Cao, S. Ma, R. Dong, W. Meng, M. Ying, Q. Weng, Z. Chen, J. Ma, Q. Fang, Q. He, and B. Yang. 2014b. Tumor hypoxia enhances Non-Small Cell Lung Cancer metastasis by selectively promoting macrophage M2 polarization through the activation of ERK signaling. *Oncotarget*. 5:9664-9677.

Zhao, H., and H. Piwnica-Worms. 2001. ATR-mediated checkpoint pathways regulate phosphorylation and activation of human Chk1. *Mol Cell Biol*. 21:4129-4139.

Zhen, A., J. Du, X. Zhou, Y. Xiong, and X.F. Yu. 2012. Reduced APOBEC3H variant anti-viral activities are associated with altered RNA binding activities. *PLoS One*. 7:e38771.

Zhu, H., D. Wang, L. Zhang, X. Xie, Y. Wu, Y. Liu, G. Shao, and Z. Su. 2014. Upregulation of autophagy by hypoxia-inducible factor-1alpha promotes EMT and metastatic ability of CD133+ pancreatic cancer stem-like cells during intermittent hypoxia. *Oncol Rep*. 32:935-942.

Ziv, Y., D. Bielopolski, Y. Galanty, C. Lukas, Y. Taya, D.C. Schultz, J. Lukas, S. Bekker-Jensen, J. Bartek, and Y. Shiloh. 2006. Chromatin relaxation in response to DNA double-strand breaks is modulated by a novel ATM- and KAP-1 dependent pathway. *Nat Cell Biol*. 8:870-876.

Zou, L., and S.J. Elledge. 2003. Sensing DNA damage through ATRIP recognition of RPA-ssDNA complexes. *Science*. 300:1542-1548.

Zou, L., and B. Stillman. 2000. Assembly of a complex containing Cdc45p, replication protein A, and Mcm2p at replication origins controlled by S-phase cyclin-dependent kinases and Cdc7p-Dbf4p kinase. *Mol Cell Biol*. 20:3086-3096.